

**Oxidation of Endogenous Substrates and Ferrous Iron in A
Chemoautotrophic Bacterium *Acidithiobacillus (Thiobacillus)*
*ferrooxidans***

By
Yongqiang Chen

**A Thesis
Submitted to the Faculty of Graduate Studies
in Partial Fulfillment of the Requirements for the Degree of
Doctor of Philosophy**

**Department of Microbiology
University of Manitoba
Winnipeg, Manitoba
March of 2005**

THE UNIVERSITY OF MANITOBA

FACULTY OF GRADUATE STUDIES

COPYRIGHT PERMISSION

Oxidation of Endogenous Substrates and Ferrous Iron in A

Chemoautotrophic Bacterium *Acidithiobacillus (Thiobacillus)*

ferrooxidans

BY

Yongqiang Chen

A Thesis/Practicum submitted to the Faculty of Graduate Studies of The University of

Manitoba in partial fulfillment of the requirement of the degree

Doctor Of Philosophy

Yongqiang Chen © 2005

Permission has been granted to the Library of the University of Manitoba to lend or sell copies of this thesis/practicum, to the National Library of Canada to microfilm this thesis and to lend or sell copies of the film, and to University Microfilms Inc. to publish an abstract of this thesis/practicum.

This reproduction or copy of this thesis has been made available by authority of the copyright owner solely for the purpose of private study and research, and may only be reproduced and copied as permitted by copyright laws or with express written authorization from the copyright owner.

Abstract

Effects of uncouplers and electron transport inhibitors have been studied on the oxygen-coupled oxidation of Fe^{2+} , endogenous substrates and formic acid by *Acidithiobacillus ferrooxidans*. Fe^{2+} oxidation was slightly stimulated by low concentrations of uncouplers within one minute indicating a normal respiratory control during Fe^{2+} oxidation, although higher concentrations of uncouplers were inhibitory. Complex I inhibitors rotenone, amytal and atabrine, and complex III inhibitors antimycin A, myxothiazol and 2-heptyl-4-hydroxyquinoline-N-oxide (HQNO), partially inhibited Fe^{2+} oxidation and the reduced activities by these inhibitors were stimulated by an uncoupler 2,4-dinitrophenol or carbonyl cyanide *m*-chlorophenylhydrazone with the exception of atabrine-reduced activity. These results support the interpretation that some electrons were flowing along the uphill (endergonic) electron transport pathway to reduce NAD^+ during Fe^{2+} oxidation. Complex I inhibitor piericidin A showed no effect on Fe^{2+} oxidation and the reduced activity of Fe^{2+} oxidation by atabrine could be further inhibited by the addition of an uncoupler. Some organic compounds such as ascorbic acid, propyl gallate (PG), salicylhydroxamic acid (SHAM), L-cysteine, glutathione and tiron can be oxidized by *A. ferrooxidans* using the Fe^{2+} -oxidizing system. These compounds could chemically reduce Fe^{3+} to Fe^{2+} and their oxidation by the cells was greatly stimulated by the addition of FeCl_3 . Their oxidation was also not sensitive to the inhibition by piericidin A but was inhibited by atabrine and the reduced activities by atabrine can also be further inhibited by an uncoupler. Other inhibitors and uncouplers showed qualitatively similar but quantitatively different effects on the oxidation of these organic compounds compared to those on Fe^{2+} oxidation.

The oxidation of endogenous substrates in *A. ferrooxidans* by O_2 or Fe^{3+} (endogenous oxidation) was greatly stimulated by uncouplers, ionophores and weak acids, indicating a normal respiratory control during endogenous oxidation. Complex I inhibitors, rotenone, amytal and piericidin A, strongly inhibited endogenous oxidation indicating a downhill (exergonic) electron transport pathway for this oxidation. Atabrine did not inhibit endogenous oxidation but inhibited Fe^{2+} oxidation while piericidin A inhibited endogenous oxidation but did not inhibit Fe^{2+} oxidation, suggesting the possibility of two types of complex I (NDH-1) in *A. ferrooxidans*: one (NDH-1_{down}) involved in the downhill reaction (NADH oxidation) and the other (NDH-1_{up}) involved in the uphill reaction (NAD⁺ reduction). This is also supported by the identification of the genes coding for two types of NDH-1 in the partial genome sequence of *A. ferrooxidans*. Complex IV inhibitors, KCN and NaN_3 at concentrations strongly inhibitory to Fe^{2+} oxidation, only partially inhibited endogenous respiration indicating the involvement of other terminal oxidases in addition to cytochrome *c* oxidase in endogenous respiration. The reduced activity of endogenous respiration by KCN or NaN_3 was further inhibited by the addition of HQNO, an inhibitor of complex III and heme *b*-containing quinol oxidases, and the remained activity was strongly inhibited by rotenone, indicating the involvement of quinol oxidases (*bd* and *bo*₃) and an unknown terminal oxidase that is not sensitive to KCN, NaN_3 and HQNO. HQNO alone, however, greatly stimulated endogenous oxidation. KCN or NaN_3 more strongly inhibited the enhanced activity of endogenous respiration by HQNO than that by uncouplers. It was interpreted that HQNO stimulation was due to the shifting of electrons to a fast electron transport pathway involving iron and the cytochrome *c* oxidase pathway. The respiratory quotient

(CO₂ / O₂ ratio) of endogenous respiration was close to 1.0 indicating the carbohydrate nature of endogenous substrates. A model for the electron transport pathways of endogenous oxidation in this organism was proposed.

Fructose, yeast extract and casamino acids were also oxidized by *A. ferrooxidans* by using at least the major parts of the electron transport pathways of endogenous oxidation.

Formate oxidation by O₂ and Fe³⁺ in *A. ferrooxidans* was strongly inhibited by HQNO even at low concentrations while it was only partially inhibited by complex I inhibitors rotenone and piericidin A but not by amytal and atabrine, supporting the view that the formate dehydrogenase (FDH) in this bacterium contains heme *b* and directly transfers electrons to ubiquinone instead of NAD⁺. Complex III inhibitors antimycin A and myxothiazol partially inhibited formate oxidation suggesting the involvement of complex III. In the presence of HQNO, the activity of formate oxidation was slow initially but increased with time, indicating the shifting of electrons to the fast iron-containing pathway as mentioned in endogenous oxidation. KCN and NaN₃ at low concentrations showed less inhibition of formate oxidation than of Fe²⁺ oxidation but at high concentrations showed stronger inhibition on formate oxidation than on Fe²⁺ oxidation, suggesting that the FDH in this organism may be inhibited by KCN or NaN₃. Formate oxidation was more sensitive to the inhibition by uncouplers than the oxidation of Fe²⁺ and endogenous substrates. The inhibitors of alternative oxidase of plants, SHAM and PG, significantly inhibited formate oxidation.

Based on this study and the currently available information in the literature, a model for the electron transport pathways involving the oxidation of different substrates was proposed.

Acknowledgements

First of all, I would like to give my sincere gratitude to my advisor **Dr. Isamu Suzuki** for his guidance and financial support through NSERC during the course of this work. In the first two years since September of 2000 when I came to Canada from China, **Dr. Suzuki** generously and patiently helped me and allowed me to take a lot of time in conquering my language (English) problem and adapting to the new environment in Canada, without which the unique discoveries in this work would never have been made so quickly. **He** is not only excellent in advising his students academically but also in demonstrating his students how to be a good person and how to successfully manage the problems in life.

I am greatly indebted to **Reuben Saba**, my previous work colleague, for tons of help. **Reuben** helped me in learning English, familiarizing in Canadian culture, demonstrating me how to use laboratory equipment, driving me to parties or to do my personal things, and doing as many kind and beneficial things for me as he can. I thank my previous work colleague **Dr. Jae Key Oh** who also gave me helps in teaching me lab techniques and giving me encouragement.

Many thanks are due to **Dr. Richard Sparling**, one of my committee members. **Dr. Sparling** gave me much important advice and ideas during my annual review meetings and in other times. When I took his graduate course “Advanced Physiology of Bacteria”, I benefited from his “critical thinking style” which greatly influenced some of my discoveries in this work. **He** is a great teacher! My previous committee member **Dr. Feiyue Wang** spent a lot of time in helping me to work out questions in chemistry and also in my other personal things. I thank him very much. I also thank my committee

member **Dr. Frank Hruska** and my external examiner **Dr. Willian Douglas Gould** who generously agreed to take their time in reading my thesis and giving me important advices.

I appreciate the help from **Dr. Georg Hausner** who kindly and enthusiastically spent lots of time in teaching me some knowledge in bioinformatics and how to do bioinformatics searches on internet. I thank **Dr. Glen Klassen** and **Dr. Peter Loewen** who also gave me some helps in bioinformatics. **Dr. Klassen** is a very nice person and gave me many encouragements in my adapting to the life in Canada. **Dr. Loewen**, the head of the department, kindly took some of his busy time to help me solving the problems in computer. **Dr. Elizabeth Worobec** and **Dr. Linda Cameron** helped me a lot in my personal things and **Dr. Cameron** also helped me in teaching.

I am indebted to the staff and graduate students in Department of Microbiology. The secretary **Sharon Berg** spent extra time in helping my personal things. **Diana Gadway** nicely gave me help. **Andrew Schurko** nicely helped me in adapting to the life in Canada. **Rahul Singh, Taweewat Deemagarn, George Golding, Patrick Chong** and **Julius Csotonyi** kindly took their time showing me how to use machines. **Ayush Kumar, Matt Young, Prashen Chelikani, Tamiko Hisanaga, Ben Wiseman, Inderpal Saini, Christopher Rathgeber, Kari Kutcher, Sahra-Taylor O'Neil, Jyothi Sethuraman, Rahim Habibyan, Heather Grover, Maureen Spearman, Nicole Poritsanos** and others also helped me in English learning and other things.

My deepest gratitude is to my family. My wife **Hongjie** always supports me with unhesitating faith and by doing all the housework. My parents and my brothers and sisters always trust that I will do my best.

Table of Contents

Abstract	i
Acknowledgements	iv
Table of Contents	vi
List of Tables	xii
List of Figures	xvii
List of Abbreviations	xxv

Chapter I General Introduction and Literature Reviews1

(I) Electron transport pathways in biology	2
(i) The classical electron transport pathway	2
(ii) Flexibility of electron transport pathways	3
(iii) Terminal electron acceptors and terminal oxidases	5
(iv) Regulation of different electron transport pathways	9
(v) Respiratory control	15
(1) Uncouplers	15
(2) Ionophores	16
Valinomycin	17
Nigericin	17
(3) Lipophilic anions	18
(4) Weak acids	18
(vi) Inhibitors of the classical electron transport pathway	18
(1) Inhibitors of complex I	19
(2) Inhibitors of complex II	20
(3) Inhibitors of complex III	21
(4) Inhibitors of complex IV	21

(5) Inhibitors of ATP synthase	22
(II) Electron transport pathways in <i>Acidithiobacillus ferrooxidans</i>	23
(i) General features of <i>Acidithiobacillus ferrooxidans</i>	23
(ii) Electron transport pathways in <i>Acidithiobacillus ferrooxidans</i>	25
(III) Study objectives	32
Chapter II Materials and Methods	34
(I) Chemicals	35
(II) Bacterial growth and preparation of cell suspension	37
(III) Preparation of spheroplasts	38
(IV) Preparation of cell free extracts	39
(V) Determination of protein concentration	39
(VI) Measurement of O ₂ consumption and CO ₂ production	40
(VII) Measurement of Fe ³⁺ reduction	41
(VIII) Measurement of external pH change	43
(IX) Bioinformatics searches	43
Chapter III Results, Discussion and Conclusions	45
Part I Oxidation of Fe²⁺ and compounds interacting	
with Fe³⁺	46
Abstract	47
Introduction	48
Results	50
1.1. Fe ²⁺ oxidation	51
1.1.1. Effect of uncouplers, other Δp dissipators, and phosphate	51
1.1.2. Effect of inhibitors of ATP synthase	52

1.1.3. Effect of inhibitors of complex IV	53
1.1.4. Effect of inhibitors of complex I and complex III	53
1.2. Oxidation of ascorbic acid (Vc)	54
1.2.1. Effect of FeCl ₃	54
1.2.2. Effect of uncouplers	55
1.2.3. Effect of electron transport inhibitors	55
1.3. Oxidation of propyl gallate (PG) and SHAM	56
1.3.1. Effect of FeCl ₃	56
1.3.2. Effect of uncouplers on PG oxidation	57
1.3.3. Effect of electron transport inhibitors on PG oxidation	57
1.4. Oxidation of L-cysteine (Cys)	58
1.4.1. Effect of FeCl ₃	58
1.4.2. Effect of uncouplers	58
1.4.3. Effect of electron transport inhibitors	58
1.5. Oxidation of glutathione (GSH)	59
1.5.1. Effect of FeCl ₃	59
1.5.2. Effect of uncouplers	59
1.5.3. Effect of electron transport inhibitors	59
1.6. Oxidation of tiron	60
1.6.1. Effect of FeCl ₃	60
1.6.2. Effect of uncouplers	60
1.6.3. Effect of electron transport inhibitors	60
1.7. Chemical reduction of Fe ³⁺ by these organic compounds (Vc, PG, SHAM, tiron, Cys and GSH)	61
1.8. Oxidations by spheroplasts and cell free extracts	64
Discussion and conclusions	66

Part II Oxidation of endogenous substrates	115
Abstract	116
Introduction	117
Results	120
2.1. Oxidation of endogenous substrates by O ₂ (endogenous respiration)	121
2.1.1. Effect of uncouplers, ionophores, anions, weak acids, thiol agents, phosphate and arsenate	121
2.1.2. Effect of complex I inhibitors	122
2.1.3. Effect of complex IV inhibitors	123
2.1.4. Effect of inhibitors of complex III and quinol oxidases	126
2.1.5. Effect of complex II inhibitor (TTFA)	128
2.1.6. Effect of iron chelators	129
2.1.7. Change of external pH of cells	131
2.1.8. Respiratory quotient of endogenous respiration	132
2.1.9. Endogenous respiration by spheroplasts and cell free extracts	133
2.2. Oxidation of endogenous substrates by Fe ³⁺	134
2.2.1. Effect of complex I inhibitors	135
2.2.2. Effect of inhibitors of complex III and quinol oxidases	136
2.2.3. Effect of complex II inhibitor (TTFA)	137
2.2.4. Effect of uncouplers, ionophores, anions, weak acids, thiol agents and inhibitors of ATP synthase	137
Discussion and conclusions	140
 Part III Oxidation of Fructose	 201

Abstract	202
Introduction	203
Results	205
3.1. Fructose may be oxidized by <i>A. ferrooxidans</i>	206
3.2. Effect of uncouplers and iron chelators	208
3.3. Effect of complex I inhibitors	208
3.4. Effect of inhibitors of complex IV	209
3.5. Effect of inhibitors of complex III and quinol oxidase	209
3.6. Respiratory quotient of fructose respiration	210
3.7. Change of external pH of cells during fructose respiration	211
3.8. Fructose respiration by spheroplasts and cell free extracts	211
Discussion and conclusions	213

Part IV Oxidation of yeast extract (YE) and

casamino acids (CA)	229
----------------------------------	------------

Subtract	230
Introduction	231
Results	232
4.1. Oxidation of YE and CA by O ₂ and Fe ³⁺	233
4.2. Effect of electron transport inhibitors	234
4.3. Effect of uncouplers and FeCl ₃	234
4.4. Oxidation of YE and CA by spheroplasts and cell free extracts	235
Discussion and conclusions	236

Part V Oxidation of Formic Acid

Abstract	251
Introduction	252

Results	254
5.1. Oxidation of formic acid at different concentrations	255
5.2. Effect of uncouplers	256
5.3. Effect of complex I inhibitors	256
5.4. Effect of inhibitors of complex III and quinol oxidase	257
5.5. Effect of complex IV inhibitors	257
5.6. Effect of iron chelators	258
5.7. Oxidation of formic acid by spheroplasts and cell free extracts	259
Discussion and conclusions	260
Chapter IV General Summary	285
Chapter V Discoveries and Future Studies	299
References	306

List of Tables

Chapter I General Introduction and Literature Reviews

Table

1	Properties of different groups of terminal oxidases	6
2	Terminal oxidases in some bacteria and archaea	8
3	The relative activities of O ₂ consumption rates of cell suspensions of <i>P. denitrificans</i> wild type and different mutant strains during succinate oxidation	14
4	The structures and pK _a values of several uncouplers	16

Chapter II Materials and Methods

Table

5	Amount of cells, substrates and the reaction times used during the oxidation of different substrates by O ₂ in <i>A. ferrooxidans</i> in oxygraph (1.2 mL	41
6	The conditions of Fe ³⁺ reduction by different substrates in 1 mL reaction system	43

Chapter III Results, Discussion and Conclusions

Tables of Part I	73
------------------------	----

Table

1-1	Effect of uncouplers on Fe ²⁺ oxidation	74
1-2	Inhibition by uncouplers of Fe ²⁺ oxidation in the absence and presence of 4 mM KH ₂ PO ₄	74

1-3	Effect of CH ₃ COOK on Fe ²⁺ oxidation	75
1-4	KCN and NaN ₃ on Fe ²⁺ oxidation	75
1-5	Effects of complex I inhibitors on Fe ²⁺ oxidation in the presence and absence of DNP	76
1-6	Effects of complex III inhibitors and combinations of complex I and III inhibitors on Fe ²⁺ oxidation in the presence and absence of DNP	77
1-7	Stimulation by FeCl ₃ of Vc oxidation	78
1-8	Effect of uncouplers on Vc oxidation	78
1-9	Effect of inhibitors of complex IV on Vc oxidation	79
1-10	Effect of inhibitors of complex III on Vc oxidation	79
1-11	Effect of inhibitors of complex I on Vc oxidation	80
1-12	Effect of FeCl ₃ on PG oxidation	81
1-13	Effect of uncouplers on PG oxidation	81
1-14	Effect of KCN and NaN ₃ on PG oxidation	82
1-15	Effect of inhibitors of complex I and complex III on PG oxidation	82
1-16	Effect of uncoupler on Cys oxidation	83
1-17	Effect of complex IV inhibitors (KCN and NaN ₃) on Cys oxidation	83
1-18	Effects of inhibitors complex I and complex III on Cys oxidation in the absence and presence of DNP	84
1-19	Effect of uncouplers on GSH oxidation	85
1-20	Effect of complex IV inhibitors (KCN and NaN ₃) on GSH oxidation	85
1-21	Effect of inhibitors of complex I and complex III on GSH oxidation	86
1-22	Effect of inhibitors of complex I, complex III, and complex IV, uncouplers and FeCl ₃ on tiron oxidation	87
1-23	Reduction of Fe ³⁺ by various Fe ³⁺ -reactive compounds in the absence and presence of cells	88

1-24 Comparison of oxidation rates of Fe^{2+} , Vc, PG, GSH and Cys by intact cells and spheroplasts.	89
1-25 Effect of uncouplers on Fe^{2+} oxidation by spheroplasts in 0.1 M β -alanine- H_2SO_4 of pH 3.5.	89
1-26 Inhibition (%) of oxidation of FeSO_4 (Fe(II)), ascorbic acid (Vc), L-cysteine (Cys), Glutathione (GSH), propyl gallate (PG) and tiron by electron transport inhibitors of complexes I and III	90

Tables of Part II 150

Table

2-1 Effect of complex I inhibitors on endogenous respiration	151
2-2 Effect of complex III inhibitors (myxothiazol and antimycin A) on endogenous respiration	152
2-3 O_2 consumption and CO_2 production during endogenous respiration in the absence and presence of different compounds	153
2-4 Effect of rotenone, amytal, atabrine, CCCP and HQNO on endogenous respiration by spheroplasts	154
2-5 Effect of complex I inhibitors on Fe^{3+} reduction	155
2-6 Effect of HQNO on Fe^{3+} reduction	155
2-7 Effect of complex II inhibitor TTFA on Fe^{3+} reduction at pH 3.5	156
2-8 Effect of uncouplers on Fe^{3+} reduction in the absence and presence of complex I inhibitors	157
2-9 Effect of nigericin and valinomycin on Fe^{3+} reduction in the absence and presence of complex I inhibitors	158
2-10 Effect of KSCN on Fe^{3+} reduction in the absence and presence of complex I inhibitors	159
2-11 Effect of CH_3COOK and KF on Fe^{3+} reduction in the absence and presence of complex I inhibitors	160

2-12 Effect of Na₂-succinate and Na₂-malonate on Fe³⁺ reduction in the absence and presence of complex I inhibitors and TTFA at pH 3.5 161

2-13 Effect of thiol agents on Fe³⁺ reduction in the absence and presence of complex I inhibitors 162

Tables of Part III 218

Table

3-1 Effect of complex I inhibitors on fructose oxidation 219

3-2 Effect of inhibitors of complex III and quinol oxidase on fructose oxidation 219

Tables of Part IV 240

Table

4-1 Effect of electron transport inhibitors on oxidation of YE and CA 241

4-2 Effect of uncouplers on oxidation of YE and CA 242

4-3 Comparison of the rates of oxidation of YE and CA by spheroplast and whole cells 242

Table 4-4. Summary of the oxidation of 2 mM Cys, 1% YE and 3% CA by *A.*

ferrooxidans 243

Tables of Part V 268

Table

5-1 Effect of uncouplers on oxidation of formic acid by O₂ 269

5-2 Effect of complex I inhibitors on formic acid oxidation 270

5-3 Comparison of effects of complex I inhibitors on oxidation of different substrates by *A. ferrooxidans* at pH 3.5 271

5-4 Effect of inhibitors of complex III and quinol oxidases on formic acid oxidation 272

Tables of Chapter IV 294

Table

7 Comparison of the effects of uncouplers (CCCP and DNP) and complex IV inhibitors (KCN and NaN_3) on the oxidation of Fe^{2+} , Vc, PG, Cys, GSH and tiron 295

8 Effect of an uncoupler (CCCP or DNP) on the atabrine-reduced activities during the oxidation of Fe^{2+} and the organic compounds that interact with Fe^{3+} 295

9 Comparison of the effects of the inhibitors of complex I, complex III and complex IV, uncouplers and Fe^{3+} on the oxidation of different substrates 296

List of Figures

Chapter I General Introduction and Literature Reviews

Figure

1	The classical electron transport pathway in biology	3
2	The electron transport pathway in a mammalian mitochondrion	4
3	The electron transport pathway in a plant mitochondrion	4
4	The respiratory flexibility in <i>Paracoccus denitrificans</i>	5
5	Four models for the electron transport pathways of Fe ²⁺ oxidation in <i>A. ferrooxidans</i>	26
6	Proposed model for electron transport pathway of Fe ²⁺ oxidation in <i>A. ferrooxidans</i> based on the published data	31
7	Model for the electron transport pathways of thiosulfate oxidation in <i>A. ferrooxidans</i>	32

Chapter III Results, Discussion and Conclusions

Figures of Part I	91
--------------------------------	----

Figure

1-1	Effect of CCCP and DNP on Fe ²⁺ oxidation	92
1-2	Effect of CCCP and DNP on Fe ²⁺ oxidation in the presence and absence of 4 mM KH ₂ PO ₄ (Pi)	93
1-3	Effect of KH ₂ PO ₄ (Pi, 4 mM) on Fe ²⁺ oxidation by cells with and without the treatment of CCCP	94
1-4	Effect of KSCN on Fe(II) oxidation	96
1-5	Effect of nigericin and valinomycin on Fe ²⁺ oxidation	96

1-6	Effect of oligomycin and DCCD on Fe ²⁺ oxidation	97
1-7	Effect of KCN concentration on Fe ²⁺ oxidation	97
1-8	Effect of NaN ₃ concentration on Fe ²⁺ oxidation	98
1-9	Effect of KCN and NaN ₃ on Fe ²⁺ oxidation	98
1-10	Combinations of complex I inhibitors on Fe ²⁺ oxidation in the absence and presence of 0.1 mM DNP	99
1-11	Combinations of complex III inhibitors on Fe ²⁺ oxidation	100
1-12	Combinations of inhibitors of complex I and III on Fe ²⁺ oxidation in the absence and presence of DNP	100
1-13	The relative activities of Fe ²⁺ oxidation in the presence of inhibitors of complex I and complex III and different concentrations of DNP	101
1-14	Ascorbic acid (Vc) oxidation stimulated by FeCl ₃ and inhibited by atabrine and CCCP	102
1-15	Stimulation of PG (4 mM) oxidation by different concentrations of FeCl ₃ ...	102
1-16	Oxidation of SHAM	103
1-17	Effect of FeCl ₃ on Cys oxidation	104
1-18	The relative activities of Cys oxidation in the presence of inhibitors of complex I and complex III with and without 10 μM DNP	104
1-19	Effect of FeCl ₃ on GSH oxidation	105
1-20	Oxidation of tiron at different concentrations	106
1-21	FeCl ₃ , atabrine and CCCP on tiron (T) oxidation	106
1-22	HQNO on tiron oxidation in the absence and presence of FeCl ₃	107
1-23	Oxidation of Fe ²⁺ by spheroplasts at pH 3.5 of buffers of different components	108
1-24	Oxidation of Fe ²⁺ by cell free extracts (CFE) in 0.1 M β-alanine-H ₂ SO ₄ at pH 3.5	108
1-25	The bioinformatics search results of the putative ORF containing the	

subunit 6 of the two types of complex I in <i>A. ferrooxidans</i>	109
1-26 Proposed model for the electron transport pathways of the oxidations of Fe ²⁺ and some iron-interacting organic compounds by <i>A. ferrooxidans</i> based on experimental data	113
Figures of Part II	163
Figure	
2-0 The hypothetical model for the electron transport pathways of endogenous substrate oxidation in <i>A. ferrooxidans</i>	164
2-1 Effect of DNP and CCCP on endogenous respiration at pH 3.5 in 0.1 M β-alanine-H ₂ SO ₄ (a) and water (b)	165
2-2 Effect of valinomycin and nigericin on endogenous respiration	166
2-3 Effect of KSCN on endogenous respiration in the presence and absence of FeCl ₃ and / or rotenone	166
2-4 Effect of weak acids on endogenous respiration in the presence and absence of KCN	167
2-5 Effect of thiol agents NEM, HgCl ₂ and ANO ₃ on endogenous respiration	168
2-6 Effect of arsenate (Na ₂ HAsO ₄) and its combination with KCN or rotenone on endogenous respiration	169
2-7 Complex I inhibitors on endogenous respiration	169
2-8 Effect of KCN concentration on endogenous respiration	170
2-9 Effect of KCN on endogenous respiration in the presence of DNP	170
2-10 Effect of KCN and chloramphenicol (Ch, 0.31 mM) on endogenous respiration in the presence and absence of CCCP	171
2-11 Effect of KCN and NaN ₃ on endogenous respiration in the presence of FeCl ₃ ...	171
2-12 Effect of NaN ₃ on endogenous respiration	172
2-13 Effect of HQNO on endogenous respiration in 0.1 M β-alanine-H ₂ SO ₄ buffer (a) and water (b)	173

2-14	Effect of HQNO and CCCP on endogenous respiration in the absence and presence of KCN and rotenone at pH 3.5 (a, b)	174
2-15	Comparison of the effects of HQNO and CCCP on endogenous respiration in the presence of NaN ₃	175
2-16	Effect of TTFA on endogenous respiration in the absence and presence of other reagents	175
2-17	Effect of ferrozine, oxalic acid and NaP ₂ O ₇ on endogenous respiration	176
2-18	Effect of tiron on endogenous respiration in the absence and presence of o-phenanthroline (O-phen.), 2,2'-dipyridyl, DNP and rotenone	176
2-19	Effect of SHAM on endogenous respiration in the absence and presence of rotenone, amytal, KCN, o-phenanthroline (O-phen.) and 2,2'-dipyridyl	177
2-20	Effect of SHAM on endogenous respiration in the absence and presence of (a) HQNO and KCN and (b) CCCP and KCN	178
2-21	Effect of propyl gallate (PG) on endogenous respiration in the absence and presence of KCN or o-phenanthroline (O-phen.)	179
2-22	External pH change during endogenous respiration in cells of 100 mg / mL ...	180
2-23	External pH change during endogenous respiration in cells of 20 mg / mL in the presence of different compounds	180
2-24	O ₂ consumption and CO ₂ production in the absence and presence of different compounds	181
2-25	Effect of KCN and NaN ₃ on Fe ³⁺ reduction by endogenous substrates at pH 3.5	185
2-26	Effect of amytal on Fe ³⁺ reduction by endogenous substrates at (a) pH 2.3 and (b) pH 3.5	186
2-27	Effect of rotenone on Fe ³⁺ reduction by endogenous substrates at (a) pH 2.3 and (b) pH 3.5	187
2-28	Effect of piericid A (PA, 0.5 μM) and combination of PA, 0.1 mM rotenone (R) and 2 mM amytal (Am) on Fe ³⁺ reduction by endogenous substrates at pH 3.5	188
2-29	Effect of atabrine on Fe ³⁺ reduction by endogenous substrates	

at pH 2.3 and pH 3.5	188
2-30 Effect of antimycin A on Fe ³⁺ reduction by endogenous substrates at pH 3.5 ...	189
2-31 Effect of myxothiazol on Fe ³⁺ reduction by endogenous substrates at pH 2.3 and pH 3.5	189
2-32 Effect of HQNO on Fe ³⁺ reduction by endogenous substrates	190
2-33 Effect of TTFA on Fe ³⁺ reduction by endogenous substrates at pH 3.5	191
2-34 Effect of CCCP on Fe ³⁺ reduction by endogenous substrates at (a) pH 2.3 and (b) pH 3.5	192
2-35 Effect of DNP on Fe ³⁺ reduction by endogenous substrates at (a) pH 2.3 and (b) pH 3.5	193
2-36 Effect of nigericin on Fe ³⁺ reduction by endogenous substrates in the absence and presence of complex I inhibitors at pH 3.5	194
2-37 Effect of valinomycin on Fe ³⁺ reduction by endogenous substrates in the absence and presence of complex I inhibitors at pH 3.5	194
2-38 Effect of KSCN on Fe ³⁺ reduction by endogenous substrates at (a) pH 2.3 and (b) pH 3.5	195
2-39 Effect of CH ₃ COOK on Fe ³⁺ reduction by endogenous substrates in the absence and presence of complex I inhibitors at pH 3.5	196
2-40 Effect of KF on Fe ³⁺ reduction by endogenous substrates in the absence and presence of complex I inhibitors at pH 3.5	196
2-41 Effect of Na ₂ -succinate and Na ₂ -malonate on Fe ³⁺ reduction by endogenous substrates at pH 3.5	197
2-42 Effect of NEM on Fe ³⁺ reduction by endogenous substrates in the absence and presence of complex I inhibitors at pH 3.5	198
2-43 Effect of HgCl ₂ and AgNO ₃ on Fe ³⁺ reduction by endogenous substrates at pH 2.3 and pH 3.5	198
2-44 Effect of inhibitors of ATP synthase, DCCD (a) and oligomycin (b), on Fe ³⁺ reduction by endogenous substrates at pH 2.3 and pH 3.5	199
2-45 Proposed model for electron transport pathways of oxidation of endogenous substrates in <i>A. ferrooxidans</i>	200

Figures of Part III 220

Figure

- 3-1** Relative activities of respiration by 24 mg cells in Oxygraph (1.2 mL) in the presence of different alcohols (a) and sugars (b) 221
- 3-2** Rates of oxidation of fructose at different concentrations by 10 mg and 24 mg cells in Oxygraph (1.2 mL) 222
- 3-3** Oxidation of fructose (F) at 80 mM and 160 mM and effect of sucrose on fructose oxidation and endogenous respiration by 24 mg cells in Oxygraph (1.2 mL) 222
- 3-4** Rates of respiration by 24 mg cells in Oxygraph (1.2 mL) in the presence of 4 mM FeCl₃, fructose (F), fructose-6-phosphate (F-6-P), fructose-1,6-diphosphate (F-1,6-P), glucose (G), glucose-6-phosphate (G-6-P) and glucose-1-phosphate (G-1-P) 223
- 3-5** Effect of complex I inhibitors on fructose oxidation by O₂ (a) and Fe³⁺ (b) 224
- 3-6** Effect of KCN and NaN₃ on fructose oxidation 225
- 3-7** Effect of antimycin A, myxothiazol and HQNO on fructose oxidation by Fe³⁺ 225
- 3-8** Oxidation of fructose (F, 80 mM) with and without the combinations of CCCP (10 μM) and HQNO (H, 40 μM) after cells (24 mg / 1.2 mL) had been preincubated with 2 mM KCN for 25 min 226
- 3-9** O₂ consumption and CO₂ production during endogenous and fructose oxidation 227
- 3-10** Change of external pH of cells during endogenous and fructose oxidation tested in 2 ml system included 40 mg cells in water of pH 3.5 228

Figures of Part IV 244

Figure

- 4-1** Effect of complex I inhibitors on oxidation of YE (1 %, a)

and CA (3 %, b)	245
4-2 Effect of complex III inhibitors on oxidation of YE (1 %, a) and CA (3 %, b)	246
4-3 Effect of complex IV inhibitors on oxidation of YE (1 %, a) and CA (3 %, b)	247
4-4 Effect of FeCl ₃ on oxidation of YE (1 %, a) and CA (3 %, b)	248
4-5 Oxidation of YE and CA by spheroplasts	249
Figures of Part V	273
Figure	
5-1 Oxidation of formic acid at different concentrations by O ₂ and Fe ³⁺	274
5-2 Effect of uncouplers CCCP (a) and DNP (b) on formate oxidation by Fe ³⁺ ...	276
5-3 Effect of rotenone on formic acid oxidation by O ₂ (a) and Fe ³⁺ (b)	277
5-4 Effect of combination of CCCP and atabrine on formate oxidation by O ₂	278
5-5 Effect of HQNO on formate oxidation by O ₂ (a) and Fe ³⁺ (b)	279
5-6 Effect of KCN (a) and NaN ₃ (b) on formate oxidation by O ₂	280
5-7 Effect of KCN, SHAM and FeCl ₃ on the formate (0.5 mM) oxidation by 24 mg cells	281
5-8 Effects of FeCl ₃ , tiron and SHAM on formate oxidation	281
5-9 Formate oxidation in the absence and presence of FeCl ₃	282
5-10 Effects of PG on formate oxidation	283
5-11 Proposed model for electron transport pathways of formate oxidation in <i>A. ferrooxidans</i>	284

Figures of Chapter IV 297

Figure

8 The electron transport pathways in *A. ferrooxidans* 298

List of Abbreviations

ADP	adenosine diphosphate
Am	amytal; amobarbital; 5-ethyl-5-isoamylbarbituric acid
An	antimycin A
AOX	alternative oxidase
At	atabrine; quinacrine dihydrochloride
ATP	adenosine triphosphate
bc_1I	the cytochrome bc_1 involved in the uphill reaction
bc_1II	the cytochrome bc_1 involved in the downhill reaction
CA	casamino acids
CCCP	carbonyl cyanide <i>m</i> -chlorophenylhydrazone
CO ₂ / O ₂ ratio	CO ₂ production / O ₂ consumption
Cys	L-cysteine
Cyt.	cytochrome
DCCD	dicyclohexylcarbodiimide
DHase	dehydrogenase
DNP	2,4-dinitrophenol
EDTA	ethylenediaminetetraacetic acid disodium salt, dihydrate
FDH	formate dehydrogenase
ferrozine	3-(2-pyridyl)-5,6-bis(4-phenylsulfonic acid)-1,2,4-triazine), monosodium salt
Fig	figure

GSH	reduced glutathione
h	hour
H	HQNO: 2-heptyl -4-hydroxyquinoline-N-oxide
HQSA	8-hydroxyquinoline-5-sulfonic acid
KCN	potassium cyanide
K_m	the Michaelis-Menten constant as the substrate concentration at which the velocity is half of the maximum velocity
KSCN	Potassium thiocyanate
μM	micromolar (10^{-6} molar)
μmol	micromole (10^{-6} mole)
MES buffer	2-morpholinoethanesulfonic acid, monohydrate buffer
mM	millimolar (10^{-3} molar)
mL	millilitre (10^{-3} litre)
min	minute
My	myxothiazol
NDH-1	prokaryotic complex I; the proton-translocating NADH:quinone oxidoreductase in prokaryotes
NDH-2	a NADH-ubiquinol oxidoreductase involving no proton pumping
NDH-1 _{down}	the NDH-1 involved in the downhill reaction (NADH oxidation)
NDH-1 _{up}	the NDH-1 involved in the uphill reaction (NAD ⁺ reduction)
NEM	N-ethyl maleimide
nmol	nanomole (10^{-9} mole)
N side	mitochondrial matrix, or bacterial cytoplasm
<i>o</i> -phen.	<i>ortho</i> -phenanthroline (1,10-phenanthroline), monohydrate

ORF	open reading frame
Δp	proton motive force ($\Delta\Psi - 59\Delta\text{pH}$)
P side	intramembrane space in mitochondria, or periplasm in bacteria
PA	piericidin A
PG	propyl gallate
Pi	phosphate (KH_2PO_4)
Q	ubiquinone / ubiquinol pool
R	rotenone
SHAM	salicylhydroxamic acid
TPB ⁻	tetraphenylboron sodium
tiron	4,5-dihydroxy-1,3-benzene disulfonic acid, disodium salt
TTFA	thenoyltrifluoroacetone; 4,4,4-trifluoro-1[2-thienyl]-1,3-butanedione
V _c	ascorbic acid
V _{max}	the maximum velocity with the enzyme concentration and the conditions used
vol	volume
wt	weight
YE	yeast extract

Chapter I

General Introduction and Literature Reviews

(I) Electron transport pathways in biology

An electron transport pathway is also called “an electron transport chain”. It is composed of different electron carriers on a biological membrane. Electrons sequentially flow along these carriers to a terminal electron acceptor. In most cases, an electron transport pathway, or most parts of it, is reversible and carries out both the forward and reverse reactions. In the forward exergonic (downhill) direction, electrons flow spontaneously from an electron carrier with a low redox potential to one with a high redox potential. In fact energy is often conserved as proton motive force (Δp) or ATP. In the reverse endergonic (uphill) direction, electrons flow from high-redox-potential carriers to low-redox-potential carriers and energy is required for the reaction.

(i) The classical electron transport pathway

The classical electron transport pathway in biology starting from complex I (proton-pumping NADH dehydrogenase) or complex II (succinate dehydrogenase) and ending at complex IV (cytochrome *c* oxidase aa_3) is shown in Fig. 1. ATP is generated when proton flow from outside of the membrane into inside of the membrane via the ATP synthase (complex V) consuming Δp . Electrons are transferred along this pathway with a redox potential span of 1.14 V or 0.79 V since $E_{m,7}$ is -0.32 V for the $\text{NAD}^+ / \text{NADH}$ couple, +0.031 V for the fumarate / succinate couple and +0.82 V for the $\text{O}_2 / 2\text{H}_2\text{O}$ couple. Complex I, complex III (cytochrome bc_1 complex) and cytochrome aa_3 oxidase are proton-pumps generating Δp .

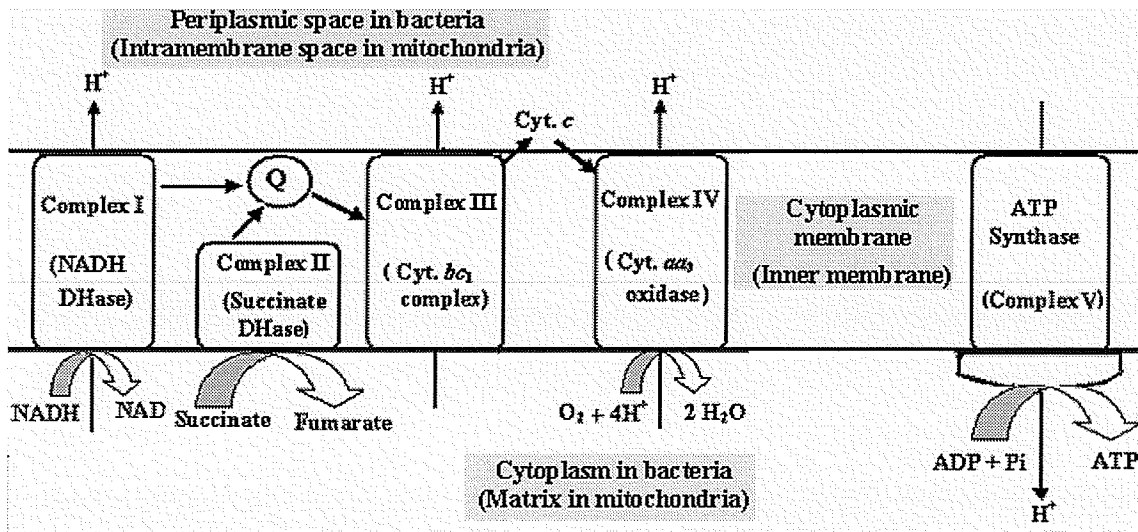


Fig. 1. The classical electron transport pathway in biology. DHase: dehydrogenase; Q: ubiquinone / ubiquinol pool; Cyt.: cytochrome.

(ii) Flexibility of electron transport pathways

The classical electron transport pathway is not used for oxidation of all substrates or by all organisms. Many organisms have more than one pathway for the oxidation of the same substrate, especially when oxygen is used as the terminal electron acceptor. The multiplicity of electron transport pathways is also called “respiratory flexibility”. The respiratory flexibility is: bacteria and archaea > mitochondria of plants, yeasts, filamentous fungi and ancient protozoa > mitochondria of animals (Richardson 2000).

In mammalian mitochondria, there is some respiratory flexibility at the level of electron input, but none at the level of electron output where the only terminal oxidase is cytochrome aa_3 oxidase as shown in Fig. 2.

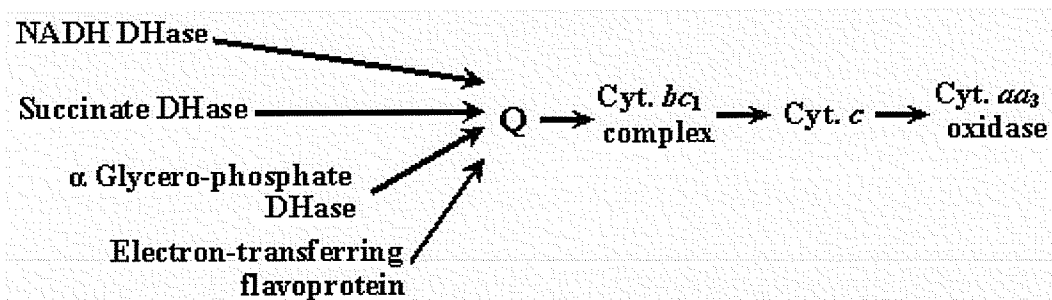


Fig. 2. The electron transport pathway in a mammalian mitochondrion. DHase: dehydrogenase; Q: ubiquinone / ubiquinol pool; Cyt.: cytochrome. (Richardson 2000).

In plant mitochondria, respiratory flexibility is reflected by a number of alternative dehydrogenases at the level of electron input and two types of terminal oxidases as shown in Fig. 3.

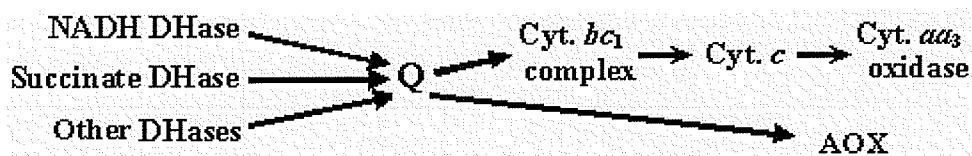


Fig. 3. The electron transport pathway in a plant mitochondrion. DHase: dehydrogenase; Q: ubiquinone / ubiquinol pool; Cyt.: cytochrome; AOX: alternative oxidase. (Millenaar and Lambers 2003).

The most complex pathways, allowing greatest respiratory flexibility are found in bacteria and archaea which could have many choices in electron donors, electron acceptors and electron carrier enzymes. Many bacteria have been reported to have multiple electron transport pathways but such examples in archaea are smaller in numbers (Nunoura et al. 2003; Schafer et al. 1996). Fig. 4 shows an example of the respiratory flexibility in the bacterium *Paracoccus denitrificans*.

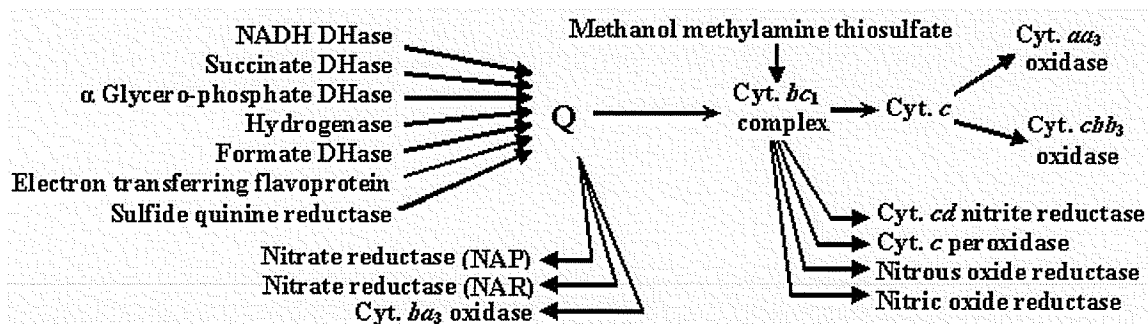


Fig. 4. The respiratory flexibility in *Paracoccus denitrificans*. DHase: dehydrogenase; Q: ubiquinone / ubiquinol pool; Cyt.: cytochrome. (Otten et al. 2001; Richardson 2000).

Respiratory flexibility gives an organism advantage in surviving under a wide range of environmental conditions. Flexibility at the level of electron input enables an organism to obtain energy by oxidizing different kinds of substrates. The ability of an organism to use O_2 and other compounds (Fe^{3+} , NO_3^- , etc.) as terminal electron acceptors makes it be able to live in aerobic and anaerobic environments.

(iii) Terminal electron acceptors and terminal oxidases

Plants and mammals use only O_2 as a terminal electron acceptor while microorganisms can also use other species (Fe^{3+} , Mn^{4+} , NO_3^- , SO_4^{2-} , etc.) under an anoxic condition (Jørgensen 1982; Lovley 2000; Richardson 2000).

A terminal oxidase is a membrane-bound enzyme transferring electrons to O_2 in the last step of an electron transport pathway. Terminal oxidases can be divided into three groups: cytochrome *c* oxidases, quinol oxidases and alternative oxidase. A cytochrome *c* oxidase accepts electrons transferred from quinol pool to complex III (cytochrome *bc*₁ complex), then to a cytochrome *c*. This class involves proton pumping and is sensitive to cyanide and azide inhibition. A quinol oxidase accepts electrons directly from quinol pool and contains cytochromes, but is insensitive to cyanide and azide inhibition. Some

quinol oxidases pump protons. Alternative oxidase accepts electrons also directly from quinol pool but contains no cytochromes. It does not pump protons and is insensitive to cyanide and azide inhibition. Some properties of these three oxidases are summarized in Table 1.

Table 1. Properties of different groups of terminal oxidases.

	Cytochrome <i>c</i> oxidase	Quinol oxidase	Alternative oxidase (AOX)
Mammals	+ (<i>aa₃</i>)	-	-
Plants, fungi, protozoa	+ (<i>aa₃</i>)	-	+
Prokaryotes	+ (<i>aa₃</i> and others)	+	- (^a)
Characteristic	Heme-copper enzymes	Some are heme- copper enzymes	di-iron proteins
Sensitivity to CN ⁻ and NaN ₃	Sensitive	Insensitive	Insensitive
Proton pumping	+	+ or -	-
Cytochromes	+	+	-
References	I	II	III

+: existent; -: not existent.

^aOne gram-negative bacterium *Novoshingobium aromaticivorans* was reported to have AOX (Stenmark and Nordlund 2003).

I: Ferguson-Miller and Babcock 1996; Garcia-Horsman et al.1994; Musser and Chan.1998.

II: Garcia-Horsman et al.1994; Puustinen et al.1989; Tsubaki et al. 2000; Watmough et al.1998.

III: Albury et al.2002; Millenaar and Lambers 2003.

The more wide spread terminal oxidase, cytochrome *c* oxidase *aa₃*, is present in mammals, plant, fungi, protozoa as well as in prokaryotes that include bacteria and archaea (Table 1). Action of cytochrome *c* oxidases contributes to ATP generation because they pump protons.

Alternative oxidase (AOX), which is mainly found in plant, fungi and protozoa, does not pump protons (Table 1) and so it is not involved in ATP generation. The energy available in the reduced-quinol pool, normally used by complex III and complex IV (cytochrome *c* oxidase) of the respiratory chain, is lost as heat when electrons flow to AOX (Millenaar and Lambers 2003; Stenmark and Nordlund 2003). AOX, instead of ATP production, gives its host advantages such as (a) preventing the production of excess reactive oxygen species (H_2O_2 , $\cdot\text{OH}$, OH^- , $\cdot\text{O}_2^-$) by stabilizing the redox state of the mitochondrial ubiquinone / ubiquinol pool making TCA cycle operate smoothly (Vanlerberghe et al. 2002; Millenaar and Lambers 2003); (b) helping pollination via volatilizing insect aromatic attractants by the heat produced (Vanlerberghe et al. 2002; Richardson 2000); (c) supporting growth of American skunk cabbage at subzero temperatures using the heat produced (Richardson 2000); (d) modulating the initiation of a programmed cell death pathway responsive to mitochondria respiratory status when the pathway to cytochrome *c* oxidase was inhibited (Vanlerberghe et al. 2002).

The extensively reported terminal oxidases in prokaryotes are cytochrome *c* oxidases and quinol oxidases. Many bacteria and some archaea have more than one terminal oxidase. Quinol oxidases in some organisms can pump protons (Garcia-Horsman et al. 1994) and so are involved in ATP generation but quinol oxidases cannot in others (Azarkina et al. 1999). Table 2 shows the multiplicity of terminal oxidases in bacteria and archaea.

Table 2. Terminal oxidases in some examples of bacteria and archaea.

Organism	Cytochrome <i>c</i> oxidase	Quinol oxidase	References
<i>Acidithiobacillus ferrooxidans</i>	<i>aa</i> ₃ , <i>ba</i> ₃	<i>bd</i> , <i>bo</i> ₃	Brasseur et al. 2004; Kamimura et al. 2001
<i>Acidithiobacillus thiooxidans</i>	<i>aa</i> ₃	<i>bd</i>	Masau et al. 2001
<i>Escherichia coli</i>		<i>bd</i> , <i>bo</i> ₃	Alexeeva et al. 2003; Garcia-horsman et al. 1994
<i>Bacillus subtilis</i>	<i>caa</i> ₃	<i>aa</i> ₃ , <i>bd</i> , <i>bb'</i>	Azarkina et al. 1999; Winstedt and von Wachenfeldt. 2000
<i>Paracoccus denitrificans</i>	<i>cbb</i> ₃ , <i>aa</i> ₃	<i>ba</i> ₃	Otten et al. 2001; Richardson 2000
<i>Rhodobacter sphaeroides</i>	<i>cbb</i> ₃ , <i>aa</i> ₃		Daldal et al. 2001
<i>Azotobacter vinelandii</i>	<i>bo</i> ₃ , <i>cbb</i> ₃	<i>bd</i>	Bertsova, et al. 2001; Poole and Hill 1997
<i>Pyrobaculum oguniense</i> *	SoxB, SoxM		Nunoura et al. 2003
<i>Aeropyrum pernix</i> *	<i>aa</i> ₃ , <i>ba</i> ₃		Ishikawa et al. 2002
<i>Acidianus ambivalens</i> *		<i>aa</i> ₃	Purschke et al. 1997

* Archaea

Although several terminal oxidases can exist in one organism, they operate at different oxygen concentrations since they have different affinities for O₂ and H⁺ / e⁻ ratios. For example in *E. coli* quinol oxidases *bd* operates at low O₂ concentrations and has a high affinity for O₂ ($K_m = 0.024 \mu\text{M O}_2$, $V_{\max} = 42 \mu\text{M O}_2 \text{ (nmol cytochrome o)}^{-1} \text{ h}^{-1}$), whereas the heme-copper *bo*₃ type oxidase operates at high O₂ concentrations and has a low affinity for O₂ ($K_m = 0.2 \mu\text{M O}_2$, $V_{\max} = 66 \mu\text{M O}_2 \text{ (nmol cytochrome o)}^{-1} \text{ h}^{-1}$) (Alexeeva et al. 2003). Furthermore, the *bd* oxidase pumps about one proton per electron transferred (H⁺ / e⁻ ratio ≈ 1.0) (Miller and Gennis 1985), while the *bo*₃ oxidase is more efficient with a H⁺ / e⁻ ratio ≈ 2.0 (Puustinen et al. 1989). The H⁺ / e⁻ ratio of

cytochrome *c* oxidase *aa₃* (~1.0), is similar to that of *bd* quinol oxidase (Musser and Chan. 1998; Namslauer et al. 2003), but is only half of that of *E. coli bo₃* oxidase. The existence of terminal oxidases with different affinities for O₂ makes it possible for an organism to shift from one to another as O₂ concentration changes (Alexeeva et al. 2003), and to prevent the overproduction of reactive oxygen species. In *Azotobacter vinelandii*, which has *bo₃*, *cbb₃* and *bd* oxidases (Table 2), the high-oxygen-affinity *bd* oxidase could protect the oxygen-labile nitrogenase by keeping the oxygen concentration at a low level (Poole and Hill 1997).

(iv) Regulation of different electron transport pathways

When a substrate can be oxidized through different electron transport pathways, interesting questions are raised including (a) how electrons would be partitioned among different pathways? and (b) what consequences would be if one (or more) pathway has been inhibited by electron transport inhibitors or blocked by genetic mutation of genes coding for enzyme(s) on the electron transport pathways or by other stresses ?

The regulation of electron transport pathways in plants has been extensively studied, especially on the pathway from Q to AOX (AOX pathway) and from Q to cyt. *aa₃* oxidase (*aa₃* pathway) (Fig. 3) (Millenaar and Lambers 2003). It was once thought that, under normal conditions, electrons only flowed to the *aa₃* pathway and electrons overflowed to AOX pathway only after *aa₃* pathway was saturated and the Q pool was highly reduced (Day 1992; Douce and Neuberger 1989). Later it was proven that, in some plant species, electrons can also flow to AOX pathway even when the *aa₃* pathway was not fully engaged (Atkin et al. 1995). The activity of AOX can be regulated by the

following factors (Hoefnagel et al. 1995; Millar et al. 1996; Millenaar and Lambers 2003).

- (a) When the intramolecular disulfide bonds of AOX dimer are reduced, AOX becomes active, while the oxidative formation of AOX dimer bonds would inactivate this enzyme.
- (b) Some α -keto organic acids such as pyruvate, glyoxylate and hydroxypyruvate, measured with an oxidative substrate, for example succinate or NADH, stimulate AOX pathway activity by reducing the disulfide bonds of AOX and also lowering the K_m of AOX to Qr (reduced ubiquinone).
- (c) Higher ratios of reduced ubiquinone over total ubiquinone result in higher activity of AOX.

Atkin et al. (1995) studied the diversion of electrons from AOX pathway to aa_3 pathway in the intact roots of 8 plant species. They found that SHAM, a inhibitor of AOX, did not inhibit the respiration in 6 species and showed only 10 – 20% inhibition on the other 2 species when the inhibitor of aa_3 oxidase KCN was not present. The authors explained that the lack of SHAM inhibition was due to the diversion of electrons from the AOX pathway to the unsaturated aa_3 pathway since KCN in the presence of SHAM inhibited respiration more than KCN alone. The fact that SHAM alone showed inhibition of respiration in 2 plant species may be due to the near saturation of aa_3 pathway.

Hoefnagel et al. (1995) investigated the switching of electrons between the AOX and aa_3 pathways in the isolated soybean cotyledon mitochondria. Succinate was used as a

substrate during oxidation of which, the *aa*₃ pathway has two sites of proton pumping involved in ATP generation, while the AOX pathway is completely uncoupled (Figs. 1 & 3). When succinate was oxidized, electrons went to both *aa*₃ and AOX pathways since propyl gallate (PG, an inhibitor of AOX) at 50 μM, inhibited the O₂ consumption rate by 46% in the absence of ADP and by 16% in the presence of 1 mM ADP. The switching of electrons from AOX pathway to *aa*₃ pathway was supported by the stimulation of the ATP generation rate upon the addition of PG. In the presence of 5 mM pyruvate, the respiration was stimulated by 21% and 9% in the absence and presence of ADP, respectively, while ATP generation rate was inhibited by 19%. Therefore, pyruvate activated the AOX pathway and made more electrons be switched from *aa*₃ pathway to AOX pathway. ATP generation rate in the presence of pyruvate was stimulated by 7% by the addition of PG again indicating electron switching from AOX pathway back to *aa*₃ pathway. Electron switching was also demonstrated by testing ferricyanide (Fe(CN)₆³⁻) reduction and O₂ consumption simultaneously. FeCN accepts electrons from Cyt. *bc*₁ complex preventing O₂ consumption by *aa*₃ oxidase and thus making O₂ reduction be carried out by AOX alone. In the absence of pyruvate, myxothiazol (4 μM), an inhibitor of Cyt. *bc*₁ complex, stimulated O₂ consumption rate by 355% but inhibited FeCN reduction by 95% indicating electron switching to AOX pathway. PG inhibited the myxothiazol-stimulated rate by 64% confirmed that the O₂ was consumed by AOX. In the presence of 5 mM pyruvate, myxothiazol stimulated the O₂ consumption rate only by 175% and PG inhibited the increased activity by 85% indicating larger portion of electrons flowed to AOX before the addition of myxothiazol

and smaller part of electrons switched to AOX upon the addition of myxothiazol when compared to the situation in the absence of pyruvate.

Cysteine can trigger a signal pathway leading to the loss of the mitochondrial *aa₃* pathway activity and greatly increase AOX protein and activity in tobacco cells (Vanlerberghe et al. 2002). Transgenic cells (AS8) which were not able to induce AOX lost all respiratory activity upon the treatment with cysteine. Therefore, cysteine treatment down-regulated *aa₃* pathway but up-regulated AOX pathway to modulate the initiation of a programmed cell death pathway which is responsive to mitochondria respiration.

Temperature also regulates electron partition between the *aa₃* and AOX pathways in plants. Cold-grown mung bean, but not soybean, up regulated the level of AOX protein and enhanced electron partitioning to AOX pathway when measured at cold temperatures (González-Meler et al. 1999). A chilling treatment led to a 40% inhibition of the respiration rate via the *aa₃* pathway but stimulated the respiration rate via the AOX pathway by 167% in a chilling-sensitive maize cultivar (Ribas-Carbo et al. 2000). Cold temperatures place a stress on plants forcing the activation of AOX pathway which may play a role in preventing the formation of toxic reactive oxygen species when the activity of *aa₃* pathway is restricted.

The regulation of electron transport pathways have also been investigated in some bacteria. *E. coli* has two quinol oxidases (Table 2). Under low O₂ concentrations (aerobiosis < 40%, the minimum O₂ input rate required for complete oxidation of glucose to CO₂ is defined as 100% aerobiosis), electrons flow to the high-affinity (for O₂) *bd* oxidase responsible for O₂ consumption, while when aerobiosis > 40%, electrons

are shifted from *bd* oxidase to the low-affinity *bo*₃ oxidase (Alexeeva et al. 2003). Distribution of electron flux between these two pathways (to *bd* oxidase and *bo*₃ oxidase) in *E. coli* is controlled by a two-component regulatory ArcAB system (Alexeeva et al. 2003). The effect of ArcA regulator on the electron distribution between the two oxidases was investigated by studying the wild type and a mutant ($\Delta arcA$) strains. In the wild type, *bd* oxidase was solely responsible for O₂ consumption in aerobiosis < 40%. The respiration rate by *bd* oxidase increased with the increase in aerobiosis percentage and reached a maximum at 50% aerobiosis and then quickly decreased, while the activity of *bo*₃ oxidase appeared at 40% aerobiosis and increased to a maximum at about 99% aerobiosis. In $\Delta arcA$, the activities of both oxidases were already present from 0% aerobiosis. The activity of *bo*₃ oxidase increased much faster than that of *bd* oxidase with the increase in aerobiosis percentage and reached a maximum at about 99% aerobiosis, while the activity of *bd* oxidase quickly reached a maximum at around 30% aerobiosis. Furthermore, the maximum activity of *bo*₃ oxidase was about 4.3 times of that of *bd* oxidase. The total maximum O₂ consumption rate in $\Delta arcA$ was about 40% higher than that of the wild type. Therefore, ArcA regulator may control electron flow to *bd* oxidase in low O₂ concentrations and switch electrons to *bo*₃ oxidase in high O₂ concentrations. When ArcA regulator is destroyed, the produced stress will force the main flow of electrons to *bo*₃ oxidase in any O₂ concentrations.

Paracoccus denitrificans has three terminal oxidases: cytochrome *c* oxidases *aa*₃ and *cbb*₃, and quinol oxidase *ba*₃ (Table 2 and Fig. 4). Otten et al. (2001) investigated the O₂ consumption rates during succinate oxidation by different mutants of *P. denitrificans*. Their results shows that O₂ consumption rate of the wild type strain can be compensated

or slightly stimulated after the pathways to one or more terminal oxidases were blocked via genetic mutation (Table 3).

Table 3. The relative activities of O₂ consumption rates of cell suspensions of *P. denitrificans* wild type and different mutant strains during succinate oxidation. (Otten et al. 2001).

Strain *	Relative activity
Wild type	1.00
<i>bc₁</i> ⁻	1.05
<i>ba₃</i> ⁻	0.95
<i>cbb₃</i> ⁻	1.13
<i>aa₃</i> ⁻	1.11
<i>aa₃</i> srm	0.92
<i>cbb₃</i> srm	0.97
<i>ba₃</i> srm	0.88

*⁻: negative mutants (electrons cannot be transferred to these enzymes);
srm: single-route mutants (electrons can only be transferred to these enzymes).

The three terminal oxidases in *P. denitrificans* function at different O₂ concentrations: *aa₃* under aerobic conditions, *cbb₃* under semiaerobic conditions and *ba₃* under denitrifying conditions. The dysfunction of one or two terminal oxidases must have lead to the highly reduced state of the ubiquinone pool (high ratio of reduced ubiquinone over oxidized ubiquinone). This will force the electron flow to other oxidase(s) to be faster compared to the situation in the wild type preventing the production of reactive oxygen species.

(v) Respiratory control

Respiratory control means that the rate of respiration is controlled by the thermodynamic disequilibrium between the redox potential (ΔE) spanning across the proton-translocating regions of the respiratory chain and the proton motive force Δp ($\Delta \Psi - 59\Delta pH$). The greater the difference between ΔE and Δp is, the faster the rate of respiration will be. Any process that decreases Δp will accelerate the respiration. (Nicholls and Ferguson 2002).

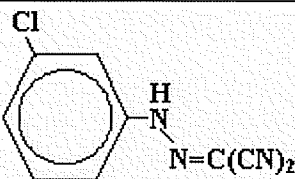
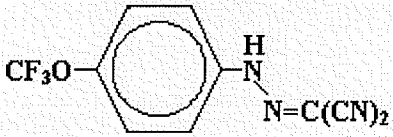
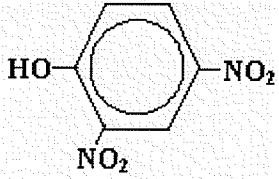
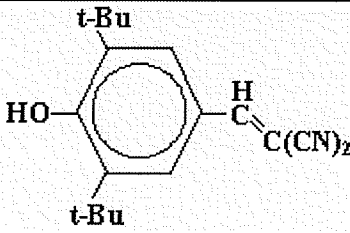
In mitochondria, respiratory control can be directly demonstrated by the addition of ADP and phosphate (P_i). The respiratory rate in the absence of ATP synthesis is significantly lower than the maximum. The addition of ADP and P_i will accelerate ATP generation consuming Δp . After ADP and P_i have been converted to ATP, Δp will increase due to proton pumping, which will slow down the respiration rate. The ratio of rates of respiration in the presence and absence of ADP and P_i (stimulated rate/control rate) is defined as “respiratory control index (RCI)” (Tsuchiya and Rosen 1980). Respiratory control has not been directly demonstrated by adding ADP + P_i in the intact cells of bacteria. But it can be indirectly demonstrated by using uncouplers and other Δp dissipaters, the addition of which could accelerate respiration. Examples of some Δp dissipaters are introduced in the following.

(1) Uncouplers (Nicholls and Ferguson 1992; 2002)

Uncouplers (protonophores) are lipophilic weak acids with a pK_a value not far below 7. The outside pH of the inner membrane is usually lower than the inside pH of inner membrane. An uncoupler existing as an undissociated form with H^+ in the outside can

move across the inner membrane (cell membrane) to the side of cytoplasm or matrix where it dissociates and releases H^+ , and then move back to the outside to bring H^+ again. The increase of proton concentration in the inside would destroy Δp by decreasing ΔpH and also $\Delta \Psi$ (H^+ brings a positive charge) ($\Delta pH = pH_{in} - pH_{out}$; $\Delta \Psi = \Psi_{in} - \Psi_{out}$). The structures and pK_a values of some uncouplers are listed in Table 4.

Table 4. The structures and pK_a values of several uncouplers. (Terada 1981)

Uncoupler (MW)	Structure	pK_a
CCCP (204.62) (carbonyl cyanide <i>m</i> -chlorophenylhydrazone)		5.95
FCCP (254.17) (carbonyl cyanide <i>p</i> -trifluoromethoxyphenylhydrazone)		6.2
DNP (184.11) (2,4-dinitrophenol)		4.1
SF6847 (282.39) (3,5-di(<i>tert</i> -butyl)-4-hydroxybenzylidenemalononitrile)		6.83

(2) Ionophores (Nicholls and Ferguson 1992; 2002)

Ionophores are compounds with a molecular weight of 500 – 2000 and have a hydrophobic exterior making them lipid soluble. They can function as mobile carriers of

charge or protons (uncouplers are also ionophores carrying both protons and charge), or as channel formers (e.g. gramicidin) through which monovalent cations such as K^+ and NH_4^+ can diffuse.

Valinomycin

Valinomycin is a mobile carrier ionophore. It carries charge but not protons catalyzing the electrical uniport of Cs^+ , Rb^+ , K^+ or NH_4^+ . An ion (e.g. K^+) loses its water of hydration when it binds to valinomycin to form a complex. Then the complexed valinomycin will carry the ion from one side of the membrane and release it to the other side and the uncomplexed valinomycin will move across the membrane back to carry more ions. When a cation (K^+) is brought from the outside of the inner membrane to the inside, $\Delta\Psi$ (Ψ negative inside in mitochondria and neutrophiles) will be destroyed. On the other hand, if the cation is brought from the inside to the outside, $\Delta\Psi$ will be again restored and the decrease of positive charge in the inside will lead to the fast leaking in of protons from the outside reducing ΔpH . In both cases, Δp may be destroyed.

Nigericin

Free nigericin is a molecule which possesses heterocyclic oxygen-containing rings with hydroxyl groups. When bound to the membrane nigericin cyclizes to form a structure similar to that of valinomycin. Nigericin always is in an uncharged form when it moves across the membrane. In one side of the membrane it loses a proton by binding a cation (e.g. K^+) and in the other side of the membrane it loses the cation by binding a

proton. When a cation in the inside of the membrane is exchanged for protons in the outside of the membrane by nigericin, Δp will be destroyed by the decrease of ΔpH .

(3) Lipophilic anions (Nicholls and Ferguson 1992; 2002)

Some anions move across lipophilic membranes even though they carry charge. Examples include TPB^- (tetraphenylborate) and SCN^- (thiocyanate ion). When these anions diffuse into the inside of the membrane $\Delta \Psi$ will be destroyed (Ψ positive inside in acidophiles) and more protons will leak in destroying ΔpH and therefore Δp .

(4) Weak acids (Nicholls and Ferguson 1992; 2002)

Some weak acids can also diffuse into the inside of cells or mitochondria by carrying protons from the outside if their pK_a values are higher than the outside pH but lower than the inside pH. The consequence is to decrease ΔpH and therefore may destroy Δp .

The pK_a values of some weak acids are: CH_3COOH , 4.75; HF, 3.45; succinic acid, 4.21, 5.64; malonic acid, 2.85; HN_3 , 4.72.

(vi) Inhibitors of the classical electron transport pathway

The complexes on the classical electron transport pathway (Fig. 1) include complex I, complex II, complex III, complex IV and the related ATP synthase (complex V). To study electron transport pathways, it is essential to test the effects of inhibitors of different components on the pathways. The commonly used inhibitors of the complexes on the classical electron transport pathway are summarized in the following.

(1) Inhibitors of complex I

Complex I, a proton-pumping NADH: ubiquinone oxidoreductase (NADH dehydrogenase) catalyzes the transfer of 2 electrons from NADH to quinone which couples to the pumping of 4 protons out of the cytoplasmic membrane (Fig. 1) (Holt et al. 2003). The mitochondrial complex I consists of 43 – 46 subunits with a combined molecular mass of about 1, 000 KDa, while the prokaryotic complex I (also called NDH-1) has only 14 subunits, all of which have analogues in the mitochondrial complex I, with a combined molecular mass of about 550 KDa (Holt et al. 2003; Okun et al. 1999). Complex I in both mitochondria and prokaryotes has a L-shaped structure with two domains which are called peripheral and membrane arms perpendicular to each other (Holt et al. 2003; Okun et al. 1999). The peripheral arm carries the NADH binding site, the noncovalently bound FMN and the iron-sulfur centers. The membrane arm probably contains the proton translocation site. However, the mechanisms of electron transport and proton translocation, the binding sites and the functional mechanism of the large number of inhibitors of complex I are still unclear (Okun et al. 1999).

Many structurally diverse hydrophobic compounds have been reported to inhibit complex I by binding at or close to the ubiquinone binding site(s) (Degli Esposti 1998; Friedrich et al. 1994; Miyoshi 1998; Okun et al. 1999). Degli Esposti (1998) has reviewed the characteristics and the possible mechanism of action of different inhibitors of complex I. Based on kinetic studies, these inhibitors were grouped into two classes (Friedrich et al.1994) or three types (Degli Esposti 1998; Okun et al. 1999), represented by piericidin A (class I / A-type), rotenone (class II / B-type), and capsaicin (C-type), respectively. According to the classification by Friedrich et al. (1994), class I inhibitors,

represented by piericidin A, inhibit complex I in a competitive manner with regard to ubiquinone and also inhibit glucose dehydrogenase, while class II inhibitors represented by rotenone, inhibit complex I in a non-competitive manner but do not inhibit glucose dehydrogenase. In the classification proposed by Degli Esposti (1998), three types of inhibitors can bind at three different sites on complex I. The first site is bound by Type A inhibitors represented by piericidin A, the second site by Type B inhibitors including rotenone, amytal and also piericidin A and others, and the third site by Type C inhibitors represented by capsaicin. Okun et al. (1999) demonstrated that these three types of inhibitors all bind to a large pocket in the hydrophobic part of complex I and the binding sites of these three types of inhibitors partially overlap. The rotenone binding site overlapped with both piericidin A and capsaicin binding sites but the latter two sites did not overlap. The flavin antagonist atabrine is also believed to inhibit complex I by binding to the FMN site (Arnold et al. 1986; Blaylock and Nason 1963; Elbehti et al. 2000).

(2) Inhibitors of complex II

Complex II, a succinate: ubiquinone oxidoreductase (succinate dehydrogenase), catalyzes the oxidation of succinate to fumarate and does not pump protons. A well-known inhibitor of complex II is TTFA (thenoyltrifluoroacetone, or 4,4,4-trifluoro-1[2-thienyl]-1,3-butanedione) which inhibits the succinate dehydrogenase by chelating non-heme iron (Ulvik and Romslo 1975). Another commonly used complex II inhibitor is malonate which is an analogue of the substrate succinate (competitive inhibitor) (Thorn 1953a, 1953b).

(3) Inhibitors of complex III

The formal name of complex III is ubiquinol: cytochrome *c* oxidoreductase, and is also called cytochrome *bc*₁ complex. It has a protonmotive Q cycle with two centers: P center in the P side (intramembrane space in mitochondria, periplasm in bacteria) and N center in the N side (mitochondrial matrix, bacterial cytoplasm) (Trumpower 1990). Two electrons from ubiquinol diverge at the P center with one electron recycling in the Q cycle and reducing ubiquinone to ubiquinol at the N center and the other electron being transferred to cytochrome *c* in the P side. Two protons are translocated from the N side to the P side and additional two are released into P side from ubiquinol upon the transport of two electrons. Inhibitors myxothiazol, stigmatellin, MOA-stilbene ((E, E)-methyl 3-methoxy-2-(styrylphenyl) propenoate) and UHDBT (5-undecyl-6-hydroxy-4,7-dioxobenzothiazol) inhibit complex III by binding at the P center, while inhibitors HQNO and antimycin A inhibit it by binding at the N center (Chen et al. 2003; Degli Esposti et al. 1994; Kim et al. 1998; Trumpower 1990). HQNO was previously treated as a specific inhibitor of complex III but now it has been found to be an inhibitor of all enzymes containing quinone-reacting *b* type cytochromes such as cytochrome *bd* type quinol oxidase, thiosulfate-quinone reductase and formate dehydrogenase-N (Brasseur et al. 2004; Jormakka et al. 2003; Kamikura et al. 2001).

(4) Inhibitors of complex IV

Complex IV is called cytochrome *c* oxidase, ferrocyclochrome *c*: O₂ oxidoreductase. It contains 3 copper atoms two of which form the binuclear copper centre (Cu_A). Electrons from cytochrome *c* at the P side are sequentially transferred to the Cu_A centre, haem *a*,

to haem a_3 . O_2 is reduced to H_2O by the cooperation of haem a_3 and Cu_B (the third copper atom) using the electron from haem a_3 . For every $4e^-$ transferred, $8H^+$ are consumed at the N side: $4H^+$ are used to produce $2H_2O$ with $1O_2$ while the other $4H^+$ are pumped out into the P side. Inhibitors of complex IV including cyanide (CN^-), azide (N_3^-), nitric oxide (NO) and carbon monoxide (CO), bind haem a_3 , the O_2 binding site. (Nicholls and Ferguson 2002).

Nitric oxide is a reversible inhibitor of complex IV because it can be slowly reduced to the non-inhibitory nitrous oxide (N_2O) (Nicholls and Ferguson 2002).

Azide is also a Δp dissipater (pK_a of HN_3 , 4.72) and an inhibitor of mitochondrial F_1F_0 -ATPase (Harold 1972; Hesse et al. 2002).

(5) Inhibitors of ATP synthase

Complex V is an ATP synthase. It is usually referred to as the proton-translocating ATP synthase, which is known as an F_1F_0 -ATPase different from E_1E_2 -ATPase in eukaryotic plasma membrane and the V ATPase (for vacuolar). The F_0 sector of ATP synthase, located in the inner membrane, translocates protons from the P side to the N side, and the F_1 sector in mitochondrial matrix or bacterial cytoplasm catalyzes ATP production from ADP and Pi. (Nicholls and Ferguson 2002).

Inhibitors of ATP synthase include venturicidin, oligomycin, DCCD (dicyclohexylcarbodiimide), Nbf-Cl (7-chloro-4-nitrobenzofurazan), efrapeptin and aurovertin. Venturicidin and oligomycin interact with F_0 sector but their exact binding sites are not known. DCCD binds both F_0 and F_1 . It specifically reacts with an aspartate or glutamate residue on a c subunit of F_0 . DCCD and Nbf-Cl bind one of the three β -

subunits of F_1 . Aurovertin and efrapetin also bind F_1 . Aurovertin binds two of the three β -subunits and efrapetin binds in the central cavity between the three β -subunits and the three α -subunits. (Nicholls and Ferguson 2002).

DCCD is not a specific inhibitor of ATP synthase. It can also inhibit other enzymes in some organisms such as complex I (Degli Esposti 1998) and complex IV (Prochaska et al. 1981).

Oligomycin did not inhibit ATP generation in the intact cells but inhibited it in the membrane vesicles of *Acidithiobacillus caldus* (Dopson et al. 2002). However, DCCD inhibited ATP generation in the intact cells of *Acetobacterium woodii* (Imkamp and Müller 2002) and in the membrane vesicles of *A. caldus* (Dopson et al. 2002) and *Acidithiobacillus ferrooxidans* (Apel et al. 1980).

(II) Electron transport pathways in *Acidithiobacillus ferrooxidans*

(i) General features of *Acidithiobacillus ferrooxidans*

Acidithiobacillus (Thiobacillus) ferrooxidans is a gram-negative, motile, non-sporulating rod. It is a chemolithoautotrophic bacterium, which obtains carbon by fixing CO_2 using the reducing power (NADH) produced via an uphill electron transport pathway, and the energy obtained by oxidizing inorganic compounds such as ferrous iron, reduced sulfur compounds, H_2 and formic acid (Drobner et al. 1990; Fischer et al. 1996; Harahuc et al. 2000; Harahuc and Suzuki 2001; Jensen and Webb 1995; Pronk et al. 1991a, 1991b).

A. ferrooxidans, a typical aerobic bacterium, can also grow anaerobically by using ferric iron as a terminal electron acceptor (Jensen and Webb 1995; Ohmura et al. 2002;

Pronk et al. 1991a). It is an acidophile, which can grow in the pH range of 1.0 – 4.5 with an optimum pH of 2.0 – 2.3. It cannot survive at a pH above pH 6.5 or below pH 1.0 (Jensen and Webb 1995; Leduc and Ferroni 1994; Smith et al. 1988).

The range of growth temperatures of *A. ferrooxidans* is between 15°C and 40 °C, designating it as a mesophilic bacterium (Leduc and Ferroni 1994; McDonald and Clark 1970).

Since the first strain of *A. ferrooxidans* was isolated in 1947 (Colmer and Hinkle 1947), its name has been changed from *Ferrobacillus ferrooxidans* to *Thiobacillus ferrooxidans* (Leathen et al. 1956; Silver and Lundgren 1968; Temple and Colmer 1951), and finally to *Acidithiobacillus ferrooxidans* based on physiological characters and 16S rRNA gene sequence comparisons (Kelly and Wood 2000). After the reclassification, *A. ferrooxidans* belongs to the new genus *Acidithiobacillus* which only contains 3 species in the γ -subclass of the *Proteobacteria* including *A. ferrooxidans*, *Acidithiobacillus thiooxidans* (previous *Thiobacillus thiooxidans*) and *Acidithiobacillus caldus* (previously *Thiobacillus caldus*) (Kelly and Wood 2000).

A. ferrooxidans is a unique bacterium in that it has been extensively studied in the oxidation of both Fe^{2+} and reduced inorganic sulfur compounds. Sulfur oxidation has also been extensively studied in other organisms such as *Acidithiobacillus thiooxidans* and *Paracoccus pantotrophus* (Friedrich et al. 2001; Suzuki 2001), but Fe^{2+} oxidation has been studied extensively and its electron transport pathways have been proposed only in *A. ferrooxidans* although Fe^{2+} can also be oxidized by other organisms such as *Leptospirillum ferrooxidans* and *Acidimicrobium ferrooxidans* (Rawlings 2002; Rohwerder et al. 2003; Suzuki 2001).

A. ferrooxidans has been extensively studied since it is the most important organism used in microbial leaching by extracting metals such as copper, uranium and gold from their ores (Bosecker 1997; Edwart and Hugues 1991; Ingledeu 1992; Suzuki 2001) and it is also environmentally important such as in the treatment of acid mine drainage and desulfurization of waste gases (SO₂ and H₂S) (Harahuc et al. 2000).

(ii) Electron transport pathways in *Acidithiobacillus ferrooxidans*

Although *A. ferrooxidans* can grow on Fe²⁺, reduced sulfur compounds, H₂ and formic acid, the emphasis of oxidation studies has been put on: Fe²⁺ > reduced sulfur compounds > H₂, formic acid and others. However, the electron transport pathways for the oxidation of none of these compounds are clear. Four groups of authors have proposed their models for electron transport pathways of Fe²⁺ oxidation (Fig. 5), and one model has been proposed for the oxidation of thiosulfate (Fig. 7) but no models have been proposed for the oxidation of other compounds.

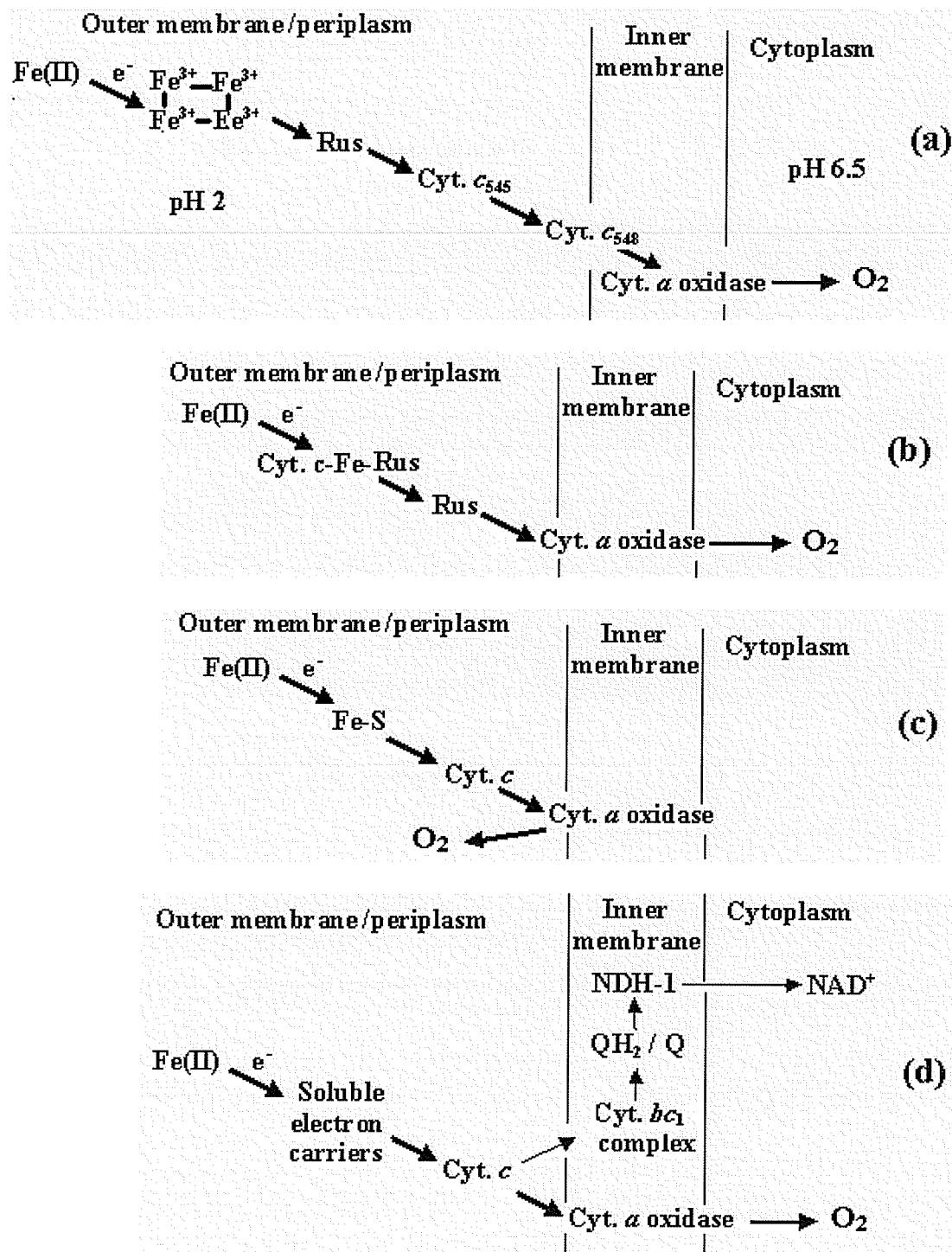


Fig. 5. Four models for the electron transport pathways of Fe^{2+} oxidation in *A. ferrooxidans*. (a) model of Ingledew's group (Blake and Shute 1994; Ingledew 1982, Ingledew and Houston 1986); (b) model of Blake's group (Blake and Shute 1994); (c) model of Yamanaka's group (Yamanaka et al. 1991); (d) model of Elbehti's group (Elbehti et al. 2000). Rus: rusticyanin; Cyt.: cytochrome; Fe-S: iron-sulfur protein; Cyt. c -Fe-Rus: cytochrome c -containing iron: rusticyanin oxidoreductase; NDH-1: NADH-Q oxidoreductase complex.

In the model of Ingledew's group (Fig. 5a), electrons from Fe^{2+} are first transferred to an extracellular polynuclear Fe^{3+} grid on the outer membrane and then sequentially to the blue copper protein rusticyanin, cytochrome c_{545} and cytochrome c_{548} in periplasm and finally to cytochrome oxidase a in the inner membrane, and O_2 is reduced to H_2O in cytoplasm. Although not shown in their model, Ingledew's group agrees that electrons from Fe^{2+} are also transferred along an uphill pathway from a cytochrome c to NAD^+ . NAD^+ will be reduced to NADH providing reducing power (NADH) for CO_2 fixation (Ingledew 1982).

In the model of Blake's group (Fig. 5b), electrons derived from Fe^{2+} oxidation first flow to a cytochrome c -containing iron: rusticyanin oxidoreductase, and then to rusticyanin to cytochrome oxidase a . The reduction of O_2 also occurs in the cytoplasm.

In the model of Yamanaka's group (Fig. 5c), electron from Fe^{2+} oxidation first flow to an iron-sulfur protein, and then to cytochrome c to cytochrome oxidase a . However, O_2 reduction occurs in periplasm and rusticyanin is not involved in the pathway.

In the model of Elbehti's group (Fig. 5d), electrons from Fe^{2+} oxidation flow to soluble electrons carriers to cytochrome c , then mainly to cytochrome oxidase. Some electrons will be transferred from cytochrome c along the uphill pathway to reduce NAD^+ to NADH. O_2 will be reduced in the cytoplasm.

Before the proposal of the model of Elbehti et al.(2000), the model of electron transport pathways for Fe^{2+} oxidation proposed by Ingledew's group (Fig. 5a) was considered more reasonable than the other two models (Fig. 5b and Fig. 5c), and had become the textbook model (Nicholls and Ferguson 2002). One big difference between the two models proposed by Ingledew's group and Elbehti' group (Fig. 5a and Fig. 5d)

is that the latter proposed proton pumping by Cyt. *c* oxidase but the former did not. The non-proton pumping model by Ingledew's group was probably proposed because (a) the big difference of pH ($\Delta\text{pH} = 3 - 4$) between the inside and outside of the cells was considered to make the proton pumping "unnecessary" and (b) uncouplers only inhibited but did not stimulate Fe^{2+} oxidation (Beck and Shafia 1964; Ingledew et al. 1977).

Elbehti's group reported indirect evidence for the existence of the uphill electron transport pathway from cytochrome *c* to NDH-1 by studying the oxidation of external reduced cytochrome *c* instead of Fe^{2+} or other growth substrates used by this organism (Elbehti et al. 2000). Their proton pumping (by Cyt. *c* oxidase) model is consistent with the situations in mitochondria and heterotrophic bacteria. However, they did not give the evidence for proton pumping by Cyt. *c* oxidase. Recently, Chen and Suzuki (2004) reported for the first time that uncouplers could stimulate Fe^{2+} oxidation and greatly stimulate endogenous respiration in *A. ferrooxidans*. This may support proton pumping by Cyt. *c* oxidase. Therefore, the model proposed by Elbehti's group better fits the current data for Fe^{2+} oxidation in *A. ferrooxidans* at present.

Knowledge of the sequence and types of the electron carriers between Fe^{2+} and cytochrome *c* oxidase is still poor. However, the blue copper protein rusticyanin must be an essential component. The gene for rusticyanin (*rus*) in *A. ferrooxidans* has been sequenced and corresponding protein isolated and sequenced (Ronk et al. 1991; Yano et al. 1991). The *in vivo* concentration of rusticyanin may represent 5% of the total cell protein in *A. ferrooxidans* (Casimiro et al. 1995). When rusticyanin was added to the membrane preparations of this organism, the rate of Fe^{2+} oxidation could be increased by up to 10-folds (Cox and Boxer 1986). The detailed studies of rusticyanin in the recent

years (Donaire et al. 2002; Grossmann et al. 2002; Jiménez et al. 2003; Kanbi et al. 2002; Sasaki et al. 2003; Yarzabal et al. 2004) further indicate its importance. The interesting discovery of two types of rusticyanin (Sasaki et al. 2003) as well as two types of cytochrome *bc*₁ complex (*bc*₁I only works in the uphill reaction, e.g. during Fe²⁺ oxidation, while *bc*₁II only works in the downhill reaction) (Brasseur et al. 2002, 2004), two sets of structural genes (form I and form II) coding for the CO₂ fixation enzyme, ribulose-1,5-bisphosphate carboxylase/oxygenase (RuBisCO) (Kusano et al. 1991; Shively et al. 1998) and two copies of form I RuBisCO genes (Heinhorst et al. 2002) in *A. ferrooxidans*, makes it more challenging to understand the physiology and the electron transport pathways in this organism.

The Fe²⁺-oxidizing enzyme (Fe-S protein in Fig. 5c), Fe²⁺ oxidase Iro, which rapidly reduced *A. ferrooxidans* ferricytochrome *c*₅₅₂ with Fe²⁺ at pH 3.5, was considered to be the first enzyme to accept electrons from Fe²⁺ but it did not reduce rusticyanin with Fe²⁺ (Fukumori et al. 1988; Kusano et al. 1992). Although the authors did not give the evidence for the location (outer membrane or periplasm) of Fe²⁺ oxidase Iro, it is possible that this protein is an outer membrane protein. More recently some outer membrane proteins, for example cytochrome *c* C_{yc2}, have been isolated in this organism (Yarzabal et al. 2002b).

The bioinformatics information and experimental studies of cytochromes *c* in *A. ferrooxidans* has been reviewed by Yarzabal et al. (2002a). Eleven genes encoding the putative cytochromes *c* have been identified in the genome sequence of ATCC23270 and most genes are duplicated. In ATCC3320 strain cells, at least 8 putative cytochromes *c* were differentiated on gels. Twenty-three cytochromes *c* have been

identified in different strains, two of which are an outer membrane protein, six soluble proteins, thirteen inner-membrane bound proteins, and two of uncertain location. Four cytochromes belonging to the c_4 cytochrome family have been found in *A. ferrooxidans*. The total content of cytochrome c was higher in Fe^{2+} -grown cells than in S^0 -grown cells. As the authors explained, Fe^{2+} oxidation may require higher concentrations of electron transport carriers, such as cytochromes c , to catalyze the fast oxidation of Fe^{2+} since much less energy is available for biosynthesis from Fe^{2+} oxidation than from S^0 oxidation. Three cytochromes c including the outer membrane protein Cyc2 and two c_4 (c_{552}) cytochromes are specific for Fe^{2+} oxidation while a 24.5 kDa cytochrome c is specific for S^0 oxidation.

Therefore, an outer membrane protein (possibly cytochromec c Cyc2 or Iro), rusticyanin and cytochrome c_4/c_{552} (one or two) are essential electron carriers between Fe^{2+} and O_2 . Since the redox potential of $\text{Fe}^{3+} / \text{Fe}^{2+}$ couple is high ($E_{m,2} = +0.65 \text{ V}$) (Ingledeu 1982), the electron carrier following Fe^{2+} should have an even higher redox potential. A possible candidate could be rusticyanin ($E_{m,2} = +0.68 \text{ V}$) but not cytochrome c_4 ($E_m = +0.48 \text{ V}, +0.385 \text{ V}$) (Giudici-Orticoni et al. 1999) or c_{552} (also a c_4 -type, $E_m = 0.36 \text{ V}$) (Sato et al. 1989). Giudici-Orticoni et al. (1999) reported that the redox potential of rusticyanin at pH 4.8 was +0.59 V and but decreased to +0.49 V after it formed a complex with cytochrome c_4 whose redox potential remained unchanged after complexation. This complex-induced tuning makes electron transfer possible in the energy requiring step from rusticyanin to cytochrome c_4 . Thus, according to current published data, electron transport between Fe^{2+} and O_2 probably follows $\text{Fe}^{2+} \rightarrow \text{Fe}^{2+}$ oxidase (cytochromec c Cyc2 or Fe-S protein Iro) \rightarrow rusticyanin \rightarrow cytochrome c_4/c_{552}

→ cytochrome *c* oxidase → O₂, and a model for electron transport pathway of Fe²⁺ oxidation is shown in Fig. 6.

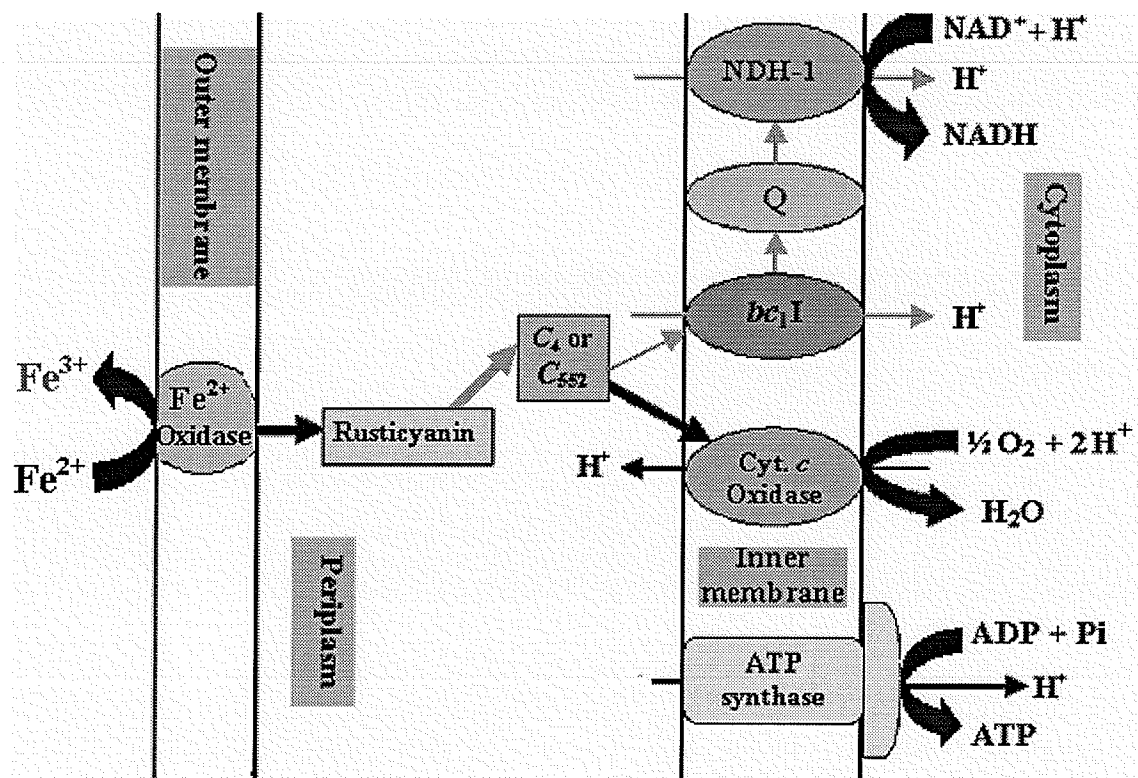


Fig. 6. Proposed model for electron transport pathway of Fe²⁺ oxidation in *A. ferrooxidans* based on the published data. Q: ubiquinone / ubiquinol pool; bc₁I: the bc₁ complex participating in the uphill reaction (NAD⁺ reduction); NDH-1: NADH-Q oxidoreductase complex; c₄ or c₅₅₂: cytochrome c₄ or cytochrome c₅₅₂; Cyt.: cytochrome; Fe²⁺ oxidase: an putative enzyme that accepts electron from Fe²⁺, it may be the same enzyme (Fe-S protein Iro) proposed by Yamanaka's group (see the text). The thickness of straight arrows (not including the arrows pointing at H⁺) represents the speed of electron flow in a qualitative manner

The model for thiosulfate oxidation (Fig. 7) by *A. ferrooxidans* is the first model for the oxidation of a substrate other than Fe²⁺. The most important contribution of this model is that it suggests for the first time the existence of multiple terminal oxidases being responsible for the oxidation of a substrate in *A. ferrooxidans*. Therefore, a

network of multiple electron transport pathways also exists in *A. ferrooxidans* as in other prokaryotes.

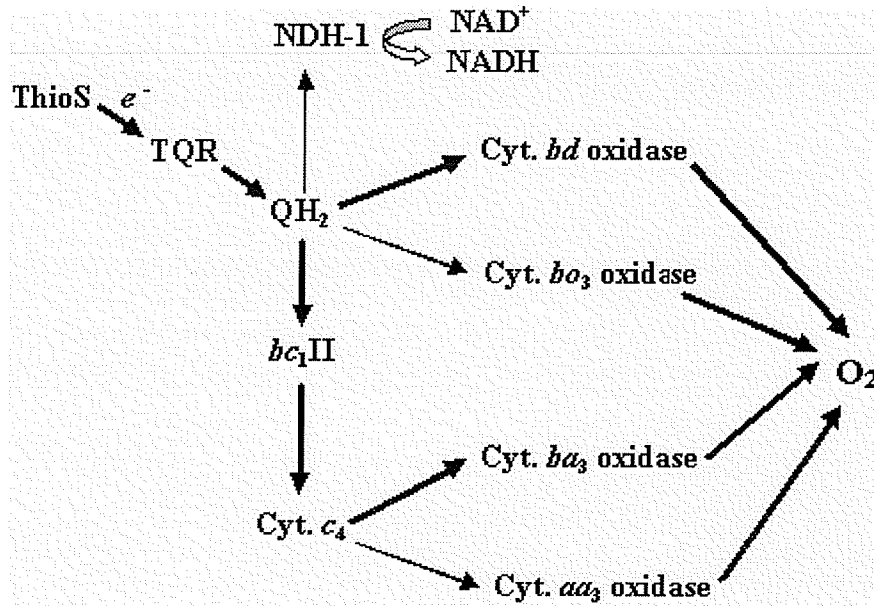


Fig. 7. Model for the electron transport pathways of thiosulfate oxidation in *A. ferrooxidans*. ThioS: thiosulfate; TQR: thiosulfate-quinol reductase; NDH-1: NADH-Q oxidoreductase complex (complex I); QH₂: ubiquinol pool; *bc*₁II: the second cytochrome *bc*₁ complex in *A. ferrooxidans*, which only transfers electrons in the downhill reaction (from QH₂ to Cyt. *c*₄); Cyt.: cytochrome. (Bresseur et al. 2004).

(III) Study objectives

Since no evidence has been reported to show the electron transport along the uphill pathway to reduce NAD⁺ during Fe²⁺ oxidation in *A. ferrooxidans*, one of the objectives of this dissertation is to provide such an evidence.

Secondly, the oxidation of all known growth substrates of *A. ferrooxidans* is believed to involve the transport of electrons via the uphill pathway to reduce NAD⁺, but the preliminary study by Chen and Suzuki (2004) showed that endogenous respiration only takes a downhill pathway involving NADH oxidation in this bacterium. This is the first

report of an electron transport pathway starting from complex I (NDH-1) to oxidize a substrate (endogenous substrate) in this organism, the same as the situation in mitochondria and heterotrophic bacteria. This interesting discovery makes it important to study the possible electron transport pathways for the oxidation of endogenous substrates(s), which will add new information to the physiology of this organism and may help the understanding of the oxidation mechanisms of Fe^{2+} and other substrates. Since four terminal oxidases have been discovered in *A. ferrooxidans* (Brasseur et al. 2004), it is quite possible that these oxidases are involved in endogenous respiration, that is, more than one electron transport pathway may be used for endogenous respiration.

Therefore, the second objective of this dissertation is to investigate the possible electron transport pathways and their regulation during the oxidation of endogenous substrates and other possible organic compounds.

Chapter II
Materials and Methods

(I) Chemicals

All chemicals used were the highest grade commercially available and obtained from the following companies: J. T. **Baker** Chemical Co. (Phillipsburg, New Jersey, U. S. A); **BDH** (The British Drug Houses Ltd., Poole, England); **Calbiochem** (San Diego, California, U. S. A); **Difco** laboratories (Detroit, Michigan, U. S. A); **Eastman** Organic Chemicals (New York, U. S. A); **Fisher** Scientific (Fair Lawn, New Jersey, U. S. A); **Malinkrodt** Canada Inc.(Pointe Clarie, Quebec, Canada); **Mann** Research Laboratories Inc. (New York, U. S. A); **McAthur** Chemical Co. Ltd.(Montreal, Canada); **MC/B-** Matheson Coleman & Bell, Los Angeles, California, U. S. A; **Sigma-Aldrich** Canada (Oakville, ON, Canada).

β -alanine -----	Sigma
Ammonium sulfate -----	Malinkrodt
Amytal (amo barbital; 5-ethyl-5-isoamylbarbituric acid) -----	Sigma
Antimycin A -----	Sigma
L-ascorbic acid -----	Baker
Atabrine (Quniacrine dihydrochloride) -----	Mann
Bacto yeast extract -----	Difco
Casamino acids -----	Difco
CCCP (carbonyl cyanide <i>m</i> -chlorophenylhydrazone) -----	Sigma
L-cysteine -----	Sigma
DCCD (dicyclohexylcarbodiimide) -----	Sigma
Deferoxamine mesylate -----	Sigma

2,2'-dipyridyl -----	Sigma
DNP (2,4-dinitrophenol) -----	Calbiochem
EDTA (Ethylenediaminetetraacetic acid disodium salt, dihydrate) -----	Sigma
Ferrous sulfate, heptahydrate -----	Fisher
Ferrozine (3-(2-pyridyl)-5,6-bis(4-phenylsulfonic acid)-1,2,4-triazine), monosodium salt -----	Sigma
Formic acid, 88% -----	Fisher
D-fructose, and other sugars and sugar alcohols -----	Sigma
Glutathione (reduced form) -----	Sigma
HQNO (2-heptyl-4-hydroxyquinoline-N-oxide) -----	Sigma
HQSA (8-Hydroxyquinoline-5-sulfonic acid) -----	Eastman
Lysozyme -----	Sigma
Magnesium sulfate, heptahydrate -----	Fisher
Malonic acid, disodium salt, monohydrate -----	MC/B
Myxothiazol -----	Sigma
NEM (N-ethyl maleimide) -----	Sigma
Nigericin, sodium salt -----	Sigma
Oligomycin -----	Sigma
Oxalic acid -----	McAthur
PG (Propyl gallate; 3,4,5-trihydroxybenzoic acid propyl ester) -----	Sigma
Piericidin A -----	Sigma
Potassium cyanide -----	Baker
Potassium acetate -----	Baker

Potassium fluoride -----	Fisher
Potassium thiocyanate -----	Sigma
o-phenanthroline (1,10-phenanthroline), monohydrate -----	Sigma
Rotenone -----	Sigma
SHAM (salicylhydroxamic acid) -----	Sigma
Succinic acid, disodium salt, hexahydrate -----	MC/B
Sodium arsenate, disodium salt, heptahydrate -----	MC/B
Sodium azide -----	BDH
Tetraphenylboron, sodium -----	Sigma
Tetra-sodium pyrophosphate -----	BDH
Tiron (4,5-dihydroxy-1,3-benzene disulfonic acid)-disodium salt -----	Sigma
TTFA (thenoyltrifluoroacetone) -----	Sigma
Valinomycin -----	Sigma

(II) Bacterial growth and preparation of cell suspension

A. ferrooxidans (ATCC19859) was grown in the modified 9 K medium (Harahuc et al. 2000) containing 0.4 g of $MgSO_4 \cdot 7H_2O$, 0.1 g of K_2HPO_4 , 0.4 g of $(NH_4)_2SO_4$, and 33.3 g of $FeSO_4 \cdot 7H_2O$ per liter, adjusted to pH 2.3 with H_2SO_4 . The ferrous sulfate solution (33.3%) was sterilized separately by passing through a 115-mL Nalgene filter unit with 0.45 μm pores. Other components in the medium were mixed and autoclaved at 121°C for 20 min. The organism was cultured in Erlenmeyer flasks using a 10% inoculum at 25°C and on a rotary shaker at 150 rpm for 50 h. Cells were harvested by passing the culture through Whatman no. 1 filter paper to remove most of the

precipitated ferric iron. The supernatant was centrifuged at $8000 \times g$ for 10 min. The cell pellet was resuspended in 0.1 M β -alanine- H_2SO_4 buffer of pH 2.3 or 3.5 and centrifuged at $1000 \times g$ for 5 min to further remove ferric iron precipitate. The supernatant was centrifuged at $10,000 \times g$ for 10 min to collect the cell pellet. The cell pellet was resuspended in the same buffer and centrifuged a fourth time generating a cell suspension of 100 mg per mL in the same buffer. Cell suspensions (normally 4 to 5 mL from 4 to 5 L of culture) were stored in one plastic centrifuge tube for oxidation of substrates other than endogenous substrates and fructose or in Eppendorf tubes (one tube for one test) for oxidation of endogenous substrates and fructose (0.21 mL / tube 1.2 cm deep for Fe^{3+} reduction or 0.25 mL / tube 1.3 cm deep for O_2 consumption) without shaking at $4^\circ C$ and used within 3 days.

(III) Preparation of spheroplasts

Spheroplasts were made by following the method of Apel et al. (1980). Cells (0.5 g) were washed twice in 10 mL 0.05 M Tris- H_2SO_4 buffer of pH 7.8 (at $10,000 \times g$ for 10 min) and then once in 10 mL 0.05 M Tris buffer containing 10% (wt / vol) sucrose. The cell pellet was suspended in 10 mL 0.05 M Tris-10% sucrose buffer containing 0.2% (wt / vol) EDTA- Na_2 and 0.1% (wt / vol) lysozyme. The cell suspension was treated with liquid nitrogen by freezing-and-thawing for 4 times and then was incubated in a water bath at $37^\circ C$ for 30 min. The suspension was centrifuged at $10,000 \times g$ for 10 min at $4^\circ C$. The pellet was washed first with 0.05 M Tris-10% sucrose buffer containing 0.02 M $MgSO_4$ and then with 0.05 M Tris-10% sucrose buffer containing 0.01 M $MgSO_4$. The pellet was finally suspended in 0.1 M β -alanine- H_2SO_4 containing 10% (wt / vol)

sucrose at pH 3.5. The spheroplast suspension was kept on ice or at 4°C without stirring and was used within 1 – 2 days. The osmotic sensitivity was checked by comparing the activities of Fe²⁺ oxidation in 0.1 M β-alanine-H₂SO₄ buffer of pH 3.5 with and without 10% sucrose and also in H₂O of pH 3.5. All experiments with spheroplasts were carried out in duplicates.

(IV) Preparation of cell free extracts

Cell free extracts were made by using the method modified from Bodo and Lundgren (1974): cells harvested in H₂O of pH 3.5 was suspended in 10 mM K₂HPO₄-KH₂PO₄ buffer of pH 7.0 and centrifuged at 10,000 × g for 10 min. Cell pellet (0.3 g) resuspended in 10 mL 10 mM K₂HPO₄-KH₂PO₄ buffer of pH 7.0 was stored at 4°C overnight. Ten mL double-distilled water was added and the mixture was centrifuged at 10,000 × g for 10 min. The pellet was suspended in 20 mL double-distilled water and centrifuged at 10,000 × g for 10 min. The pellet was suspended in 5 mL double-distilled water and was passed through a French Press Cell at 20 kg for 3 times. The mixture was centrifuged at 3,500 × g for 10 min to remove the whole cells and the supernatant (cell free extracts, pH 6.5) was stored at 4°C without stirring and was used within 1 – 2 days.

(V) Determination of protein concentration

Protein concentration was determined by using Lowry's method (Lowry et al. 1951): 4 mg wet cells in 0.1 mL H₂O was mixed with 0.9 mL 0.1 N NaOH, boiled for 10 min, centrifuged for 3 min in Micro-centrifuge. Supernatant (0.8 mL) was mixed with 4mL reagent D and after 10 min at room temperature, 0.2 mL 2 N phenol reagent and 0.2 mL

H₂O were added. After standing for at least 30 min at room temperature. The absorbance at 660 nm (A_{660}) was measured and the protein concentration was calculated using a standard curve determined with bovine serum albumin. Experiments were carried out in triplicates. Protein concentration was finally determined to be about 8 mg protein per 100 mg cells.

(VI) Measurement of O₂ consumption and CO₂ production

Rates of O₂ consumption were measured polarographically in a Gilson Oxygraph (1.2 mL) with a Clark oxygen electrode. Unless otherwise stated, all experiments of O₂ consumption were carried out in 0.1 M β -alanine-H₂SO₄ buffer of pH 3.5 at 25°C and, except for Fe²⁺ oxidation, reactions were started by the addition of cells. Other conditions for the measurement of O₂ consumption rates of the oxidation of different substrates are summarized in Table 5. Experiments were carried out at least in duplicates. Rates were expressed as nmol or μ mol O₂ min⁻¹ (mg protein)⁻¹ (\pm SD, n = 2 – 5).

Warburg respirometer and manometric methods (Umbreit et al. 1949) were used to follow O₂ consumption and CO₂ production during oxidations of endogenous substrates and fructose for 6 to 8 h at 30°C in 3.2 mL reaction system (64 mg cells, 5.1 mg protein) with and without 10 N NaOH in the center wells. The consumption of O₂ is calculated based on the pressure change in the flask with NaOH and CO₂ production is calculated using the pressure change in the flask without NaOH subtracting the pressure change due to the consumption of O₂. Experiments were carried out in duplicates. Rates were expressed as nmol O₂ or CO₂ min⁻¹ (mg protein)⁻¹ (\pm SD, n = 2).

When the effect of a compound (inhibitors, uncouplers, etc.) was studied, it was added with cells at zero time unless otherwise stated. This is the same in other experiments (e.g. Fe^{3+} reduction).

Table 5. Amount of cells, substrates and the reaction times used during the oxidation of different substrates by O_2 in *A. ferrooxidans* in oxygraph (1.2 mL).

Substrate	Concentration (mM)	Cells (mg) *	Reaction time (min)
FeSO_4 (Fe^{2+}) **	4	2.4	1
Ascorbic acid (Vc)	2	2.4	1 – 2.5
Propyl gallate (PG)	4	2.4	10
SHAM	2	4.8	5
Tiron	4	4.8	10
L-cysteine (Cys)	2	2.4	7 – 8
Glutathione (GSH)	8	4.8	7 – 8
Endogenous		24	60
Fructose	80	24	45 – 50
Formic acid	0.1	2.4	15 – 20
Yeast extract (YE)	1%	4.8	10
Casamino acids (CA)	3%	4.8	5 – 6

* Cell suspension of 100 mg per mL contained about 8% protein; ** Unless otherwise stated, cells were preincubated with or without other compounds (uncouplers, inhibitors, etc.) for 5 min before the addition of Fe^{2+} .

(VII) Measurement of Fe^{3+} reduction

Fe^{3+} reduction was measured by determining the formation of Fe^{2+} . The mechanism for Fe^{2+} determination is based on the red color density of Fe^{2+} and 1,10-phenanthroline

(C₁₂H₈N₂, *ortho*-phenanthroline or *o*-Phen.) complex {[*o*-phen.)₃Fe]²⁺} (Diehl and Smith. 1952; Harvey et al. 1955; Skoog et al. 2000).

The reduction of Fe³⁺ was carried out in 1 mL reaction system by measuring the rate of Fe²⁺ formation after cytochrome *c* oxidases in *A. ferrooxidans* were inhibited by KCN. The reaction mixture in a glass tube (up to 8 tubes can be used at the same time) contained cells, 4 μmol FeCl₃, 2 μmol KCN, with and without other compounds in 0.1 M β-alanine-H₂SO₄ buffer of pH 2.3 or pH 3.5 with a total volume of 1 mL (see Table 6) and was stirred magnetically at 25 °C. A sample of 0.1 mL was taken at 10 min intervals and mixed with 1 mL 0.1% *o*-phen. (pH 2.3 or 3.5) and the mixture was immediately centrifuged for 2 min in a micro-centrifuge to remove cells (centrifugation was not required for oxidation of YE, CA, formic acid and for chemical reactions). The supernatant was diluted with 0.9 mL buffer and the absorbance at 510 nm (A₅₁₀) (the feature absorbance of [(*o*-phen.)₃Fe]²⁺) was measured in a Hewlett-Packard 8452A Diode array spectrophotometer. Experiments were carried out in duplicates or triplicates and figures were drawn using Excel and Sigma Plot showing standard error bars at each time point. The amount of Fe²⁺ formed was calculated according to the relationship Y = 0.005 X (Y: A₅₁₀, X: nmol Fe²⁺ produced) which was determined by using known concentrations of FeSO₄. The factor 0.005 is close to the theoretical value (0.00555) calculated according to the molar extinction coefficient (E = 11,100 M⁻¹ cm⁻¹) of [(*o*-phen.)₃Fe]²⁺ (Skoog et al. 2000). Rates of Fe³⁺ reduction were expressed as nmol Fe²⁺ min⁻¹ (mg protein)⁻¹ (± SD, n = 2 – 3).

Table 6. The conditions of Fe³⁺ reduction by different substrates in 1 mL reaction system.

Substrate	Endogenous	Fructose	Formic acid	YE	CA
Concentration		80 mM	1 mM	1%	3%
Cells (mg)	20	20	4	4	4
pH	2.3, 3.5	3.5	3.5	3.5	3.5
Centrifugation	Yes	Yes	No	No	No

(VIII) Measurement of external pH change

Changes in pH during oxidation of endogenous substrates and fructose by O₂ were followed in a Radiometer pH meter 28 in a 2-mL reaction system with 40 mg (200 mg to show proton leaking in during endogenous respiration) wet cells harvested and tested in water of pH 3.5 (0.48 mM H₂SO₄).

(IX) Bioinformatics searches

Bioinformatics searches were carried out according to the methods by Altschul et al. (1997). The amino acid sequence of a protein from a known source was used as the query sequence to do the tblastn search (amino acid sequence searching DNA databases) in the partial genome of *A. ferrooxidans* ATCC 23270 at the NCBI (National Center for Biotechnology Information) web site (http://www.ncbi.nlm.nih.gov/sutils/genom_table.cgi) contributed by TIGR Microbial Database (<http://www.tigr.org/tdb/mdb/mdbinprogress.html>). Amino acid sequences obtained and putative open reading frames (ORFs) were found via the ORF Finder (<http://www.ncbi.nlm.nih.gov/gorf/gorf.html>) from the nucleotide sequences that produced significant alignments. Then the putative amino acid sequence of a target

protein was found by blasting the ORFs (blastp) against the genomes of known organisms.

Sequence comparisons were directly taken from the website or were carried out by using the GeneDoc program downloaded from GeneDoc website (<http://www.psc.edu/biomed/genedoc/>).

Chapter III

Results, Discussion and Conclusions

Part I

Oxidation of Fe^{2+} and Compounds Interacting with Fe^{3+}

Abstract

The effects of uncouplers and electron transport inhibitors were studied on the oxidation of Fe^{2+} and the compounds interacting with ferric iron. Fe^{2+} oxidation was sensitive to the inhibition by uncouplers and it could be stimulated only to a small extent by uncouplers at low concentrations and in the initial 1 min. Fe^{2+} oxidation was strongly inhibited by complex IV inhibitors but only slightly by inhibitors of complex I (except piericidin A) and complex III, and the reduced activities caused by inhibitors of complex I and III were released by the addition of an uncoupler with the exception of atabrine inhibition. The inhibition of Fe^{2+} oxidation by complex I inhibitor atabrine was unique in that the inhibited activity was not released but it was further inhibited by the addition of an uncoupler. Ascorbic acid, propyl gallate, salicylhydroxamic acid, L-cysteine and glutathione chemically reduced ferric iron to ferrous iron. These compounds were oxidized by the cells and the oxidation activities were greatly stimulated by the addition of FeCl_3 . The oxidations of these compounds, similar to Fe^{2+} oxidation, were sensitive to the inhibition by uncouplers and could be inhibited by some electron transport inhibitors. They were also inhibited by atabrine and the inhibition was magnified by the addition of an uncoupler. It was interpreted that (a) the slight stimulation of Fe^{2+} oxidation by uncouplers indicated a normal respiratory control; (b) the inhibition of Fe^{2+} oxidation by inhibitors of complexes I and III and the stimulation of the inhibited activities by an uncoupler, indicated an uphill reaction (NAD^+ reduction); (c) the compounds interacting with ferric iron were oxidized by using the Fe^{2+} oxidation system; (d) the evidence that two NDH-1s may exist in this organism is based on the opposite effects of atabrine and piericidin A on Fe^{2+} oxidation and endogenous respiration.

Introduction

According to previous studies uncouplers showed only an inhibitory effect on the oxidation of Fe^{2+} (Beck and Shafia 1964; Ingledew et al. 1977). Because the oxidation of Fe^{2+} involves ATP generation (Adapoe and Silver 1975; Elbehti et al. 2000; Ingledew 1982; Mignone and Donati 2004) and because of the controversy about the H^+ pumping during Fe^{2+} oxidation (Elbehti et al. 2000; Ingledew et al. 1977), the effect of uncouplers, CCCP and DNP, were re-investigated to see if a normal respiratory control exists during Fe^{2+} oxidation. Elbehti et al. (2000) indirectly showed the existence of an uphill reaction from cytochrome *c* to NDH-1 (NAD^+ reduction) in *A. ferrooxidans* (see Fig. 6) by testing the oxidation of external reduced cytochrome *c* after cytochrome *c* oxidase was inhibited by KCN. However, no evidence has been reported to show electron transport along the uphill electron transport pathway to reduce NAD^+ during oxidation of Fe^{2+} or other substrates used by this organism. This investigation has attempted to present such evidence by studying the effects of different electron transport inhibitors.

Some organic compounds were reported to be oxidized by *A. ferrooxidans* or to interact with ferric iron. Ascorbic acid oxidation by *A. ferrooxidans* was earlier reported (Cox et al. 1979; Tikhonova et al. 1967). L-cysteine and glutathione are known to interact with iron (Timmerman and Woods 1999). Propyl gallate (PG) and SHAM, inhibitors of alternative oxidase (Atkin et al. 1995; Siedow and Bickett 1981), and tiron all as chelators of iron greatly increased the rate of endogenous respiration by the cells of *A. ferrooxidans* and seem to be oxidized by the cells (see Part II in this dissertation). Since *A. ferrooxidans* is an autotroph and therefore not likely to obtain carbon and reducing power by oxidizing organic compounds (via the downhill electron transport

pathway starting from NDH-1), one possible mechanism for the oxidation of the above-mentioned compounds involves the use of the Fe^{2+} oxidation system in this organism after Fe^{3+} on the cell surface was chemically reduced by these compounds. Therefore, the interaction of these organic compounds with ferric iron and the responses of their oxidation to uncouplers and electron transport inhibitors have been investigated to see if the features of their oxidation agree with those of Fe^{2+} oxidation.

Results

1.1. Fe²⁺ oxidation

1.1.1. Effect of uncouplers, other Δp dissipators, and phosphate

Table 1-1 and Fig. 1-1 show that, when cells were added to start the reaction, the activity of Fe²⁺ oxidation was maximally stimulated 25% and 28% by 0.5 μ M CCCP and 20 μ M DNP, respectively. Lower and higher concentrations of CCCP or DNP showed less stimulation. CCCP at 5 μ M and 10 μ M showed 3% and 10% inhibition, respectively. When cells were preincubated with uncouplers for 5 min before the addition of Fe²⁺, the activity of Fe²⁺ oxidation was inhibited 73% and 87% by 5 μ M and 10 μ M CCCP, respectively and 19% and 40% by 0.1 mM and 1.0 mM DNP, respectively (Table 1-2 and Fig. 1-2).

The effect of phosphate (KH₂PO₄, Pi) on Fe²⁺ oxidation is different in the absence and presence of uncouplers. In the absence of uncouplers Fe²⁺ oxidation was stimulated 24% by 4 mM Pi, but was unaffected in the presence of uncouplers CCCP or DNP (Table 1-2 and Fig. 1-2). Since CCCP at 10 μ M greatly stimulated endogenous respiration for 1 h in *A. ferrooxidans* (see Part II), Fe²⁺ oxidation was tested by using the same concentrations of cells and uncoupler. Cells (20 mg / mL) were incubated in the presence and absence of 10 μ M CCCP at 25°C for 30 min with magnetic stirring. Then samples were taken either directly or after 6-times and 10-times washing by centrifugation (10,000 \times g for 10 min in 20 mL buffer) to test Fe²⁺ oxidation in oxygraph. CCCP-treated cells only showed 10% of the activity of Fe²⁺ oxidation compared to control cells (without the addition of CCCP) when 24 mg cells (data not shown) or 2.4 mg cells were used (Fig. 1-3a) before washing, but CCCP-treated cells (2.4 mg) showed 92% and 79% of the activity of control cells (2.4 mg) after 6-times and

10-times washing, respectively although the activity of control cells decreased to 65% and 58%, respectively by washing (Fig. 1-3). When 4 mM Pi was added with Fe^{2+} before the addition of these washed cells (2.4 mg), the activity of control cells after 6-times and 10-times washing was restored to 97% and 93% of the unwashed cells (no Pi), respectively, and the CCCP-treated cells was 99% and 81% of the activity of control cells, respectively (Fig. 1-3). After 6-time washing, Pi stimulated the activities of control cells and CCCP-treated cells by 50% and 61%, respectively. After 10-time washing, Pi stimulated the activities of control cells and CCCP-treated cells by 61% and 65%, respectively.

Effects of other Δp dissipators CH_3COOK , KSCN, nigericin and valinomycin on Fe^{2+} oxidation were also tested. CH_3COOK at 0.2 mM showed a maximal stimulation of 15% on Fe^{2+} oxidation and showed 29% and 68% inhibition at very high concentrations of 10 mM and 40 mM, respectively (Table 1-3). KSCN stimulated Fe^{2+} oxidation only by 6% at 0.1 mM and 0.5 mM and it inhibited it progressively with time and with concentrations at 1mM, 2 mM and 5 mM (Fig. 1-4). Valinomycin had no effect on Fe^{2+} oxidation when its concentration was increased up to 100 μM either in the absence (Fig. 1-5) or presence of 1 mM K_2SO_4 (data not shown). Nigericin had no effect on Fe^{2+} oxidation when its concentration was increased up to 0.5 μM but inhibited Fe^{2+} oxidation by 13% and 20% at 1 μM and 5 μM , respectively (Fig. 1-5).

1.1.2. Effect of inhibitors of ATP synthase

Inhibitors of ATP synthase, DCCD and oligomycin, were tested at different concentrations. Oligomycin up to 1 μM and DCCD up to 100 μM had no effect on Fe^{2+}

oxidation (Fig. 1-6). This is different from the membrane vesicle experiment reported by Apel et al (1980) in that 100 μM DCCD inhibited ATP synthesis by 40%, but agrees with the report by Adapoe and Silver (1975) that the isolated ATPase was not inhibited by DCCD.

1.1.3. Effect of inhibitors of complex IV

Fig. 1-7 shows the effect of KCN on Fe^{2+} oxidation when 2.4 mg cells were added to start the reaction. KCN showed time-dependent inhibition on Fe^{2+} oxidation. KCN at 5 μM and 10 μM showed 16% and 35% inhibition, respectively, and showed 97% inhibition at 50 μM after 100 s, 100% inhibition at 0.1 mM to 2 mM after 50 s. NaN_3 , on the other hand, showed instant inhibition on Fe^{2+} oxidation initially but time-dependent activity recovery (Fig. 1-8). NaN_3 at 5 μM showed 100% and 92% inhibition before and after 40 s, respectively. The higher the concentration of NaN_3 was used, the later the activity recovery would appear and the less the activity recovery was.

When 24 mg cells were added to start the reaction Fe^{2+} oxidation was inhibited 100% by 2 mM KCN and 98.1%, 99.8% and 100% by 0.1 mM, 1 mM and 2 mM NaN_3 , respectively (Table 1-4 and Fig. 1-9).

1.1.4. Effect of inhibitors of complex I and complex III

Since Fe^{2+} oxidation would finish within 80 s when 2.4 mg cells and 4 mM Fe^{2+} were used in oxygraph (1.2 mL) and the oxidation was less sensitive to inhibitors of complex I and complex III when cells were added to start the reaction (data not shown), cells were preincubated with inhibitors for 5 min before the addition of Fe^{2+} . Inhibitors of

complex I (amytal, atabrine and rotenone) and complex III (antimycin A, HQNO and myxothiazol) inhibited Fe^{2+} oxidation by 7 – 18% and the inhibition was enhanced up to 30 – 40% by the combinations of these inhibitors (Tables 1-5, 1-6 and Fig. 1-10a, 1-11). Another complex I inhibitor piericidin A, at a concentration of 0.5 μM , which strongly inhibited the oxidation of endogenous substrates (see Part II), had no effect on Fe^{2+} oxidation (Table 1-5).

When DNP (10 μM or 100 μM) was added the residual activities of Fe^{2+} oxidation with inhibitors of complex I and complex III were stimulated (increase in relative activities) with the sole exception of atabrine (Tables 1-5, 1-6 and Fig. 1-10, 1-12, 1-13). DNP at 10 μM raised the inhibited activities more than DNP at 100 μM . The inhibited activities in the presence of atabrine were not stimulated by DNP and the inhibition of Fe^{2+} oxidation was enhanced in the presence of both 100 μM DNP and atabrine (Table 1-5 and Fig. 1-10, 1-12, 1-13). When CCCP was used the same phenomena were observed (data not shown).

1.2. Oxidation of ascorbic acid (Vc)

1.2.1. Effect of FeCl_3

Oxidation of Vc was stimulated 59%, 70%, 72% and 59% by FeCl_3 at 0.4 mM, 1 mM, 2 mM and 4 mM, respectively (Table 1-7 and Fig. 1-14). Vc can be chemically oxidized by O_2 with a rate of 2% of that of the biological reaction. However, the chemical reaction was zero in the presence of FeCl_3 (Table 1-7 and Fig. 1-14). The stimulation of Vc oxidation by FeCl_3 indicates that Vc oxidation may have been achieved by first

reducing the Fe^{3+} on the cell surface to Fe^{2+} and then using the Fe^{2+} oxidation system in *A. ferrooxidans*

1.2.2. Effect of uncouplers

Vc oxidation, similar to Fe^{2+} oxidation, was slightly stimulated by uncouplers CCCP and DNP at low concentrations (Table 1-8). The maximal stimulation was 13% by 0.5 μM CCCP, 12% by 20 μM DNP and 17% by 0.5 μM CCCP plus 30 μM DNP. Lower and higher concentrations of CCCP or DNP showed less stimulation. CCCP at 5 μM and 10 μM showed 9% and 19% inhibition, respectively. DNP at 100 μM only showed 2% inhibition.

1.2.3. Effect of electron transport inhibitors

Vc oxidation is sensitive to the inhibition by complex IV inhibitors KCN and NaN_3 similar to Fe^{2+} oxidation. KCN inhibited Vc oxidation by 23%, 98% and 100% at 10 μM , 0.1 mM and 1 mM, respectively, and NaN_3 inhibited it by 51%, 91% and 100% at 1 μM , 10 μM and 0.1 mM, respectively (Table 1-9).

The effects of complex III inhibitors on Vc oxidation are different from those on Fe^{2+} oxidation (Table 1-10). Myxothiazol and antimycin A had no effect on Vc oxidation. HQNO showed no effect at 5 – 20 μM but showed about 10% stimulation at 30 μM and 40 μM . HQNO, however, showed only 6% stimulation when tested in the presence of 4 mM FeCl_3 . The reason for stimulation of Vc oxidation by HQNO is unknown. It is probably due to the fact that some Vc could directly donate electrons to ubiquinone and to quinol oxidase(s). If quinol oxidase(s) is inhibited by HQNO that electron flow could

shift to the more efficient Fe^{3+} reduction and Fe^{2+} oxidation pathway and a faster respiration would be observed. Table 1-11 showed the inhibitory effect of complex I inhibitors and the combination of atabrine and CCCP on Vc oxidation. Vc oxidation was inhibited 13%, 6% and 19% by 1 mM amytal, 0.1 mM rotenone and the combination of 1 mM amytal and 0.1 mM rotenone, respectively. Compared to Fe^{2+} oxidation, Vc oxidation was more sensitive to the inhibition by atabrine. Atabrine at 0.1 mM, 1 mM and 2 mM showed 46 – 49%, 84% and 90% inhibition, respectively. Similar to Fe^{2+} oxidation, the atabrine-inhibited Vc oxidation was further inhibited by an uncoupler CCCP at a high concentration of 10 μM . Atabrine at 0.1 mM, CCCP at 10 μM and the combination of the two inhibited Vc oxidation by 46%, 27% and 62%, respectively. Piericidin A had no effect on Vc oxidation.

1.3. Oxidation of propyl gallate (PG) and SHAM

1.3.1. Effect of FeCl_3

PG can be oxidized by *A. ferrooxidans* and the oxidation rate of PG increased with the concentration of PG up to 60 mM beyond which the rate decreased (data not shown). The concentration of PG, 4 mM, was used for detailed studies. FeCl_3 from 0.5 mM to 10 mM greatly stimulated PG oxidation by 2 – 27 folds and the chemical oxidation of PG by O_2 in the presence of FeCl_3 was 7 – 40% (Table 1-12 and Fig. 1-15).

SHAM could also be oxidized by *A. ferrooxidans*. However the oxidation was too slow to be measured. In the presence of FeCl_3 , the oxidation rate of SHAM was fast enough to be measured (Fig. 1-16). SHAM, however, would form a precipitate complex with FeCl_3 , which coated the electrode of the oxygraph with a film making it difficult to

accurately measure O_2 consumption. Therefore further studies of SHAM oxidation were stopped. The stimulation of the oxidations of PG and SHAM by $FeCl_3$ indicates these two compounds may reduce Fe^{3+} on the cell surface to Fe^{2+} which will be oxidized using the Fe^{2+} oxidation system in this organism.

1.3.2. Effect of uncouplers on PG oxidation

The oxidation of PG was more sensitive to inhibition by uncouplers than Fe^{2+} oxidation. CCCP and DNP inhibited PG oxidation only slightly in the concentration range that stimulated Fe^{2+} oxidation (Table 1-13).

1.3.3. Effect of electron transport inhibitors on PG oxidation

PG oxidation was sensitive to the inhibition of complex IV inhibitors KCN and NaN_3 . KCN and NaN_3 both at 1 mM almost completely inhibited PG oxidation (Table 1-14).

Table 1-15 shows the effect of inhibitors of complex I and complex III. Complex I inhibitors amytal and piericidin A had no effect on PG oxidation. Complex I inhibitors, rotenone and atabrine, and complex III inhibitors, HQNO, myxothiazol and antimycin A, individually inhibited PG oxidation by 9 – 29% . Combination of complex III inhibitors resulted in 40% inhibition. The addition of 10 μ M CCCP magnified the inhibition by atabrine.

1.4. Oxidation of L-cysteine (Cys)

1.4.1. Effect of FeCl₃

Cys was oxidized by *A. ferrooxidans*. FeCl₃ at 1 mM, 4 mM and 8 mM stimulated Cys oxidation by 370%, 340% and 320%, respectively (Fig. 1-17). Cys could not be chemically oxidized by O₂ in the presence of FeCl₃. Thus Cys oxidation, similar to oxidations of Vc, PG and SHAM, may also use the Fe²⁺ oxidation system.

1.4.2. Effect of uncouplers

During a 6 min time-course experiment, CCCP at 0.5 μM, 1 μM had no effect and at 10 μM showed 19% inhibition on Cys oxidation, and DNP at 30 μM showed 7% stimulation and at 100 μM showed 4% inhibition (Table 1-16). When reactions were observed for only 90 s, 30 μM DNP and 0.5 μM CCCP stimulated Cys oxidation by 25% and 4%, respectively (Table 1-16).

1.4.3. Effect of electron transport inhibitors

The oxidation of Cys was sensitive to the inhibition by complex IV inhibitors KCN and NaN₃. KCN at 2 mM and 1 mM NaN₃ both inhibited Cys oxidation by 100% (Table 1-17).

Oxidation of Cys, like that of Fe²⁺, was also sensitive to the inhibition by inhibitors of both complex I (except piericidin A) and complex III (Table 1-18). Thus, the experiment was also carried out to test if an uncoupler could stimulate the activities which were reduced by these inhibitors. Oxidation of Cys was inhibited by inhibitors of complex I (rotenone and amytal) and III (antimycin A, myxothiazol and HQNO) by 5 –

39% (Table 1-18) and these inhibited activities were stimulated in the presence of 10 μM DNP (Table 1-18 and Fig. 1-18). Atabrine strongly inhibited Cys oxidation and the inhibited activity was further inhibited by the addition of an uncoupler CCCP (Table 1-18).

1.5. Oxidation of glutathione (GSH)

1.5.1. Effect of FeCl_3

GSH was oxidized by *A. ferrooxidans* and FeCl_3 at 2 mM stimulated GSH oxidation by 790% (Fig. 1-19). There was no O_2 consumption without cells (Fig. 1-19). So GSH oxidation also used the Fe^{2+} oxidation system.

1.5.2. Effect of uncouplers

Oxidation of GSH was slower than Cys oxidation and less sensitive to inhibition by uncouplers. The maximal stimulations were 14% and 15% by 0.5 μM CCCP and 100 μM DNP, respectively, within a reaction time of 7 min (Table 1-19).

1.5.3. Effect of electron transport inhibitors

Table 1-20 shows that GSH oxidation was sensitive to the inhibition by complex IV inhibitors KCN and NaN_3 . KCN at 2 mM and NaN_3 at 1 mM both completely inhibited GSH oxidation. GSH was oxidized by O_2 at a rate 1% of that of the biological oxidation.

Table 1-21 shows the effects of inhibitors of complex I and complex III on GSH oxidation. Atabrine at 2 mM inhibited GSH oxidation by 25% and the inhibition was magnified to 65% by the addition of 100 μM CCCP which alone showed only 14%

inhibition. Complex I inhibitors rotenone, amytal and piericidin A and complex III inhibitors myxothiazol, antimycin A and HQNO showed no effect.

1.6. Oxidation of tiron

1.6.1. Effect of FeCl₃

The oxidation of tiron was very slow in the absence of FeCl₃ (Table 1-22 and Fig. 1-20). FeCl₃ at 4 mM stimulated tiron oxidation by 31 folds with the chemical oxidation rate amounting to only 1% (Table 1-22 and Fig. 1-21). So tiron oxidation used the Fe²⁺ oxidation system and detailed studies of tiron oxidation have been carried out by using 4 mM tiron and 4 mM FeCl₃.

1.6.2. Effect of uncouplers

Tiron oxidation was more sensitive to inhibition by uncouplers than Fe²⁺ oxidation. CCCP at 0.5 μM and 10 μM inhibited tiron oxidation by 13% and 57%, respectively and DNP at 20 μM and 0.1 mM inhibited tiron oxidation by 17% and 45%, respectively (Table 1-22).

1.6.3. Effect of electron transport inhibitors

Complex IV inhibitors KCN at 2 mM and NaN₃ at 1 mM both completely inhibited tiron oxidation (Table 1-22).

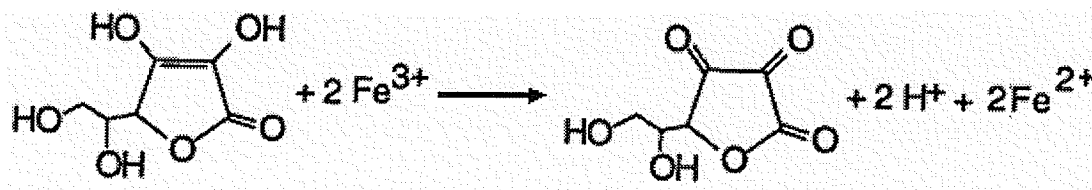
Oxidation of tiron, similar to Fe²⁺ oxidation, was inhibited 58% by 2 mM atabrine and the inhibition was amplified to 74% in the presence of 10 μM CCCP (Table 1-22 and Fig. 1-21). Complex III inhibitor HQNO inhibited tiron oxidation by 59% in the

presence of 4 mM FeCl_3 but had no effect in the absence of FeCl_3 (Table 1-22 and Fig. 1-22). The inhibition in the presence of FeCl_3 could be due to some unknown interaction among HQNO, FeCl_3 and tiron which affected the consumption of O_2 . Complex III inhibitors antimycin A and myxothiazol and complex I inhibitors amytal, rotenone and piericidin A showed no effect (Table 1-22).

1.7. Chemical reduction of Fe^{3+} by these organic compounds (Vc, PG, SHAM, tiron, Cys and GSH)

Since the oxidation of Vc, PG, SHAM, tiron, Cys and GSH was greatly stimulated by FeCl_3 , possibility that these compounds could chemically reduce Fe^{3+} to Fe^{2+} was investigated. The results shown in Table 1-23 indicate that these compounds indeed reduce Fe^{3+} to Fe^{2+} .

Vc, a well-known reducing agent, reduced Fe^{3+} instantly with a stoichiometry of 2 Fe^{2+} production for every Vc in agreement with the formation of dehydroascorbic acid (Reaction 1).

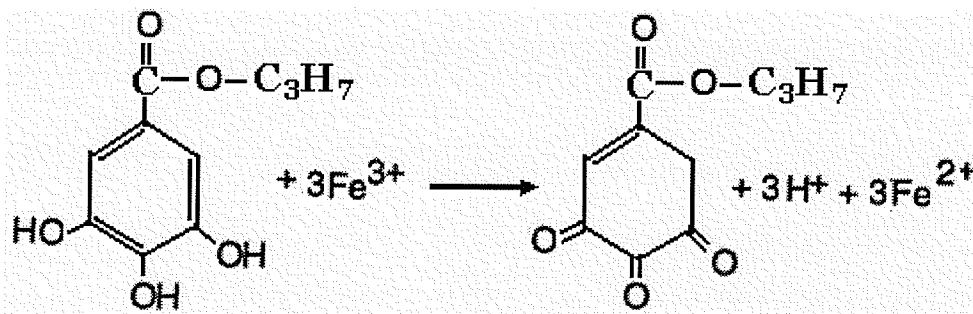


Reaction 1. Ascorbic acid (Vc) oxidation by Fe^{3+} .

PG binds Fe^{3+} forming a black complex, SHAM a red complex and tiron a blue complex. All three of them are hydroxy benzene compounds with one (SHAM), two

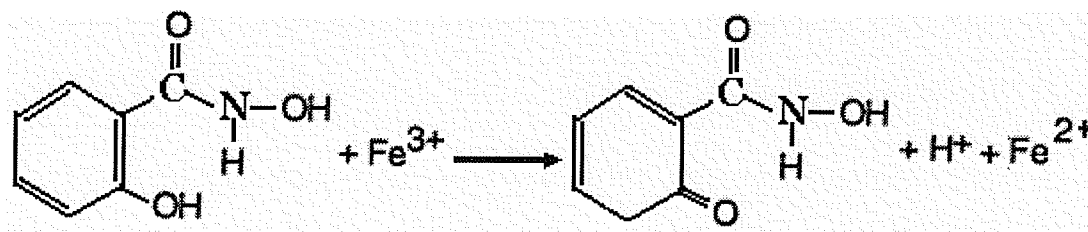
(tiron) or three (PG) hydroxyl groups, which are possibly oxidized to keto groups by reducing Fe^{3+} to Fe^{2+} .

PG reduced 3 Fe^{3+} instantly possibly following reaction 2, then the reduction continued with time for a further 5 Fe^{3+} in 60 min perhaps due to unstable nature of the keto products.



Reaction 2. Propyl gallate (PG) oxidation by Fe^{3+} .

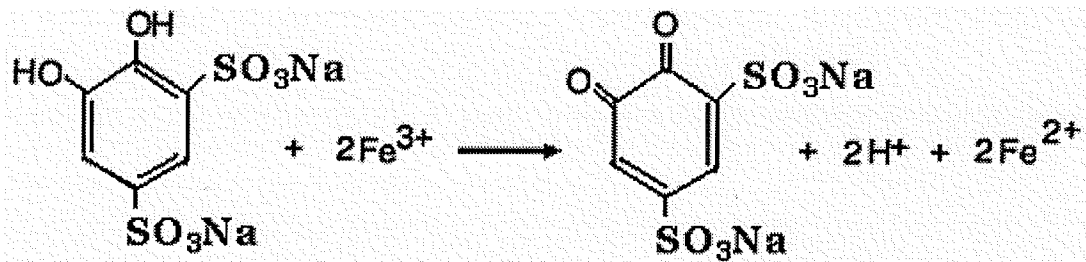
SHAM reduced one Fe^{3+} per SHAM molecule instantly in the presence of cells possibly according to reaction 3.



Reaction 3. SHAM oxidation by Fe^{3+} .

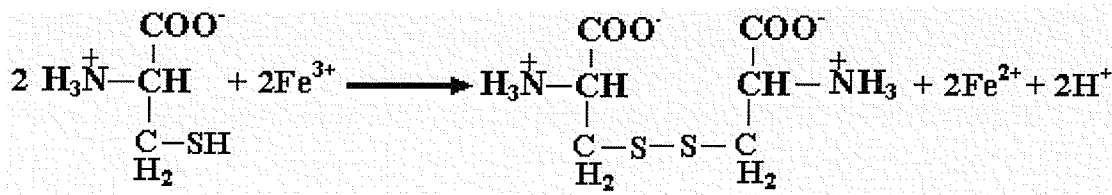
Tiron at 4 mM instantly reduced 1 mM and 2.6 mM Fe^{3+} without and with cells, respectively, and in 60 min reduced 1.1 mM and 2.9 mM Fe^{3+} , respectively.

Theoretically, one tiron could reduce 2 Fe^{3+} to 2 Fe^{2+} (Reaction 4) if both hydroxyl groups were oxidized.

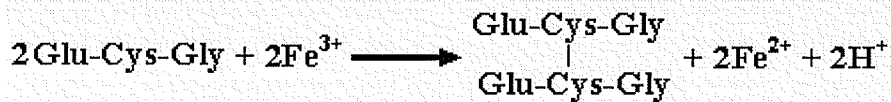


Reaction 4. Tiron oxidation by Fe^{3+} .

Cys and GSH contain sulfhydryl (thiol) groups which rapidly reduced Fe^{3+} to Fe^{2+} with a stoichiometry of 1 mM Fe^{2+} for 1 mM Cys or GSH in agreement with the formation of disulfide bonds (Reactions 5 and 6).



Reaction 5. Cys oxidation by Fe^{3+} .



Reaction 6. GSH oxidation by Fe^{3+} .

O_2 consumption experiments (without external Fe^{3+}) have been carried out to check the stoichiometry for the oxidation of these compounds by cells. The oxidations of Vc, Cys and GSH agreed with the stoichiometries of 1 O_2 consumed from 2 Vc, 4 Cys and 4 GSH, respectively. The oxidations of PG, SHAM and tiron with and without Fe^{3+} were too slow to successfully show the stoichiometry (data not shown).

1.8. Oxidations by spheroplasts and cell free extracts

The spheroplasts of *A. ferrooxidans* were made according to the method used by Apel et al. (1980). Table 1-24 shows that spheroplasts could oxidize Fe^{2+} , Vc, PG, GSH and Cys when tested in 0.1 M β -alanine- H_2SO_4 buffer of pH 3.5 in 10% sucrose.

Spheroplasts showed 60%, 12%, 82%, 19% and 16% of the oxidation activities of Fe^{2+} , Vc, PG, GSH and Cys by intact cells, respectively. The decrease of oxidation activities may be due to the loss, damage or disorganization of electron transport enzyme(s) during the preparation of spheroplasts. When Fe^{2+} oxidation by spheroplasts was tested in 0.1 M β -alanine- H_2SO_4 buffer of pH 3.5 without sucrose and in water of pH 3.5 without sucrose, the activity, compared to that in the presence of sucrose, decreased 41% and 88%, respectively (Figs. 1-23 & 1-24). This confirmed that at least the main products by the method of Apel et al. (1980) were spheroplasts. The spheroplasts could

be stored at 4°C (no stirring) for 3 days without loss of Fe²⁺ oxidation activity (data not shown). Detailed studies with spheroplasts were only carried out on Fe²⁺ oxidation affected by uncouplers. Fe²⁺ oxidation was more sensitive to inhibition by uncouplers in spheroplasts than in intact cells. DNP at 20 μM and 100 μM showed 9% and 15% inhibition, respectively, on Fe²⁺ oxidation by spheroplasts, and CCCP at 0.5 μM and 10 μM showed 4% and 29% inhibition, respectively (Table 1-25).

Cell free extracts also showed 4 – 5% Fe²⁺ oxidation activity of intact cells (Fig. 1-24). Oxidations of other compounds interacting with ferric iron were not tested.

Discussion and conclusions

Uncouplers CCCP and DNP stimulated Fe^{2+} oxidation suggesting proton pumping by cytochrome *c* oxidase (Fig. 6) and a normal respiratory control during Fe^{2+} oxidation. That uncouplers stimulated Fe^{2+} oxidation maximally by only 30% may be due to that (1) the rate of Fe^{2+} oxidation by resting cells was very close to the maximal rate of oxygen consumption by growing cells; (2) some energy from Δp was used for the uphill reaction to reduce NAD^+ and for the energy requiring step from rusticyanin to cytochrome c_4/c_{552} (Fig. 6). It was reported that the rate of Fe^{2+} oxidation was 10 times faster than the respiration rate of mitochondria (Ingledeew 1982). Previous studies only showed inhibition but not stimulation of Fe^{2+} oxidation by uncouplers (Beck and Shafia 1964; Ingledeew et al. 1977). The reason may have been due to the Warburg manometric methods used could not measure O_2 consumption within one minute. P_i stimulated Fe^{2+} oxidation by 20% in the absence of an uncoupler but did not show stimulation in the presence of an uncoupler. After cells with and without the treatment of uncoupler have been washed for several times, P_i greatly stimulated Fe^{2+} oxidation by 60%. These results indicate that cells may lose P_i when washed and the addition of P_i may have stimulated ATP generation via increasing substrate (P_i) concentration. Thus Fe^{2+} respiration is controlled by ATP generation. The effects of other Δp dissipators CH_3COOK and KSCN on Fe^{2+} oxidation also support a respiratory control during Fe^{2+} oxidation. The high sensitivity of Fe^{2+} oxidation to the inhibition by uncouplers in *A. ferrooxidans* is similar to the situation in other autotrophic bacteria such as *Nitrobacter*, *Nitrosomonas europaea* and *Acidithiobacillus thiooxidans* (previously *Thiobacillus thiooxidans*). In *Nitrobacter*, electrons from nitrite have to go through an energetically uphill reaction from cytochrome a_1 to cytochrome *c* (Aleem 1977; Kiesow 1967). In

Nitrobacter, nitrite oxidation is inhibited by uncouplers, while NADH oxidation is stimulated by them (Aleem 1977; Cobley 1976a, 1976b; Kiesow 1967). Ammonia oxidation by *N. europaea* (Whittaker et al. 2000) and the oxidation of sulfur or sulfite by *A. thiooxidans* (Masau et al. 2001; Suzuki et al. 1999) are also inhibited by uncouplers. The inhibition of the oxidation of inorganic compounds by uncouplers in these autotrophic bacteria supports that energy (Δp) is required in an uphill electron transport pathway in these organisms.

Inhibitors of ATP synthase, DCCD and oligomycin, had no effect on Fe^{2+} oxidation. The reason may be due to that these two compounds cannot go through the cell wall of this organism as oligomycin did not inhibit ATP generation in the intact cells but inhibited it in the membrane vesicles of *Acidithiobacillus caldus* (Dopson et al. 2002) and DCCD inhibited ATP generation in the membrane vesicles of *A. ferrooxidans* (Apel et al. 1980).

Complex IV inhibitors KCN and NaN_3 strongly inhibited Fe^{2+} oxidation supporting that cytochrome *c* oxidases (aa_3 and ba_3) are the terminal oxidases for Fe^{2+} respiration. It was observed that KCN inhibition was progressive with time while NaN_3 showed complete inhibition initially and then some activity recovered when the concentrations used were not very high (Figs. 1-7 & 1-8). The pattern of KCN inhibition is possibly due to the difficulty cyanide anion would have in penetrating the cells. The pattern of NaN_3 inhibition may be interpreted by the additional effects of NaN_3 besides inhibiting cytochrome *c* oxidase, that is, inhibiting ATPase and destroying Δp by working as a weak acid (Harold 1972; Hesse et al. 2002). The inhibition of electron flow via ATP synthase by NaN_3 may account for the initial complete inhibition while the later activity

recovery may be due to uncoupling of respiration from ATP synthesis by the weak acid effect of NaN_3 when the concentration of NaN_3 was not too high to completely inhibit cytochrome *c* oxidase. In fact, NaN_3 could inhibit ATP synthase in *A. ferrooxidans* although DCCD was not effective (Adapoe and Silver 1975). The effect of NaN_3 may indicate an obligatory coupling between Fe^{2+} oxidation and ATP generation.

The partial inhibition (9 – 30%) of Fe^{2+} oxidation by complex I inhibitors rotenone, amytal and atabrine, and complex III inhibitors HQNO, antimycin A and myxothiazol, indicates that some electrons from Fe^{2+} oxidation also flow along the uphill electron transport pathway from cytochrome *c* to NDH-1 to reduce NAD^+ (Fig. 6). The inhibition was not high in agreement with the idea that only a small portion of electrons (about 10%) may be used for NAD^+ reduction (Ingledeew 1982). The effect observed was indirect, that is, the effect on Fe^{2+} oxidation but consistent with the DNP stimulation after the inhibition by rotenone, amytal, HQNO, antimycin A and myxothiazol. This is different from the situation where the most portion of electrons supplied were directly used for NAD^+ reduction demonstrated by Elbehti et al. (2000). Elbehti et al. (2000) studied the oxidation of external reduced cytochrome *c* in spheroplasts in the presence of KCN. In their case, complex I inhibitors (rotenone, amytal and atabrine) showed 65 – 85% inhibition and complex III inhibitors (HQNO, antimycin A, myxothiazol and others) showed 30 – 75% inhibition on cytochrome *c* oxidation.

The flow of some electrons in the uphill pathway (NAD^+ reduction) could release the “pressure” by excess energy (Δp). When the uphill pathway was inhibited, the excess Δp would make Fe^{2+} oxidation slow down. So the uphill electron transport pathway is the other respiratory controller for Fe^{2+} oxidation in addition to ATP synthase. Therefore, it

is expected that uncouplers will stimulate the inhibited-activities of Fe^{2+} oxidation by inhibitors of complexes I and III, as the experiments showed (Tables 1-5 & 1-6 and Fig. 1-13). Proton motive force (Δp) is also required for generation of the reducing power (NAD(P)H) in other autotrophic organisms such as the photosynthetic purple bacterium *Rhodospseudomonas sphaeroides* (now *Rhodobacter sphaeroides*) (Armitage et al. 1985), the ammonia oxidizer *N. europaea* (Whittaker et al. 2000), the nitrite oxidizer *Nitrobacter* (Kiesow 1967) and the sulfur oxidizer *A. thiooxidans* (Masau et al. 2001; Suzuki et al. 1999). The similar experiment (inhibitors plus an uncoupler) providing an evidence for the uphill electron transport pathway has not been performed in these organisms.

The effect of complex I inhibitor atabrine is unusual. The reduced activity of Fe^{2+} oxidation by atabrine was not stimulated by an uncoupler but the inhibition could be magnified by the addition of an uncoupler (Fig. 1-13). This indicates that atabrine may also inhibit Fe^{2+} oxidation at other place(s) than at complex I.

Another complex I inhibitor piericidin A had no effect on Fe^{2+} oxidation (Table 1-5). The effects of atabrine and piericidin A on Fe^{2+} oxidation are different from their effects on the oxidations of endogenous substrates (Part II), fructose (Part III), YE and CA (Part IV) and formic acid (Part V). The oxidations of these substrates used downhill electron transport pathways starting from complex I (involving NADH oxidation) or other dehydrogenases. They were also inhibited by piericidin A but not by atabrine (see Part II to Part V). Since complex I inhibitors inhibited Fe^{2+} oxidation indirectly by affecting reverse (uphill) electron transport, the opposite effects of atabrine and piericidin A on NAD^+ reduction and NADH oxidation may indicate two types of complex I (NDH-1) in

A. ferrooxidans responsible for the uphill reaction (NAD⁺ reduction) and the downhill reaction (NADH oxidation), respectively. In fact the genes encoding the subunits of two types of complex I have been found in the partial genome sequence of *A. ferrooxidans* strain 23270. The Nuo subunit genes of one type of complex I (Type I) have high similarity to those from archaea and proteobacteria and the subunit genes of the other type of complex I (Type II) have high similarity to those from eukaryote and cyanobacteria. The amino acid sequences for some subunits (especially the corresponding subunits) of these two types of complex I are from different parts in a same putative ORF (open reading frame) with substantial overlapping. Fig. 1-25 shows an example of the putative ORF containing the subunits 6 of the two types of complex I. The existence of two types of complex I (NDH-1) has been reported in the cyanobacteria *Synechocystis* sp. strain PCC6803 (Cournac et al. 2004; Ohkawa et al. 2000) and *Synechococcus* sp. PCC7942 (Maeda et al. 2002). The amino acid sequence of the subunit 6 of the Type II complex I in *A. ferrooxidans* has 22% of identity and 43% of conserved replacement with the subunit 6 of one type of complex I in the cyanobacterium *Synechocystis* sp. strain PCC6803 (Fig. 1-25c). Therefore, it is quite possible that two types of complex I (NDH-1) exist in *A. ferrooxidans* although it is uncertain which type (Type I or Type II) is involved in the uphill (or downhill) reaction. One type of NDH-1 (NDH-1_{up}) is responsible for the uphill reaction (NAD⁺ reduction) and the other type (NDH-1_{down}) is responsible for the downhill reaction (NADH oxidation).

It is obvious that the oxidations of Vc, PG, SHAM, Cys, GSH and tiron were using the Fe²⁺ oxidation system since these compounds reduced Fe³⁺ to Fe²⁺ (Table 1-23) and

their oxidation by O_2 were greatly stimulated by $FeCl_3$. The effects of complex I inhibitors atabrine and piericidin A and complex IV inhibitors KCN and NaN_3 on these oxidations were same as on Fe^{2+} oxidation: atabrine showed inhibition and the inhibition could be magnified by an uncoupler; piericidin A had no effect, and KCN and NaN_3 showed strong inhibition.

Table 1-26 shows the comparison of the inhibition of the oxidations of these organic compounds and Fe^{2+} by inhibitors of complexes I and III. Except for the effects by atabrine and piericidin A, the inhibition by these inhibitors roughly follows the trend: the faster the oxidation, the higher the inhibition by inhibitors. This agrees with the hypothesis that the faster the oxidation is, the more electrons will flow along the uphill pathway to NAD^+ . The oxidation of Cys was inhibited by all inhibitors tested of complexes I and III except piericidin A, and the inhibited-activities of Cys oxidation by these inhibitors (except atabrine), similar to those of Fe^{2+} oxidation, were stimulated by uncoupler DNP (Fig. 1-18). This further confirmed that Cys oxidation was using the Fe^{2+} oxidation system in the presence of an uphill reaction pathway.

According to the studies in this dissertation combining the information in Fig. 6, a new model for the electron transport pathway of the oxidations of Fe^{2+} and the above-mentioned organic compounds by *A. ferrooxidans* is shown in Fig. 1-26.

Tables of Part I

Table 1-1. Effect of uncouplers on Fe²⁺ oxidation.*

CCCP (μM)	Rate **	R.A	DNP (μM)	Rate **	R.A
0	1.45 \pm 0.01	1.00	0	1.45 \pm 0.01	1.00
0.2	1.56 \pm 0.01	1.08	10	1.60 \pm 0.04	1.10
0.5	1.81 \pm 0.02	1.25	20	1.86 \pm 0.09	1.28
1.0	1.78 \pm 0.06	1.23	30	1.74 \pm 0.01	1.20
5.0	1.41 \pm 0.07	0.97	40	1.67 \pm 0.06	1.15
10.0	1.30 \pm 0.01	0.90	60	1.62 \pm 0.02	1.12
			100	1.54 \pm 0.04	1.06
0.5 μM + 30 μM DNP				1.70 \pm 0.01	1.17

*Cells were added to start the reaction.

** Rate: $\mu\text{mol O}_2 \text{ min}^{-1} \text{ mg protein}^{-1}$ (\pm SD, n = 3 – 5). R.A: relative activity, a ratio of the rate in the presence of an uncoupler over that in the absence (0 μM).

Table 1-2. Inhibition by uncouplers of Fe²⁺ oxidation in the absence and presence of 4 mM KH₂PO₄.*

	In the absence of KH ₂ PO ₄		In the presence of 4 mM KH ₂ PO ₄	
	Rate **	R.A	Rate **	R.A
Control	1.21 \pm 0.03	1.00	1.50 \pm 0.02	1.24
5 μM CCCP	0.33 \pm 0.00	0.27	0.34 \pm 0.00	0.28
10 μM CCCP	0.16 \pm 0.02	0.13	0.17 \pm 0.02	0.14
0.1 mM DNP	0.98 \pm 0.01	0.81	0.98 \pm 0.00	0.81
1 mM DNP	0.73 \pm 0.02	0.60	0.74 \pm 0.00	0.61

*Cells were pre-incubated with uncouplers for 5 min.

** Rate: $\mu\text{mol O}_2 \text{ min}^{-1} (\text{mg protein})^{-1}$ (\pm SD, n = 3). R.A: relative activity, a ratio of a rate over that of control in the absence of KH₂PO₄.

Table 1-3. Effect of CH₃COOK on Fe²⁺ oxidation.*

CH ₃ COOK	Rate **	R.A
Control	1.11 ± 0.00	1.00
50 µM	1.22 ± 0.01	1.10
0.1 mM	1.24 ± 0.01	1.12
0.2 mM	1.28 ± 0.01	1.15
0.5 mM	1.26 ± 0.02	1.14
1 mM	1.20 ± 0.02	1.08
2 mM	1.14 ± 0.02	1.03
10 mM	0.79 ± 0.01	0.71
40 mM	0.35 ± 0.01	0.32

*Cells were added to start the reaction. *Cells were added to start the reaction.

** Rate: µmol O₂ min⁻¹ mg protein⁻¹ (± SD, n = 3). R.A: relative activity, a ratio of the rate in the presence of CH₃COOK over that in the absence (control).

Table 1-4. KCN and NaN₃ on Fe²⁺ oxidation.*

Concentration		Rate **	R.A
Endogenous		0.92 ± 0.08	0.002
Control		590.94 ± 8.44	1.00
KCN	2 mM	0.58 ± 0.02	0.001
NaN ₃	0.1 mM	11.52 ± 0.29	0.019
	1 mM	0.87 ± 0.01	0.002
	2 mM	0.59 ± 0.02	0.001

*Cells (24 mg / mL) were added to start the reaction.

** Rate: nmol O₂ min⁻¹(mg protein)⁻¹. R.A: relative activity, a ratio of the rate in the presence of KCN or NaN₃ over that in the absence (control) or the rate of endogenous respiration over that of control.

Table 1-5. Effects of complex I inhibitors on Fe^{2+} oxidation in the presence and absence of DNP.*

	No DNP		Plus 10 μM DNP		Plus 100 μM DNP	
	Rate **	R.A	Rate **	R.A	Rate **	R.A
Only cells	1.31 \pm 0.03	1.00	1.30 \pm 0.03	0.96	1.25 \pm 0.02	1.16
DNP			1.35 \pm 0.03	1.00	1.08 \pm 0.01	1.00
Am	1.12 \pm 0.04	0.85	1.33 \pm 0.02	0.99	0.98 \pm 0.02	0.91
At	1.09 \pm 0.02	0.83	1.08 \pm 0.01	0.80	0.55 \pm 0.00	0.51
R	1.08 \pm 0.05	0.82	1.30 \pm 0.01	0.96	0.90 \pm 0.01	0.83
<hr/>						
Only cells	1.37 \pm 0.01	1.00	1.69 \pm 0.03	0.96	1.64 \pm 0.02	1.16
DNP			1.76 \pm 0.01	1.00	1.41 \pm 0.03	1.00
R + Am	1.11 \pm 0.03	0.81	1.75 \pm 0.02	0.99	1.20 \pm 0.01	0.85
R + At	0.97 \pm 0.04	0.71	1.39 \pm 0.04	0.79	0.56 \pm 0.01	0.40
Am + At	1.05 \pm 0.01	0.77	1.50 \pm 0.02	0.85	0.71 \pm 0.02	0.50
Am + At + R	0.92 \pm 0.02	0.67	1.29 \pm 0.01	0.73	0.52 \pm 0.01	0.37
<hr/>						
Only cells	1.35 \pm 0.13	1.00				
PA	1.36 \pm 0.04	1.01				
PA + R + Am	1.18 \pm 0.03	0.87				

*Cells (2.4 mg / mL) were pre-incubated with inhibitors plus / minus DNP for 5 min before addition of Fe^{2+} .

** Rate: $\mu\text{mol O}_2 \text{ min}^{-1}(\text{mg protein})^{-1}$ ($\pm\text{SD}$, $n = 3 - 6$); R.A: relative activity, a ratio of the rate in the presence of electron transport inhibitor(s) over that in the absence (control activity). When DNP was absent control activities were those with "Only cells". When DNP was present control activities were those in the presence of 10 μM or 100 μM DNP. Am: 1 mM amytal; R: 0.1 mM rotenone; PA: 0.5 μM Piericidin A; At: 2 mM atabrine.

Table 1-6. Effects of complex III inhibitors and combinations of complex I and III inhibitors on Fe^{2+} oxidation in the presence and absence of DNP.*

	No DNP		Plus 10 μM DNP		Plus 0.1 mM DNP	
	Rate **	R.A	Rate **	R.A	Rate **	R.A
Only cells	1.35 \pm 0.11	1.00	1.61 \pm 0.03	0.97	1.20 \pm 0.04	1.19
DNP			1.66 \pm 0.04	1.00	1.01 \pm 0.02	1.00
An	1.13 \pm 0.03	0.84	1.51 \pm 0.02	0.91	0.97 \pm 0.01	0.96
My	1.25 \pm 0.01	0.93	1.69 \pm 0.03	1.02	1.00 \pm 0.01	0.99
H	1.16 \pm 0.05	0.86	1.52 \pm 0.00	0.92	0.92 \pm 0.01	0.91
Only cells	1.52 \pm 0.03	1.00	1.48 \pm 0.03	0.92	1.43 \pm 0.03	1.13
DNP			1.61 \pm 0.04	1.00	1.27 \pm 0.04	1.00
An + My	1.38 \pm 0.01	0.91	1.54 \pm 0.03	0.96	1.20 \pm 0.04	0.94
An + H	1.10 \pm 0.01	0.72	1.44 \pm 0.06	0.89	1.09 \pm 0.03	0.86
My + H	1.27 \pm 0.01	0.84	1.52 \pm 0.07	0.94	1.19 \pm 0.03	0.94
An + H + My	1.05 \pm 0.01	0.69	1.52 \pm 0.06	0.94	1.07 \pm 0.02	0.84
Only cells	1.49 \pm 0.05	1.00	1.49 \pm 0.05	0.93	1.49 \pm 0.05	1.17
DNP			1.61 \pm 0.04	1.00	1.27 \pm 0.04	1.00
I + III	0.89 \pm 0.01	0.60	0.65 \pm 0.04	0.40	0.37 \pm 0.01	0.29

*Cells were pre-incubated with inhibitors plus / minus DNP for 5 min before addition of Fe^{2+} .

** Rate: $\mu\text{mol O}_2 \text{ min}^{-1}(\text{mg protein})^{-1}$ ($\pm\text{SD}$, n = 3 - 6); R.A: relative activity (definition is same as in Table 1-4); An: 10 μM antimycin A; My: 10 μM myxothiazol; H: 40 μM HQNO; I + III: R + Am + At + An + H + My. The concentrations of R, Am and At are same as in Tabel 1-5.

Table 1-7. Stimulation by FeCl₃ of Vc oxidation.

Concentration		Rate *	R.A
Endogenous respiration		0.0 ± 0.0	0
Only Vc **		12.5 ± 3.1	0.02
Vc + 4 mM FeCl ₃ **		3.1 ± 0.0	0.00
Control		750.0 ± 50.0	1.00
FeCl ₃	0.4 mM	1190.0 ± 6.3	1.59
	1 mM	1271.9 ± 6.3	1.70
	2 mM	1287.5 ± 6.3	1.72
	4 mM	1193.8 ± 18.8	1.59

* Rate: nmol O₂ min⁻¹(mg protein)⁻¹ (±SD, n = 3); ** Cells were not added and rates were converted to values as if cells were present; R.A: relative activity, a ratio of a rate over the rate of control.

Table 1-8. Effect of uncouplers on Vc oxidation.

[CCCP] (μM)	Effect of CCCP		DNP (μM)	Effect of DNP	
	Rate *	R.A		Rate *	R.A
0	674.0 ± 18.6	1.00	0	674.0 ± 18.6	1.00
0.1	681.9 ± 15.1	1.01	5	684.5 ± 0.7	1.02
0.2	701.0 ± 20.2	1.04	10	727.1 ± 4.0	1.08
0.5	762.1 ± 24.8	1.13	20	754.2 ± 40.3	1.12
1.0	730.2 ± 11.3	1.08	30	751.3 ± 44.1	1.11
5.0	616.2 ± 15.4	0.91	40	678.1 ± 4.1	1.01
10.0	544.4 ± 14.9	0.81	60	677.2 ± 19.1	1.00
			100	660.1 ± 28.3	0.98
0.5 μM CCCP + 30 μM DNP				791.4 ± 18.1	1.17

* Rate: nmol O₂ min⁻¹(mg protein)⁻¹ (±SD, n = 3); R.A: relative activity, a ratio of a rate over the rate of control (0 μM).

Table 1-9. Effect of inhibitors of complex IV on Vc oxidation.

	Concentration	Rate *	R.A
Control		771.9 ± 46.9	1.00
KCN	10 µM	590.6 ± 9.4	0.77
	0.1 mM	17.2 ± 0.0	0.02
	1 mM	0.0 ± 0.0	0.00
NaN ₃	1 µM	375.0 ± 40.6	0.49
	10 µM	68.2 ± 6.3	0.09
	0.1 mM	0.0 ± 0.0	0.00

* Rate: nmol O₂ min⁻¹(mg protein)⁻¹ (±SD, n = 3); R.A: relative activity, a ratio of a rate over the rate of control.

Table 1-10. Effect of inhibitors of complex III on Vc oxidation.

	Concentration	Rate *	R.A
In the absence of FeCl ₃			
Control		739.1 ± 39.4	1.00
Myxothiazol	40 µM	768.8 ± 11.7	1.04
Antimycin A	0.1 mM	742.7 ± 10.7	1.00
HQNO	5 µM	746.4 ± 8.7	1.01
	10 µM	715.0 ± 9.0	0.97
	20 µM	711.5 ± 10.8	0.96
	30 µM	845.5 ± 11.5	1.14
	40 µM	837.0 ± 6.7	1.13
In the presence of 4 mM FeCl ₃			
Control		1037.5 ± 3.1	1.00
HQNO	40 µM	1103.1 ± 3.1	1.06

* Rate: nmol O₂ min⁻¹(mg protein)⁻¹ (±SD, n = 3); R.A: relative activity, a ratio of a rate over the rate of control.

Table 1-11. Effect of inhibitors of complex I on Vc oxidation.

	Concentration	Rate *	R.A
Control		839.8 ± 31.5	1.00
Atabrine	10 µM	839.0	1.00
	0.1 mM	425.0 ± 9.3	0.51
	1 mM	134.4 ± 6.3	0.16
	2 mM	81.3 ± 6.2	0.10
Amytal (Am)	1 mM	728.1 ± 9.4	0.87
Rotenone (R)	0.1 mM	787.5 ± 9.3	0.94
R + Am		681.3 ± 12.5	0.81
Piericidin A	0 µM	881.3 ± 0.2	1.00
	0.5 µM	871.9 ± 3.1	0.99
Control		750.0 ± 50.0	1.00
Atabrine (At)	0.1 mM	403.1 ± 53.1	0.54
CCCP	10 µM	550.0 ± 15.6	0.73
At + CCCP		281.3 ± 12.5	0.38

* Rate: $\text{nmol O}_2 \text{ min}^{-1}(\text{mg protein})^{-1}$ ($\pm\text{SD}$, $n = 3$); R.A: relative activity, a ratio of a rate over the rate of control.

Table 1-12. Effect of FeCl₃ on PG oxidation.

[FeCl ₃] (mM)	With cells (biological oxidation)		Without cells (chemical oxidation)	
	Rate *	R.A	Rate **	R.A
0	40.2 ± 0.3	1.00	2.7 ± 2.0	0.07
0.5	85.5 ± 1.1	2.13	4.1 ± 0.5	0.10
1	104.6 ± 0.7	2.60	4.2 ± 0.1	0.10
2	252.9 ± 1.4	6.29	6.5 ± 0.3	0.16
5	1058.7 ± 26.2	26.33	12.8 ± 0.7	0.32
10	1082.7 ± 7.6	26.93	16.2 ± 0.4	0.40

* Rate: nmol O₂ min⁻¹ (mg protein)⁻¹ (±SD, n = 2); R.A: relative activity, a ratio of a rate over the rate of control (0 mM FeCl₃ in the presence of cells); ** rates were converted to values as if cells were present.

Table 1-13. Effect of uncouplers on PG oxidation.

[CCCP or DNP] (μM)	CCCP		DNP	
	Rate *	R.A	Rate *	R.A
0	40.9 ± 0.1	1.00	57.7 ± 0.4	1.00
0.02	40.2 ± 0.7	0.98	57.6 ± 0.6	1.00
0.1	39.5 ± 0.1	0.97	57.7 ± 0.2	1.00
0.5	35.8 ± 0.3	0.88	54.9 ± 0.4	0.95
1	33.3 ± 0.1	0.81	53.1 ± 1.1	0.92
5	32.2 ± 0.3	0.79		
10	30.4 ± 0.1	0.74	52.0 ± 0.5	0.90
20			50.6 ± 0.5	0.88
100			49.0 ± 0.4	0.85

* Rate: nmol O₂ min⁻¹(mg protein)⁻¹ (±SD, n = 2); R.A: relative activity, a ratio of a rate over the rate of control (0 μM).

Table 1-14. Effect of KCN and NaN₃ on PG oxidation.

[KCN or NaN ₃] (mM)	KCN		NaN ₃	
	Rate *	R.A	Rate *	R.A
Only PG **	1.51 ± 0.03	0.03	1.51 ± 0.03	0.03
0	47.24 ± 0.42	1.00	43.07 ± 0.05	1.00
0.1	10.16 ± 0.42	0.22	7.03 ± 0.05	0.16
0.5	4.22 ± 0.47	0.09	2.76 ± 0.73	0.06
1	2.19 ± 0.42	0.05	1.30 ± 0.10	0.03
2	1.98 ± 0.31	0.04	1.82 ± 0.26	0.04

* Rate: nmol O₂ min⁻¹(mg protein)⁻¹ (±SD, n = 2); R.A: relative activity, a ratio of a rate over the rate of control (0 mM); ** rates were converted to values as if cells were present.

Table 1-15. Effect of inhibitors of complex I and complex III on PG oxidation.

Effect of complex I inhibitors			Effect of complex III inhibitors		
	Rate *	R.A		Rate *	R.A
Control	41.9 ± 0.8	1.00	Control	46.8 ± 0.1	1.00
Am	41.8 ± 0.4	1.00	H	33.3 ± 0.3	0.71
R	37.5 ± 0.3	0.89	My	39.4 ± 0.3	0.84
R + Am	35.6 ± 0.3	0.85	An	35.3 ± 0.1	0.75
Control	57.9 ± 0.7	1.00	H + An + My	27.9 ± 0.9	0.60
PA	56.0 ± 0.1	0.97			
At	52.5 ± 0.5	0.91			
10 μM CCCP	51.3 ± 0.2	0.89			
CCCP + At	44.3 ± 0.2	0.77			

* Rate: nmol O₂ min⁻¹(mg protein)⁻¹ (±SD, n = 2); R.A: relative activity, a ratio of a rate over the rate of control; Am: 1 mM amytal; R: 0.1 mM rotenone; PA: 0.5 μM Piericidin A; At: 2 mM atabrine; H: 40 μM HQNO; My: 40 μM myxothiazol; An: 0.1 mM antimycin A.

Table 1-16. Effect of uncoupler on Cys oxidation.

	Concentration	Rate *	R.A
Reactions within 6 min			
Control		335.9 ± 0.7	1.00
DNP	30 µM	359.4 ± 1.5	1.07
	100 µM	321.6 ± 18.0	0.96
CCCP	0.5 µM	334.4 ± 10.3	1.00
	1 µM	334.4 ± 3.0	1.00
	10 µM	272.2 ± 5.7	0.81
Reactions within 90s			
Control		368.8 ± 25.0	1.00
DNP	30 µM	462.5 ± 90.6	1.25
CCCP	0.5 µM	384.4 ± 9.4	1.04

* Rate: $\text{nmol O}_2 \text{ min}^{-1}(\text{mg protein})^{-1}$ ($\pm\text{SD}$, $n = 2$); R.A: relative activity, a ratio of a rate over the rate of control.

Table 1-17. Effect of complex IV inhibitors (KCN and NaN_3) on Cys oxidation.

	Concentration	Rate *	R.A
Only Cys, no cells		0.0 ± 0.0	0.00
Endogenous		0.0 ± 0.0	0.00
Control		226.9 ± 6.3	1.00
KCN	2 mM	0.9 ± 0.0	0.00
NaN_3	1 mM	1.0 ± 0.2	0.00

* Rate: $\text{nmol O}_2 \text{ min}^{-1}(\text{mg protein})^{-1}$ ($\pm\text{SD}$, $n = 2$); R.A: relative activity, a ratio of a rate over the rate of control.

Table 1-18. Effects of inhibitors complex I and complex III on Cys oxidation in the absence and presence of DNP.

Complex I inhibitors	No DNP		Plus 10 μ M DNP	
	Rate *	R.A	Rate *	R.A
Only cells	232.0 \pm 0.5	1.00	312.0 \pm 7.7	0.95
DNP			326.8 \pm 3.6	1.00
0.1 mM rotenone (R)	219.7 \pm 0.7	0.95	332.2 \pm 5.2	1.02
1 mM amytal (Am)	205.4 \pm 1.0	0.89	330.2 \pm 1.9	1.01
R+Am	209.1 \pm 1.5	0.90		
0.4 mM atabrine (At)			122.3 \pm 0.6	0.37
Only cells	335.9 \pm 0.7	1.00		
40 μ M atabrine	298.7 \pm 1.8	0.89		
0.4 mM atabrine (At)	125.3 \pm 7.0	0.37		
2 mM atabrine	51.9 \pm 1.1	0.15		
10 μ M CCCP (CCCP)	272.2 \pm 5.7	0.81		
At + CCCP	93.8 \pm 5.9	0.28		
Only cells	264.2 \pm 0.2	1.00		
0.5 μ M Piericidin A	259.4 \pm 6.6	0.98		
Complex III inhibitors				
Only cells	232.0 \pm 0.5	1.00	312.0 \pm 7.7	0.95
DNP			326.8 \pm 3.6	1.00
10 μ M antimycin A (An)	203.7 \pm 0.3	0.88	328.2 \pm 0.9	1.00
40 μ M myxothiazol (My)	177.2 \pm 5.9	0.76	312.3 \pm 2.2	0.96
40 μ M HQNO (H)	162.2 \pm 8.0	0.70	303.7 \pm 9.8	0.93
An+My+H	141.4 \pm 10.4	0.61	288.5 \pm 5.2	0.88

* Rate: $\text{nmol O}_2 \text{ min}^{-1}(\text{mg protein})^{-1}$ (\pm SD, n = 2); R.A: relative activity, a ratio of the oxidation rate in the presence of electron transport inhibitor(s) over that in the absence (control activity). When DNP was present control activities were those in the presence of 10 μ M DNP.

Table 1-19. Effect of uncouplers on GSH oxidation.

	Concentration	Rate *	R.A
Control		107.6 ± 1.0	1.00
No cells		1.4 ± 0.3	0.01
CCCP	0.5 µM	122.6 ± 0.4	1.14
	1 µM	121.4 ± 0.3	1.13
	5 µM	119.8 ± 1.8	1.11
	10 µM	112.2 ± 2.2	1.04
	100 µM	92.7 ± 1.2	0.86
DNP	30 µM	115.9 ± 1.9	1.08
	100 µM	124.0 ± 4.3	1.15

* Rate: $\text{nmol O}_2 \text{ min}^{-1}(\text{mg protein})^{-1}$ ($\pm\text{SD}$, $n = 2$); R.A: relative activity, a ratio of a rate over the rate of control.

Table 1-20. Effect of complex IV inhibitors (KCN and NaN_3) on GSH oxidation.

	Concentration	Rate *	R.A
Control		107.6 ± 1.0	1.00
Only GSH, no cells		1.4 ± 0.3	0.01
KCN	2 mM	1.0 ± 0.0	0.01
NaN_3	1 mM	0.6 ± 0.1	0.01

* Rate: $\text{nmol O}_2 \text{ min}^{-1}(\text{mg protein})^{-1}$ ($\pm\text{SD}$, $n = 2$); R.A: relative activity, a ratio of a rate over the rate of control.

Table 1-21. Effect of inhibitors of complex I and complex III on GSH oxidation.

	Concentration	Rate *	R.A
Complex I inhibitors			
Control		107.6 ± 1.0	1.00
Atabrine (At)	2 mM	81.1 ± 2.9	0.75
Rotenone (R)	0.1 mM	106.9 ± 1.7	0.99
Amytal (Am)	1 mM	104.9 ± 1.0	0.97
R + Am		107.8 ± 3.5	1.00
R + Am + At		78.5 ± 0.7	0.73
CCCP	100 µM	92.7 ± 1.2	0.86
CCCP + At		37.7 ± 1.3	0.35
Complex III inhibitors			
Control		85.2 ± 0.4	1.00
Piericidin A	0.5µM	87.9 ± 0.1	1.03
Complex III inhibitors			
Control		85.2 ± 0.4	1.00
HQNO	40 µM	84.7 ± 1.9	0.99
Myxothiazol	40 µM	81.1 ± 1.1	0.95
Antimycin A	0.1 mM	81.6 ± 0.7	0.96

* Rate: $\text{nmol O}_2 \text{ min}^{-1}(\text{mg protein})^{-1}$ ($\pm\text{SD}$, $n = 2$); R.A: relative activity, a ratio of a rate over the rate of control.

Table 1-22. Effect of inhibitors of complex I, complex III and complex IV, uncouplers and FeCl₃ on tiron oxidation.

No FeCl ₃ (Fe(III))	Concentration	Rate *	Relative activity
Tiron	0 mM	0.86 ± 0.26	0.23
	2 mM	3.67 ± 0.1	0.98
	4 mM	3.75 ± 0	1.00
	8 mM	5.1 ± 0.36	1.36
4 mM tiron + 40µM HQNO		3.91 ± 0.42	1.04 #
4 mM tiron + 4 mM FeCl ₃		115.52 ± 2.19	30.81
Effect of different reagents with 4 mM tiron plus 4 mM FeCl ₃			
No cells (chemical oxidation)		1.28 ± 0.26 **	0.01
Only cells		0.86 ± 0.26	0.01
Control		115.52 ± 2.19	1.00
KCN	2 mM	0.6 ± 0.0	0.01
NaN ₃	1 mM	0.6 ± 0.1	0.01
Piericidin A	0.5 µM	113.28 ± 0.91	0.98
Amytal	1 m M	111.93 ± 0.29	0.97
Rotenone	0.1 mM	110.49 ± 0.96	0.96
Atabrine (At)	2 mM	48.75 ± 0.42	0.42
At + 10 µM CCCP		30.29 ± 0.63	0.26
Antimycin A	0.1 mM	113.78±1.22	0.98
Mxothiazol	40 µM	110.05±0.55	0.95
HQNO	40 µM	47.27±1.95	0.41 ***
CCCP	0.5 µM	100.39 ± 3.8	0.87
	10 µM	49.58 ± 0.81	0.43
DNP	20 µM	95.47 ± 0.29	0.83
	0.1 mM	63.75 ± 0.99	0.55

* Rate: nmol O₂ min⁻¹(mg protein)⁻¹ (±SD, n = 2); ** as if cells were present. *** The inhibition did not show when external Fe(III) was not added (see #). Relative activity is a ratio of a rate over that of control or a rate over the rate with 4 mM tiron in the case when FeCl₃ was not present.

Table 1-23. Reduction of Fe^{3+} by various Fe^{3+} -reactive compounds in the absence and presence of cells.

Compound	Concentration	Cells (20 mg)	Reduction of Fe^{3+}			
			Fe^{2+} formed (mM) *			
			Initial	10 min	20 min	60 min
None		-	0.15			0.19
		+	0.29			0.66
Vc	2 mM	-	3.75			4.08
		+	4.00			4.36
PG	0.2 mM	-	0.63			0.98
		+	0.77			1.69
SHAM	2 mM	-	1.44			1.37
		+	1.93			2.08
Tiron	4 mM	-	0.97			1.12
		+	2.58			2.92
Cys	1 mM	-	1.04		1.06	
GSH	1 mM	-	0.60	0.99	0.96	

* 4 mM FeCl_3 , 2 mM KCN in 0.1 M β -alanine- H_2SO_4 buffer of pH 3.5 with (+) and without (-) cells in 1 mL reaction system. Initial samples of 0.1 mL were taken as soon as possible after mixing for Fe^{2+} determination with o-phenanthroline.

Table 1-24. Comparison of oxidation rates of Fe^{2+} , Vc, PG, GSH and Cys by intact cells and spheroplasts.

Substrate	*Rate: $\text{nmol O}_2 \text{ min}^{-1}(\text{mg protein})^{-1}$ ($\pm\text{SD}$, n = 3-10)		Rs/Rc (%)
	Cells (Rc)	SP (Rs)	
Fe^{2+}	1465 \pm 13	882 \pm 7	60
Vc	795 \pm 63	96 \pm 5	12
PG	50 \pm 5	41 \pm 6	82
GSH	108 \pm 1	20 \pm 3	19
Cys	229 \pm 4	36 \pm 9	16

*Rates are the average values from at least two experiments. *Rates are the average values from at least two experiments.

Table 1-25. Effect of uncouplers on Fe^{2+} oxidation by spheroplasts in 0.1 M β -alanine- H_2SO_4 of pH 3.5. *

	Concentration	Rate **	R.A
Control		928.1 \pm 6.3	1.00
DNP	20 μM	843.8 \pm 9.4	0.91
	100 μM	790.6 \pm 3.1	0.85
CCCP	0.5 μM	887.5 \pm 3.1	0.96
	10 μM	662.5 \pm 12.5	0.71

*Spheroplasts (0.19 mg protein) were added to start the reaction.

** Rate: $\text{nmol O}_2 \text{ min}^{-1}(\text{mg protein})^{-1}$ ($\pm\text{SD}$, n = 3); R.A: relative activity, a ratio of a rate over the rate of control.

Table 1-26. Inhibition (%) of oxidation of FeSO₄ (Fe²⁺), ascorbic acid (Vc), L-cysteine (Cys), Glutathione (GSH), propyl gallate (PG) and tiron by electron transport inhibitors of complexes I and III.

		Fe ²⁺	Vc	Cys	GSH	PG	Tiron *	
Inhibition (%)	Complex I inhibitors	0.5 μM PA	0	1	2	0	3	2
		2 mM At	17	90	85	25	9	58
		1 mM Am	15	13	11	3	0	3
		0.1 mM R	18	6	5	1	11	4
		Am + R	19	19	10	0	15	
	Complex III inhibitors	10 μM My	7					
		40 μM My		0	24	5	16	5
		10 μM An	16		12			
		0.1 mM An		0		4	15	2
		40 μM H	14	0	30	1	29	59 (0 **)
		My + An + H	31		39		40	
Chemical reaction (% of control)		0	2	0	1	1	1	
R.A, no FeCl ₃		1.00	0.50	0.22	0.07	0.04	0.003	
R.A, with FeCl ₃ ***		1.00	0.85	0.90	0.57	0.71	0.08	

R: rotenone; Am: amytal; At: atabrine; PA: piericidin A; An: antimycin A; My:

myxothiazol; H: HQNO. * Tiron oxidation was tested in the presence of 4 mM FeCl₃.

** Tested in the absence of FeCl₃. *** Different concentrations of FeCl₃ were used with different substrates and maximal rates were used for calculation of relative activities.

R.A: relative activity, a ratio of the oxidation rate [nmol O₂ min⁻¹ (mg protein)⁻¹] of a substrate over that of Fe²⁺ (no FeCl₃).

Figures of Part I

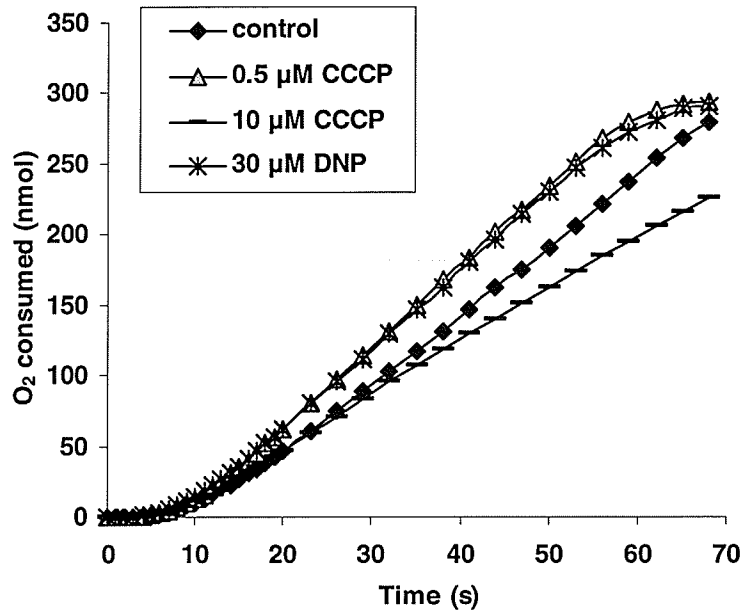
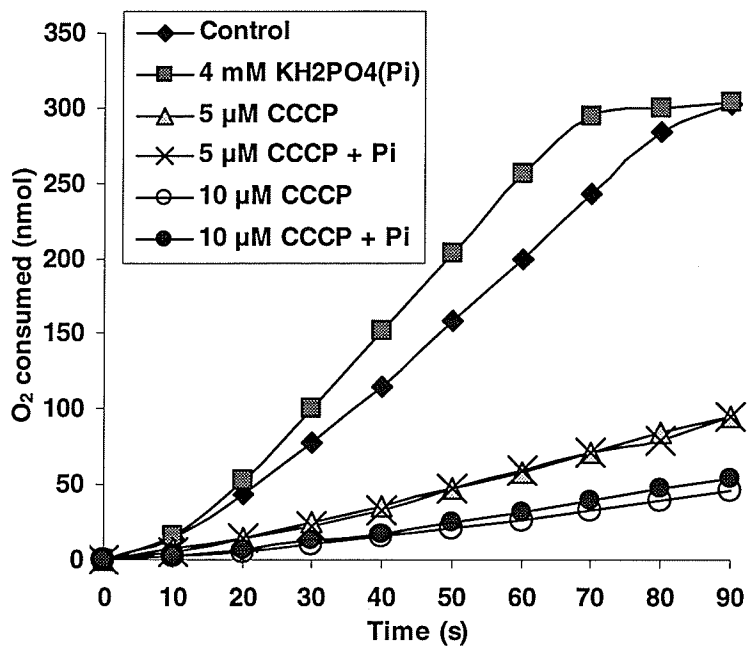
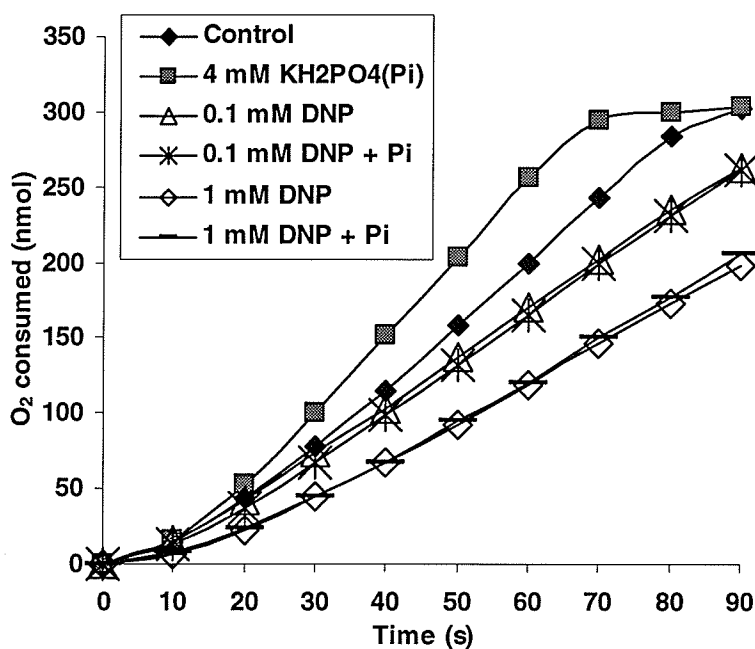


Fig. 1-1. Effect of CCCP and DNP on Fe^{2+} oxidation. Cells (2.4 mg) were added to start the reaction in Oxygraph (1.2 mL).



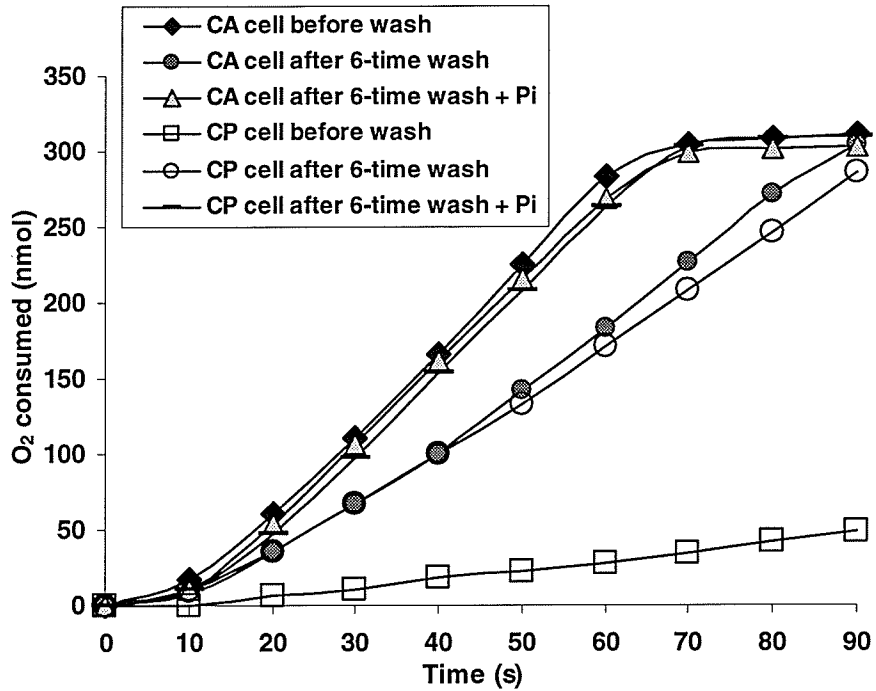
(a)



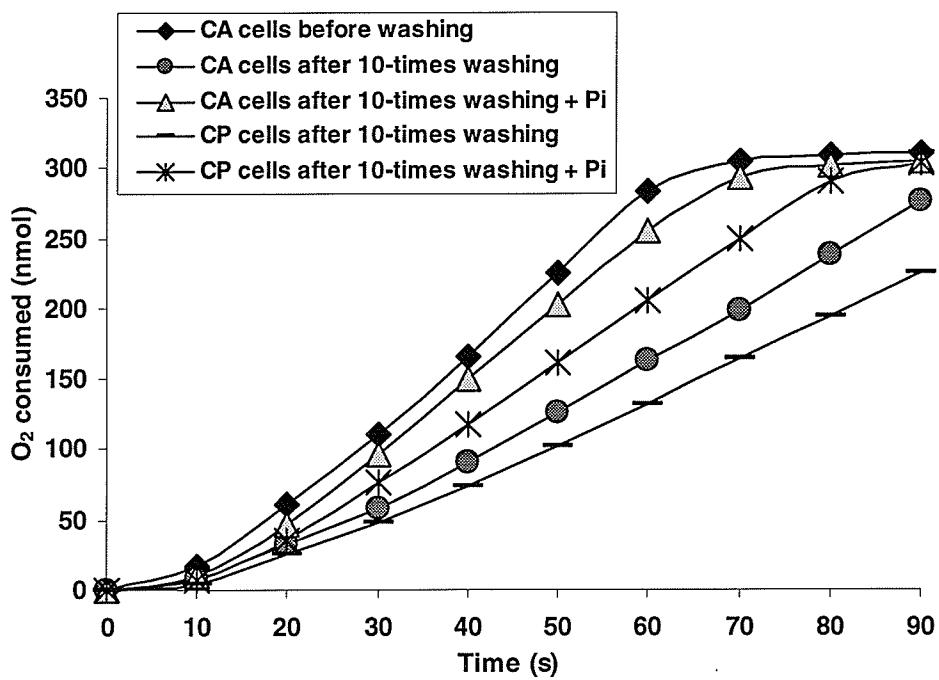
(b)

Fig. 1-2. Effect of CCCP and DNP on Fe^{2+} oxidation in the presence and absence of 4 mM KH_2PO_4 (Pi). (a) Effect of CCCP, (b) effect of DNP. Cells (2.4 mg) were preincubated with and without uncouplers for 5 min before the addition of Fe^{2+} in Oxygraph (1.2 mL).

Fig. 1-3. Effect of KH_2PO_4 (Pi, 4 mM) on Fe^{2+} oxidation by cells with and without the treatment of CCCP. Cells (20 mg / mL) were preincubated in the absence (CA cells, control cells) and presence (CP cells) with CCCP (10 μM) at 25°C for 30 min by magnetic stirring. Then cells were washed for 6 times (a) and 10 times (b) with 20 mL buffer (at 10,000 $\times g$, 10 min). Fe^{2+} oxidation was initiated by adding 2.4 mg cell in Oxygraph (1.2 mL) with and without the addition of Pi.



(a)



(b)

Fig. 1-3.

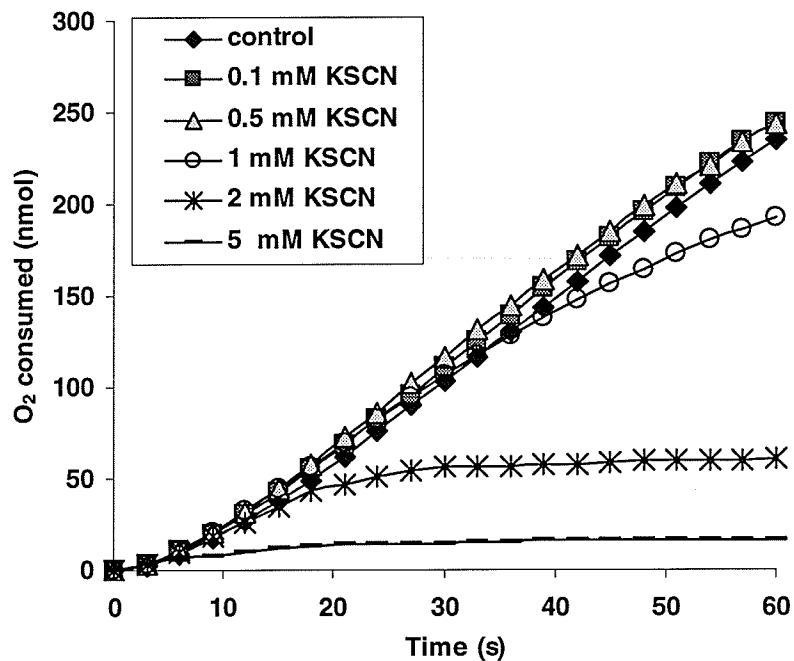


Fig.1-4. Effect of KSCN on Fe^{2+} oxidation. Cells (2.4 mg / 1.2 mL) were added to start the reaction.

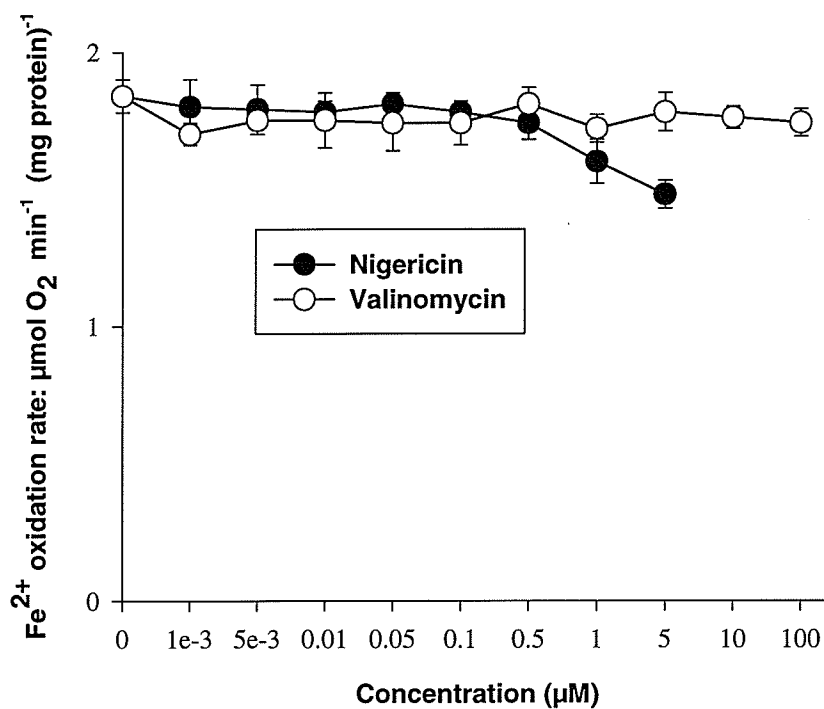


Fig. 1-5. Effect of nigericin and valinomycin on Fe^{2+} oxidation. Cells (2.4 mg / 1.2 mL) were added to start the reaction.

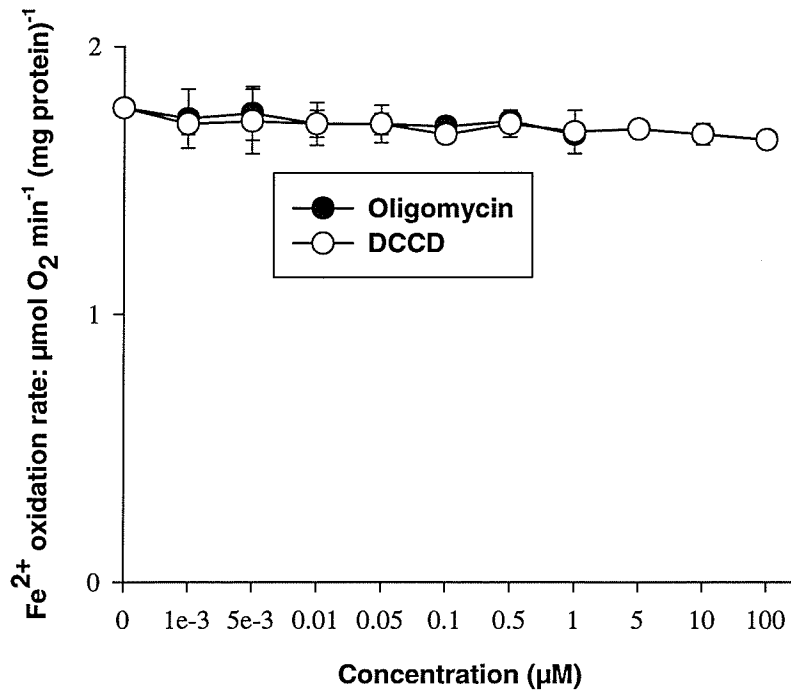


Fig. 1-6. Effect of oligomycin and DCCD on Fe^{2+} oxidation. Cells (2.4 mg / 1.2 mL) were preincubated with and without oligomycin or DCCD for 5 min before the addition of Fe^{2+} .

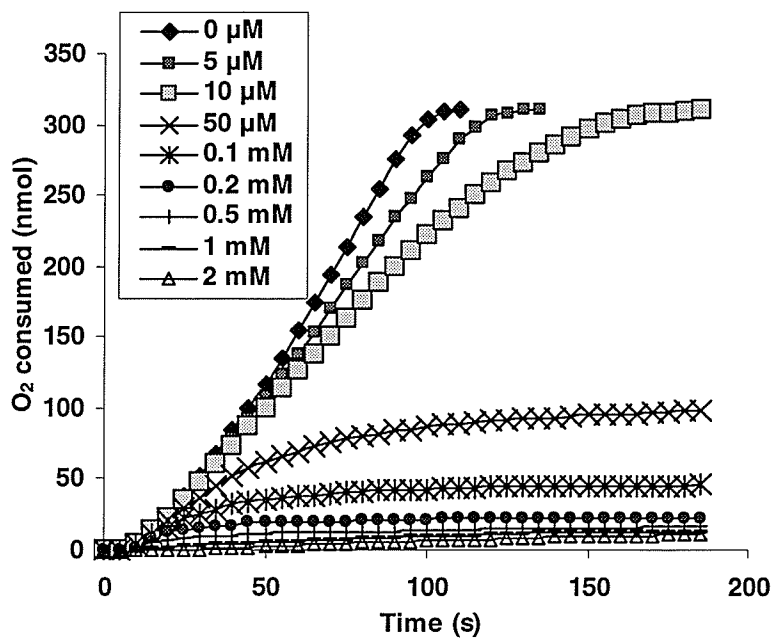


Fig. 1-7. Effect of KCN concentration on Fe^{2+} oxidation. Cells (2.4 mg) were added to start the reaction after KCN and Fe^{2+} .

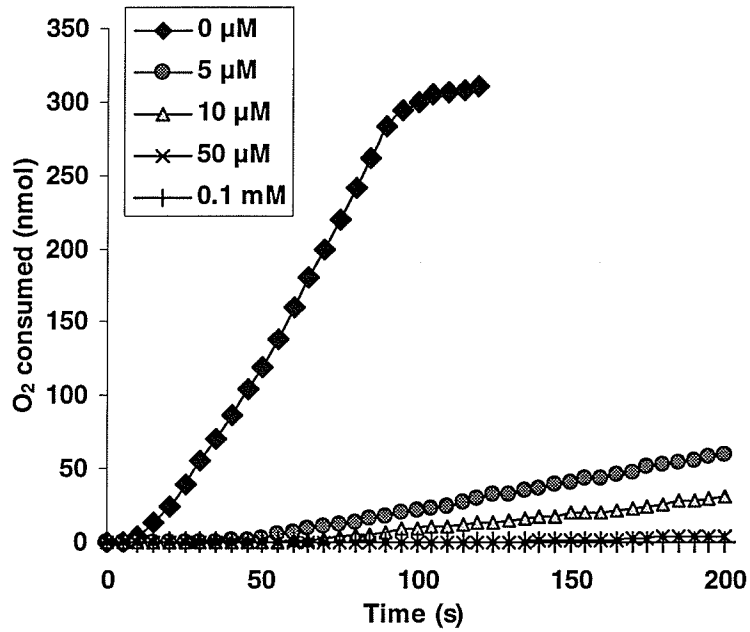


Fig. 1-8. Effect of NaN_3 concentration on Fe^{2+} oxidation. Cells (2.4 mg) were added to start the reaction after NaN_3 and Fe^{2+} .

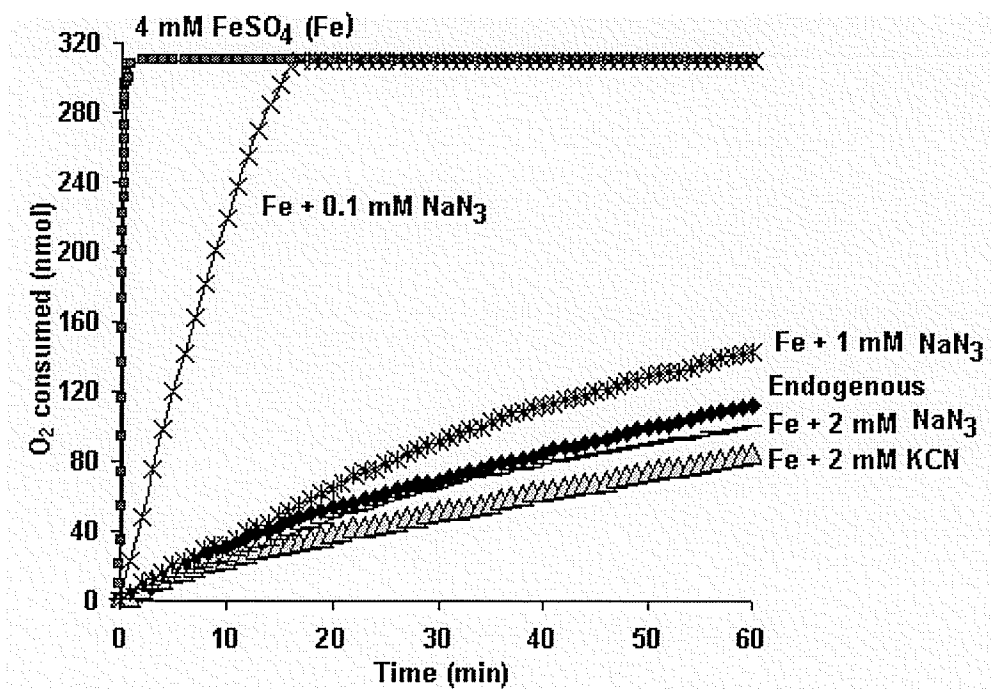
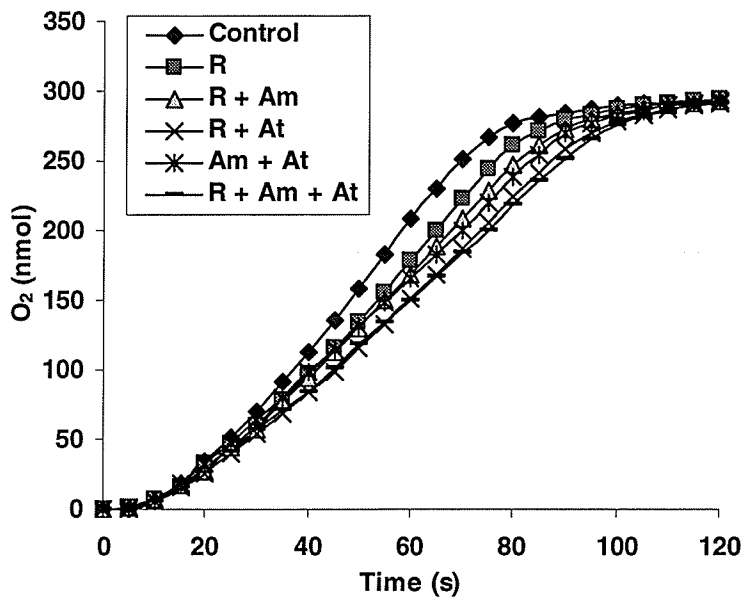
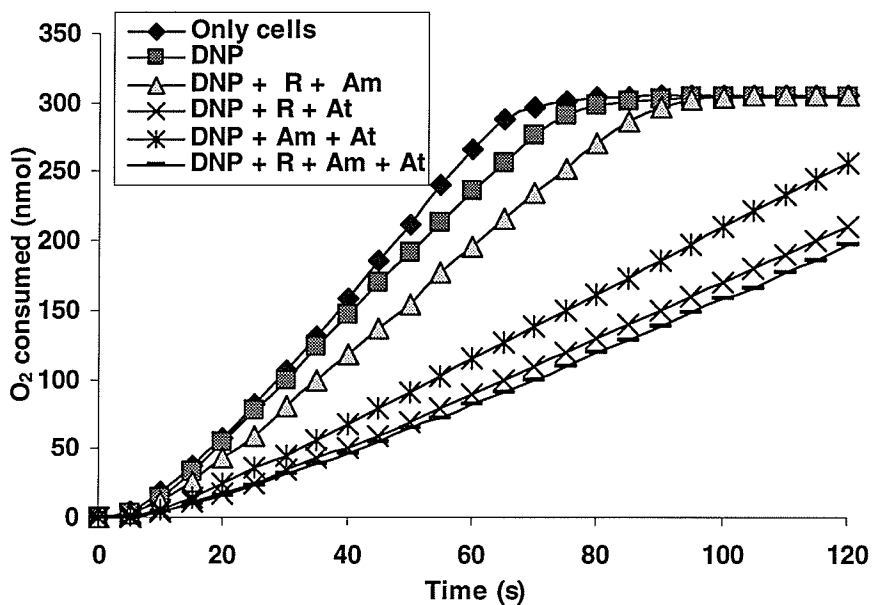


Fig. 1-9. Effect of KCN and NaN_3 on Fe^{2+} oxidation. Cells (24 mg / 1.2 mL) were added to start the reaction.



(a)



(b)

Fig. 1-10. Combinations of complex I inhibitors on Fe^{2+} oxidation in the absence and presence of 0.1 mM DNP. Cells (2.4 mg / 1.2 mL) were preincubated with and without inhibitors and / or DNP for 5 min before the addition of Fe^{2+} . R: 0.1 mM rotenone; Am: 1 mM amytal; At: 2 mM atabrine.

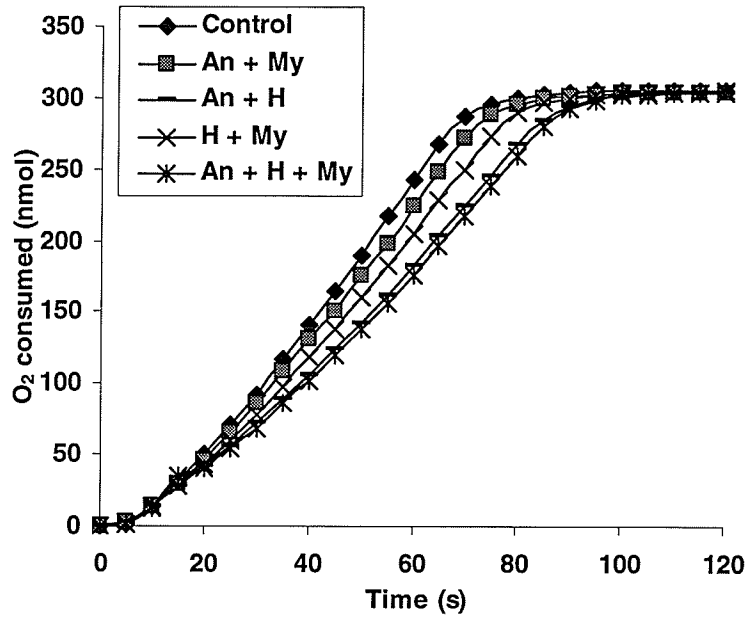


Fig. 1-11. Combinations of complex III inhibitors on Fe^{2+} oxidation. Cells (2.4 mg / 1.2 mL) were preincubated with and without inhibitors for 5 min before the addition of Fe^{2+} . An: 10 μM Antimycin A; H: 40 μM HQNO; My: 10 μM Myxothiazol.

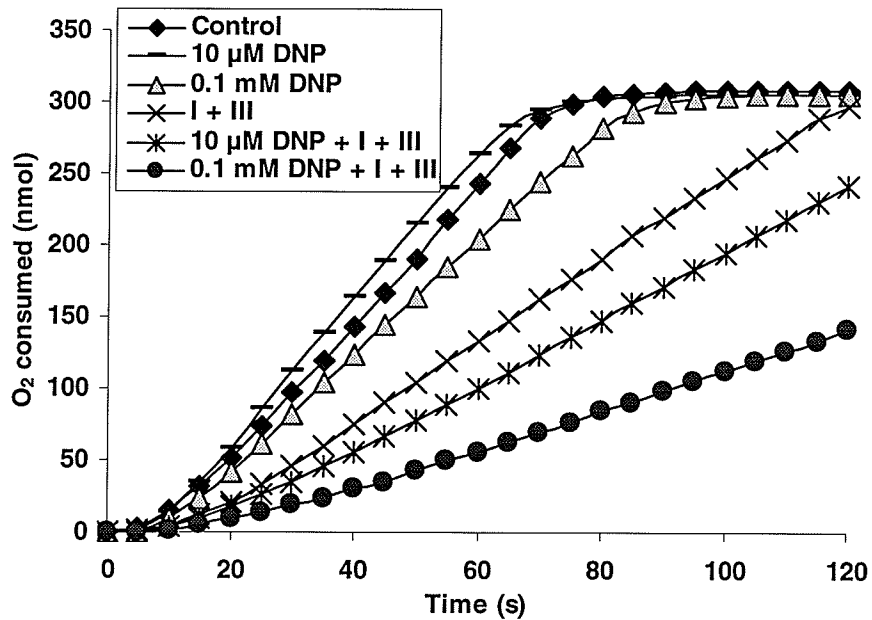
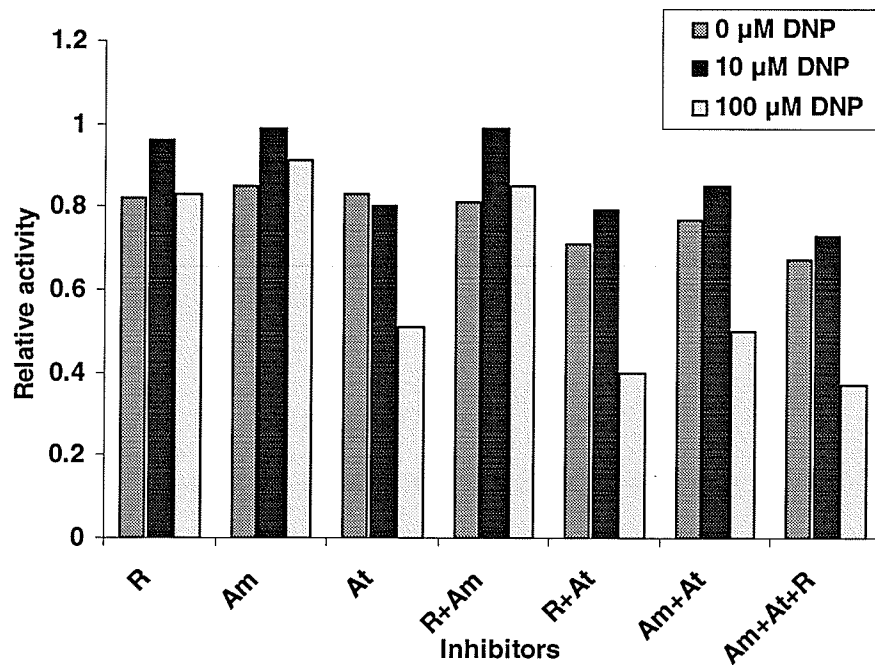
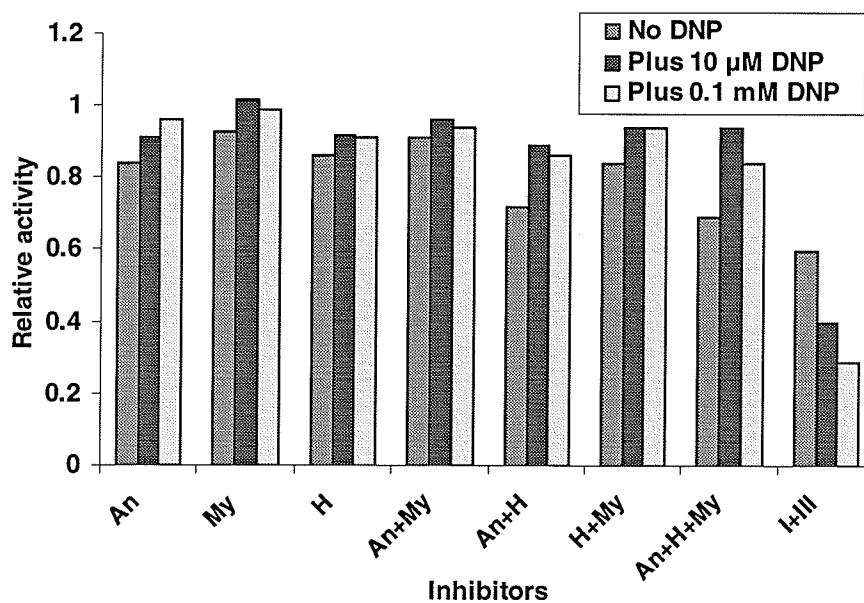


Fig. 1-12. Combinations of inhibitors of complex I and III on Fe^{2+} oxidation in the absence and presence of DNP. I + III: R + Am + At + An + H + My. Letter abbreviations are same as in Fig. 1-10 and 1-11.



(a)



(b)

Fig. 1-13. The relative activities of Fe^{2+} oxidation in the presence of inhibitors of complex I and complex III and different concentrations of DNP. Letter abbreviations and definition of relative activity are the same as in Tables 1-5 and 1-6.

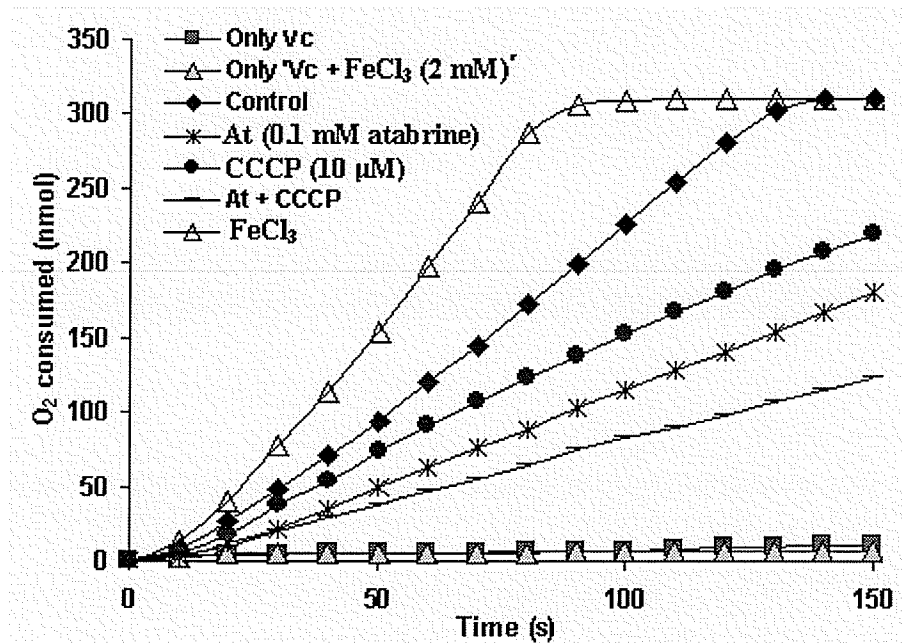


Fig. 1-14. Ascorbic acid (Vc) oxidation stimulated by FeCl₃ and inhibited by atabrine and CCCP. Only Vc / 'Vc + Fe(III)' means cells were not added.

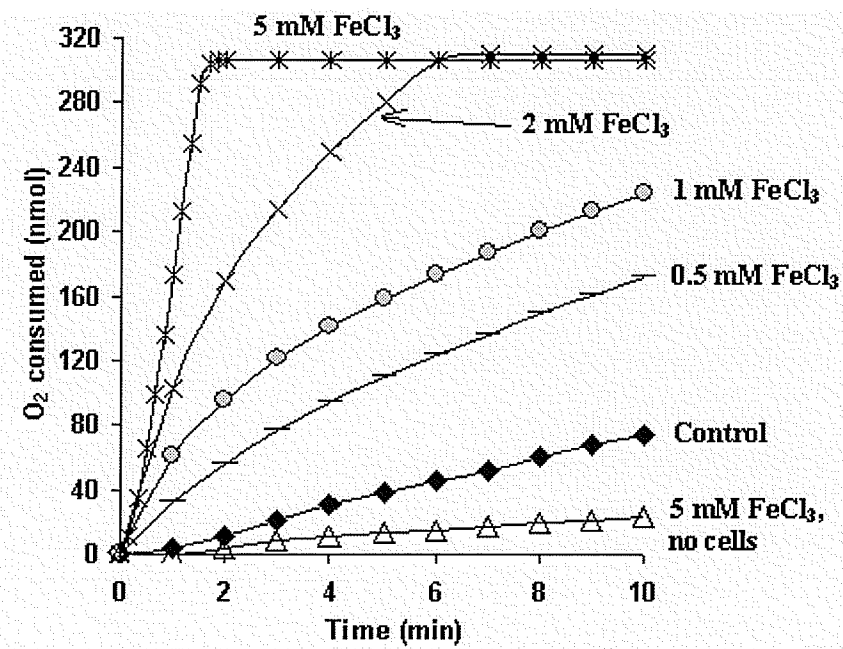


Fig. 1-15. Stimulation of PG (4 mM) oxidation by different concentrations of FeCl₃.

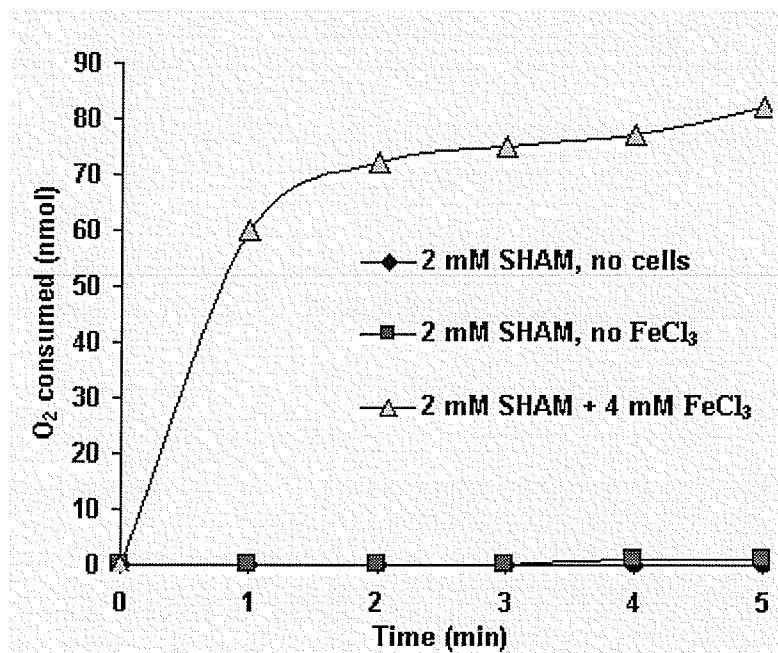


Fig. 1-16. Oxidation of SHAM. Due to the SHAM-Fe³⁺ (FeCl₃) complex precipitate coated on the electrode film of oxygraph, the O₂ consumption recording by oxygraph was almost stopped after 2 min.

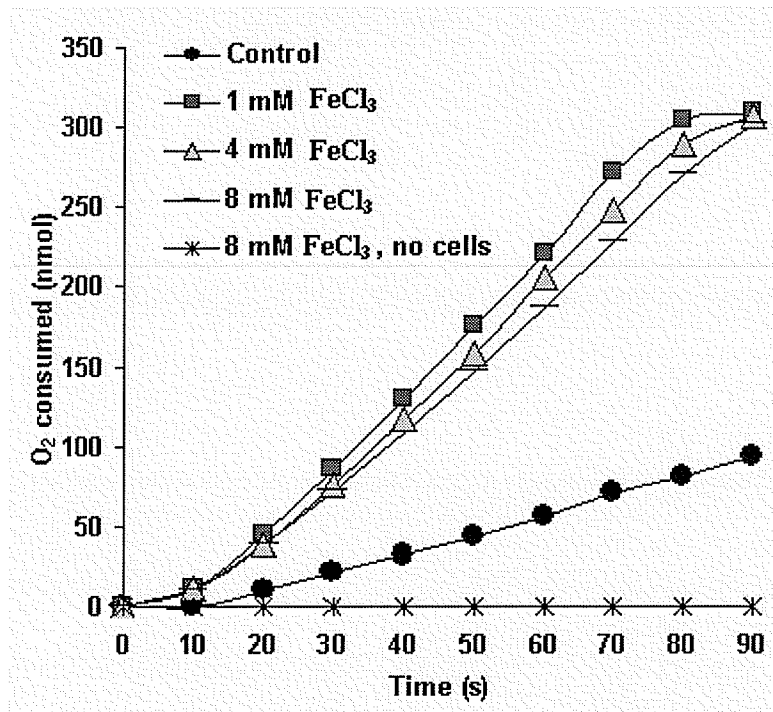


Fig. 1-17. Effect of FeCl₃ on Cys oxidation.

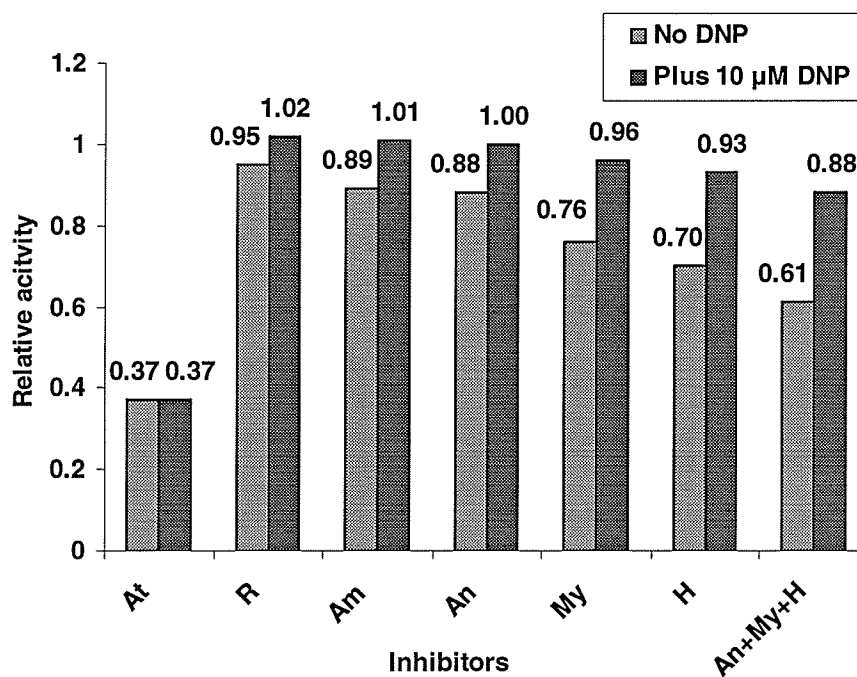


Fig. 1-18. The relative activities of Cys oxidation in the presence of inhibitors of complex I and complex III with and without 10 μM DNP. Letter abbreviations and definition of relative activity are the same as in Table 1-18. Piericidin A was not shown in this figure.

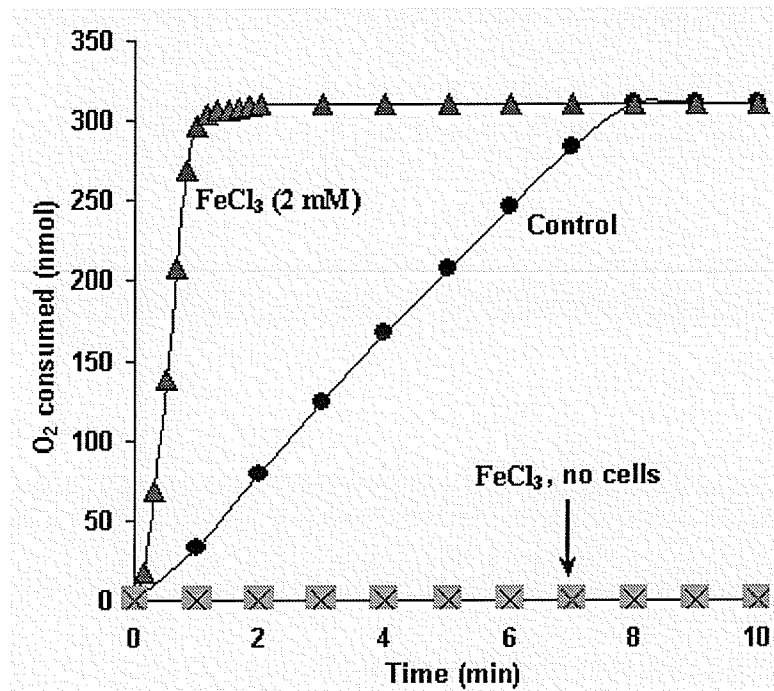


Fig. 1-19. Effect of FeCl₃ (2 mM, Fe(III)) on GSH oxidation.

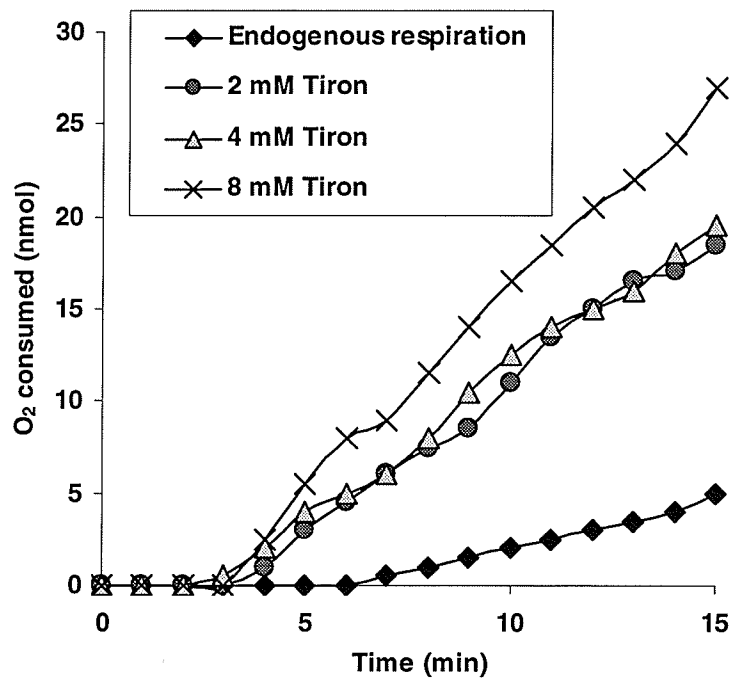


Fig. 1-20. Oxidation of tiron at different concentrations.

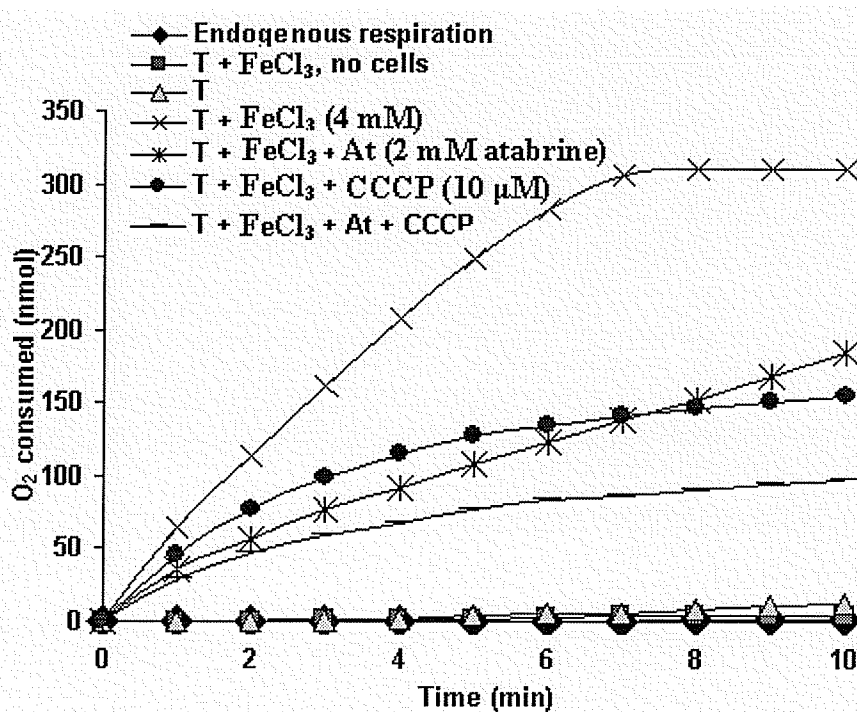
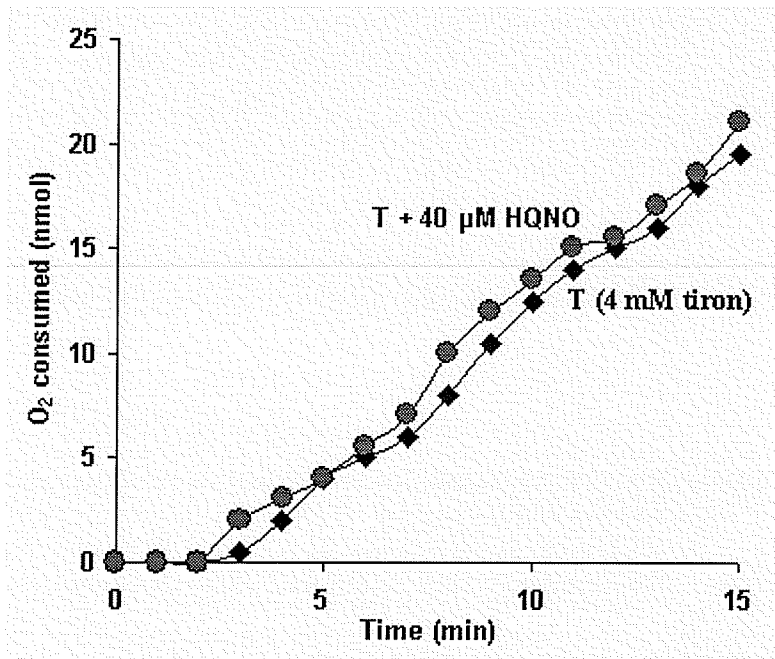
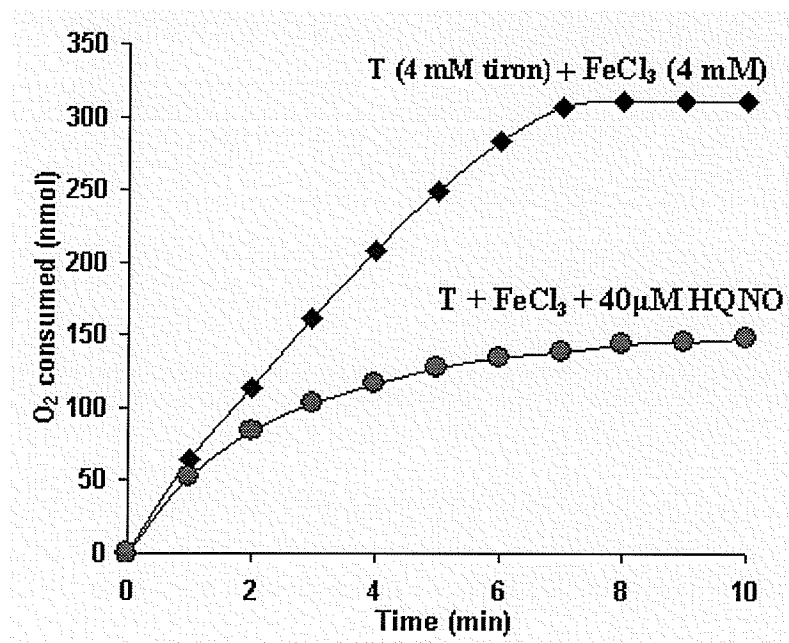


Fig. 1-21. FeCl₃, atabrine and CCCP on tiron (T) oxidation.



(a)



(b)

Fig. 1-22. HQNO on tiron oxidation in the absence and presence of $FeCl_3$.

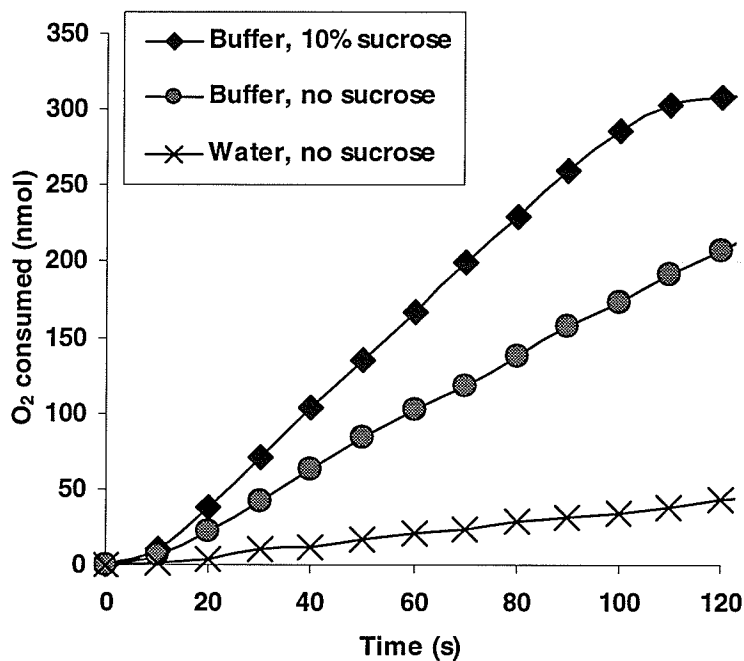


Fig. 1-23. Oxidation of Fe^{2+} by spheroplasts at pH 3.5 of buffers of different components. Buffer: 0.1 M β -alanine- H_2SO_4 . 2.4 mg spheroplasts (0.19 mg protein) were added to start the reaction.

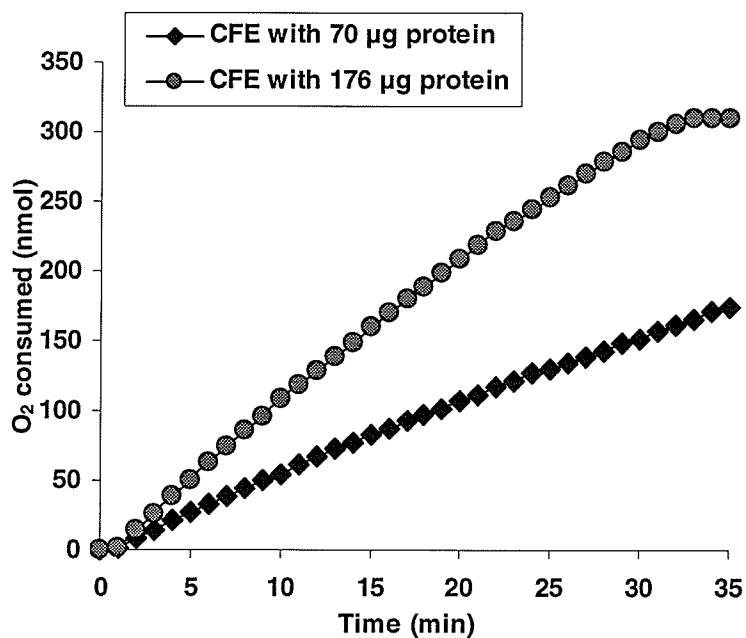


Fig. 1-24. Oxidation of Fe^{2+} by cell free extracts (CFE) in 0.1 M β -alanine- H_2SO_4 at pH 3.5. CFE was added to start the reaction.

Fig. 1- 25. The bioinformatics search results of the putative ORF containing the subunit 6 of the two types of complex I in *A. ferrooxidans*. The amino acid sequence of the subunit 1 of *Nitrosomonas europaea* ATCC 19718 NDH-1 (accession number **NP_841800**) was used as the query sequence to search the partial genome sequence (tblastn) of *A. ferrooxidans* ATCC 23270 at the NCBI (National Center for Biotechnology Information) web site (http://www.ncbi.nlm.nih.gov/sutils/genom_table.cgi) contributed by TIGR Microbial Database (<http://www.tigr.org/tdb/mdb/mdbinprogress.html>). Amino acid sequences were obtained and putative ORFs were found via ORF Finder (<http://www.ncbi.nlm.nih.gov/gorf/gorf.html>) from the nucleotide sequences that produced significant alignments. Then putative amino acid sequences coding for the subunits of complex Is have been found by blasting the putative ORFs (blastp) against the genomes of known organisms. Sequence comparisons were directly taken from the website. (a) The putative ORF in *A. ferrooxidans*; (b) the putative conserved domains that contain the subunits 6 of the two types of complex I; (c) amino acid sequence alignments of the proteins corresponding to each subunit 6 of the two putative complex Is: NADH-ubiquinone / plastoquinone oxidoreductase chain 6 and NADH:ubiquinone oxidoreductase subunit 6 (chain J) [Energy production and conversion], respectively. Sequences can be obtained from the GenBank under the accession numbers listed at the bottom of each alignment.

Length: 153 aa

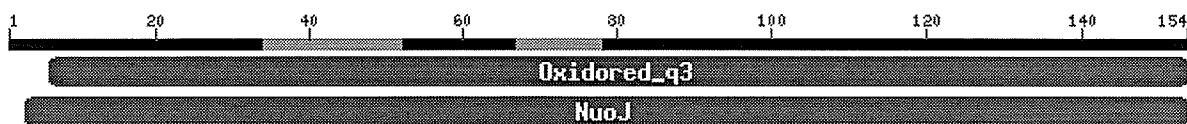
```

2445 atgctgccagtaaccacgattctgttttatatcttctccgctata
      M L P V T T I L F Y I F S A I
2490 ttgctgggctctgcaacgctggtgatcacggcgcgtaatccgggtg
      L L G S A T L V I T A R N P V
2535 tacgcgaccctgtatctggtgctggcggttttttaatgctgccgcc
      Y A T L Y L V L A F F N A A A
2580 ctgttcacacctgctgggagctgaattcctgggggttgattctgatt
      L F I L L G A E F L G L I L I
2625 ctgggtctatgtgggcgcggtgatgggtgcttttcctctttgtggtg
      L V Y V G A V M V L F L F V V
2670 atgatgctggatatcaacctggcacgtatcaaggaaggctttctc
      M M L D I N L A R I K E G F L
2715 agttatctgccattgggtcttgctattgccatcctcgggtgttctg
      S Y L P L G L A I A I L G V L
2760 gagctggcggtcgttttctggacgtcttcctcctgggccatatacct
      E L A V V F W T S S L G H I P
2805 ggcgccgcgcactcccggcggataccgacaatacccgggcactg
      A P A A L P A D T D N T R A L
2850 gggatcctactgtataccaaatatctgtatccatttgaaatagca
      G I L L Y T K Y L Y P F E I A
2895 gcagtaattctg 2906
      A V I L

```

Fig. 1-25 (a)

Putative conserved domains



PSSMs producing significant alignments:	Score (bits)	E value
gnlCDD11058 pfam00499, Oxidored_q3, NADH-ubiquinone/plastoquinone oxidored...	<u>34.0</u>	0.007
gnlCDD110706 COG0839, NuoJ, NADH:ubiquinone oxidoreductase subunit 6 (chain...	<u>57.9</u>	5e-10

Fig. 1-25 (b)

Sequence alignment of NADH-ubiquinone/plastoquinone oxidoreductase chain 6

	10	20	30	40	50	60
consensus******
A. f	1	MTYIVLILSIGLVLGLVASKPSP	10	YAGLGLIVAFVGVCGLYLLLG	20	ASFVALALFLIYL 60
E. c	5	TTILFYIFSAILLGSATLVIT	10	ARNPVYATLYLVLAFFNAAAL	20	FILLGAEFLGLLILLVYV 64
G. c	1	MTYFVIFLGVICFMLGVLAV	10	ASNPSPIYGVVGLVVASVMG	20	CGWLVSLGVSVFVSLALFLVYL 60
D. v	2	KMMTIYIISLLMIGFVAFAS	10	KPSPYGGLSLVVSGGLGCGM	20	VVSLEDFLGLVFLVYL 61
S. P	8	QYISFLILAFLVIGAALGVV	10	LLSNIVYSAFLLGGVFLSIS	20	GIYILLNADFVAAAQVLVYV 67
L. b	8	QIVSFAILAAMMIGSAIGV	10	VLEENVYSAFLLGGVFISIA	20	GLYLLLNADFVAAAQVLIYV 67
M. p	8	YETIFLFLFESGLILGSLG	10	VILLTNIVYSAFLGDFVFC	20	ISLLYLLLNADFVAAAQILYV 67
Z. m	8	HEILVLFGGFGLLLGGLGV	10	VLLTNPIYSAFSLGLVLCI	20	SFLYLLNSYFVAVAQLLIYV 67
	70	80	90	100	110	120
consensus******
A. f	61	GCMLVVFYTVAMANEPEAWG	70	SNKVVW---GGTLVVLGLGIE	80	VLLGGYFLGWTEVVIV 116
E. c	65	GAVMVLFLFVMMMLDINLAR	70	IKEGFLSYL---PLG--LAI	80	AILGVLELAVVFWTSSLGH 118
G. c	61	GCMLVVFYTVAMANEPEAWG	70	DWRVVG---yGLGFVLVVMG	80	VVLLGGVDFWVGVVVT 117
D. v	62	GCMLVVFYTVAMATEEYPET	70	WVGN-----VVAFIMLLF	80	VLLQVGVYFMSKLVYII 113
S. P	68	GAVSVLILFAIMLVNKRED--	70	FSKIPGRwl-rnVSTALVCT	80	GIFALLST-MVLITPWQIN 123
L. b	68	GAVNVLILFAIMLVNKREA--	70	FQPIAKSwi-rrAATALVC	80	AGIFALLSA-MVLITPWAI 123
M. p	68	GAVNVLIIFAVMLINKKQ--	70	YSNFFVYwtigdGITLTLCT	80	SIFLLLN-FISNTSWSKI 123
Z. m	68	GAINVLIIFAVMVFVNGSE--	70	WSKDKNYwtigdGFTLLLC	80	ITIPFSLMT-TIPDTSWYGI 123
	130	140	150	160	170	
consensus******
A. f	117	VAFT-----VEGSLIR-ED	120	ITGGAALYSCGVLPFELAG	130	VLLVALFVAIELAR 164
E. c	119	IPAP-----AALPADTD-N	120	TRALGILLYTKYLYPFEIA	130	AVIL----- 154
G. c	117	FKFSgvawaiydTGDSGAFS	120	-EEIMGAAALYSYGAWVVIV	130	TGWSLLVGVVLVILEVTR 173
D. v	118	VDG-----GGVSFAR-LD	120	FSGVAVFYSCGVGLFLVAG	130	WGLLLALFVVLVLELVR 163
S. P	114	MAIKlf-----dfVETSLV	120	G-QDYNGVSQLYYCGGWA	130	LALGWLFMFTIYVVLVLR 164
L. b	124	ETGPF-----VENT-----	130	LVTIGKHFFSDYLLPFEL	140	ASVLLMAMVGAIIAR 167
M. p	124	TAVP-----IESS-----	130	IITIGLHFFTFDFFLPFEL	140	ASILLMALVGAIVLAR 166
Z. m	124	FLMTkpn----lvVKDIILIN	130	-TVRHIGSELLTEFLLPFEL	140	MSIILLVALIGAITLAR 176
	124	LWTTrsn----qiVEQG-LIN	130	-NVQQIGIHLATDFYLPFEL	140	ISLILLVSLIGAITMAR 175

A. f. *Acidithiobacillus ferrooxidans* (Proteobacteria)

E. c. *Equus caballus* (Eukaryota); accession number (AN): P48657

G. g. *Gallus gallus* (Eukaryota); AN: P18941

D. v. *Didelphis virginiana* (Eukaryota); AN: P41315

S. P. *Synechocystis* sp. PCC 6803 (Cyanobacteria); AN: P26523

L. b. *Leptolyngbya boryana* (Cyanobacteria); AN: Q00243

M. p. *Marchantia polymorpha* (Eukaryota); AN: P06266

Z. m. *Zea mays* (Eukaryota); AN: P46621

Sequence alignment of NADH:ubiquinone oxidoreductase subunit 6 (chain J)

[Energy production and conversion]

		10	20	30	40	50	60		
	******		
consensus	1	MMIETLAFYLF	FAVLAI	AFALGV	VLAKNP	VVSALY	LALTL	LSIAALFFLLGAEFLGVVQVL 60	
A.f	2	1PVTILFYIF	SAILLGS	ATLVIT	ARNPVY	ATLYLV	LAFNAAL	FILLGAEFLGLLIL 61	
B.m	1	-----	MIASAF	MVIAAR	NPVHSV	LFLLT	FFNAAL	FLLTGAEFLAMILLV 46	
N.m	1	MTFQLILFY	IFAVIL	LYGAIK	TVTAKN	PVHAAL	HLVLT	FCVSAAMLWMLMQAEFLGVTLVV 60	
R.s	1	MEITTIIF	YCFSL	VLVLS	SALKVI	TAKN	PVHAAL	FLVLSFFTAAIWMLLKAEFLAITLVL 60	
S.m	1	MCLQALFF	YLF	FAFI	AVASAF	MVIAAR	NPVSVL	FLILFFNAAGLFLLTGAEFLAMILLV 60	
X.f	2	MDVWNI	AFYLF	SAVAVA	AAGAVI	SVRHPV	YAVL	CLLILFFSMACIWLIVGAEFLGVTLVL 61	
M.l	3	SGLEAAFF	YLF	FAFVA	VASAF	MVISSR	NPVHSV	LVFLILFFNAAGLFMLTGAEFLAMILLV 62	
		70	80	90	100	110	120		
	******		
consensus	61	VYVGAVMVL	FLFVVM	MLNVD	GAEVRE	EEGLRG	KPLAAL	VGLVLLALLIISVAVVSGA--FV 118	
A.f	62	VYVGAVMVL	FLFVVM	MMLDIN	LARIKE	GFLSYL	PLGLAIA	AILGVLELAVVFWTSSLGhiPA 121	
B.m	47	VYVGAVAVL	FLFVVM	MMLD	VDFAE	LKRGAL	QYAPV	GALVGLILLGELIFVFASRMFT--PK 104	
N.m	61	VYVGAVMVL	FLFVVM	MLNID	IEEMR	AGFRH	APVAG	VVGTLLAVALILILVN-PKT--DL 117	
R.s	61	VYVGAVMVL	FLFVVM	MIDVD	IEHLR	DFWTV	YVPMG	AFVGA	VIIMEMAVVLT---KA--FM 115
S.m	61	VYVGAVAVL	FLFVVM	MMLD	IDFTE	LRAGV	LEYAP	IGALIGLILAAELIVVVGSSAFS--PE 118	
X.f	62	VYVGAVMVL	FLFVVM	MMLD	IDT	SRLRE	GWVRY	LPVGLLVAGVMLVQMVLVIGVKMRM--AT 119	
M.l	63	VYVGAVMVL	FLFVVM	MMLD	VDFAE	MKEGAL	QYAP	IGALVGLILAAELIIVLGGYTFA--PK 120	
		130	140	150	160	170			
	******		
consensus	119	PPS---N--	PAAIGN--	IKALGS	VLFTD	YLLP	FELAS	VLLLVAMVGAIVLARRER 166	
A.f	122	PAA---L--	PADTDN--	TRALG	ILLYT	KYLYP	FEIAA	VIL----- 154	
B.m	105	LGqg-aLp	iPDVAT	rtnTAAL	GDILY	THVYF	YFQV	AGLVLLVAMIGAIVLTMRHK 158	
N.m	118	AAFgImK	GiPADY	Nn--IR	DLGSR	IYTDY	LLPF	EAAVLLLLGMVAAIALVHRKT 170	
R.s	116	GRSqp	vQeLP	KALSG	pnTQAL	GKLIY	TDYI	YAFEVAGAVLLLLAIVAAVALTARRR 170	
S.m	119	IAKgiaM	piPAP	SERtn	TAALG	DVLYT	HYVYF	FQIAGLVLLVAMIGAIVLTTLRHR 173	
X.f	120	PPFv	dnAaa	QAHTS	n-LT	WLASH	LSFT	DFLFPFEFAAVILTVAVIAAVMLTLRKR 173	
M.l	121	LAA	tv	sKpi	PDLAT	RsnTAAL	GDILY	TDYLYYFQISGLILLVAMIGAIVLTTLRHK 175	

A.f. *Acidithiobacillus ferrooxidans* (Proteobacteria);

B.m. *Brucella melitensis* 16M (Proteobacteria); AN: NP_540066

N.m. *Neisseria meningitidis* Z2491 (Proteobacteria); AN: NP_282862

R.s. *Ralstonia solanacearum* GMI1000 (Proteobacteria); AN: NP_520174

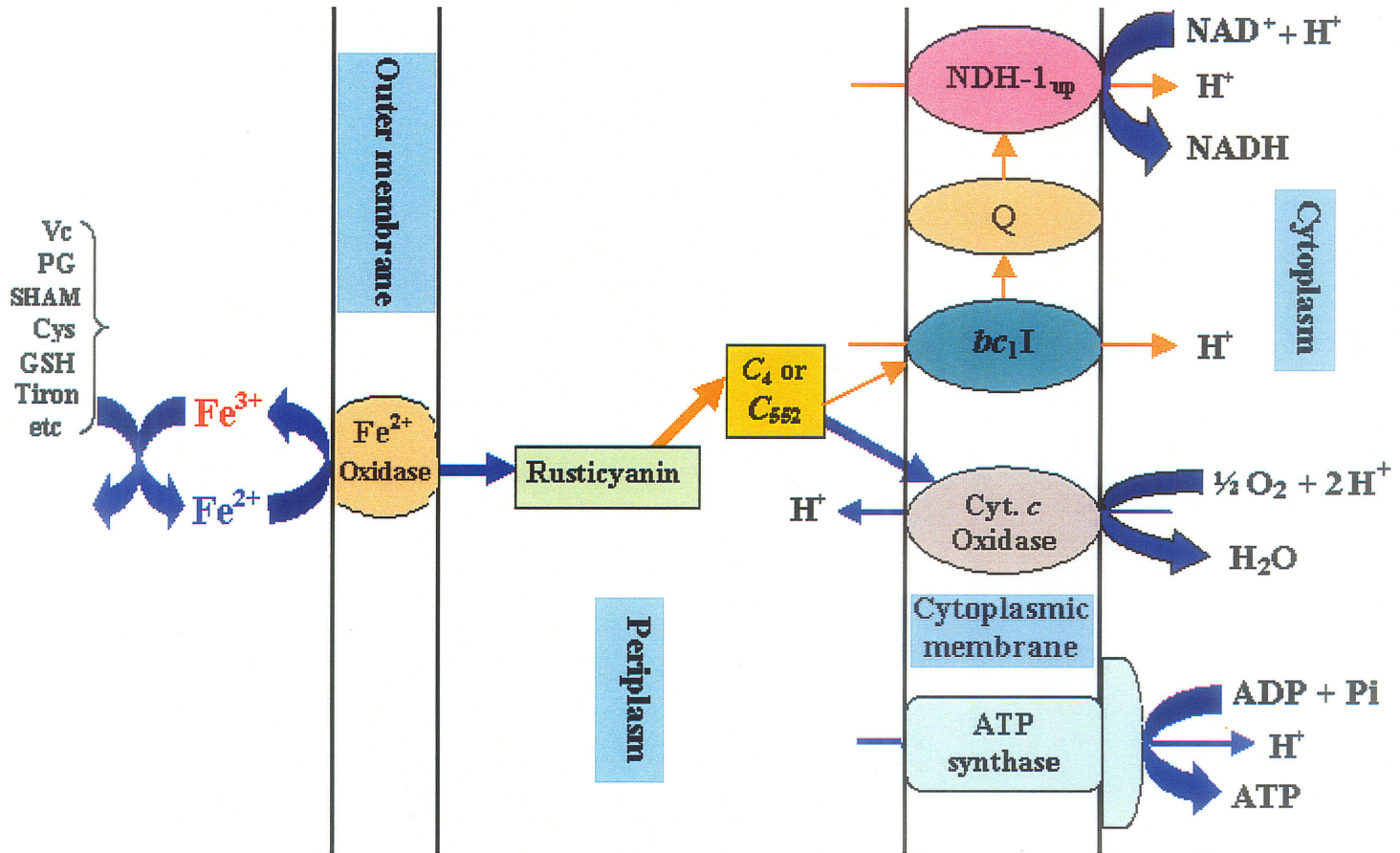
S.m. *Sinorhizobium meliloti* 1021 (Proteobacteria); AN: NP_385381

X.f. *Xylella Fastidiosa* 9a5c (Proteobacteria); AN: NP_297605

M.l. *Mesorhizobium loti* MAFF303099 (Proteobacteria); AN: NP_102963

Fig. 1-25 (c).

Fig. 1-26. Proposed model for the electron transport pathways of the oxidations of Fe^{2+} and some iron-interacting organic compounds by *A. ferrooxidans* based on experimental data. Q: ubiquinone / ubiquinol pool; bc_1I : the bc_1 complex participating in the uphill reaction (NAD^+ reduction); NDH-1_{up} : the NDH-1 involved in the uphill reaction (NAD^+ reduction); c_4 or c_{552} : cytochrome c_4 or cytochrome c_{552} ; Cyt.: cytochrome. Vc: ascorbic acid; PG: propyl gallate; Cys: L-cysteine; GSH: glutathione. The thickness of straight arrows (not including the arrows pointing at H^+) represents the speed of electron flow in a qualitative manner.



Part II

Oxidation of Endogenous Substrates

(Endogenous Oxidation)

Abstract

Effects of electron transport inhibitors, uncouplers and other Δp dissipaters, thiol reagents and iron chelators were studied on the oxidation of endogenous substrates in *A. ferrooxidans* by O_2 and Fe^{3+} . Uncouplers and other Δp dissipaters greatly stimulated the oxidation of endogenous substrates indicating a normal respiratory control. Complex I inhibitors showed strong inhibition (atabrine had no effect) indicating an overall exergonic reaction. Complex IV inhibitors KCN and NaN_3 only partially inhibited endogenous respiration suggesting the involvement of more than one type of terminal oxidase. HQNO, an inhibitor of haem *b*-containing quinol oxidases, further reduced the KCN or NaN_3 inhibited activity indicating the role of quinol oxidases. The remaining activity in the presence of KCN and HQNO was strongly inhibited by rotenone suggesting the involvement of an unknown terminal oxidase that was insensitive to KCN and HQNO. HQNO alone, however, greatly stimulated the oxidation of endogenous substrates. KCN or NaN_3 more strongly inhibited the stimulated activity of endogenous respiration by HQNO than that by uncouplers. It was interpreted that HQNO stimulation was due to the shifting of electrons to a "fast" electron transport pathway involving iron and the cytochrome *c* oxidase pathway. The respiratory quotient (CO_2 / O_2 ratio) of endogenous respiration was close to 1.0 indicating the carbohydrate nature of endogenous substrates. Based on the experimental data and the current knowledge, a model for the electron transport pathways for the oxidation of endogenous substrates has been proposed.

Introduction

A. ferrooxidans obtains energy for its growth by oxidizing inorganic substrates such as Fe^{2+} and inorganic sulfur compounds. The reducing power (NADH) for CO_2 fixation is produced via an uphill electron transport pathway (NAD⁺ reduction). When these normal growth substrates are absent, the organism survives by oxidizing endogenous substrates. Since the endogenous metabolism is required for "energy of maintenance" ('the energy consumed for purposes other than the production of new cell material') (Dawes 1976), the oxidation of endogenous substrates in *A. ferrooxidans*, different from that of its inorganic substrates, may use a downhill electron transport pathway possibly involving NADH oxidation via complex I. Very little is known, however, about the endogenous metabolism of this chemoautotrophic bacterium, the study of which would help the understanding of the overall physiology of this organism.

Endogenous metabolism in microorganisms has been studied mainly on the nature of endogenous substrates, the relationships of endogenous metabolism with the viability of the cells, and energy of maintenance (Brdar et al. 1965; Dagley and Sykes 1957; Dawes 1963, 1976; Dawes and Ribbons 1962, 1964; Postage and Hunter 1962; Strange 1968), but there is a paucity of information about the electron transport pathways of the oxidation of endogenous substrates. Although endogenous polyphosphate, proteins and RNA may be degraded by an organism, the main endogenous substrates used for survival and energy of maintenance are glycogen and glycogen-like compounds, and lipids [including poly- β -hydroxybutyrate (PHB)] (Dawes 1976). Glycogen was the preferred endogenous substrate in *E. coli* (Dawes and Ribbons 1965). It was reported that glycogen-rich *E. coli* survived better than glycogen-poor bacteria, which led to the

conclusion that only bacteria with a relatively large amount of carbohydrate have superior survival properties (Dawes 1976; Dawes and Ribbons 1963; Strange 1968). Sierra and Gibbons (1962) reported that the PHB-rich (50% of polymer) strains of *Micrococcus halodenitrificans* maintained 100% viability for 100 h whereas the PHB-poor (less than 10% of polymer) strains died rapidly and less than 10% of cells survived after 30 h starvation. It has been suggested that the rapid metabolism of endogenous substrates, which produces energy at a rate greater than that required for maintenance, would accelerate the death of starved bacteria, whereas prolonged viability is associated with a low rate of endogenous metabolism that is required for energy of maintenance (Dawes 1976).

No information is available concerning the nature of endogenous substrates and the electron transport pathways for endogenous metabolism in *A. ferrooxidans*. Electron transport pathways of *A. ferrooxidans* were shown to be complex with multiple branchings for Fe^{2+} (Fig. 1-26) or sulfur growth (Fig. 7; Brasseur et al. 2004) and the Δp requiring NAD^+ reduction for CO_2 fixation. The pathway for Fe^{2+} oxidation branches at cytochrome c_4 / c_{552} which donates electrons mainly to cytochrome c oxidase (aa_3, ba_3) to reduce O_2 by downhill reaction, and partially to cytochrome $bc_1\text{I}$ complex to reduce NAD^+ by uphill reaction. The pathways for sulfur oxidation are centered on reduced ubiquinone, ubiquinol which can reduce NAD^+ by an uphill reaction or reduce O_2 by ubiquinol oxidases, cytochrome bd and cytochrome bo_3 . Ubiquinol can also enter $bc_1\text{II}$ complex to cytochrome c to cytochrome c oxidases (aa_3 and ba_3). In addition to using O_2 as a terminal electron acceptor under aerobic conditions, *A. ferrooxidans* can also use Fe^{3+} as a terminal electron acceptor under anaerobic conditions (Ohmura et al. 2002;

Pronk et al. 1991a) and in the aerobic condition at extremely low pH values (Sand 1989). The electron transport pathways of Fe^{3+} reduction are unknown in this organism and has been poorly studied in other organisms. The pathway of Fe^{3+} reduction in *Pseudomonas ferrireductans* was proposed as: dehydrogenase \rightarrow quinones \rightarrow cytochrome bc_1 complex \rightarrow iron reductase \rightarrow Fe^{3+} (Arnold et al. 1986). According to the available information about the electron acceptors and electron transport components in *A. ferrooxidans* and the information of Fe^{3+} reduction in other organisms, a hypothetical model for the electron transport pathways of endogenous substrate oxidation in *A. ferrooxidans* is shown in Fig. 2-0. The effect of different electron transport inhibitors as well as uncouplers and other Δp dissipaters, thiol reagents and metal chelators on the oxidation was studied in an effort to understand the mechanism of endogenous metabolism and its control by checking the validity of and modifying the hypothetical model.

Results

2.1. Endogenous oxidation by O₂ (endogenous respiration)

A. ferrooxidans cells consumed O₂ in the absence of ferrous iron at 25°C at a slow rate of 0.7 – 1.2 nmol O₂ min⁻¹ (mg protein)⁻¹, which corresponded only to 0.1% the rate of Fe²⁺ oxidation. The optimal pH was 3.5 with 10 – 20% less activity at pH 2.3 – 1.7 and decreasing activity above pH 3.5 to 50% less at pH 7.0. The activity at 30°C was similar to that at 25 °C, but it doubled at 40 °C. The respiration rate changed little after cell suspensions had been stored at 4°C for one week. In fact cells were used within 3 days after harvesting.

2.1.1. Effect of uncouplers, ionophores, anions, weak acids, thiol agents, phosphate and arsenate

The effect of uncouplers was studied both in 0.1 M β-alanine-H₂SO₄ buffer and water at pH 3.5, since the pH changes of cell suspensions were tested in water of pH 3.5 (see 2.1.7). When measured in 0.1 M β-alanine-H₂SO₄ buffer, endogenous respiration was stimulated by DNP by 167% at 30 μM and was inhibited by 75% at 1 mM. CCCP at 10 μM stimulated it by 162% (Fig. 2-1a). When measured in water, DNP stimulated it by 133% at 30 μM and inhibited it by 90% at 1 mM, and 10 μM CCCP stimulated it by 116% (Fig. 2-1b).

Ionophores, 0.1 mM valinomycin, 1 μM nigericin and the combination of 0.1 mM valinomycin and 1 μM nigericin, stimulated it by 110%, 120% and 115%, respectively (Fig. 2-2).

Permeable anion KSCN at 0.1 mM stimulated it by 130% in the absence or presence of 4 mM FeCl₃ (Fig. 2-3).

Weak acids, CH_3COOK (40 mM), sodium succinate (10 mM), sodium malonate (10 mM) and KF (1 mM), stimulated it by 130%, 140%, 140% and 100%, respectively (Fig. 2-4).

Sulfhydryl-binding agents (thiol agents), NEM at 5 mM, HgCl_2 at 50 μM and AgNO_3 at 0.1 mM, stimulated it by 140%, 100% and 40%, respectively (Fig. 2-5). HgCl_2 at 10 μM only showed stimulation by 5% and at 100 μM showed 46% inhibition (Fig. 2-5b).

KH_2PO_4 at 0.1 mM and 10 mM stimulated it by 3% and 30%, respectively (data not shown). NaHAsO_4 at 0.1 mM, 2 mM and 10 mM stimulated it by 60%, 29% and 27%, respectively (Fig. 2-6).

The stimulatory effect by uncouplers, ionophores, anions, weak acids indicates the existence of a normal respiratory control during endogenous respiration. The effect of thiol agents, Pi and arsenate will be discussed later.

2.1.2. Effect of complex I inhibitors

Complex I inhibitors had a maximal inhibition of only 50% on endogenous respiration (0.1 mM rotenone: 48%, 2 mM amytal: 42%, 2.5 μM piericidin A: 51%, 2 mM atabrine had no effect) (Table 2-1 and Fig. 2-7). This indicates that, during endogenous oxidation, some electrons were transferred to NDH-1 (Fig. 2-0) and other electrons were transferred to other unknown dehydrogenase(s) before they were captured by O_2 . However, complex I inhibitors showed stronger inhibition when endogenous respiration was stimulated by various compounds. Rotenone at 0.1 mM inhibited respiration when added to a culture containing 30 μM DNP (Fig. 2-1a), 40 mM CH_3COOK (data not shown), 10 mM Na_2 -succinate (data not shown), 10 mM Na_2 -

malonate (data not shown), 0.1 mM KSCN (Fig. 2-3), 5 mM NEM (Fig. 2-5a) and 0.1 mM Na₂HAsO₄ (Fig. 2-6) by 90%, 74%, 66%, 77%, 82%, 82% and 62%, respectively. Therefore, increased electron flow went to NDH-1 when endogenous respiration was accelerated. This possibly indicates that the dehydrogenase(s) (other than NDH-1) participating in endogenous respiration could not pump protons, but NDH-1 could pump protons (Fig. 2-0) and was involved in the accelerated respiration. The effects of atabrine and piericidin A on endogenous respiration and Fe²⁺ oxidation were opposite. Atabrine inhibited Fe²⁺ oxidation (see Part I) but had no effect on endogenous respiration (Fig. 2-7). Piericidin A had no effect on Fe²⁺ oxidation (see Part I) but inhibited endogenous respiration (Fig. 2-7). The bioinformatics search of the partial genome sequence of *A. ferrooxidans* indicates that two putative types of NDH-1 (possibly NDH-1_{up} and NDH-1_{down}) exist in this organism (see Part I). These results support that the NDH-1 in Fig. 2-0 was involved in the downhill reaction and was NDH-1_{down}, different from the one involved in Fe²⁺ oxidation (NDH-1_{up}).

2.1.3. Effect of complex IV inhibitors

Complex IV inhibitors showed only a partial inhibition on endogenous respiration. Fig. 2-8 shows the effect of KCN on the rate of endogenous respiration. KCN at low concentration of 0.2 mM showed 18% inhibition for the initial 25 min and 49% after that. KCN, at high concentrations from 1 mM to 10 mM, showed a 3-phases pattern of inhibition — low – high – low inhibition from 0 – 15 min, 15 – 25 min, 25 – 60 min, respectively. The highest inhibition was achieved by 2 mM KCN between 15 min and 25 min. KCN at 2 mM (also see the time course studies in Figs. 2-9, 2-10, 2-11)

inhibited endogenous respiration by 58% in the initial 15 min, 87% between 15 min and 25 min, but only 35% between 25 min and 60 min. However, KCN, at a very high concentration of 50 mM, did not show the “3-phases pattern of inhibition”. Instead, it showed inhibition of 50%, 78% and 81%, respectively in three time periods.

In the presence of weak acids (Fig. 2-4), thiol agents (Figs. 2-5a, 2-6) and particularly uncouplers (Figs. 2-9, 2-10), 2 mM KCN also showed stronger inhibition initially and weaker inhibition in later time. Chloramphenicol, which inhibits protein synthesis in bacteria (Das et al. 1966; Vazquez 1963), did not change the pattern of KCN inhibition in the absence and presence of 10 μ M CCCP (Fig. 2-10) indicating that there were no new proteins synthesized in the presence of KCN. The “low – high – low inhibition” pattern by KCN is understandable. As shown in Part I (Fig. 1-7), the inhibition of KCN on Fe^{2+} oxidation (inhibition of cytochrome *c* oxidase) was time-dependent which agrees with the initial “low-high” inhibition on endogenous respiration. After 25 min, the activity of endogenous respiration recovered (the transition to “high-low” inhibition) which indicates that electron flow was shifted to other terminal oxidases such as quinol oxidases *bd* and / or *bo*₃ after cytochrome *c* oxidase (*aa*₃, *ba*₃) was inhibited (Fig. 2-0).

In the presence of 4 mM FeCl_3 , the above-mentioned “low – high – low inhibition” pattern by KCN (2 mM) disappeared and KCN showed strong inhibition by 84% between 25 min and 60 min although the addition of FeCl_3 did not change the control activity appreciably (10-20% stimulation in the initial 30 min and little change after 30 min) (Fig. 2-11). The results suggested that electrons were preferentially transferred to the Fe-containing pathway instead of the quinol oxidase pathway in the presence of

FeCl₃. This is the basis on which Fe³⁺ reduction can be investigated aerobically in the presence of 2 mM KCN (see the section “2.2” in the same Part II).

NaN₃ at 0.1 mM, 1 mM and 2 mM inhibited Fe²⁺ oxidation by 98.1%, 99.8% and 99.9%, respectively (Fig. 1-9). NaN₃, however, at 0.1 mM and 1 mM, inhibited endogenous respiration only in the initial 8 min by 20% and 69%, respectively and stimulated endogenous respiration after 8 min by 95%, and 38%, respectively (Fig. 2-12). NaN₃ at 2 mM and 10 mM inhibited endogenous respiration in the initial 8 min by 76% and 67%, respectively and inhibited it after 8 min only by 5% and 62%, respectively (Fig. 2-12). In the presence 4 mM FeCl₃, NaN₃ at 0.1 mM also inhibited endogenous respiration in the initial 8 min by 19% and stimulated it after 8 min by 75% (Fig. 2-11). NaN₃ not only inhibited cytochrome *c* oxidase, but inhibited ATPase and also had an uncoupling effect due to its weak acid nature (Adapoe and Silver 1975; Harold 1972; Hesse et al. 2002). There was a complete inhibition of Fe²⁺ oxidation in the initial short time possibly due to the inhibition of ATPase by 10 μM NaN₃ and the partial activity recovery of Fe²⁺ oxidation due to the uncoupling effect of 10 μM NaN₃ on cytochrome *c* oxidase when 2.4 mg cells were used in 1.2 mL (Fig. 1-8). So the stimulation by 0.1 mM NaN₃ on endogenous respiration (by 24 mg cells in 1.2 mL) could be due to the weak acid effect of 0.1 mM NaN₃ on cytochrome *c* oxidase as well as on NDH-1 (Fig. 2-11). However the activity recovery of endogenous respiration by 1 mM, 2 mM and even 10 mM NaN₃ (Fig. 2-12) should be mainly due to the roles of other oxidases (e.g. quinol oxidases) after cytochrome *c* oxidase was inhibited. NaN₃ on Fe²⁺ oxidation by 24 mg cells (Fig. 1-9) supported this interpretation.

2.1.4. Effect of inhibitors of complex III and quinol oxidases

Complex III (bc_1 complex) inhibitors, myxothiazol (10 μM) and antimycin A (0.1 mM), showed little effect on endogenous respiration in the absence of FeCl_3 but showed 20 – 35% stimulation in the presence of 4 mM FeCl_3 (Table 2-2).

HQNO, an inhibitor for both bc_1 complex and quinol oxidase (Kamikura et al. 2001; Brasseur et al. 2004), at 0.5 μM , 1 μM , 4 μM , 10 μM , 40 μM and 100 μM , stimulated endogenous respiration by 36%, 68%, 96%, 211%, 360% and 358%, respectively when FeCl_3 was absent (Fig. 2-13a). The stimulation of endogenous respiration by inhibitors of complex III and quinol oxidase was unexpected and was initially thought to be similar to effect of uncouplers (see 2.1.1). Since uncouplers led to the increase of external pH of the cells during endogenous respiration but HQNO did not when tested in water of pH 3.5 (see 2.1.7), the effect of HQNO on endogenous respiration was also studied in water instead of 0.1 M β -alanine- H_2SO_4 buffer. When tested in water of pH 3.5, HQNO at 4 μM , 10 μM and 100 μM also stimulated endogenous respiration by 44%, 73% and 114%, respectively (Fig. 2-13b). In the presence of 4 mM FeCl_3 , HQNO at 40 μM also stimulated endogenous respiration by 261% (Table 2-2), much more than myxothiazol or antimycin A.

Since endogenous respiration was greatly stimulated by both uncouplers and HQNO, it was important to compare the effects by these two groups of compounds. Fig. 2-14 shows the effects of HQNO (40 μM) and CCCP (10 μM) on endogenous respiration with and without the presence of complex IV inhibitor KCN (2 mM) and complex I inhibitor rotenone (0.1 mM). HQNO or CCCP alone or their combination gave a similar stimulation of 160%. In the initial 17 min, KCN inhibited both HQNO- and CCCP-

stimulated activities by 70%; after 17 min, it inhibited HQNO-stimulated activity by 65% (Fig. 2-14a) but inhibited CCCP-stimulated activity by only 19% (Fig. 2-14b). The activity in the presence of both CCCP and KCN was inhibited by HQNO by 52% between 17 min and 60 min and the inhibited activity was further inhibited by rotenone by 77% (Fig. 2-14b). The results indicate that the mechanism of stimulation by HQNO is different from that by CCCP. The stimulation by CCCP is due to the uncoupling of respiratory control. Since HQNO inhibits complex III and quinol oxidase (*bd*, *bo*₃), the stimulation by HQNO may be due to the opening of a new electron transport pathway (as shown later in Fig. 2-45) directly from Q (Fig. 2-0) to unknown electron carrier(s) to Fe³⁺ the reduction product of which, Fe²⁺, will be oxidized via the Fe²⁺ oxidation system. It should be mentioned that in mitochondria electron flow could bypass the Q-cycle of cytochrome *bc*₁ complex from QH₂ to a cytochrome *c* in the presence of *bc*₁ complex inhibitors (Kramer et al. 2004; Muller et al. 2002). That rotenone strongly inhibited the activity of endogenous respiration in the presence of KCN, HQNO and CCCP (Fig. 2-14b) indicates the existence of the terminal oxidase(s) which was insensitive to KCN (complex IV inhibitor) and HQNO (quinol oxidase inhibitor), but it accepted electrons from Q (Fig. 2-45).

Another complex IV inhibitor, NaN₃, was also used to test the comparative effects of CCCP (10 μM) and HQNO (40 μM) on endogenous respiration (Fig. 2-15). HQNO or CCCP alone stimulated endogenous respiration by 230%. NaN₃ at 2 mM inhibited endogenous respiration by 70% in the initial 8 min but only 18% between 8 min and 60 min. When CCCP was added at 10 min, the activity in the presence of NaN₃ was stimulated by 33%, but when HQNO was added at 10 min, it was inhibited by 20%. The

results, similar to the results in the presence of KCN, supported the concept that electrons were shifted after cytochrome *c* oxidase inhibition by NaN_3 to other oxidases some of which were inhibited by HQNO. The stimulation of endogenous respiration (presumably via quinol oxidases *bd* and / or *bo*₃) by CCCP (added at 10 min) may suggest proton pumping (by quinol oxidases *bd* and / or *bo*₃). This is also supported by the later-time stimulatory effect of DNP in Fig. 2-9, CCCP in Figs. 2-10 & 2-14b, and NaN_3 in Fig. 2-12.

2.1.5. Effect of complex II inhibitor (TTFA)

Since endogenous substrates were oxidized to CO_2 by O_2 with a respiratory quotient (CO_2 / O_2) close to 1.0 (see 2.1.8), a complete TCA cycle is indicated. Thus it was expected that endogenous substrates could be oxidized by complex I as well as by complex II. Fig. 2-16 shows the effect of complex II inhibitor TTFA (chelating non-heme iron) on endogenous respiration in the absence and presence of other compounds. TTFA at 0.1 mM and 1 mM stimulated endogenous respiration by 69% and 94%, respectively. NaN_3 at 0.1 mM inhibited 1 mM TTFA-stimulated activity by 18%, and at 2 mM inhibited it by 76%, 44% and 83% in 0 – 17 min, 17 – 25 min and 25 – 60 min, respectively. KCN at 2 mM, rotenone at 0.1 mM and HQNO at 40 μM inhibited 1 mM TTFA-stimulated activity by 70%, 75% and 1%, respectively. The stimulation of endogenous respiration by TTFA was unexpected. The results indicate that TTFA stimulation was similar to HQNO stimulation rather than CCCP stimulation although the exact mechanism is unknown. Since TTFA inhibits complex II by chelating non-heme iron (Ulvik and Romslo 1975), it may also inhibit other non-heme iron containing

enzymes. Another inhibitor of complex II sodium malonate at 10 mM, and the potential substrate of complex II sodium succinate at 10 mM, also stimulated endogenous respiration both by 140% (Fig. 2-4). The effect of malonate and succinate was treated as the effect of weak acids (see 2.1.1). The reasons will be discussed later.

2.1.6. Effect of iron chelators

Since it was proposed that the cell surface of *A. ferrooxidans* is coated by an iron-grid (Ingledew and Houston 1986), it is possible that iron chelators will affect endogenous respiration. Therefore, the effect of different iron chelators has been investigated.

O-phen. (*ortho*-phenanthroline) (0.44 mM, data not shown), 2,2'-dipyridyl (10 mM, data not shown), EDTA (2 mM, data not shown), HQSA (8-hydroxyquinoline-5-sulfonic acid, 0.5 mM, data not shown), oxalic acid (1 mM, Fig. 2-17), and sodium pyrophosphate (NaP_2O_7 , 4 mM, Fig. 2-17) stimulated endogenous respiration by 30%, 30%, 20%, 10%, 40% and 73%, respectively. Ferrozine at 2 mM inhibited endogenous respiration by 73% in the initial 15 min but stimulated it by 64% after 15 min (Fig. 2-17). Deferoxamine mesylate at 2 mM had no effect on endogenous respiration (data not shown). These iron chelators may stimulate endogenous respiration by affecting the redox potential of iron when the Fe-containing pathway was used (Fig. 2-0).

Fe^{3+} chelator, tiron at 4 mM stimulated the respiration by 380% and the stimulated activity was inhibited by 0.6 mM *o*-phen. (Fe^{2+} chelator) and 10 mM 2,2'-dipyridyl (Fe^{2+} chelator), 0.1 mM rotenone (complex I inhibitor) and 30 μM DNP by 36%, 31%, 31% and 15%, respectively (Fig. 2-18). The 4 mM tiron-stimulated endogenous respiration was inhibited by 40 μM HQNO by 9% and the inhibited activity was further inhibited

by 2 mM KCN by 73% (data not shown). The results indicate that the increased O₂ consumption rate by tiron was not mainly due to the true stimulation of endogenous respiration but mainly due to the oxidation of tiron via the Fe²⁺ oxidation system as shown in Part I.

Iron chelators SHAM and propyl gallate (PG), which are the inhibitors of plant alternative oxidase (Siedow and Bickett 1981; Murphy and Lang-Unnasch 1999; Stenmark and Nordlund 2003), also stimulated endogenous respiration. SHAM at 2 mM stimulated endogenous respiration by 200% and the stimulated activity was inhibited by 0.1 mM rotenone, 2 mM amytal, 2 mM KCN, 0.6 mM o-phenanthroline and 10 mM 2,2'-dipyridyl by 70%, 80%, 61%, 43% and 22%, respectively (Fig. 2-19). SHAM, however, at 2 mM inhibited the 40 μM HQNO-stimulated endogenous respiration by 30% and the inhibited activity was further inhibited by 2 mM KCN by 58% (Fig. 2-20a). SHAM (2 mM) also inhibited the 10 μM CCCP-stimulated endogenous respiration after 2 mM KCN inhibition by 38% (Fig. 2-20b). SHAM (2 mM) had no effect on the 10 μM CCCP-stimulated endogenous respiration in the absence of KCN (data not shown). Although SHAM could also be oxidized using the Fe²⁺ oxidation system (Part I), it may truly stimulate endogenous respiration since the stimulated activity by SHAM was strongly inhibited by complex I inhibitors rotenone and amytal (Fig. 2-19).

Propyl gallate at 0.2 mM and 2 mM increased the respiration by 8 and 25 times, respectively (Fig. 2-21), and the latter activity was inhibited by 0.6 mM o-phenanthroline and 2 mM KCN by 26% and 97%, respectively (Fig. 2-21) but not affected by 0.1 mM rotenone, 10 mM 2,2'-dipyridyl or 30 μM DNP (data not shown). So, the stimulated respiration by PG (also an antioxidant), different from that by SHAM,

was not due to the true stimulation of endogenous respiration but mainly due to the oxidation of PG via the Fe^{2+} oxidation system as shown in Part I.

2.1.7. Change of external pH of cells

When cells (100 mg / mL) in pH 3.5 water were kept at room temperature (23 – 26 °C) before the pH change experiments, the external pH during endogenous respiration by cells increased from 3.3 to 3.68 within 4 hours (Fig. 2-22). This indicates that protons leaked into the cells during endogenous respiration by *A. ferrooxidans*. The result is also similar to the observation about another acidophile *Thiobacillus acidophilus* reported by Zychlinsky and Matin (1983). The cell suspension of *T. acidophilus* in water increased 0.7 pH unit at day 12 of starvation and 1.0 pH unit at day 22 of starvation.

Fig. 2-23 shows the external pH changes during endogenous respiration in cells of 20 mg / mL with the addition of different compounds when cells were kept at 4°C before testing. The external pH did not change with the control experiment, but it changed from pH 3.4 to 3.6, 3.5, 3.5, 3.5 and 3.5 with the addition of 1 μM nigericin, 10 μM CCCP, 30 μM DNP, 0.1 mM KSCN and 0.1 mM valinomycin, respectively. The results indicate that protons were translocated into the cells with the addition of these compounds, which confirmed that the stimulation of endogenous oxidation by these compounds was due to the uncoupling of respiratory control (destroying Δp).

Similar experiments were also carried out by the addition of 5 mM NEM, 0.1 mM HgCl_2 , 0.1 mM AgNO_3 , 0.1 mM rotenone, 4 mM atabrine and 0.1 mM HQNO and no pH changes were observed with these compounds (data not shown). Therefore, the

stimulation on endogenous oxidation by NEM, HgCl₂, AgNO₃ and HQNO was different from that by Δp dissipaters.

2.1.8. Respiratory quotient of endogenous respiration

Manometric experiments at 30°C were done to determine the CO₂ / O₂ ratio during endogenous respiration. Table 2-3 and Fig. 2-24 showed CO₂ production and O₂ consumption and their ratios during endogenous respiration in the absence and presence of 10 μ M CCCP, 10 mM Na₂-succinate, 10 mM Na₂-malonate, 40 mM CH₃COOK, 0.1 mM valinomycin, 1 μ M nigericin, 5 mM NEM, 2 mM SHAM, 1 mM TTFA, 4 mM tiron and 40 μ M HQNO. All these compounds stimulated endogenous respiration in Oxygraph experiments. These compounds, except TTFA and succinate (control not tested at the same time, Fig. 2-24e), stimulated CO₂ production and O₂ consumption during endogenous respiration. The CO₂ / O₂ ratio was close to 1.0 both in the absence and presence of these compounds with the exception of 4 mM tiron where the CO₂ / O₂ ratio was only 0.79 (Fig. 2-24c). This is consistent with a carbohydrate nature [(CH₂O)_n] of endogenous substrates and also confirmed the stimulation by these compounds except tiron was due to the true stimulation of endogenous respiration. In the presence of 10 mM Na₂-malonate or 40 mM CH₃COOK, O₂ consumption and CO₂ production were linear in the initial 4 hours and then slowed down (Fig. 2-24f) suggesting their long-term weak acid effect on endogenous respiration. In the initial 4 hours, malonate stimulated O₂ consumption and CO₂ production by 13% and 16%, respectively, and acetate stimulated these by 61% and 71% as expected from their uncoupling effect, respectively. However, during 4 – 8 h periods, malonate inhibited O₂ consumption and CO₂

production by 68% and 78, respectively, and acetate inhibited these by 35% and 44%, respectively presumably by excessive acid entry into the cells (Fig. 2-24f). In the presence of 10 mM succinate (Fig. 2-24e), the CO_2 / O_2 ratio was close to 1.0 and O_2 consumption and CO_2 production were fast before 2 h but slowed down after 2 h, which suggested that succinate stimulated endogenous respiration by its weak acid effect but it was not oxidized as a substrate.

2.1.9. Endogenous respiration by spheroplasts and cell free extracts

Cell free extracts showed no detectable rate of endogenous respiration in 0.1 M β -alanine- H_2SO_4 buffer of pH 3.5 but was 20 – 80% of that of whole cells in 50 mM MES buffer of pH 6.5 and 10 mM K_2HPO_4 - KH_2PO_4 buffer of pH 7.0 (data not shown).

Detailed studies of endogenous respiration by cell free extracts were not carried out because the activities were not stable or reproducible at pH 6.5 and 7.0.

Spheroplasts could perform endogenous respiration and the respiration activity did not change within 3 days when spheroplasts were kept at 4°C (data not shown). Table 2-4 shows the activity of endogenous respiration by spheroplasts and the effects of complex I inhibitors, uncoupler CCCP and HQNO. Spheroplasts showed a similar activity as whole cells. Complex I inhibitors rotenone (0.1 mM) and amytal (2 mM) showed slightly stronger inhibition on endogenous respiration by spheroplasts (62% and 48%, respectively) than by whole cells (48% and 42%, respectively, Table 2-1) but atabrine (2 mM) still had no effect on respiration by spheroplasts as by whole cells (Table 2-1). Uncoupler CCCP, which showed strong stimulation of 162% of respiration by whole cells at 10 μM (Fig. 2-1a), showed 17% inhibition on respiration by

spheroplasts (Table 2-4). The inhibitor of complex III and quinol oxidase, HQNO, which stimulated endogenous respiration by 260% at 40 μM (Fig. 2-13a), showed 6% inhibition. Thus stimulation of endogenous respiration by uncouplers and HQNO could only be achieved by whole cells. The stimulation of endogenous respiration by CCCP and HQNO disappeared by the preparation of spheroplasts probably due to the destruction or disorganization of electron carrier(s) on the Fe-containing electron transport pathway and the loss of periplasmic content.

2.2. Endogenous oxidation by Fe^{3+}

Reduction of Fe^{3+} to Fe^{2+} by endogenous metabolism of *A. ferrooxidans* could be demonstrated only when the rapid reoxidation of Fe^{2+} to Fe^{3+} by the cells was inhibited. Fig. 2-25 shows that in the presence of complex IV (cytochrome *c* oxidase) inhibitor KCN or NaN_3 , cells can reduce Fe^{3+} to Fe^{2+} . When KCN was present, the rate of Fe^{3+} reduction reached the maximum at 2 mM and the rate did not change too much even when the concentration of KCN was increased up to 50 mM. When NaN_3 was present, the rate to Fe^{3+} reduction increased with the increase of the concentration of NaN_3 and reached the maximum at 10 mM, which then went down to the level close to zero at 50 mM. The maximal rate of Fe^{3+} reduction was 4-folds in the presence of NaN_3 as in the presence of KCN and the concentration required for a maximal rate is 5-folds for NaN_3 as for KCN. KCN may only inhibit cytochrome *c* oxidase but NaN_3 could have the additional effect by working as a weak acid (Harold 1972; Hesse et al. 2002). The Fe^{3+} reduction rate by endogenous substrates may not have been stimulated by KCN but may have been stimulated by NaN_3 . Therefore, 2 mM KCN was included to study the details

of Fe^{3+} reduction by cells. When cells were kept at 4°C for 10 days without disturbing, the rate of Fe^{3+} reduction tested at pH 2.3 did not go down (data not shown). Actually all experiments were done within 3 days after harvesting of cells. When the same batch of cells were used, the rate of Fe^{3+} reduction was identical to that of O_2 reduction in terms of electrons transferred, that is 4 Fe^{3+} reduction to 4 Fe^{2+} corresponding to the consumption of one O_2 (data not shown). This observation, similar to the demonstration in Fig. 2-11, also supports the view that electrons were preferentially transferred to the Fe^{3+} -reducing pathway instead of the quinol oxidase pathway in the presence of FeCl_3 even under aerobic conditions with the presence of 2 mM KCN. When the same batch of cells were divided into two parts which were harvested and suspended in buffers of pH 2.3 and 3.5, respectively, the Fe^{3+} reduction rate by endogenous substrates at pH 2.3 was two folds of the rate at pH 3.5 (data not shown). The difference may be due to the higher solubility of Fe^{3+} at pH 2.3 than at pH 3.5 since the O_2 reduction rate by endogenous substrates at pH 2.3 was 16% less than that at pH 3.5 (data not shown).

2.2.1. Effect of complex I inhibitors

Complex I inhibitors, rotenone, amytal and piericidin A, had strong inhibition on Fe^{3+} reduction by endogenous substrates (Table 2-5 and Figs. 2-26, 2-27, 2-28). Rotenone at 0.1 mM and amytal at 2 mM inhibited the reduction rate at pH 3.5 by 46% and 45%, respectively, but at pH 2.3 by 78% and 80%, respectively. It should be mentioned that the rate of Fe^{3+} reduction by the same batch of cells was faster at pH 2.3 than at pH 3.5. The higher inhibition by rotenone and amytal at pH 2.3 may be due to the fact that more electrons must flow to complex I whose activity becomes rate-limiting in the presence

of these inhibitors. The actual Fe^{3+} reduction rates become similar at both pH's in the presence of inhibitors (Table 2-5). Piericidin A at 0.5 μM showed a stronger inhibition (92% at pH 3.5) than rotenone and amytal. A combination of these three inhibitors was less effective than piericidin A alone. The reason for the strong inhibition by piericidin A at pH 3.5 is unknown since it inhibited O_2 reduction only by 50% as rotenone and amytal did (see 2.1.2). Another complex I inhibitor atabrine did not inhibit Fe^{3+} reduction but slightly stimulated it (10% at pH 2.3 and 20% at pH 3.5) at a high concentration of 4 mM (Fig. 2-29). Thus all inhibitors of complex I had similar effects on Fe^{3+} reduction as on O_2 reduction (shown in 2.1.2) further supporting that the NDH-1 ($\text{NDH-1}_{\text{down}}$) involved in endogenous oxidation is different from the one (NDH-1_{up}) involved in Fe^{2+} oxidation, and other dehydrogenase(s) other than $\text{NDH-1}_{\text{down}}$ may also be engaged in endogenous oxidation.

2.2.2. Effect of inhibitors of complex III and quinol oxidases

Complex III inhibitors, myxothiazol and antimycin A, had no effect on Fe^{3+} reduction by endogenous substrates (Figs. 2-30 and 2-31). HQNO, an inhibitor of both complex III and quinol oxidase, significantly stimulated Fe^{3+} reduction at pH 2.3 and pH 3.5 starting from 10 μM (Table 2-6 and Fig. 2-32). The 0.1 mM HQNO-stimulated activity (250% stimulation) at pH 3.5 was inhibited by 0.1 mM rotenone by 82% (Table 2-6 and Fig. 2-32a). Effect of HQNO on Fe^{3+} reduction agrees with its effect on O_2 reduction (see 2.1.4) supporting that electron flow was shifted to the fast Fe-containing pathway (Fig. 2-45) from Q (Fig. 2-0) to Fe^{3+} after complex III and quinol oxidases were inhibited. The stimulation of Fe^{3+} reduction by HQNO may also indicate that electrons flowed along

the slow pathway from Q to bc_1 II to an unknown cytochrome *c* to an unknown electron carrier to Fe^{3+} in the absence of HQNO (Fig. 2-0).

2.2.3. Effect of complex II inhibitor (TTFA)

Table 2-7 and Fig. 2-33 show the effect of complex II inhibitor TTFA on Fe^{3+} reduction by endogenous substrates. TTFA, similar to HQNO, starting from a concentration of 10 μ M, showed significant stimulation. The 1 mM TTFA-stimulated activity (250% stimulation) was strongly inhibited by rotenone and amytal but not affected by 0.1 mM HQNO at all. Thus TTFA with an unknown mechanism had the similar effect to HQNO on both Fe^{3+} reduction and O_2 reduction (see 2.1.5) by endogenous substrates.

2.2.4. Effect of uncouplers, ionophores, anions, weak acids, thiol agents and inhibitors of ATP synthase

Effect of uncouplers on Fe^{3+} reduction by endogenous substrates was shown in Table 2-8 and Figs. 2-34 and 2-35. CCCP at 10 μ M and DNP at 30 μ M stimulated the rate at pH 3.5 by two to three folds. Lower and higher concentrations showed less stimulation and very high concentrations showed inhibition. Fe^{3+} reduction was more sensitive to the inhibition by CCCP and DNP at pH 2.3 than at pH 3.5. Rotenone at 0.1 mM, 2 mM amytal and their combination inhibited the 10 μ M CCCP-stimulated activity at pH 3.5 by 83%, 57% and 92%, respectively and the 30 μ M DNP-stimulated activity at pH 3.5 by 78%, 59% and 84%, respectively.

Ionophores, nigericin and valinomycin also stimulated Fe^{3+} reduction by endogenous substrates (Table 2-9 and Figs. 2-36 and 2-37), more at pH 3.5 than at pH 2.3. Nigericin at 1 μM and valinomycin at 0.1 mM showed stimulation at pH 3.5 by 200% and 190%, respectively. Lower and higher concentrations showed less stimulation. Rotenone at 0.1 mM and 2 mM amytal inhibited the 1 μM nigericin-stimulated activity by 92% and 89%, respectively and inhibited the 0.1 mM valinomycin-stimulated activity by 89% and 87%. In the presence of 1 mM K_2SO_4 , valinomycin showed a similar extent of stimulation on Fe^{3+} reduction as in the absence of K_2SO_4 .

Permeable anions also stimulated Fe^{3+} reduction by endogenous substrates. KSCN showed less stimulation and more inhibition at pH 2.3 than at pH 3.5. KSCN at 0.1 mM stimulated the rate by 280% at pH 3.5 and the stimulated activity was inhibited by 0.1 mM rotenone, 2 mM amytal and their combination by 87%, 75% and 97%, respectively (Table 2-10 and Fig. 2-38). Na-tetraphenylboron at 0.1 μM only showed 7% stimulation at pH 3.5 and higher concentrations only showed inhibition (data not shown).

Weak acids, CH_3COOK ($\text{p}K_a$ 3.45) and KF ($\text{p}K_a$ 4.75), showed stimulation on Fe^{3+} reduction (Table 2-11 and Figs. 2-39, 2-40) as on O_2 reduction. Higher stimulations were observed at pH 3.5 than at pH 2.3. Rotenone at 0.1 mM and 2 mM amytal inhibited the 40 mM CH_3COOK -stimulated activity by 89% and 90%, respectively, and inhibited the 1 mM KF -stimulated activity by 88% and 85%, respectively (Table 2-11 and Figs. 2-39, 2-40). Na_2 -succinate and Na_2 -malonate also greatly stimulated Fe^{3+} reduction and complex I inhibitors, except atabrine, showed stronger inhibition on the stimulated activities (Table 2-12 and Fig. 2-41). Na_2 -succinate could not have been used as a substrate metabolized via complex II because complex II inhibitor TTFA at 1 mM

showed no inhibition (Table 2-12). Na_2 -succinate ($\text{p}K_a$ 1 4.21, $\text{p}K_a$ 2 5.64) and Na_2 -malonate ($\text{p}K_a$ 2.85), were not used as substrates but functioned as weak acids being responsible for the stimulation. As discussed before, the finding that that CO_2 production and O_2 consumption slowed down in the presence of these two compounds as well as acetate in long time experiments (Fig. 2-24e, f) also supports this interpretation.

Thiol agents NEM, HgCl_2 and ANO_3 stimulated Fe^{3+} reduction up to 90% to 200% and these stimulated activities were also strongly inhibited by complex I inhibitors rotenone and amytal (Table 2-13 and Figs. 2-42, 2-43).

Inhibitors of ATP synthase, DCCD and oligomycin, had no effect on Fe^{3+} reduction by endogenous substrates (Fig. 2-44). As discussed in Part I, the reason may be due to the lack of effect or the lack of permeability of these inhibitors into the whole cells of *A. ferrooxidans*.

Therefore, uncouplers, ionophores, anions, weak acids, thiol agents and inhibitors of ATP synthase had similar effects on the reduction of Fe^{3+} and O_2 by endogenous substrates. The stimulation of Fe^{3+} reduction by uncouplers, ionophores, anions, weak acids indicates the existence of a normal respiratory control during endogenous oxidation by Fe^{3+} . Complex I inhibitors rotenone and amytal showed inhibition on the stimulated activities of Fe^{3+} reduction by the above-mentioned stimulators more strongly than on the activity of Fe^{3+} reduction in the absence of these stimulators also supporting that increased electron flow from $\text{NDH-1}_{\text{down}}$ in the presence of these stimulators. The effect of thiol agents on Fe^{3+} reduction will be discussed later.

Discussion and conclusions

The stimulation of endogenous oxidation by uncouplers (Table 2-8 and Figs. 2-1, 2-34, 2-35), ionophores (Table 2-9 and Figs. 2-2, 2-36, 2-37), anions (Table 2-10 and Figs. 2-3, 2-38), weak acids (Tables 2-11, 2-12 and Figs. 2-4, 2-39, 2-40, 2-41) indicates the existence of a normal respiratory control during endogenous oxidation, that is, the stimulation of respiration by dissipation of Δp . This is further supported by the increase of external pH of cells with the addition of these compounds (Fig. 2-23). The genes coding for acetate kinase have been found in the partial genome sequence of *A. ferrooxidans* (data not shown). However, the stimulatory effect of acetate on endogenous oxidation in this organism is believed to be due to Δp destruction instead of acetate oxidation, because the oxygen consumption rate in the presence of acetate slowed down as with malonate and succinate (Fig. 2-24) due to H^+ increase in the cytoplasm. If acetate and other weak acids had been oxidized, the oxygen consumption should have continued.

Thiol agents NEM, $HgCl_2$ and ANO_3 tested as potential inhibitors were unexpectedly found to be stimulators of endogenous oxidation (Table 2-13 and Fig. 2-5, 2-42, 2-43). Hg^{2+} and Ag^+ are known to be inhibitors of *A. ferrooxidans* cytochrome *c* oxidase and Fe^{2+} oxidation (Sugio et al. 1981; Ingledew 1982). Mechanism of stimulation by these sulfhydryl binding agents is unknown, but could be related to NEM-induced K^+ efflux systems found in gram-negative bacteria (Booth et al. 1993; Bott and Love 2004), which might increase the rate of H^+ leaking in.

The stimulation by P_i (see 2.1.1) of endogenous respiration may be due to the accelerated dissipation of Δp via ATP synthase as discussed in Part I. The reason for the stimulation of arsenate on endogenous respiration (Fig. 2-6) may be due to the

substitution of arsenate for Pi as arsenate stimulated the respiration in washed mitochondria in the absence of Pi (Crane and Lipmann 1953).

Complex I inhibitors rotenone, amytal and piericidin A inhibited endogenous oxidation by only 50% (except piericidin A had a stronger inhibition on endogenous oxidation by Fe^{3+}) indicates the involvement of NDH-1 as well as other dehydrogenase(s) in endogenous oxidation. Since these inhibitors showed stronger inhibition on the stimulated activities by the above-mentioned stimulators, larger proportion of electrons must flow to NDH-1 under the stimulated conditions. Since the increased respiration is in response to dissipating Δp , the NDH-1 must be pumping protons, but not other dehydrogenase(s). The other dehydrogenase(s) is unknown but a candidate could be the NDH-2 (the Type-II NADH dehydrogenase; a monooxygenase NADH: quinone oxidoreductase which does not involve proton pumping and is insensitive to the inhibition by complex I inhibitors) since the gene coding for a subunit of NDH-2 like protein has been isolated and cloned in *A. ferrooxidans* (Dominy et al. 1997). The opposite effects of atabrine (inhibiting Fe^{2+} oxidation but having no effect on endogenous oxidation) and piericidin A (inhibiting endogenous oxidation but having no effect on Fe^{2+} oxidation) as well as the existence of two putative types of NDH-1 in *A. ferrooxidans* (see the discussion in Part I) may indicate that two types of NDH-1 were engaged in Fe^{2+} oxidation and endogenous oxidation, respectively. NDH-1_{up} was responsible for Fe^{2+} oxidation (electrons going uphill for NAD^+ reduction) and NDH-1_{down} for endogenous oxidation (downhill NADH oxidation).

The insensitivity of endogenous respiration to the inhibition by complex IV inhibitors KCN and NaN_3 indicates that terminal oxidases other than cytochrome *c* oxidase were

also involved in endogenous respiration. The “low-high-low inhibition” pattern by KCN (Fig. 2-8) and “high-low inhibition” pattern by NaN_3 (Fig. 2-12) indicate electron shifting from cytochrome *c* oxidase to other oxidases.

It was unexpected that HQNO, an inhibitor of complex III and quinol oxidase, greatly stimulated endogenous oxidation (Figs. 2-13 & 2-32). However, the stimulation of endogenous oxidation by HQNO was different from that by uncouplers CCCP and DNP since (1) KCN inhibited the stimulated activity of endogenous respiration by HQNO (Fig. 2-14) more strongly than by uncouplers CCCP and DNP (Figs. 2-9 & 2-14) and (2) the external pH did not change upon the addition of HQNO but it increased by the addition of CCCP or DNP (see 2.1.7). The great stimulation of endogenous oxidation by HQNO may suggest the opening of a new fast pathway from Q (Fig. 2-0) to Fe^{3+} (Fig. 2-45) after complex III and quinol oxidases were inhibited. This is similar to the case in mitochondria where electron flow could bypass the Q-cycle of cytochrome *bc*₁ complex from QH_2 to a cytochrome *c* when *bc*₁ complex was inhibited (Kramer et al. 2004; Muller et al. 2002). The extent of stimulation (250 – 360%) on endogenous oxidation by HQNO in *A. ferrooxidans* (Figs. 2-13 & 2-32) is similar to the extent of stimulation (355%) on succinate oxidation via the alternative oxidase pathway by myxothiazol in isolated soybean cotyledon mitochondria (Hoefnagel et al. 1995, also see “General Introduction and Literature Reviews”).

HQNO strongly inhibited the activities of endogenous respiration in the presence of KCN with or without CCCP (Fig. 2-14) and the activity in the presence of NaN_3 (Fig. 2-15) indicating the involvement of quinol oxidases (*bd* and / or *bo*₃) in endogenous respiration (Fig. 2-45). The HQNO-sensitive quinol oxidases (*bd* and / or *bo*₃) may

pump protons since (1) the activity of endogenous respiration was greatly stimulated by CCCP after electrons were shifted away from cytochrome *c* oxidase by KCN (Fig. 2-14b); (2) the activity in the presence of KCN and CCCP was greatly inhibited by HQNO (Fig. 2-14b); and (3) the activity in the presence of KCN, HQNO and CCCP (Fig. 2-14b) was similar to that in the presence of KCN and HQNO (Fig. 2-14a). That rotenone strongly inhibited the activity of endogenous respiration in the presence of KCN, HQNO and CCCP (Fig. 2-14b) indicates that at least one terminal oxidase other than cytochrome *c* oxidases (*aa₃* and *ba₃*) and quinol oxidases (*bd* and *bo₃*) may be involved in endogenous respiration and the unknown terminal oxidase(s) may not be able to pump protons. The possible candidate for the unknown terminal oxidase is an alternative oxidase since, according to the present knowledge, only three types of terminal oxidases in biology have been reported including cytochrome *c* oxidase, quinol oxidase and alternative oxidase (Table 1). Cytochrome *c* oxidase exists in both eukaryotes and prokaryotes. Quinol oxidase has only been reported in prokaryotes. Alternative oxidase was previously considered to be an oxidase unique to eukaryotes but it was recently reported to exist in the gram negative bacterium *Novoshingobium aromaticivorans* (Stenmark and Nordlund 2003).

The effect of the inhibitors of plant alternative oxidases (belonging to the di-iron carboxylate protein family), PG and SHAM, which are also iron chelators, has been tested on endogenous respiration (see 2.1.6). Unexpectedly PG and SHAM both greatly stimulated the respiration by the cells. The respiratory activity in the presence of 2 mM PG was as high as 25 folds the control activity (endogenous respiration) (Fig. 2-21) and the activity in the presence of 2 mM PG was sensitive to the inhibition by KCN (Fig. 2-

21) but not sensitive to the inhibition by rotenone (data not shown) making it possible that the high activity in the presence of PG was not due to the true stimulation of endogenous respiration but mainly due to the oxidation of PG via the Fe^{2+} oxidation system. The studies in Part I have confirmed this hypothesis. Although SHAM was also shown to be oxidized by cells via the Fe^{2+} oxidation system (see Part I), it only happened in the presence of externally added Fe^{3+} . SHAM at 2 mM stimulated endogenous respiration by 200% and the stimulated activity was strongly inhibited by complex I inhibitors rotenone and amytal (Fig. 2-19). So SHAM truly stimulated endogenous respiration and its effect is similar to the effect by HQNO since the SHAM-stimulated activity was also sensitive to the inhibition by complex IV inhibitor KCN (Fig. 2-19). SHAM at 2 mM, however, inhibited the 40 μM HQNO-stimulated activity of endogenous respiration by 30% and inhibited the 10 μM CCCP-stimulated activity after 2 mM KCN inhibition by 38% (Fig. 2-20b) but it had no effect on the 10 μM CCCP-stimulated activity and the activity in the presence of 2 mM KCN and 40 μM HQNO (Data not shown). Furthermore, 2 mM SHAM strongly inhibited formic acid oxidation (see Part V). These results suggested that an alternative oxidase may be involved in endogenous respiration. The genes coding for the alternative oxidase-like protein have not been found in the partial genome sequence of *A. ferrooxidans* ATCC 23270 upon the bioinformatics searching. However, the genes coding for a di-iron carboxylate protein that may be involved in ubiquinone biosynthesis, have been identified and cloned in *A. ferrooxidans* (Stenmark et al. 2001). Therefore, based on current information, it is not certain if alternative oxidase exists in *A. ferrooxidans* and is involved in endogenous respiration. Since SHAM is supposed to inhibit plant alternative

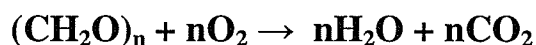
oxidase by iron chelation as well as a competitive inhibitor in binding ubiquinol (Siedow and Bichett 1981) and since it also inhibits other enzymes such as horseradish peroxidase by binding the reduced hydroquinone or forming a charge transfer complex between its hydroxamic acid and an electron-accepting group in the enzyme (Rich et al. 1987), it is possible that SHAM, similar to HQNO, inhibited cytochrome bc_1 complexes and quinol oxidases in *A. ferrooxidans* although the structures of these enzymes in this bacterium are still unknown.

Sodium succinate greatly stimulated respiration of the cells (Fig. 2-4a & 2-41). The stimulation was not due to the oxidation of succinate by the cells but due to the stimulation of endogenous respiration by the weak acid uncoupling effect of succinate since the stimulated activity by 10 mM succinate was not inhibited by the complex II inhibitor TTFA but was strongly inhibited by complex I inhibitors rotenone and amytal (Table 2-12). Another complex II inhibitor malonate also stimulated endogenous oxidation (Fig. 2-4b & 2-41) by its weak acid effect since the stimulated activity by 10 mM malonate was strongly inhibited by rotenone and amytal (Table 2-12). TTFA also greatly stimulated endogenous oxidation (Fig. 2-16 & 2-33) and the stimulated activity was strongly inhibited by rotenone and amytal (Table 2-7 and Fig. 2-16) and also by KCN (Fig. 2-16). The effect of TTFA on endogenous oxidation is similar to the effect of HQNO. Since TTFA inhibits complex II by chelating non-heme iron (Ulvik and Romslo 1975), it is possible that TTFA also inhibited cytochrome bc_1 complexes and quinol oxidases bd and bo_3 although it is unknown if these enzymes in *A. ferrooxidans* contain non-heme iron and there is no report about the inhibition of complex III and

terminal oxidases by TTFA. Thus these results indicate that complex II may not be involved in endogenous oxidation.

Spheroplasts could perform endogenous respiration with an activity similar to that of the whole cells. That the activity of endogenous respiration in spheroplasts could not be stimulated by HQNO or CCCP indicates that certain electron carrier(s) on the outer membrane or in the periplasm in the fast Fe-containing pathway from Q (Fig. 2-45) may have been damaged or disorganized or the periplasmic content has been lost during the preparation of spheroplasts. Under these conditions, electrons may flow from Q to bc_1II to the unknown cytochrome *c* to cytochrome *c* oxidase (aa_3 , ba_3) to O_2 (Fig. 2-0) in spheroplasts.

The respiratory quotient (CO_2/O_2 ratio) of endogenous respiration was close to 1.0 in the absence and presence of some stimulators (Table 2-3 and Fig. 2-24) indicating the carbohydrate nature $[(CH_2O)_n]$ of endogenous substrates which was completely oxidized to H_2O and CO_2 as shown in Reaction 7.



Reaction 7: Endogenous respiration by *A. ferrooxidans*.

This agrees with the early studies in that most prokaryotes accumulated and oxidized glycogen for survival and energy of maintenance (Dawes 1976).

Since carbohydrates are oxidized to CO_2 and H_2O via the glycolytic pathway (the Embden-Meyerhof pathway) and other pathways and the TCA cycle (the Tricarboxylic

Acid Cycle) before electrons are transferred to the electron transport chain, it is necessary to search the genes coding for the enzymes needed for the metabolism of carbohydrates in the partial genome sequence of *A. ferrooxidans*. The genes coding for glycogen (carbohydrate) phosphorylase, phosphoglucomutase and most enzymes on the glycolytic pathway, the pentose phosphate pathway and the TCA cycle have been found in this organism although the genes coding for phosphofructokinase (the key enzyme in the glycolytic pathway), α -ketoglutarate dehydrogenase (the key enzyme in the TCA cycle) and phosphogluconate dehydrase (the key enzyme in the Entner-Doudoroff pathway) have not been found. However, the failure of indentifying the genes coding for these key enzymes in the partial genome sequence does not indicate the missing of these enzymes in this organism. Actually it was reported by Ingledew (1982) that all enzymes on the glycolytic pathway and the TCA cycle exist in *A. ferrooxidans* except that the activities of succinate and α -ketoglutarate dehydrogenase are very low. The same situation also happens to another chemoautotroph *Acidithiobacillus thiooxidans* (previously *Thiobacillus thiooxidans*). Phosphofructokinase, α -ketoglutarate dehydrogenase and phosphogluconate dehydrase are considered to be missing in *A. thiooxidans* (Tian et al. 2003), but the studies by Suzuki (1958) with ^{14}C -labelled glucose suggests that all the enzymes on the glycolytic pathway and the TCA cycle exist in this organism. It may be true that the activities of these key enzymes art too low to satisfy the energetic needs during growth (Tian et al. 2003), but the activities are fast enough for the need of maintenance of energy during starvation conditions. The fact that the rate of Fe^{2+} oxidation is 1000 times faster than the rate of endogenous oxidation in *A. ferrooxidans* (studies in this dissertation) agrees with this interpretation.

Considering that the endogenous substrates in *A. ferrooxidans* may be metabolized through the TCA cycle, the electrons from endogenous metabolism are believed to enter the electron transport pathways from complex I (NDH-1) and complex II (succinate dehydrogenase). The inhibition of endogenous oxidation by complex I inhibitors are expected, but the stimulatory effect of complex II inhibitors are unexpected the reasons of which are unknown.

In all, according to this investigation, the possible electron transport pathways of endogenous oxidation in *A. ferrooxidans* are summarized in Fig. 2-45. Major additions in Fig. 2-45 compared to Fig. 2-0 are: the fast Fe-containing pathway from Q to Fe^{3+} , based on the stimulatory effect of HQNO (Figs. 2-13, 2-14 & 2-32); NDH-2, based on incomplete inhibition by rotenone or amytal (Figs. 2-7, 2-26 & 2-27); and an unknown quinol oxidase (alternative oxidase ?), based on the inhibition by rotenone of the KCN, HQNO-inhibited respiration (Fig. 2-14). Other features of the proposed pathways are also supported by experiments discussed in this section.

Tables of Part II

Table 2-1. Effect of complex I inhibitors on endogenous respiration.

	Concentration	Rate *	R.A
Control		0.86 ± 0.01	1.00
Atabrine	1 mM	0.82 ± 0.04	0.95
	2 mM	0.89 ± 0.01	1.03
	4 mM	0.88	1.02
Control		0.89 ± 0.05	1.00
Rotenone (R)	0.1mM	0.46 ± 0.09	0.52
Amytal (Am)	2 mM	0.52 ± 0.03	0.58
R + Am		0.48	0.54
Control	0	0.99 ± 0.06	1.00
Piericidin A (PA)	0.5 μM	0.53 ± 0.01	0.54
	2.5 μM	0.49 ± 0.01	0.49
	5 μM	0.56 ± 0.03	0.57
R + AM + 0.5 μM PA		0.49 ± 0.03	0.49

* Rate: $\text{nmol O}_2 \text{ min}^{-1} (\text{mg protein})^{-1}$ ($\pm\text{SD}$, $n=2$); R.A: relative activity, a ratio of a rate over that of control.

Table 2-2. Effect of complex III inhibitors (myxothiazol and antimycin A) on endogenous respiration.

	Concentration	No FeCl ₃		In 4 mM FeCl ₃	
		Rate *	R.A	Rate *	R.A
Control		0.60 ± 0.02	1.00	0.69 ± 0.08	1.00
Myxothiazol (My)	10 µM	0.63 ± 0.05	1.05	0.83 ± 0.06	1.20
Antimycin A (An)	10 µM			0.84 ± 0.01	1.22
	0.1 mM	0.58 ± 0.01	0.97	0.85 ± 0.04	1.23
My + 0.1 mM An		0.62 ± 0.03	1.03	0.93 ± 0.04	1.35
HQNO	40 µM			2.49 ± 0.05	3.61

* Rate: nmol O₂ min⁻¹ (mg protein)⁻¹ (±SD, n=2); R.A: relative activity, a ratio of a rate over that of control.

Table 2-3. O₂ consumption and CO₂ production during endogenous respiration in the absence and presence of different compounds *.

	CO ₂ production		O ₂ consumption		R _{CO2} / R _{O2}
	Rate (R _{CO2})	R.A	Rate (R _{O2})	R.A	
Control	1.32	1.00	1.22	1.00	1.08
10 μM CCCP	3.52 ± 0.05	2.67	3.48 ± 0.1	2.85	1.01
40 μM HQNO	2.96	2.25	2.82	2.31	1.05
Control	1.96	1.00	1.94	1.00	1.01
5 mM NEM	3.18	1.62	3.13	1.61	1.02
0.1 mM valinomycin	2.62	1.34	2.56	1.32	1.02
1 μM nigericin	2.11	1.08	2.08	1.07	1.01
Control	1.90	1.00	1.82	1.00	1.04
4 mM Tiron	2.77	1.46	3.51	1.93	0.79
2 mM SHAM	2.38	1.25	2.40	1.32	0.99
1 mM TTFA	1.83		1.77		1.03
10 mM Na-succinate	0.76		0.80		0.95
	0 - 4 h		0 - 4 h		0 - 4 h
Control	1.58	1.00	1.73	1.00	0.91
10 mM Na-malonnate	1.83	1.16	1.95	1.13	0.94
40 mM CH ₃ COOK	2.69	1.71	2.78	1.61	0.97

* Experiments were carried out in Warburg respirometer with 64 mg cells in 3.2 mL reaction system at 30 °C. Rate: nmol min⁻¹ (mg protein)⁻¹ (± SD, n=2). R.A: relative activity, a ratio of a rate over that of control.

Table 2-4. Effect of rotenone, amytal, atabrine, CCCP and HQNO on endogenous respiration by spheroplasts. The information of whole cells was included for comparison.

	Concentration	By spheroplasts *			By cells **
		Rate	R.A	I or S (%)	I or S (%)
With cells		0.89 ± 0.01	0.99		
Control		0.90 ± 0.01	1.00		
Rotenone	0.1 mM	0.34 ± 0.02	0.38	62 (I)	48 (I)
Amytal	2 mM	0.47 ± 0.01	0.52	48 (I)	42 (I)
Atabrine	2 mM	0.87 ± 0.20	0.97	3 (I)	3 (S)
CCCP	10 µM	0.75 ± 0.06	0.83	17 (I)	162 (S)
HQNO	40 µM	0.85 ± 0.09	0.94	6 (I)	260 (S)

* Rate: $\text{nmol O}_2 \text{ min}^{-1} (\text{mg protein})^{-1}$ ($\pm\text{SD}$, $n=2$); R.A: relative activity, a ratio of a rate over that of control; I: inhibition; S: stimulation. ** See text for the source of information.

Table 2-5. Effect of complex I inhibitors on Fe³⁺ reduction.

	Concentration	pH 2.3		pH 3.5	
		Rate *	R.A	Rate *	R.A
Control		7.85 ± 0.24	1.00	3.62 ± 0.28	1.00
Amytal (Am)	0.5 mM	4.40 ± 0.40	0.56	3.56 ± 0.26	0.98
	2 mM **	1.55 ± 0.26	0.20	2.00 ± 0.36	0.55
	6 mM			2.05 ± 0.38	0.57
Control		7.85 ± 0.24	1.00	3.53 ± 0.11	1.00
Rotenone (R)	2 µM	5.92 ± 0.32	0.75		
	5 µM			2.50 ± 0.14	0.71
	10 µM	2.72 ± 0.22	0.35	2.18 ± 0.05	0.62
	0.1 mM **	1.76 ± 0.10	0.22	1.56 ± 0.13	0.44
Control				2.99 ± 0.30	1.00
Piericidin A (PA)	0.5 µM			0.23 ± 0.05	0.08
PA + R + Am				0.61 ± 0.14	0.20

* Rate: nmol Fe²⁺ min⁻¹ (mg protein)⁻¹ (±SD, n=3); R.A: relative activity, a ratio of a rate over that of control; ** Concentrations used in combination.

Table 2-6. Effect of HQNO on Fe³⁺ reduction.

	Concentration	pH 2.3		pH 3.5	
		Rate *	R.A	Rate *	R.A
Control		6.19 ± 0.56	1.00	3.71 ± 0.26	1.00
HQNO	10 µM	8.25 ± 0.13	1.33	5.15 ± 0.04	1.39
	40 µM	9.44 ± 0.63	1.53	8.77 ± 0.71	2.36
	0.1 mM	13.06 ± 0.50	2.11	12.84 ± 0.61	3.46
0.1 mM HQNO plus 100 µM rotenone				2.36 ± 0.00	0.18 **

* Rate: nmol Fe²⁺ min⁻¹ (mg protein)⁻¹ (±SD, n=3); R.A: relative activity, a ratio of a rate over that of control; ** compared to the rate with 0.1 mM HQNO.

Table 2-7. Effect of complex II inhibitor TTFA on Fe³⁺ reduction at pH 3.5.

	Concentration	Rate *	R.A
Control		3.38 ± 0.18	1.00
TTFA	10 µM	4.10 ± 0.07	1.21
	0.1 mM	7.49 ± 0.24	2.22
	1 mM	11.65 ± 0.05	3.45
In the presence of 1 mM TTFA			
Control		11.65 ± 0.05	1.00
Rotenone (R)	0.1 mM	3.10 ± 0.21	0.27
Amytal (Am)	2 mM	1.77 ± 0.11	0.15
R + Am		1.53 ± 0.10	0.13
HQNO	0.1 mM	11.65 ± 0.02	1.00

* Rate: nmol Fe²⁺ min⁻¹ (mg protein)⁻¹ (±SD, n=3); R.A: relative activity, a ratio of a rate over that of control.

Table 2-8. Effect of uncouplers on Fe³⁺ reduction in the absence and presence of complex I inhibitors.

		pH 2.3		pH 3.5	
	Concentration	Rate *	R.A	Rate *	R.A
Control		6.88 ± 0.31	1.00	8.20 ± 0.10	1.00
CCCP	3 μM	14.31 ± 0.50	2.08		
	10 μM	13 → 4 **	1.9 → 0.5 **	15.30 ± 0.10	1.87
	30 μM			13.60 ± 0.00	1.66
	60 μM	10 → 0 **	1.5 → 0 **		
	0.2 mM			11.10 ± 0.20	0.35
In the presence of 10 μM CCCP					
Only cells				2.91 ± 0.01	0.35
Control				8.34 ± 0.05	1.00
Rotenone (R)	0.1 mM			1.43 ± 0.04	0.17
Amytal (Am)	2 mM			3.59 ± 0.10	0.43
R + Am				0.63 ± 0.02	0.08
In the presence of 30 μM DNP					
Control				8.81 ± 0.50	1.00
DNP	10 μM	14.25 ± 1.44	1.62		
	30 μM	17.31 ± 0.88	1.96	16.00 ± 0.30	1.95
	0.1 mM	15 → 0 **	1.7 → 0 **	14.30 ± 0.20	1.74
	1 mM			4.10 ± 0.20	0.50
Only cells				2.91 ± 0.01	0.33
Control				8.82 ± 0.10	1.00
Rotenone (R)	0.1 mM			1.98 ± 0.02	0.22
Amytal (Am)	2 mM			3.61 ± 0.05	0.41
R + Am				1.39 ± 0.01	0.16

* Rate: nmol Fe²⁺ min⁻¹ (mg protein)⁻¹ (±SD, n=3); ** Rate decreased from the initial rate (as in Figs. 2-24a, 2-25a); R.A: relative activity, a ratio of a rate over that of control.

Table 2-9. Effect of nigericin and valinomycin on Fe^{3+} reduction in the absence and presence of complex I inhibitors.

	Concentration	pH 2.3		pH 3.5	
		Rate *	R.A	Rate *	R.A
Control		6.99 ± 0.13	1.00	4.45 ± 0.28	1.00
Nigericin	0.5 µM	9.25 ± 0.40	1.32		
	1.0 µM	9.22 ± 0.03	1.32	13.55 ± 0.88	3.04
	10 µM	6.98 ± 0.23	1.00		
	30 µM			8.38 ± 0.48	1.88
In the presence of 1 µM nigericin					
Control				13.55 ± 0.88	1.00
Rotenone	0.1 mM			1.02 ± 0.16	0.08
Amytal	2 mM			1.45 ± 0.34	0.11
Control	0 µM	6.01	1.00	3.43 ± 0.22	1.00
Valinomycin	1 µM			6.00 ± 0.23	1.75
	10 µM	7.62	1.27	7.82 ± 0.01	2.28
	0.1 mM			9.89 ± 0.31	2.88
	0.2 mM	6.08	1.01		
In the presence of 0.1 mM valinomycin					
Control				9.89 ± 0.31	1.00
Rotenone	0.1 mM			1.10 ± 0.11	0.11
Amytal	2 mM			1.25 ± 0.14	0.13
In the presence of 1 mM K_2SO_4					
No K_2SO_4				3.43 ± 0.22	1.18
Control				2.90 ± 0.11	1.00
Valinomycin	1 µ M			5.89 ± 0.10	2.03
	10 µ M			7.03 ± 0.06	2.42

* Rate: $\text{nmol Fe}^{2+} \text{ min}^{-1} (\text{mg protein})^{-1}$ ($\pm\text{SD}$, $n=3$); R.A: relative activity, a ratio of a rate over that of control.

Table 2-10. Effect of KSCN on Fe³⁺ reduction in the absence and presence of complex I inhibitors.

	Concentration	pH 2.3		pH 3.5	
		Rate *	R.A	Rate *	R.A
Control		8.81 ± 0.50	1.00	3.80 ± 0.40	1.00
KSCN	50 µM	16.50 ± 0.06	1.87	8.50 ± 0.40	2.24
	0.1 mM	19.19 ± 0.44	2.18	14.40 ± 0.10	3.79
	1 mM	0.94 ± 0.06	0.11	14.0 → 4.0 **	3.7 → 1.0 **
In the presence of 0.1 mM KSCN					
Only cells				2.59 ± 0.18	0.33
Control	0.1 mM			7.91	1.00
Rotenone (R)	0.1 mM			1.00	0.13
Amytal (Am)	2 mM			1.98	0.25
R + Am				0.25	0.03

* Rate: nmol Fe²⁺ min⁻¹ (mg protein)⁻¹ (±SD, n=3); ** Rate decreased from the initial rate (as in Figs. 2-30b); R.A: relative activity, a ratio of a rate over that of control.

Table 2-11. Effect of CH₃COOK and KF on Fe³⁺ reduction in the absence and presence of complex I inhibitors.

	Concentration	pH 2.3		pH 3.5	
		Rate *	R.A	Rate *	R.A
Control		7.47 ± 0.40	1.00	4.45 ± 0.28	1.00
CH ₃ COOK	1 mM	8.05	1.08	5.59 ± 1.10	1.26
	40 mM	9.23	1.24	11.54 ± 0.59	2.59
In the presence of 40 mM CH ₃ COOK					
Control				11.54 ± 0.59	1.00
Rotenone	0.1 mM			1.22 ± 0.10	0.11
Amytal	2 mM			1.16 ± 0.09	0.10
In the presence of 1 mM KF					
Control		7.47 ± 0.40	1.00	3.68 ± 0.63	1.00
KF	0.5 mM	7.47	1.00		
	1 mM			8.03 ± 0.18	2.18
	10 mM	0.63 ± 0.16	0.08	5.68 ± 0.34	1.54
In the presence of 1 mM KF					
Control				8.03 ± 0.18	1.00
Rotenone	0.1 mM			0.97 ± 0.17	0.12
Amytal	2 mM			1.20 ± 0.04	0.15

* Rate: nmol Fe²⁺ min⁻¹ (mg protein)⁻¹ (±SD, n=3); R.A: relative activity, a ratio of a rate over that of control.

Table 2-12. Effect of Na₂-succinate and Na₂-malonate on Fe³⁺ reduction in the absence and presence of complex I inhibitors and TTFA at pH 3.5.

	Concentration	Rate *	R.A
Control		3.28 ± 0.16	1.00
Na-succinate	0.1 mM	4.03	1.23
	1 mM	8.86	2.70
	10 mM	13.03 ± 0.13	3.97
In the presence of 10 mM Na ₂ -succinate			
Control		13.03 ± 0.32	1.00
TTFA	1 mM	12.73 ± 0.21	0.98
Rotenone (R)	0.1 mM	0.93 ± 0.13	0.07
R + TTFA		2.62 ± 0.11	0.20
Amytal	2 mM	1.42 ± 0.05	0.11
Atabrine	2 mM	12.16 ± 0.14	0.93
In the presence of 10 mM Na ₂ -malonate			
Control		3.51 ± 0.65	1.00
Na ₂ -malonate	10 μM	3.11 ± 0.04	0.88
	0.1 mM	3.12 ± 0.17	0.89
	1 mM	3.92 ± 0.07	1.12
	10 mM	8.25 ± 0.14	2.35
In the presence of 10 mM Na ₂ -malonate			
Control		8.25 ± 0.14	1.00
Rotenone	0.1 mM	1.28 ± 0.23	0.16
Amytal	2 mM	1.54 ± 0.23	0.19

* Rate: nmol Fe²⁺ min⁻¹ (mg protein)⁻¹ (±SD, n=3); R.A: relative activity, a ratio of a rate over that of control.

Table 2-13. Effect of thiol agents on Fe³⁺ reduction in the absence and presence of complex I inhibitors.

	Concentration	pH 2.3		pH 3.5	
		Rate *	R.A	Rate *	R.A
Control		6.37 ± 0.35	1.00	3.67 ± 0.31	1.00
NEM	1 mM	8.25 ± 0.09	1.30	9.44 ± 0.19	2.57
	5 mM	10.21 ± 0.84	1.60	11.41 ± 0.51	3.11
In the presence of 5 mM NEM					
Control				11.41 ± 0.51	1.00
Rotenone	0.1 mM			0.96 ± 0.21	0.08
Amytal	2 mM			1.10 ± 0.07	0.10
Control		4.48	1.00	3.21 ± 0.00	1.00
AgNO ₃	50 μM	4.76	1.06	4.91	1.53
	0.1 mM	4.96	1.11	6.59 ± 0.24	2.05
	1 mM	6.28	1.40	2.77	0.86
In the presence of 0.1 mM AgNO ₃					
Control				6.59 ± 0.24	1.00
Rotenone	0.1 mM			0.73 ± 0.01	0.11
Amytal	2 mM			1.32 ± 0.05	0.20
Control	0 μM			2.77 ± 0.19	1.00
HgCl ₂	50 μM			3.52	1.27
	0.1 mM			5.35 ± 0.16	1.93
	1 mM			0.30 ± 0.04	0.11
0.1 mM HgCl ₂ plus 5 mM NEM				16.09	5.81
In the presence of 0.1 mM HgCl ₂					
Control				5.35 ± 0.16	1.00
Rotenone	0.1 mM			0.51 ± 0.08	0.10
Amytal	2 mM			0.45 ± 0.04	0.08

* Rate: nmol Fe²⁺ min⁻¹ (mg protein)⁻¹ (±SD, n=3); R.A: relative activity, a ratio of a rate over that of control.

Figures of Part II

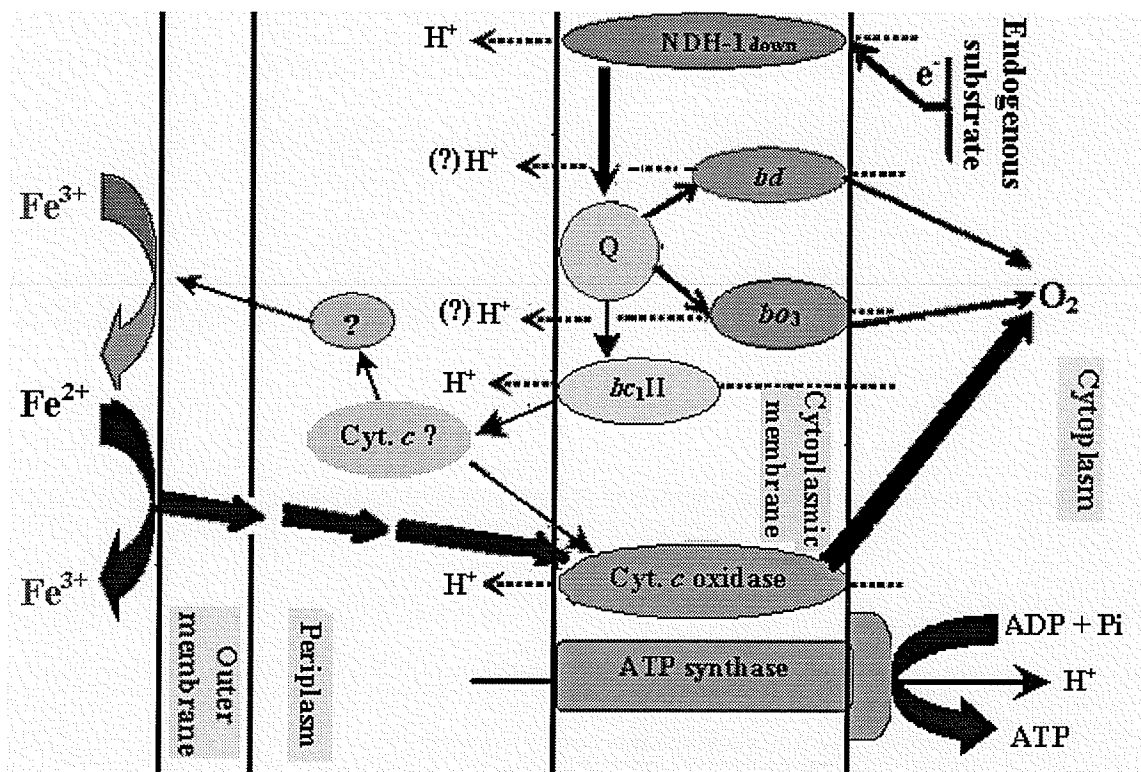
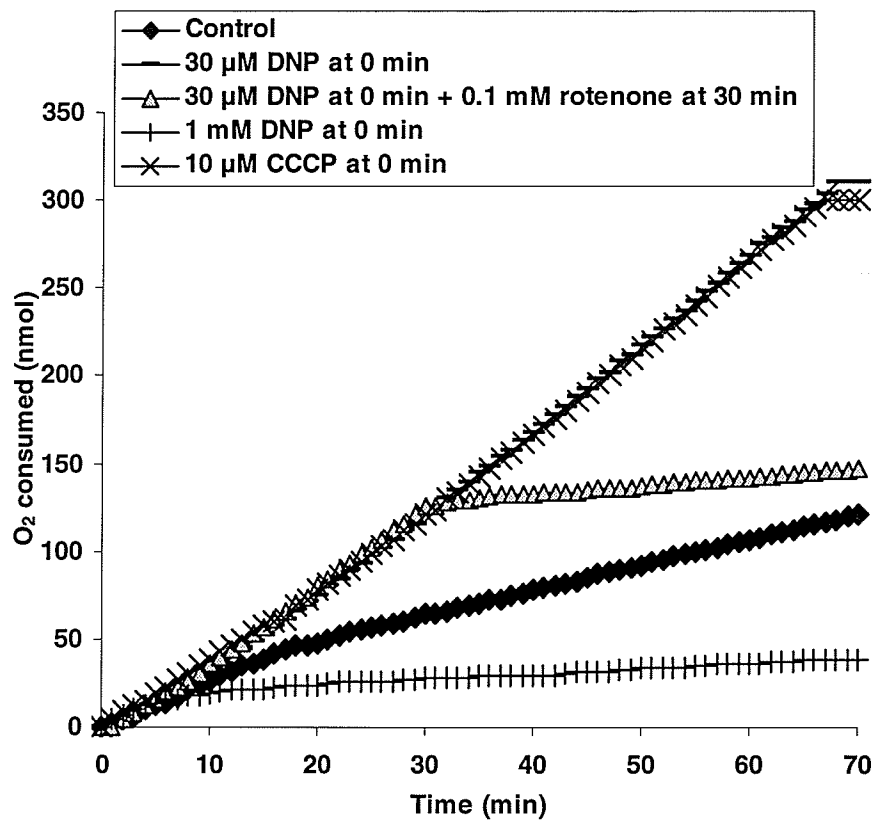
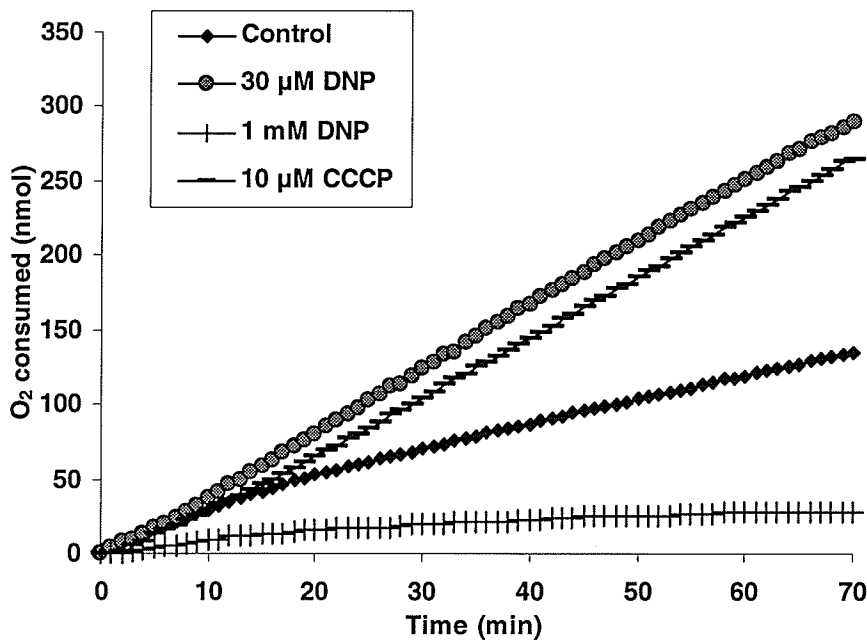


Fig. 2-0. The hypothetical model for the electron transport pathways of endogenous substrate oxidation in *A. ferrooxidans*. Q: ubiquinone/ubiquinol pool; bc_1II : the bc_1 complex participating in the downhill reaction (NADH oxidation); Cyt.: cytochrome; bd and bo_3 : cytochrome bd oxidase and cytochrome bo_3 oxidase; Cyt.: cytochrome c ; (?) H^+ : proton pumping is not sure. The thickness of straight arrows (not including the arrows pointing at H^+) represents the speed of electron flow in a qualitative manner.



(a)



(b)

Fig. 2-1. Effect of DNP and CCCP on endogenous respiration at pH 3.5 in 0.1 M β -alanine- H_2SO_4 (a) and water (b). In (a), rotenone had a strong inhibitory effect on DNP-stimulated activity.

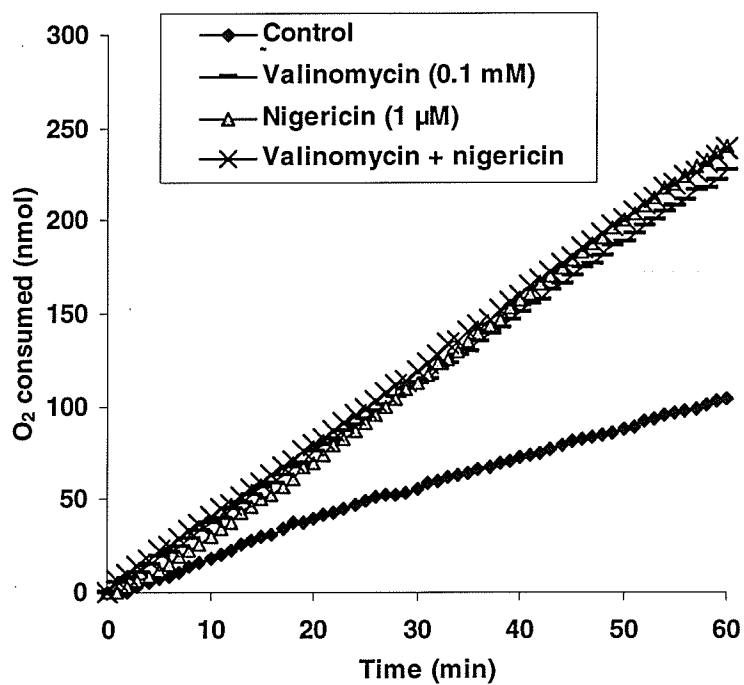


Fig. 2-2. Effect of valinomycin and nigericin on endogenous respiration.

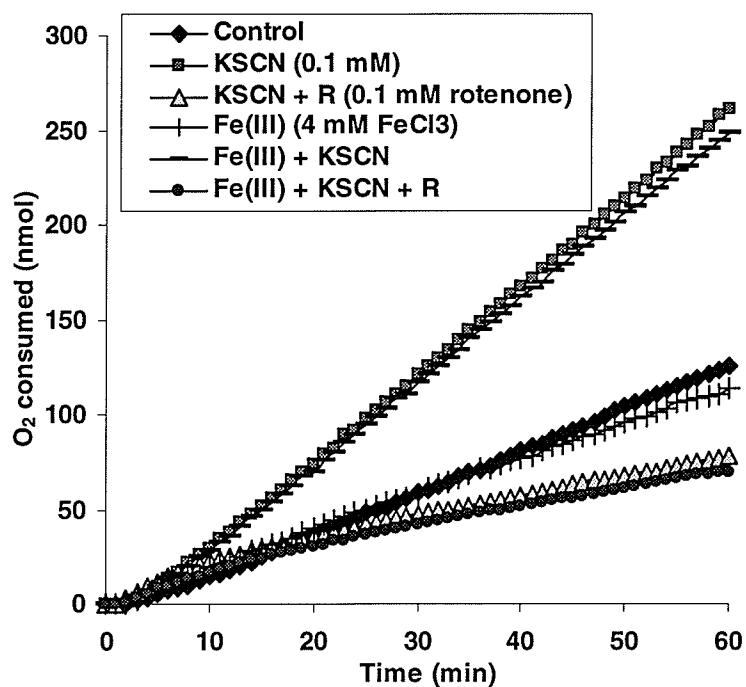
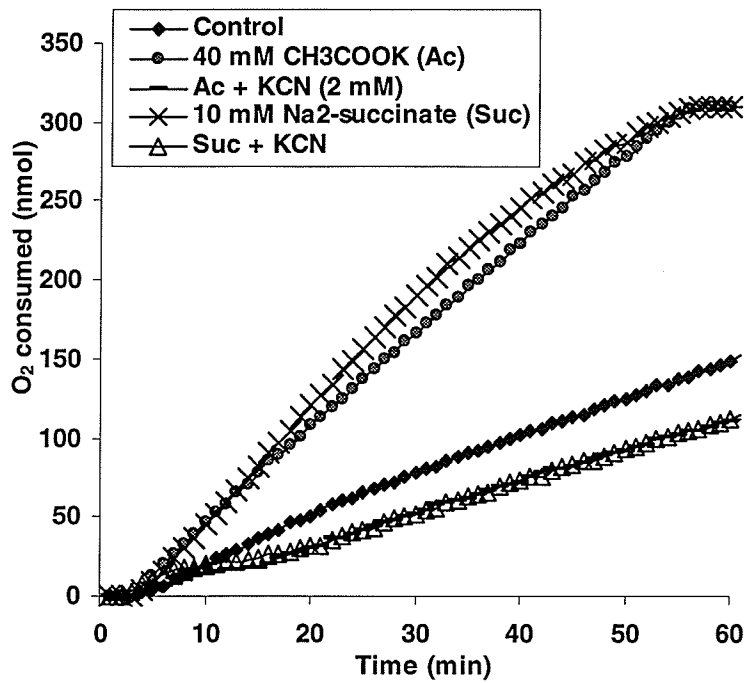
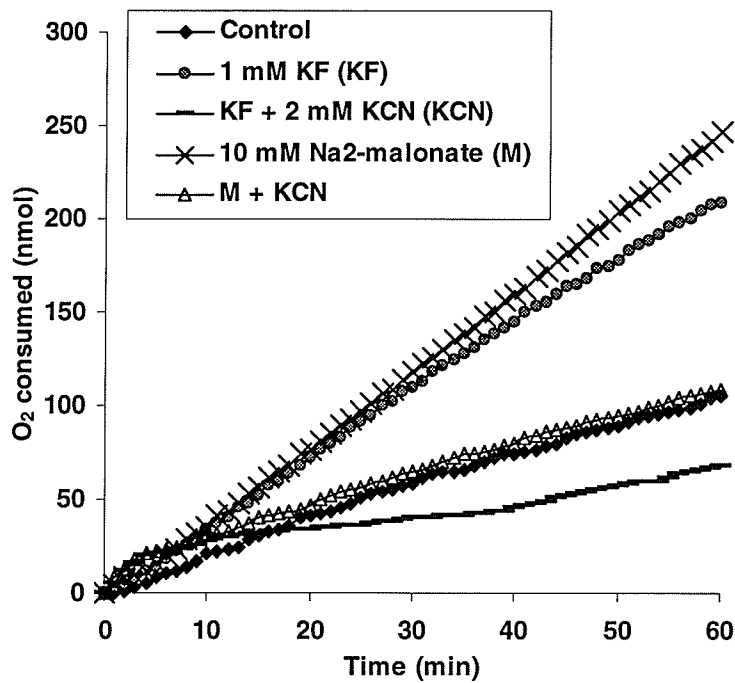


Fig. 2-3. Effect of KSCN on endogenous respiration in the presence and absence of FeCl₃ and / or rotenone.

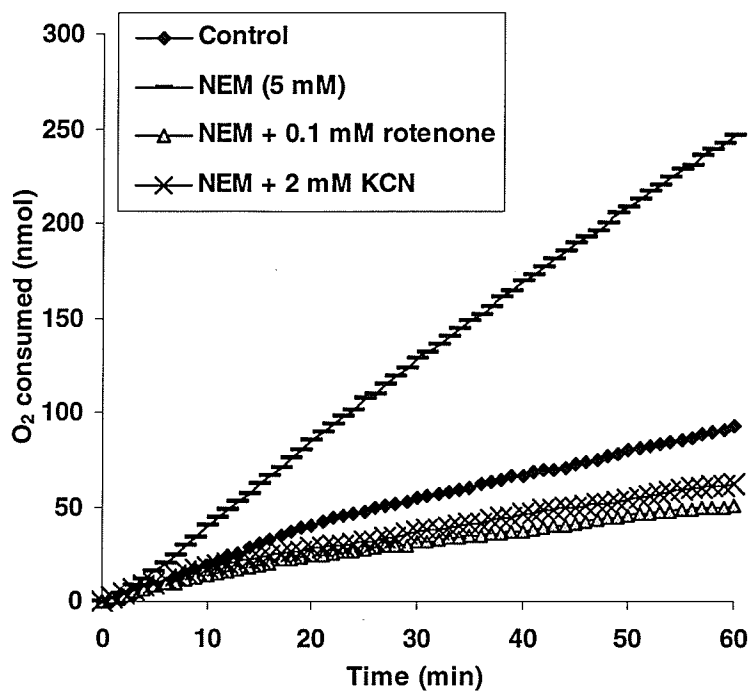


(a)

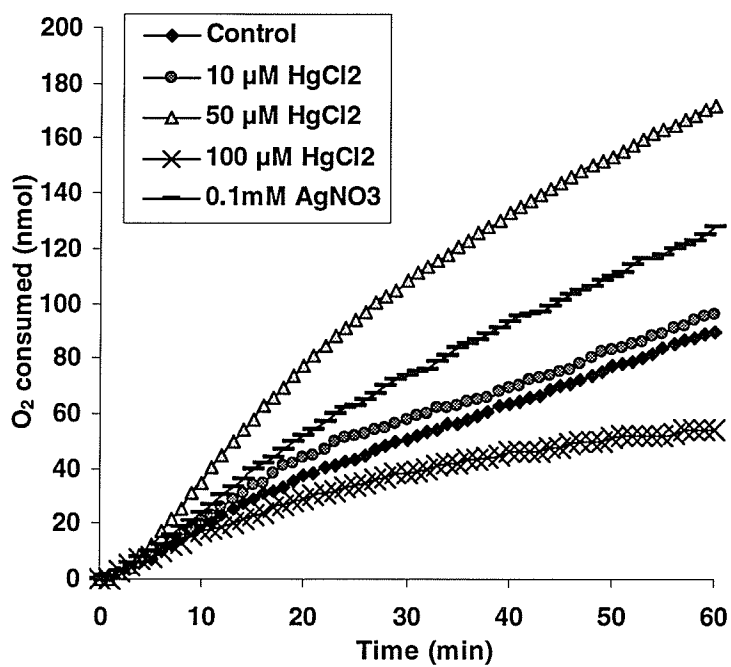


(b)

Fig. 2-4. Effect of weak acids on endogenous respiration in the presence and absence of KCN. (a) Effect of CH₃COOK and Na-succinate; (b) effect of KF and Na₂-malonate.



(a)



(b)

Fig. 2-5. Effect of thiol agents NEM, HgCl₂ and ANO₃ on endogenous respiration. (a) Effect of NEM and its combination with KCN or rotenone; (b) effect of HgCl₂ and ANO₃.

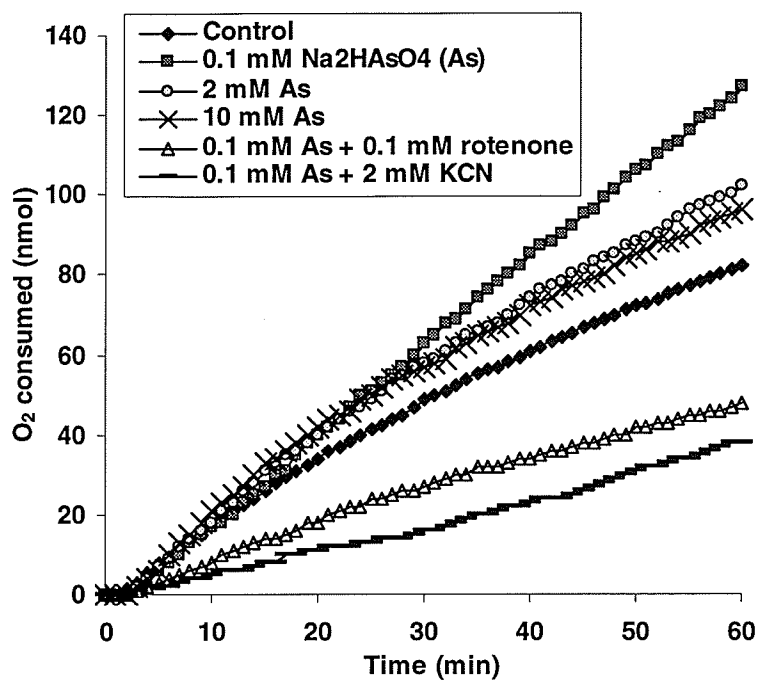


Fig. 2-6. Effect of arsenate (Na_2HAsO_4) and its combination with KCN or rotenone on endogenous respiration.

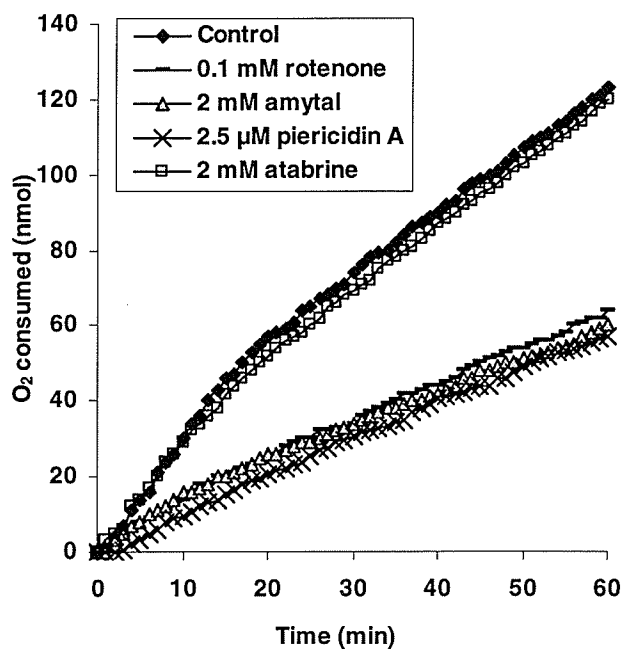


Fig. 2-7. Complex I inhibitors on endogenous respiration.

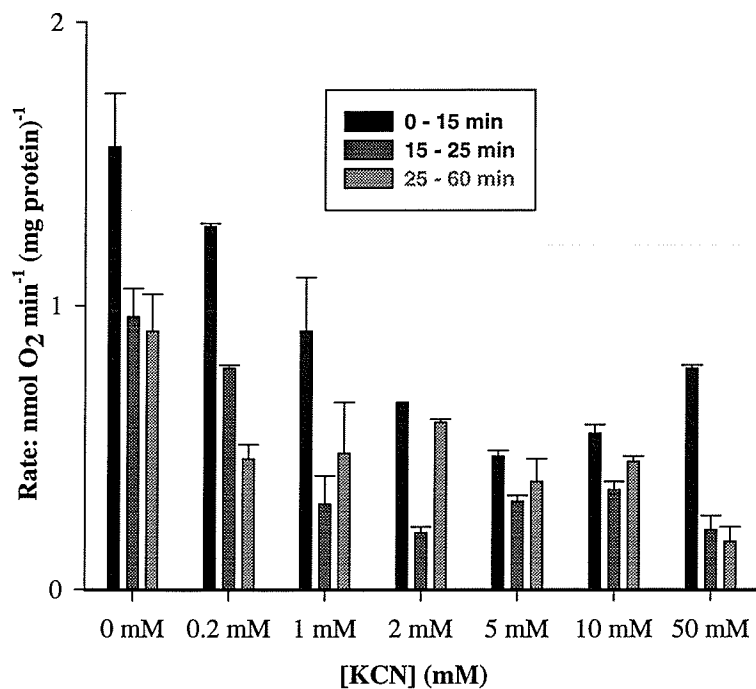


Fig. 2-8. Effect of KCN concentration on endogenous respiration (error bars, SD, n=2).

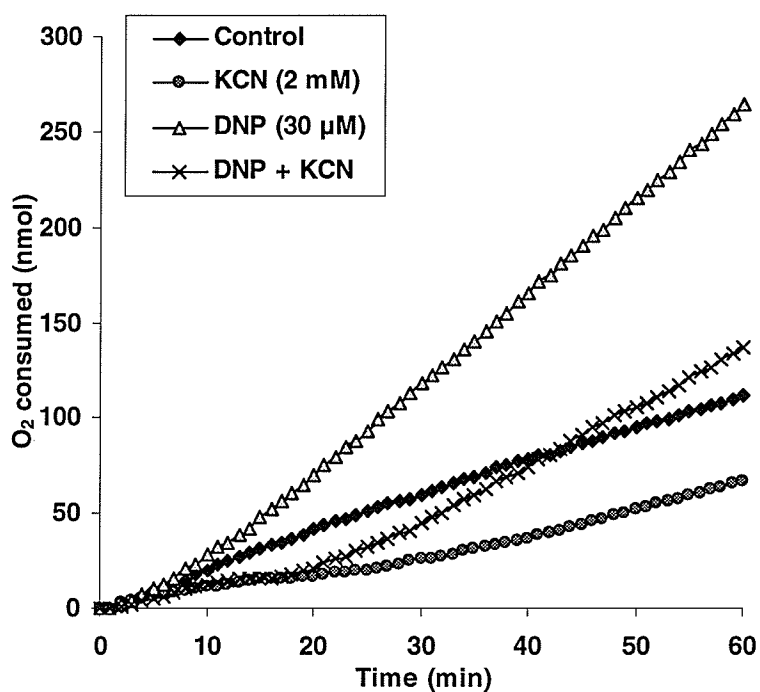


Fig. 2-9. Effect of KCN on endogenous respiration in the presence of DNP.

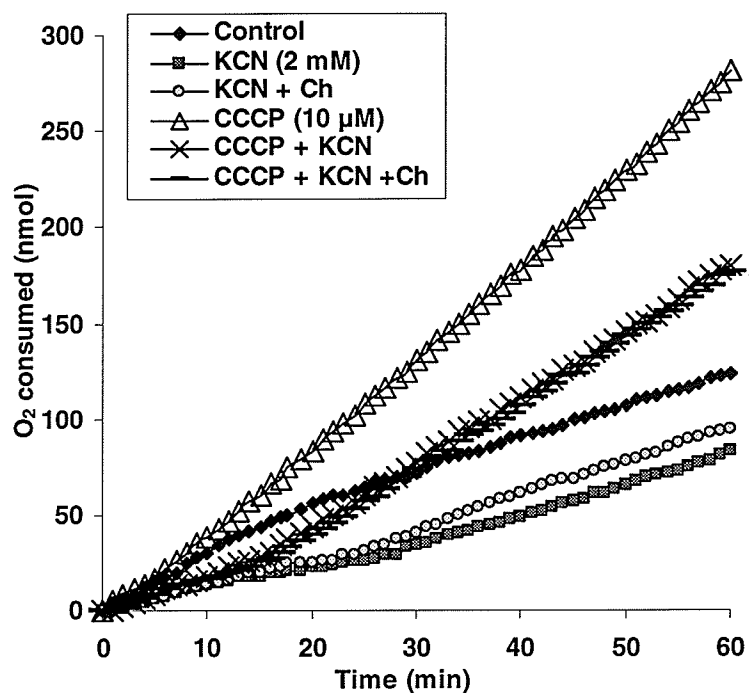


Fig. 2-10. Effect of KCN and chloramphenicol (Ch, 0.31 mM) on endogenous respiration in the presence and absence of CCCP.

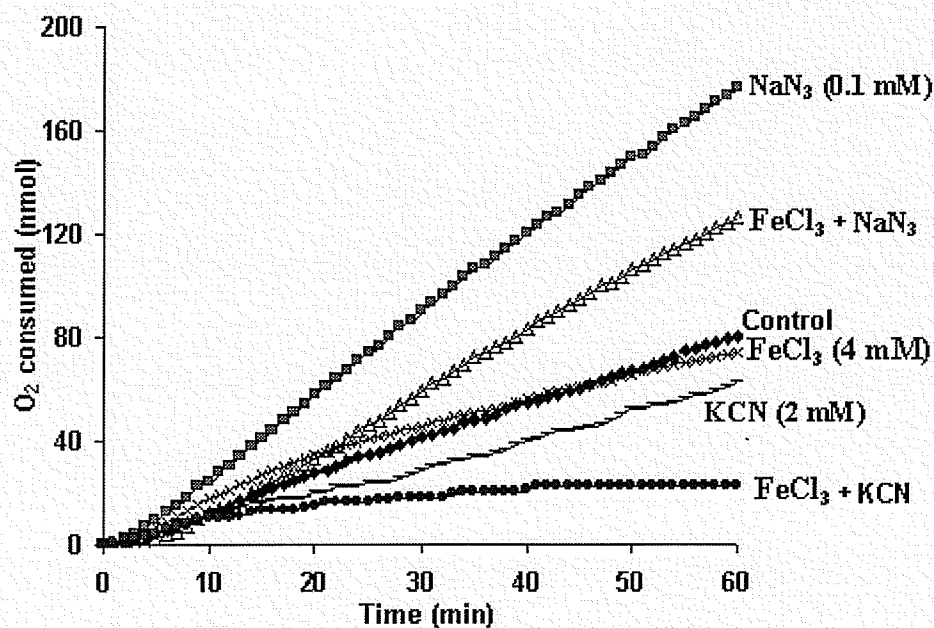


Fig. 2-11. Effect of KCN and NaN₃ on endogenous respiration in the presence of FeCl₃.

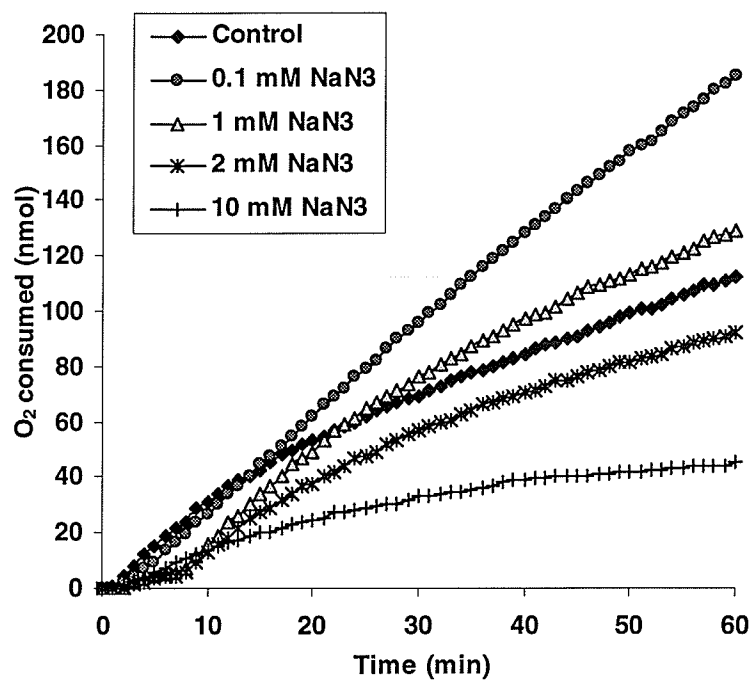
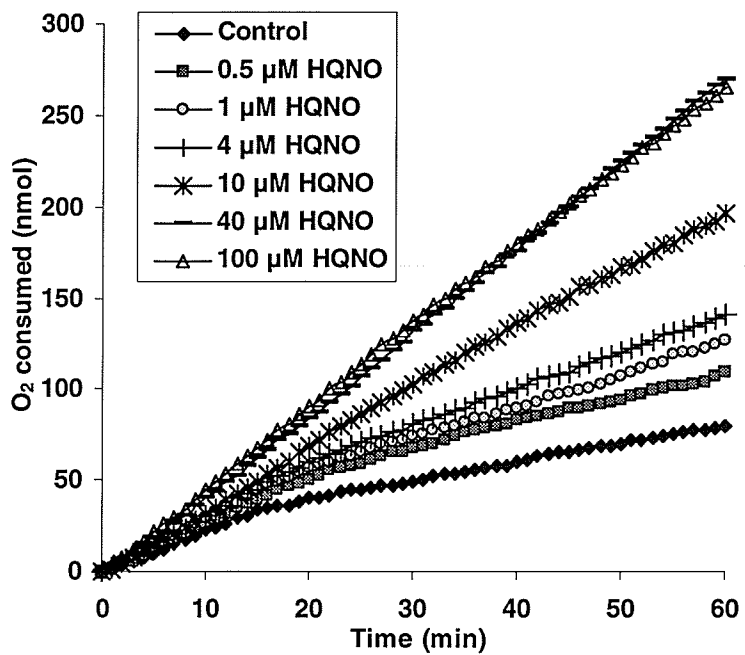
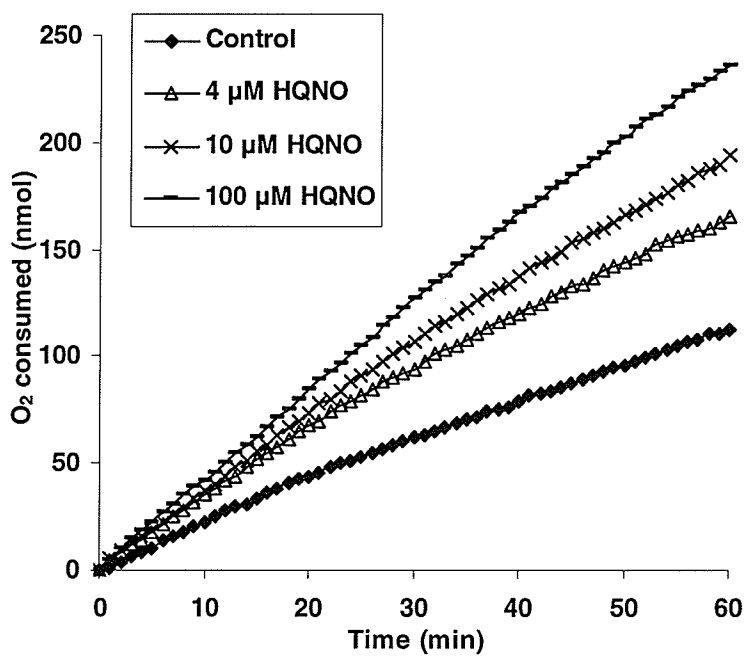


Fig. 2-12. Effect of NaN₃ on endogenous respiration.

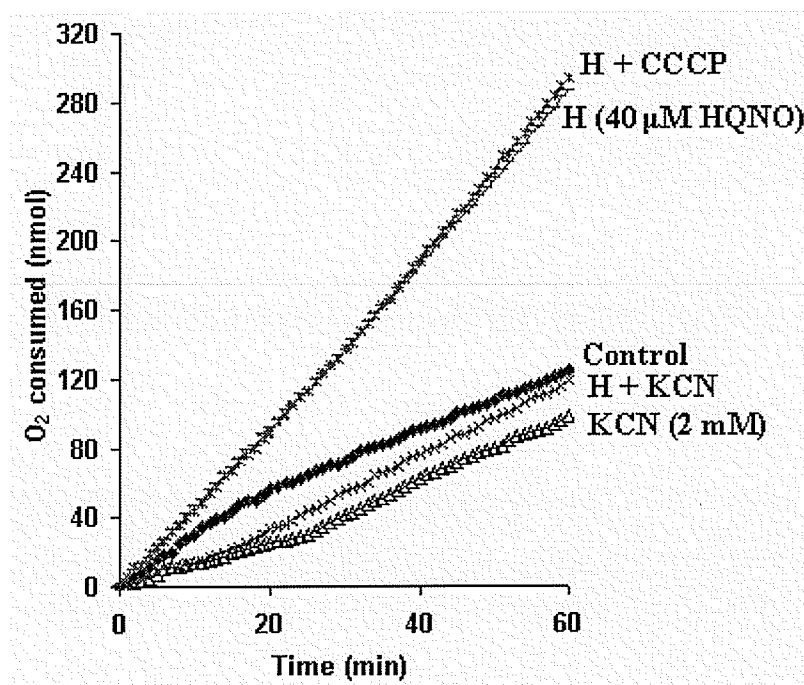


(a)

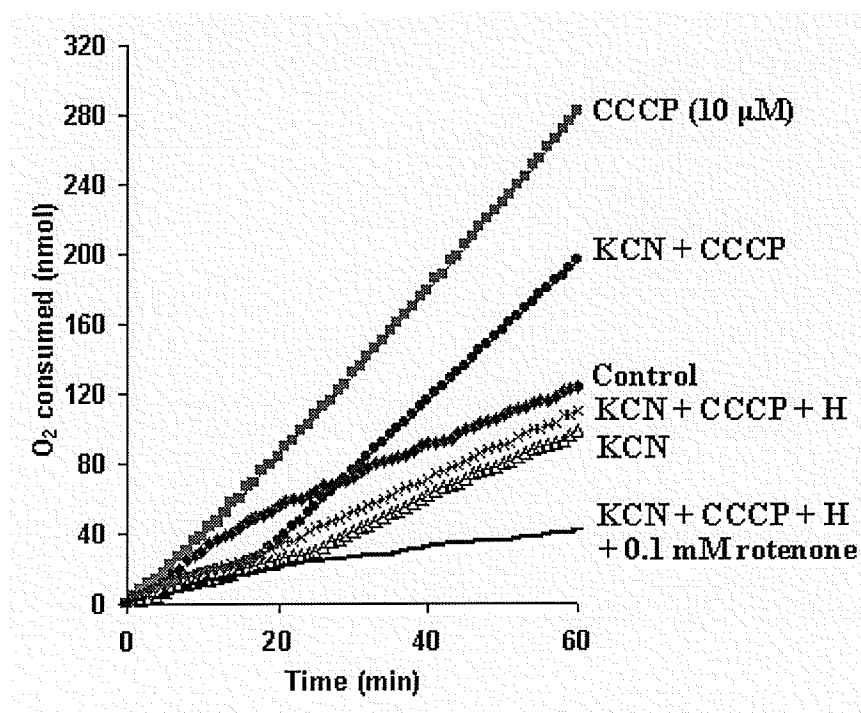


(b)

Fig. 2-13. Effect of HQNO on endogenous respiration in 0.1 M β -alanine- H_2SO_4 buffer (a) and water (b).



(a)



(b)

Fig. 2-14. Effect of HQNO and CCCP on endogenous respiration in the absence and presence of KCN and rotenone at pH 3.5 (a, b).

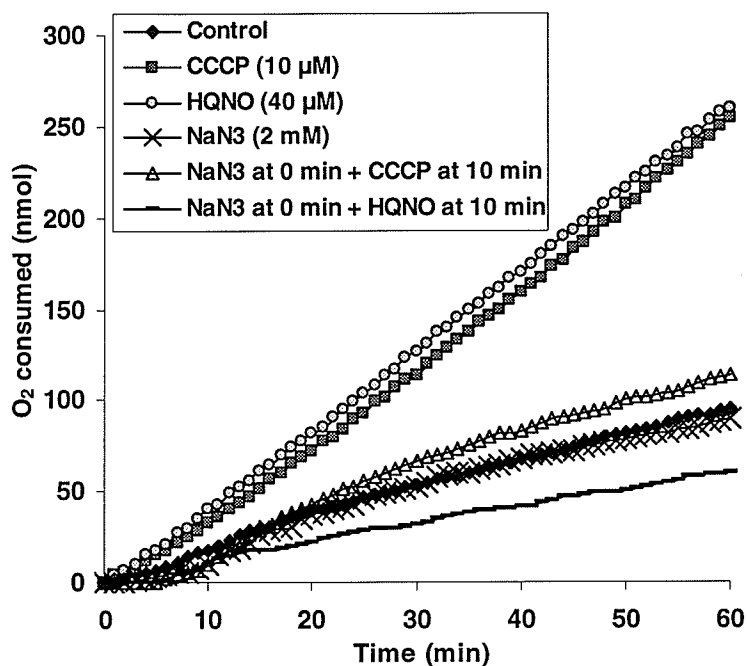


Fig. 2-15. Comparison of the effects of HQNO and CCCP on endogenous respiration in the presence of NaN₃.

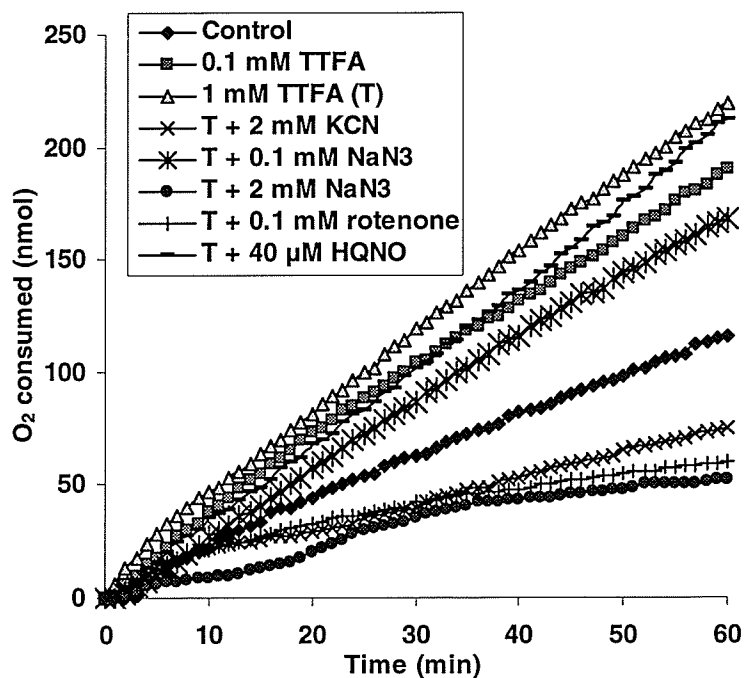


Fig. 2-16. Effect of TTFA on endogenous respiration in the absence and presence of other reagents.

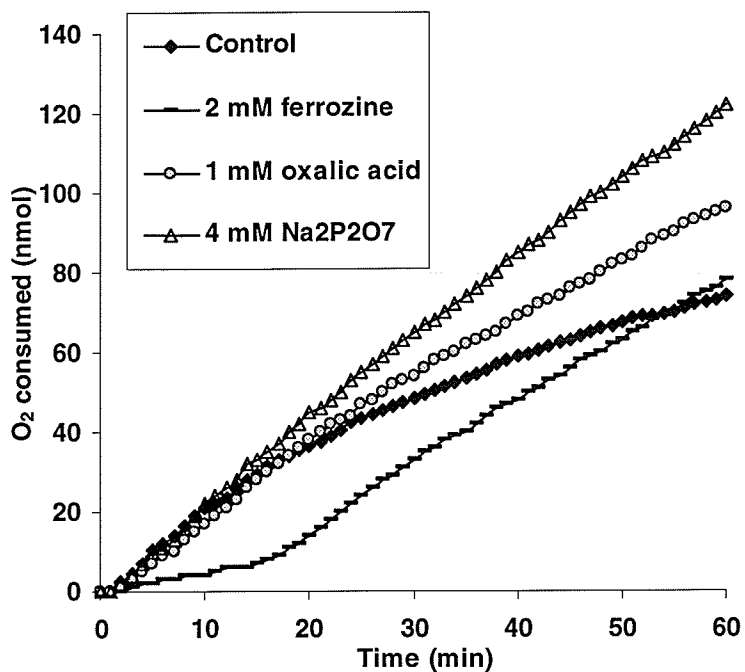


Fig. 2-17. Effect of ferrozine, oxalic acid and NaP₂O₇ on endogenous respiration.

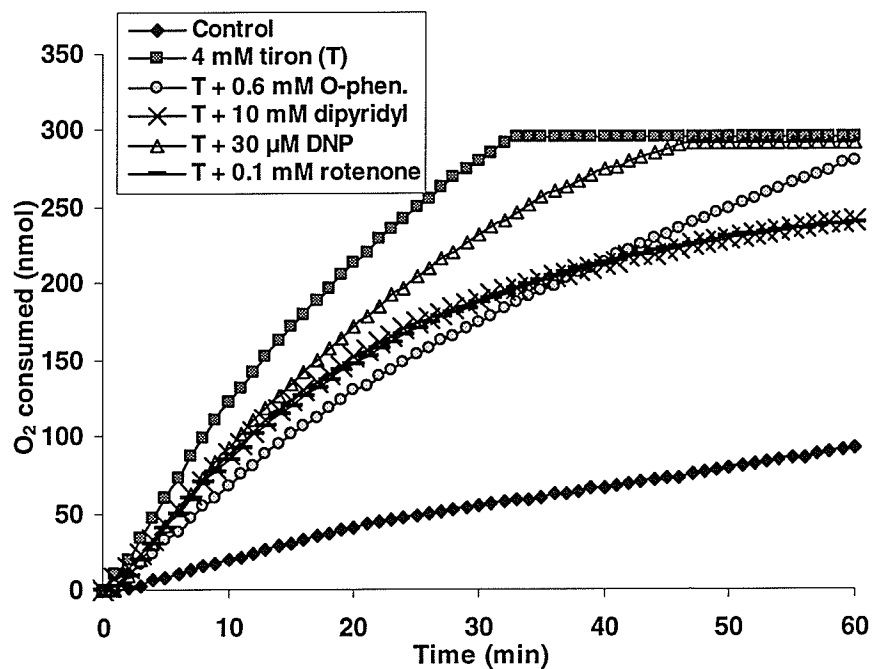


Fig. 2-18. Effect of tiron on endogenous respiration in the absence and presence of o-phenanthroline (*o*-phen.), 2,2'-dipyridyl, DNP and rotenone.

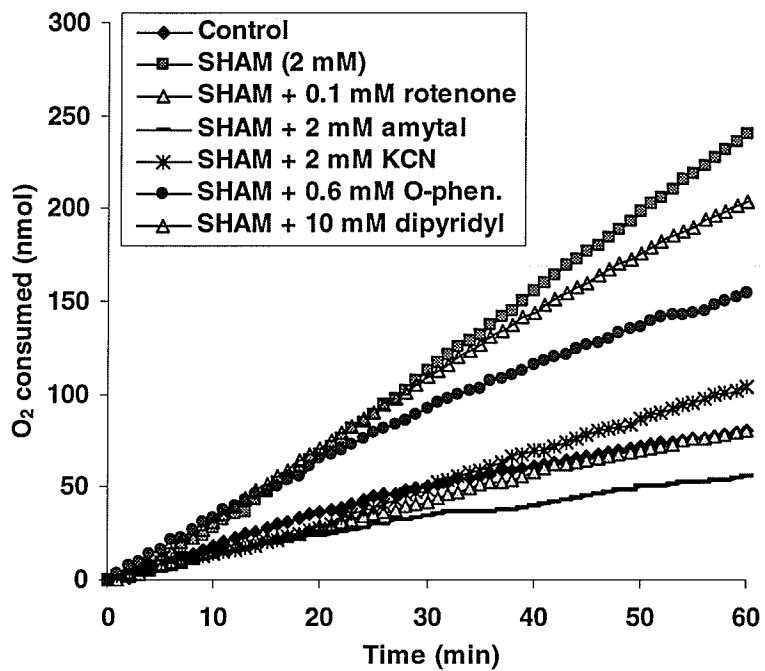
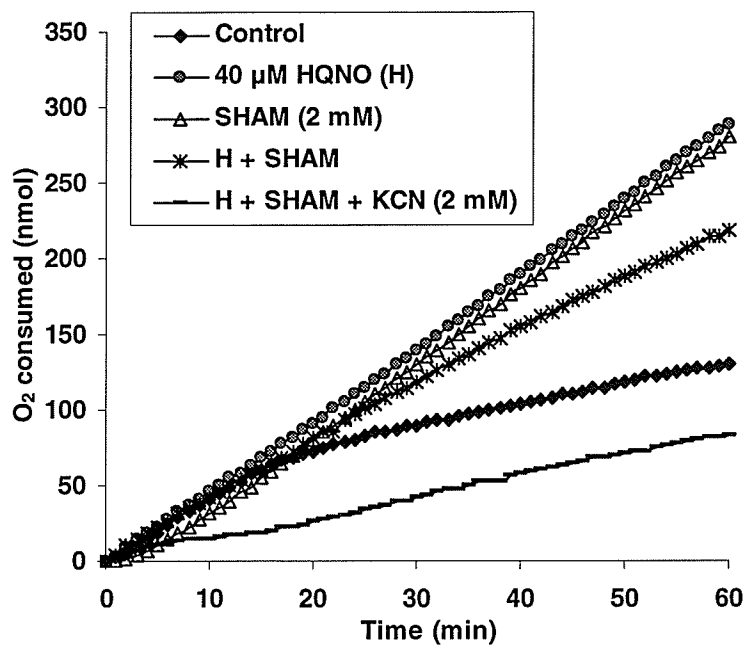
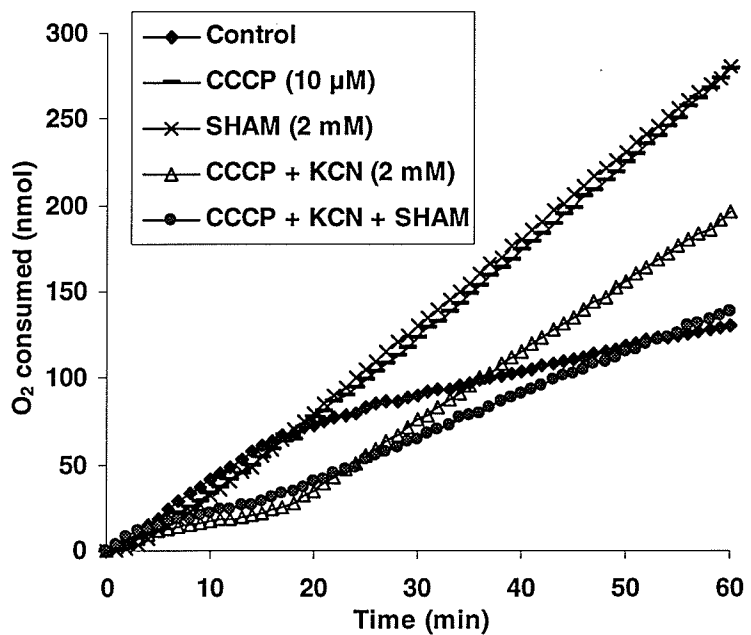


Fig. 2-19. Effect of SHAM on endogenous respiration in the absence and presence of rotenone, amytal, KCN, *o*-phenanthroline (*o*-phen.) and 2,2'-dipyridyl.



(a)



(b)

Fig. 2-20. Effect of SHAM on endogenous respiration in the absence and presence of (a) HQNO and KCN and (b) CCCP and KCN. SHAM had no effect on CCCP-stimulated activity (data not shown).

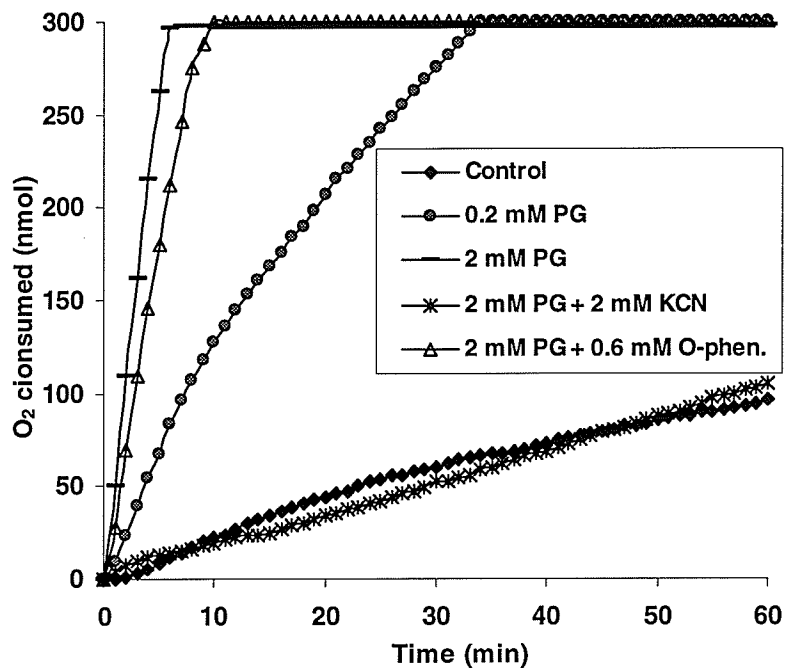


Fig. 2-21. Effect of propyl gallate (PG) on endogenous respiration in the absence and presence of KCN or *o*-phenanthroline (*o*-phen.).

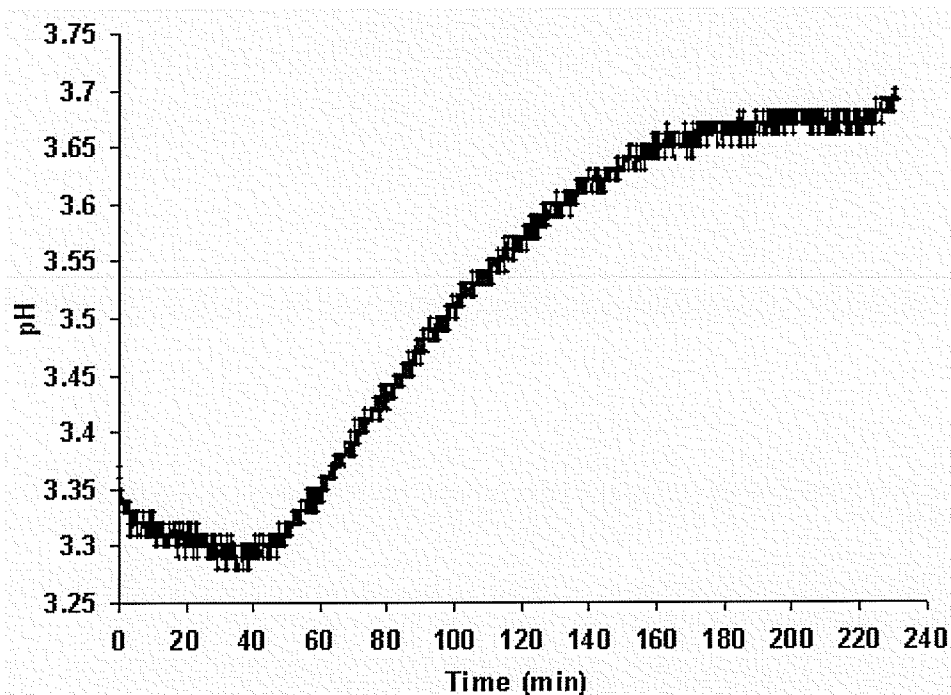


Fig. 2-22. External pH change during endogenous respiration in cells of 100 mg / mL. Cells were kept at room temperature for at least one hour before testing pH change.

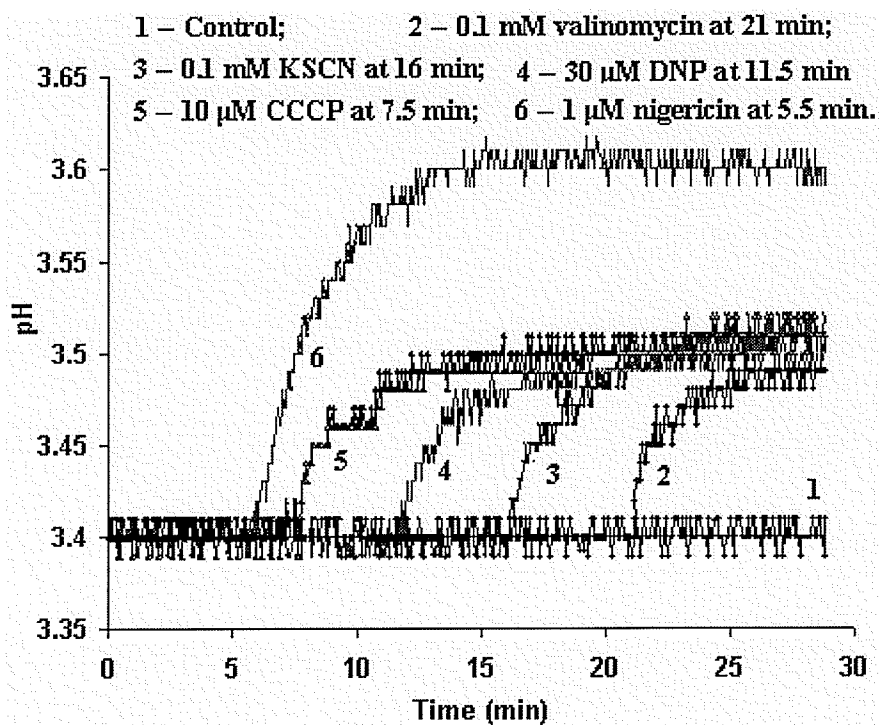
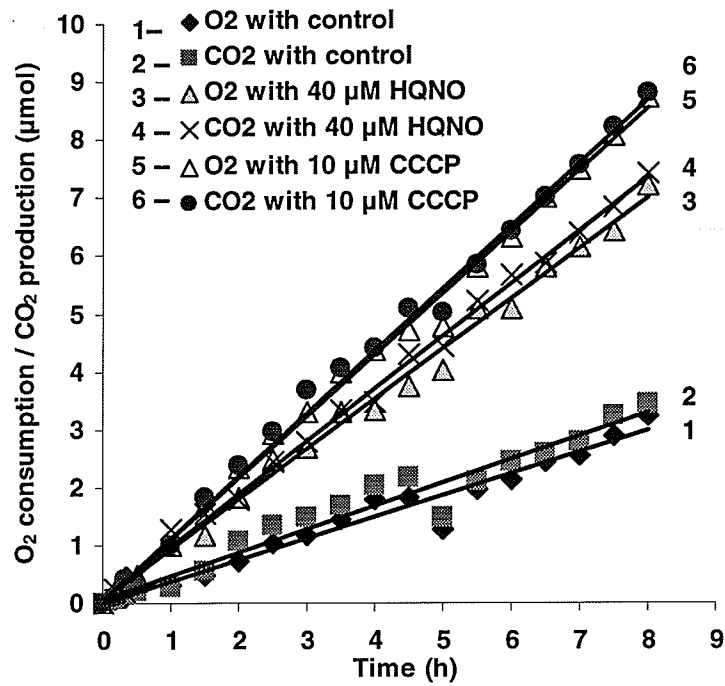
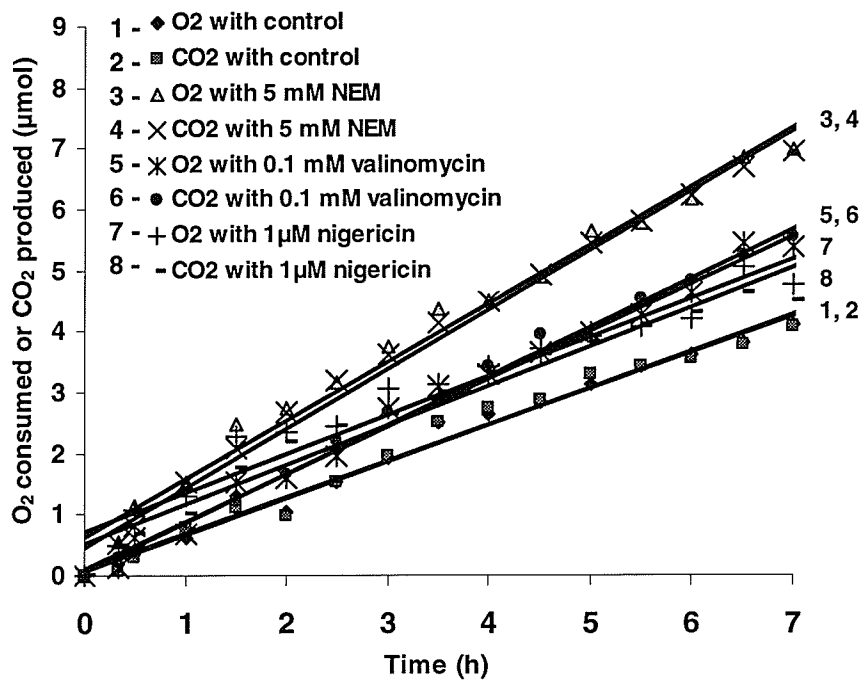


Fig. 2-23. External pH change during endogenous respiration in cells of 20 mg / mL in the presence of different compounds. Cells were kept at 4°C before testing. Compounds alone did not lead to change of pH (data not shown).

Fig. 2-24. O₂ consumption and CO₂ production in the absence and presence of different compounds. (a) HQNO and CCCP; (b) NEM, nigericin and valinomycin; (c) tiron; (d) SHAM; (e) TTFA and Na-succinate; (f) Na₂-malonate and CH₃COOK. Tests were done at 30°C in Warburg respirometer with 64 mg cells in 3.2 mL reaction system.

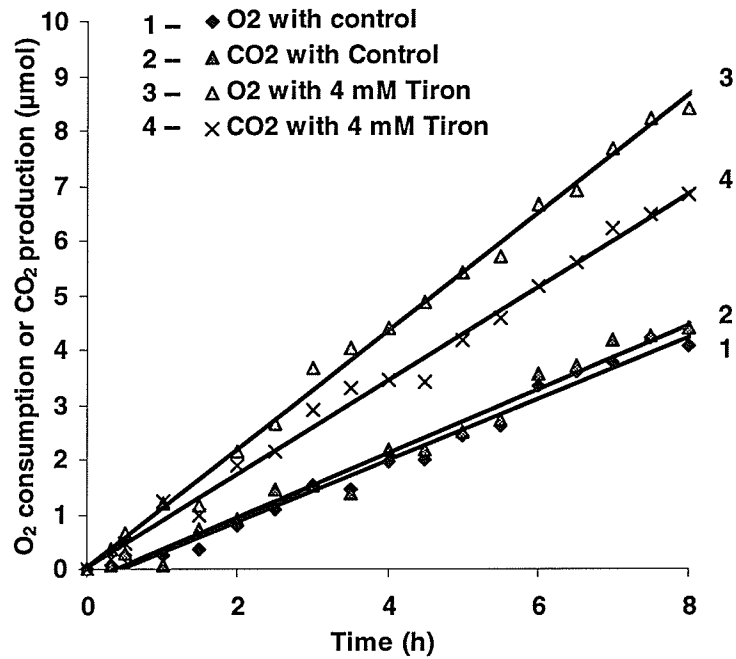


(a)

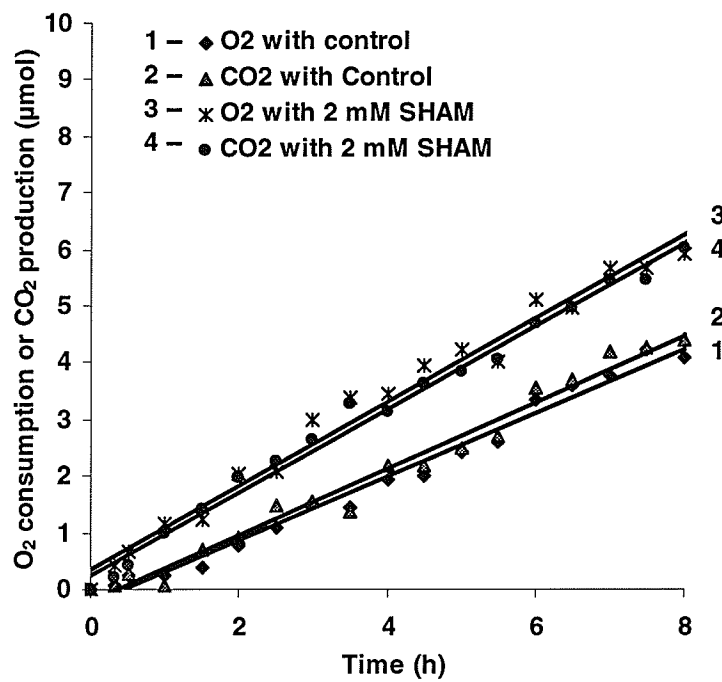


(b)

Fig. 2-24

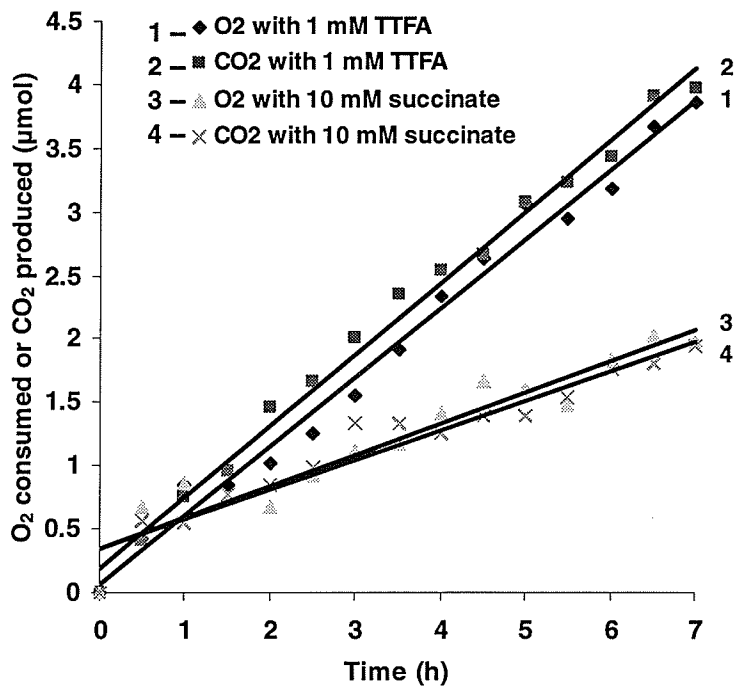


(c)

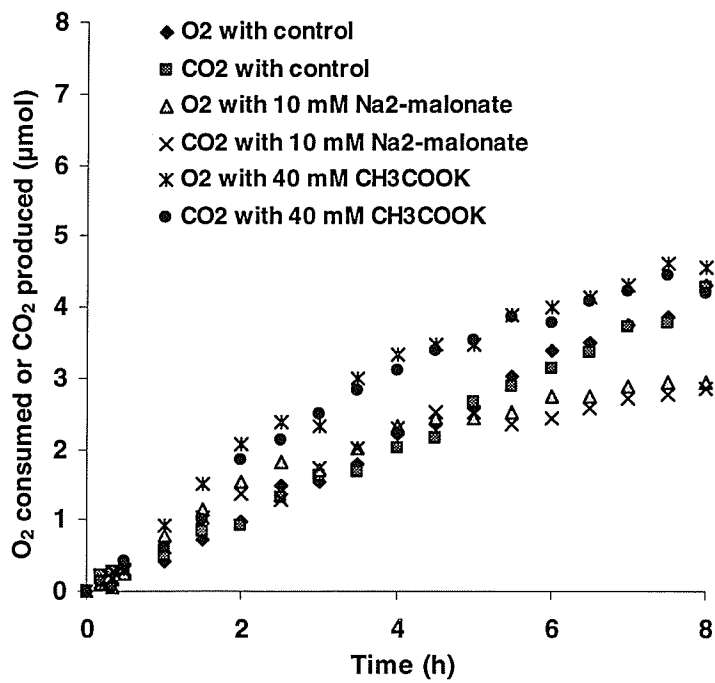


(d)

Fig. 2-24



(e)



(f)

Fig. 2-24

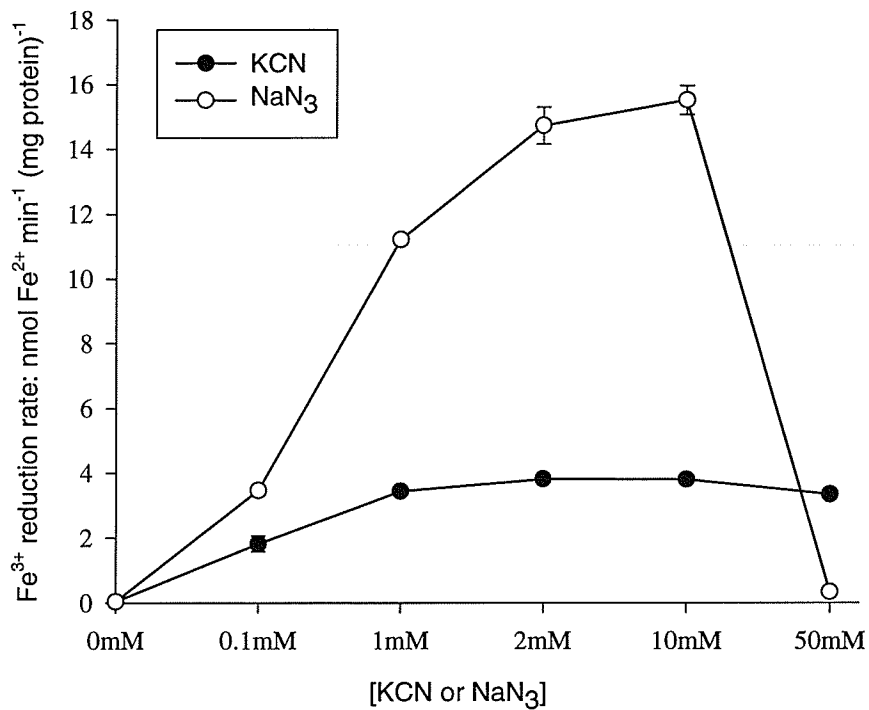


Fig. 2-25. Effect of KCN and NaN₃ on Fe³⁺ reduction by endogenous substrates at pH 3.5. The error bars at each point represent standard deviations (SD, n = 3).

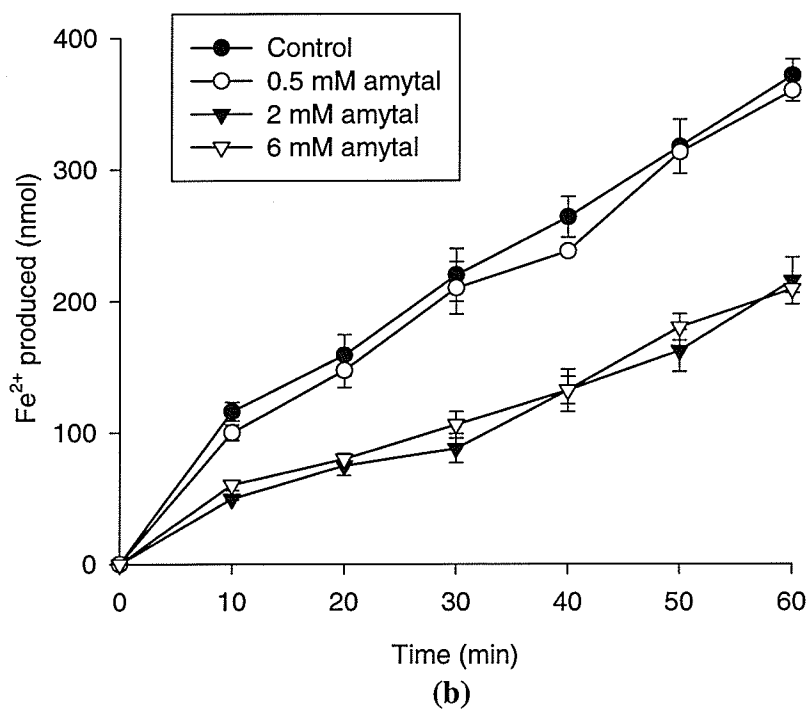
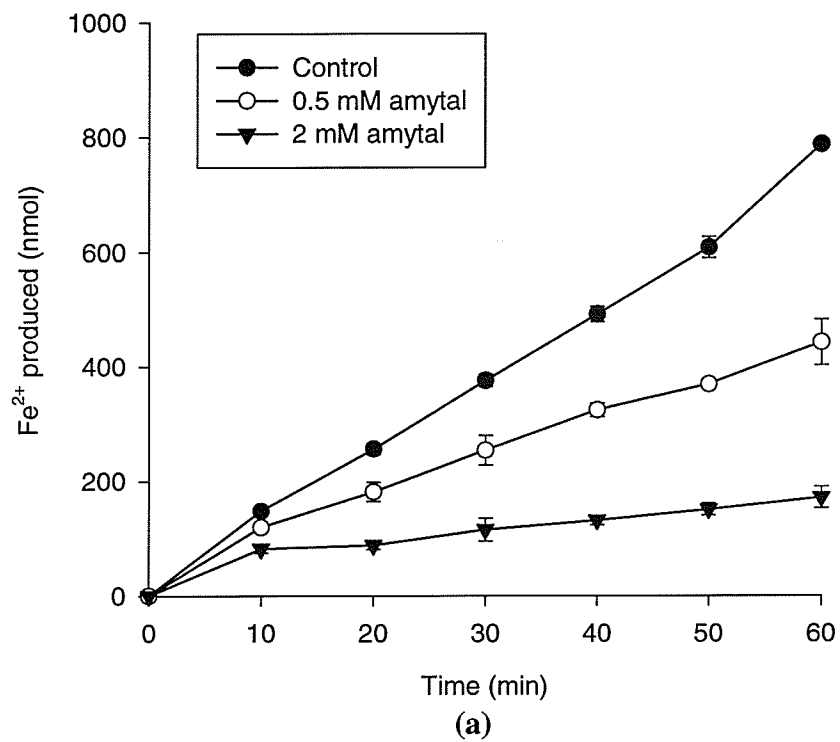
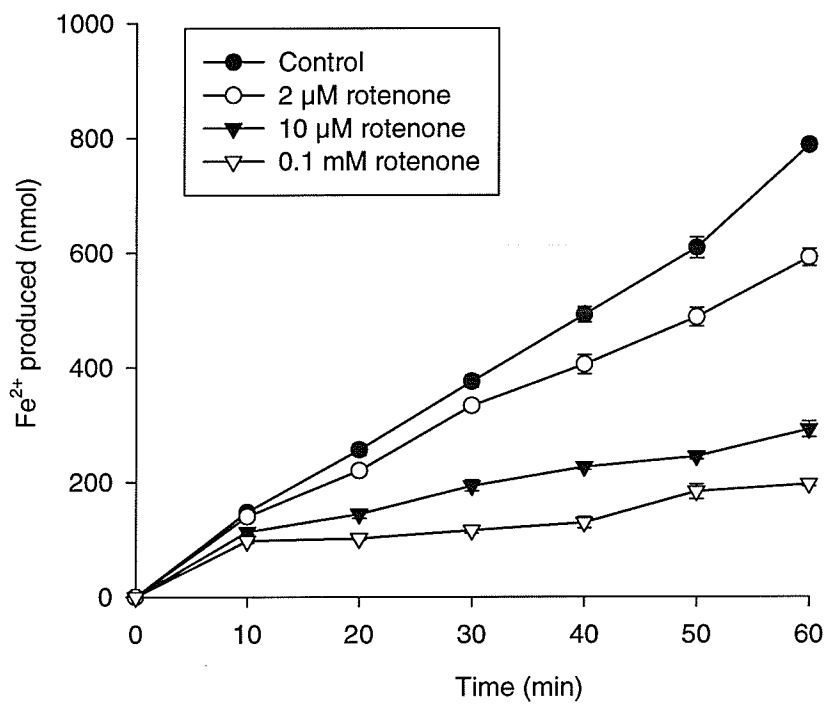
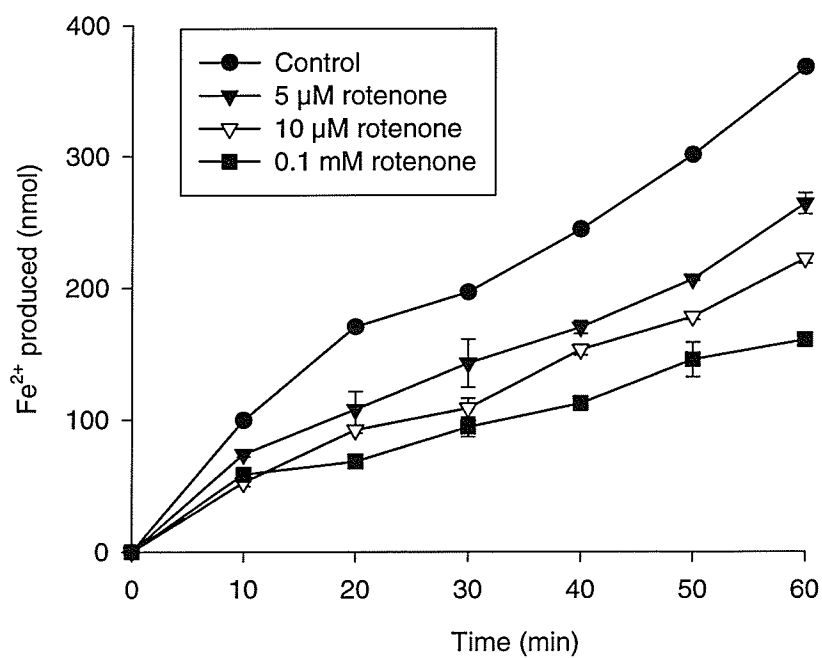


Fig. 2-26. Effect of amytal on Fe^{3+} reduction by endogenous substrates at (a) pH 2.3 and (b) pH 3.5.



(a)



(b)

Fig. 2-27. Effect of rotenone on Fe^{3+} reduction by endogenous substrates at (a) pH 2.3 and (b) pH 3.5.

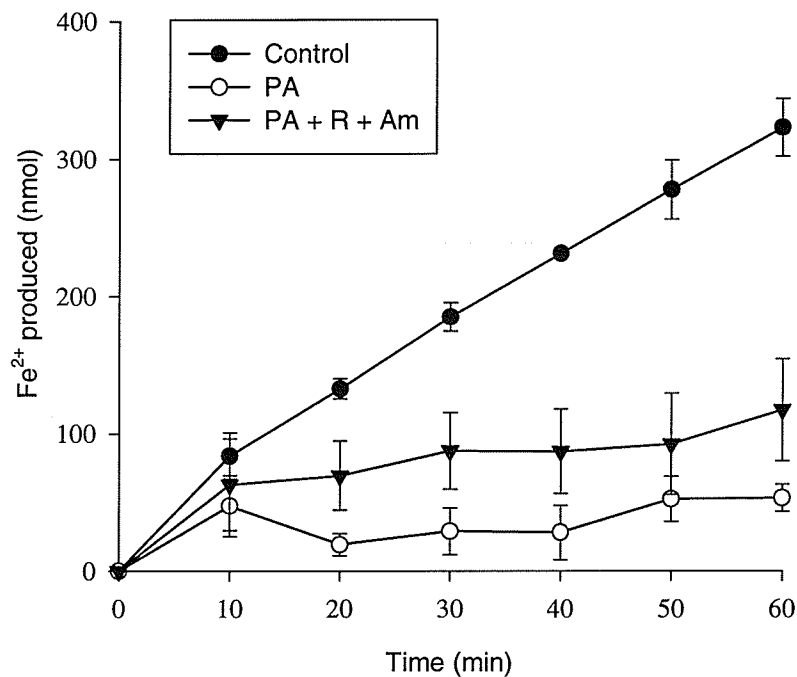


Fig. 2-28. Effect of piericid A (PA, 0.5 μ M) and combination of PA, 0.1 mM rotenone (R) and 2 mM amytal (Am) on Fe³⁺ reduction by endogenous substrates at pH 3.5.

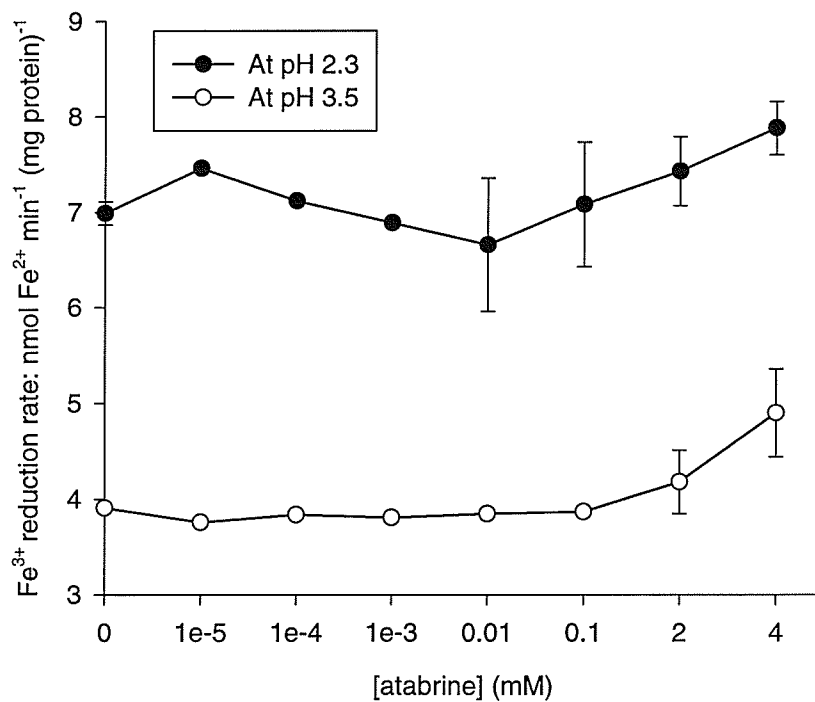


Fig. 2-29. Effect of atrabrine on Fe³⁺ reduction by endogenous substrates at pH 2.3 and pH 3.5.

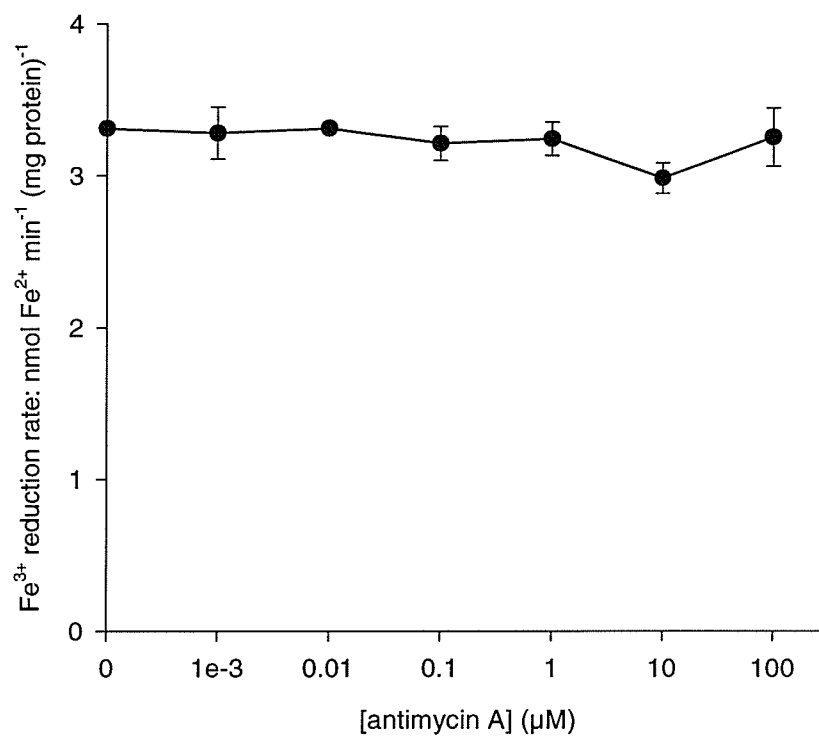


Fig. 2-30. Effect of antimycin A on Fe³⁺ reduction by endogenous substrates at pH 3.5.

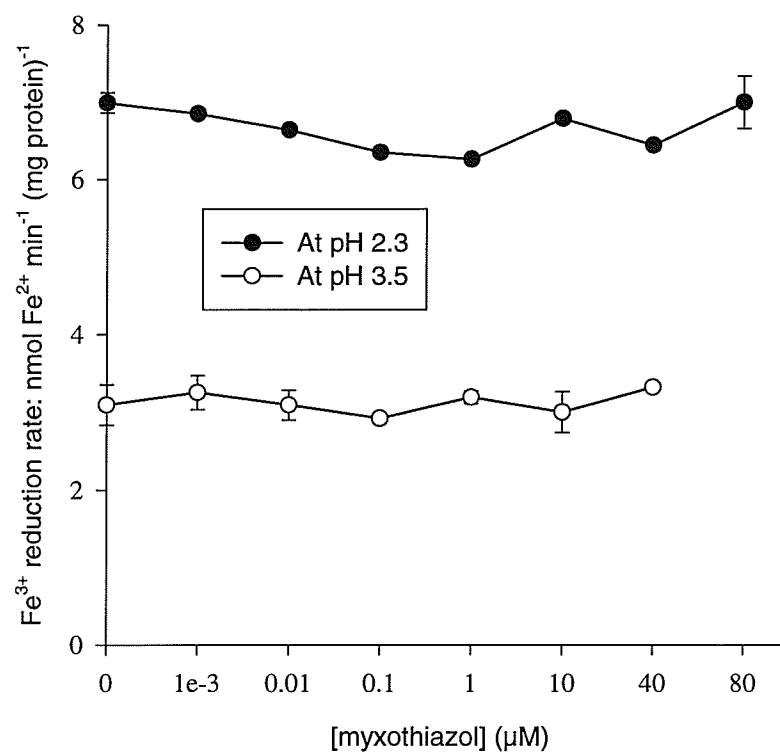
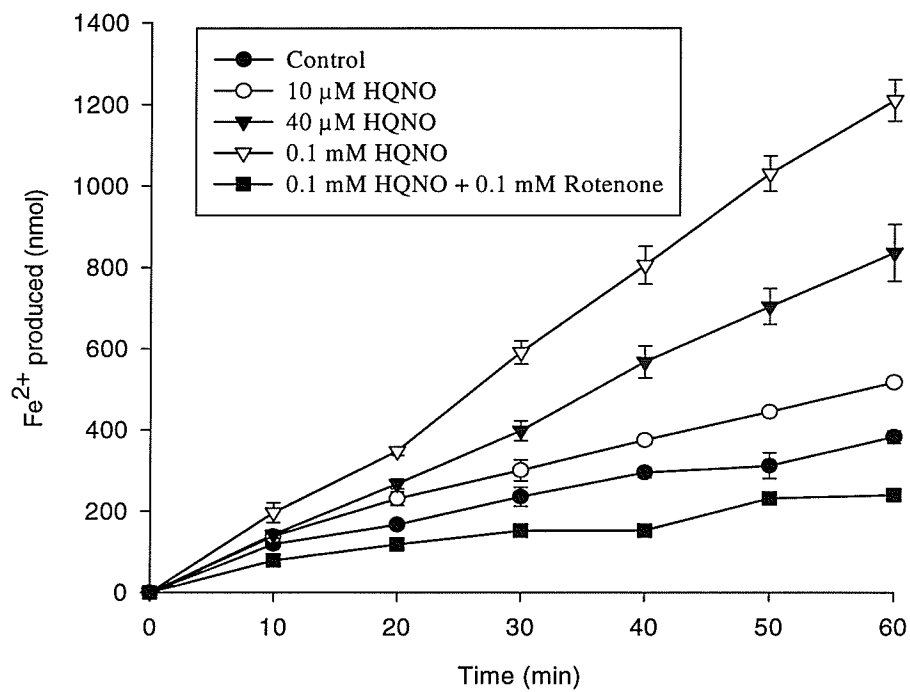
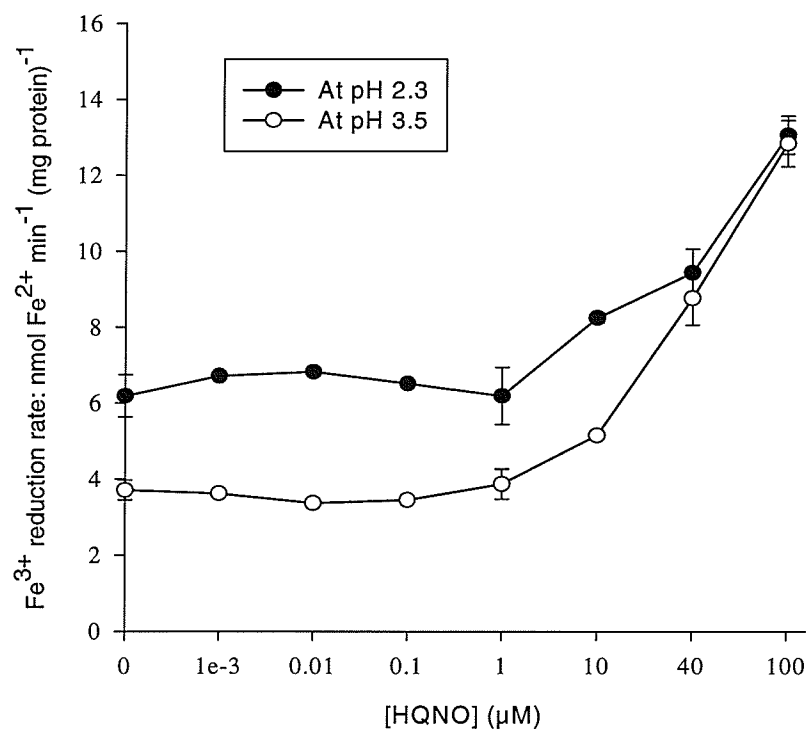


Fig. 2-31. Effect of myxothiazol on Fe³⁺ reduction by endogenous substrates at pH 2.3 and pH 3.5.

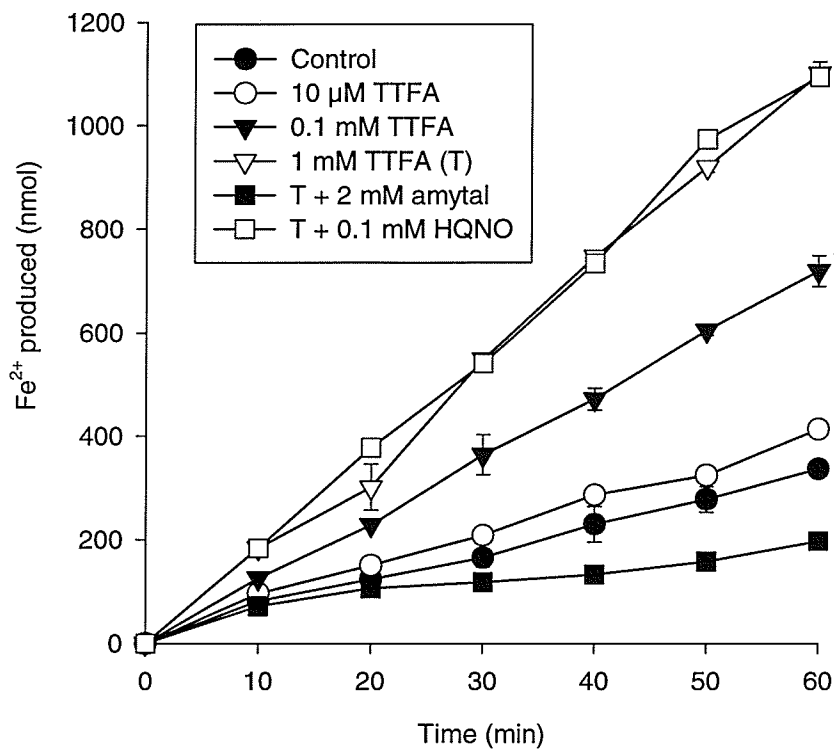


(a)

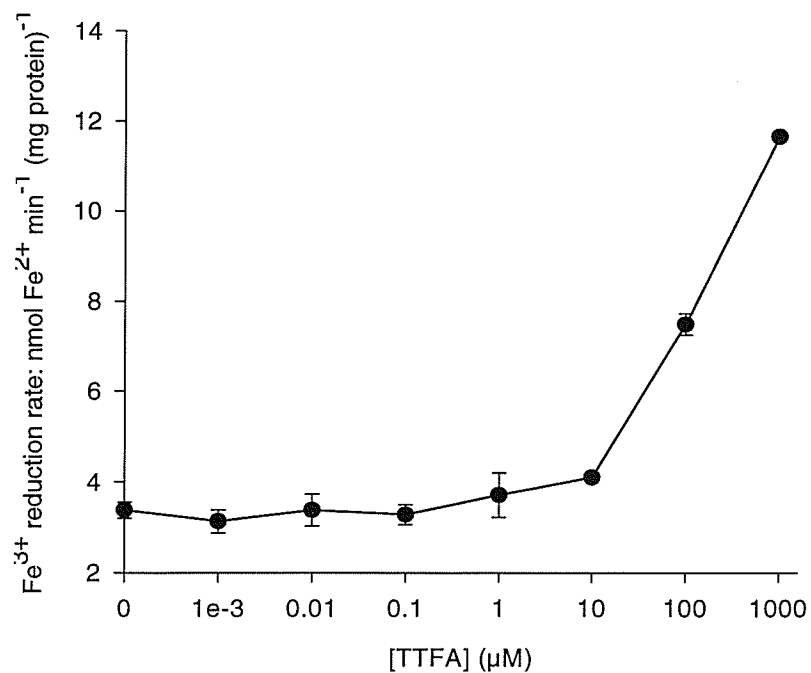


(b)

Fig. 2-32. Effect of HQNO on Fe³⁺ reduction by endogenous substrates. (a) Time evolution at pH 3.5; (b) rates at pH 2.3 and pH 3.5.



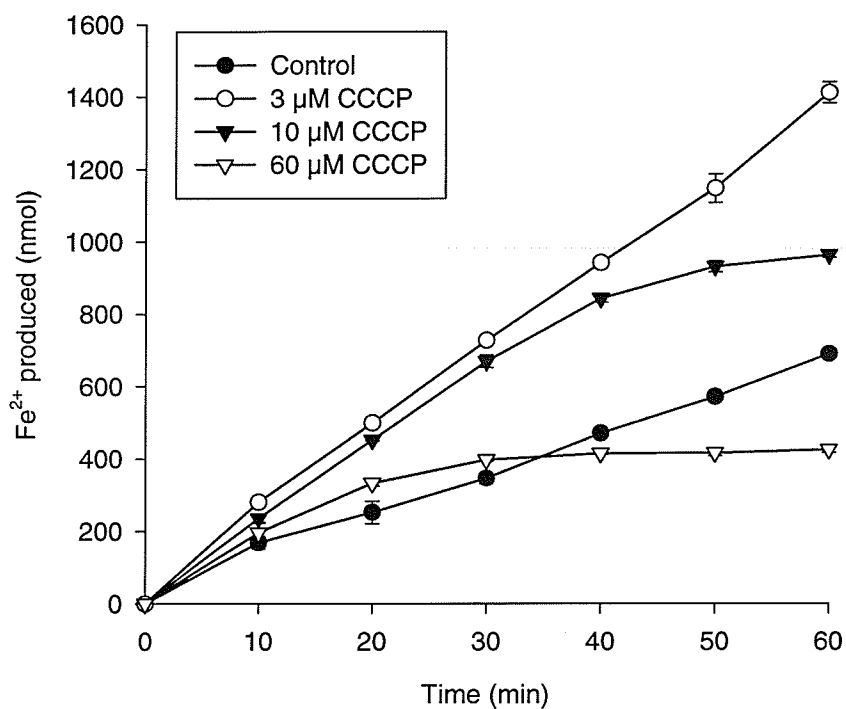
(a)



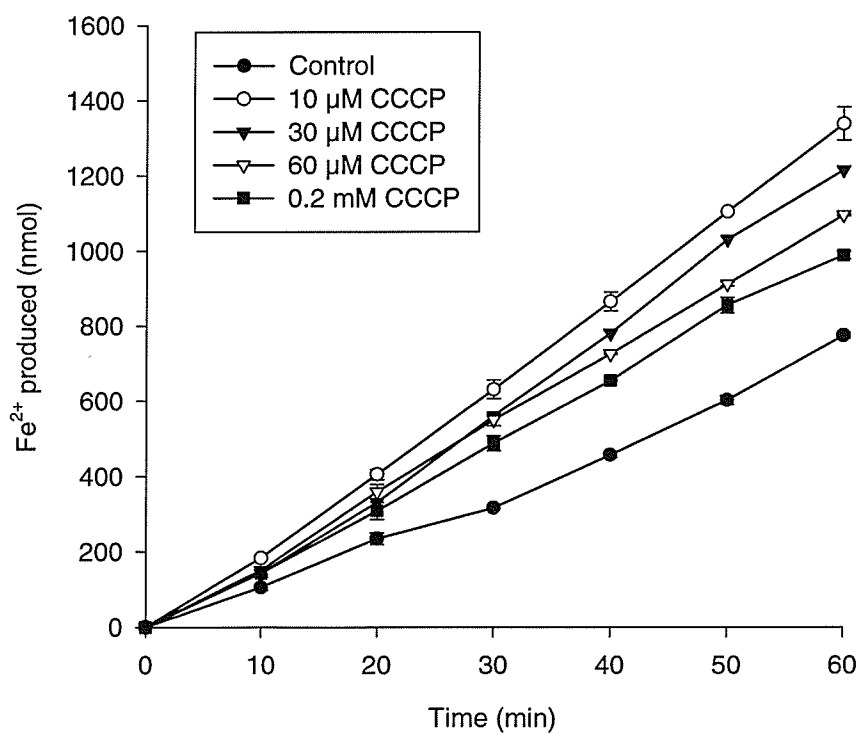
(b)

Fig. 2-33. Effect of TTFA on Fe^{3+} reduction by endogenous substrates at pH 3.5. (a)

Time evolution and the combination with amytal or HQNO; (b) rates at different concentrations of TTFA.



(a)



(b)

Fig. 2-34. Effect of CCCP on Fe^{3+} reduction by endogenous substrates at (a) pH 2.3 and (b) pH 3.5.

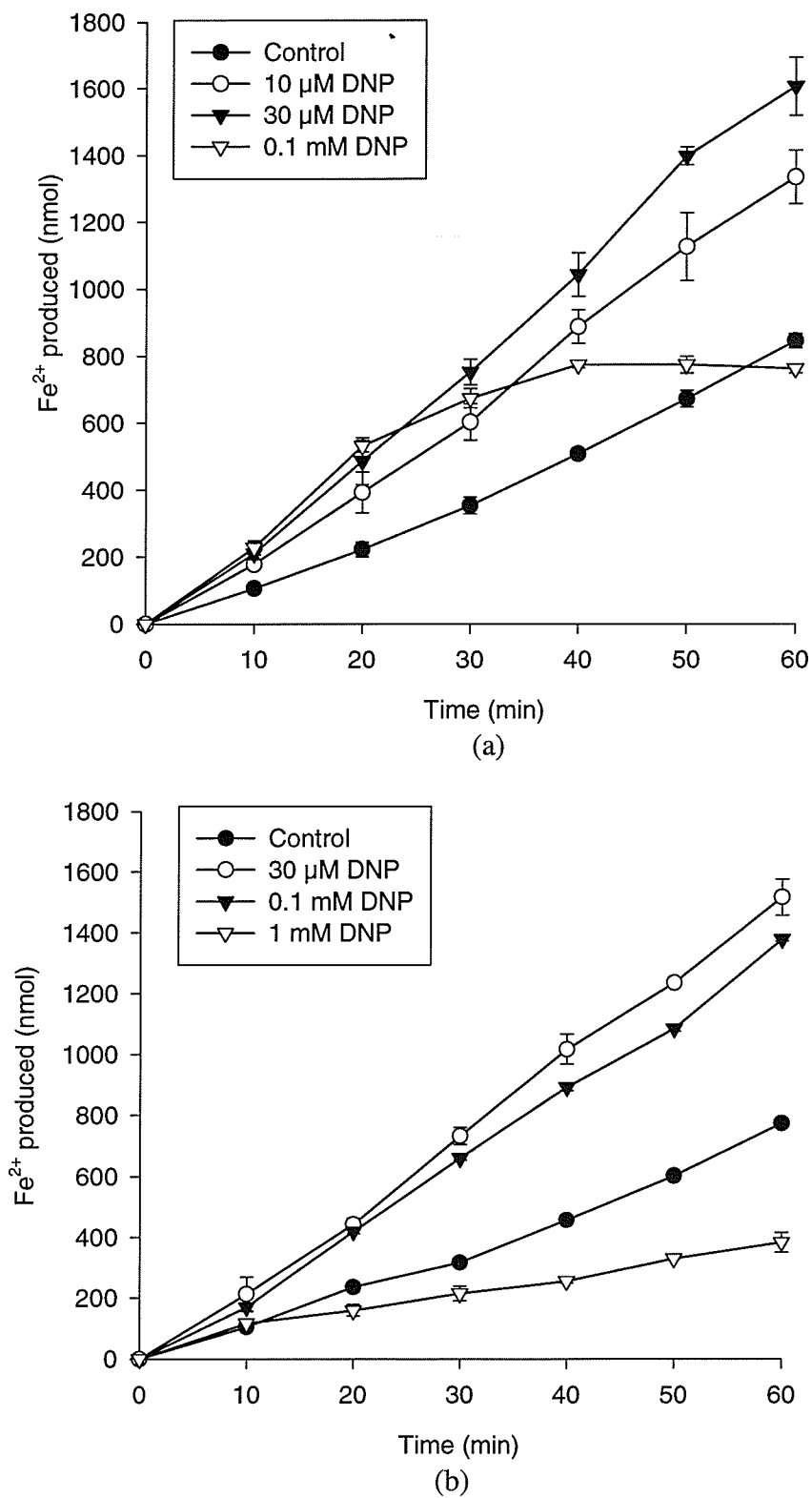


Fig. 2-35. Effect of DNP on Fe^{3+} reduction by endogenous substrates at (a) pH 2.3 and (b) pH 3.5.

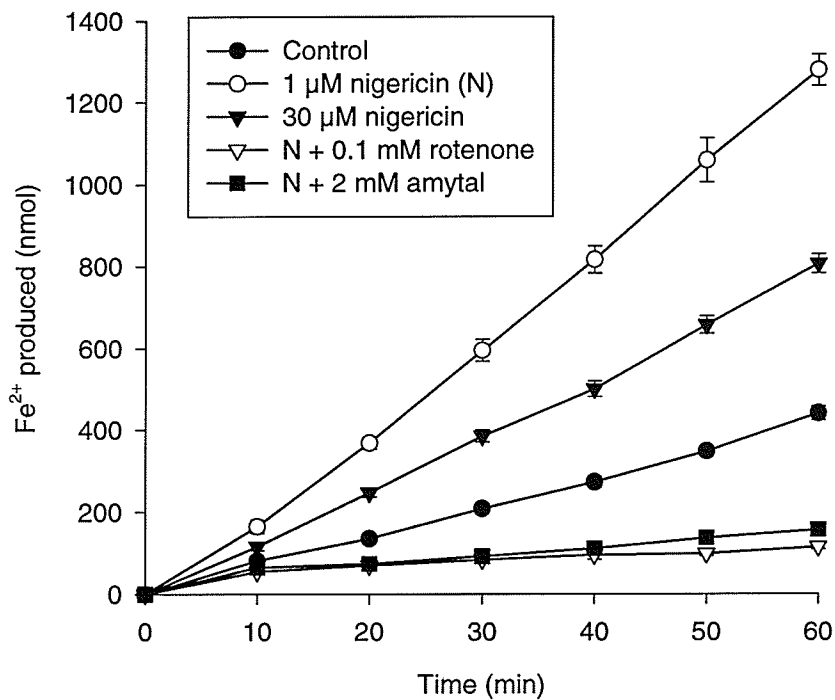


Fig. 2-36. Effect of nigericin on Fe³⁺ reduction by endogenous substrates in the absence and presence of complex I inhibitors at pH 3.5.

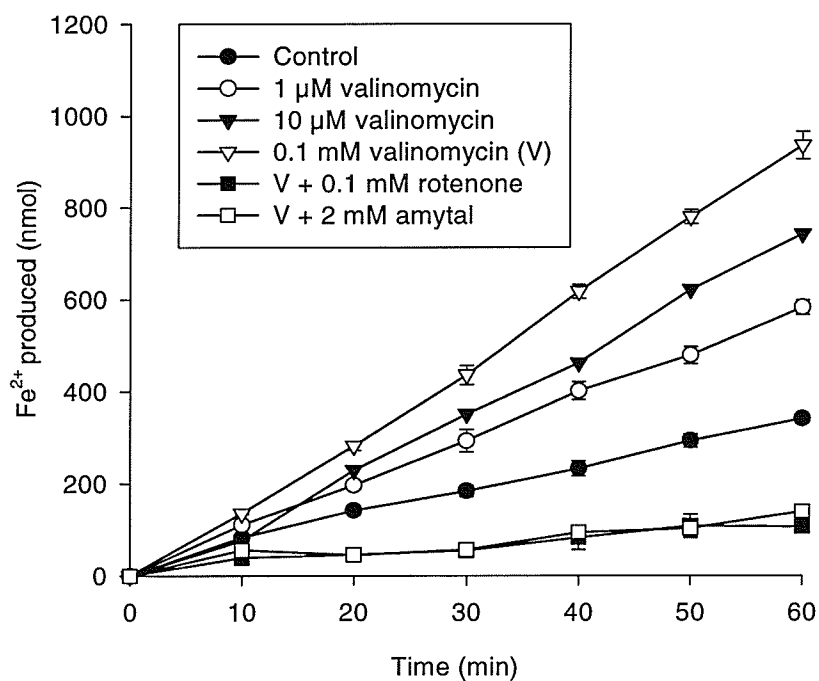


Fig. 2-37. Effect of valinomycin on Fe³⁺ reduction by endogenous substrates in the absence and presence of complex I inhibitors at pH 3.5.

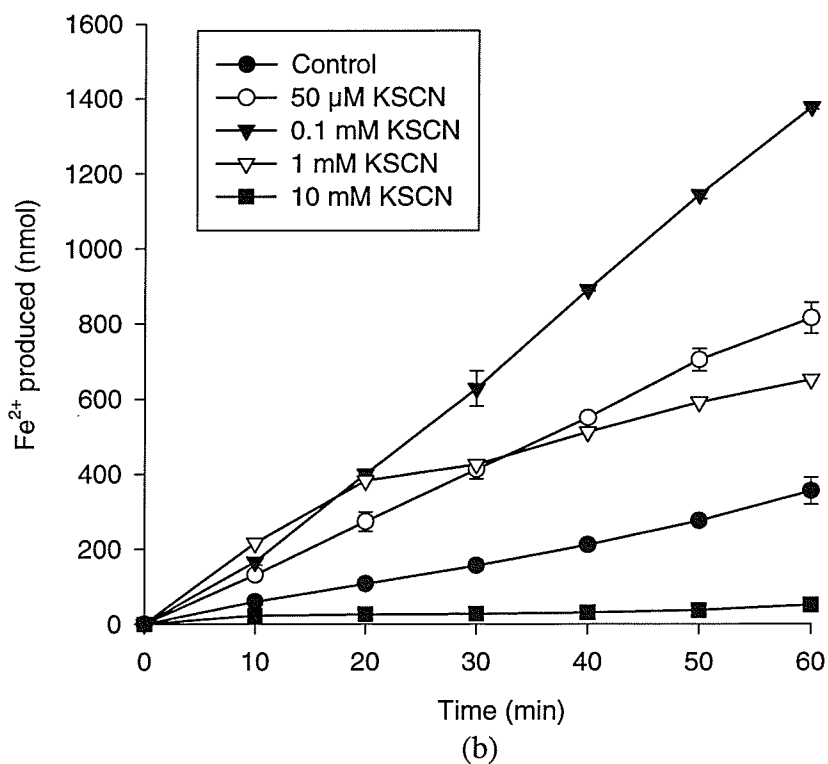
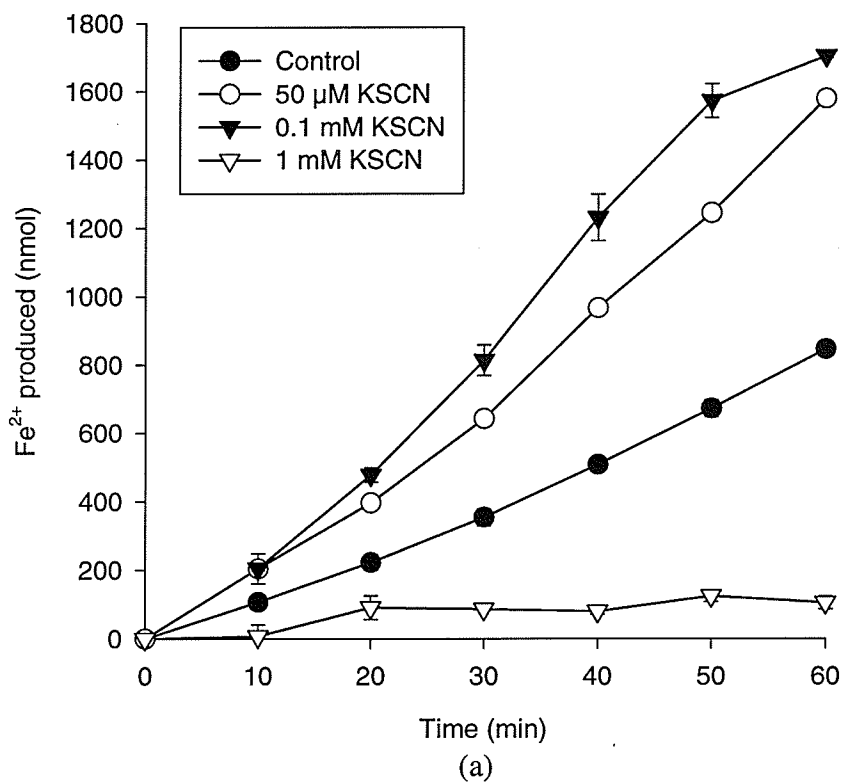


Fig. 2-38. Effect of KSCN on Fe^{3+} reduction by endogenous substrates at (a) pH 2.3 and (b) pH 3.5.

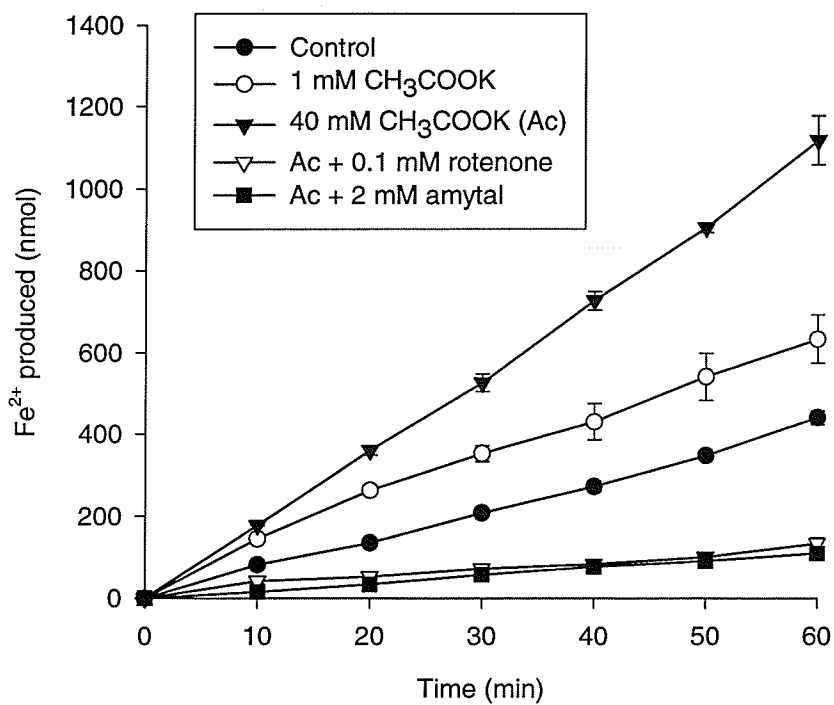


Fig. 2-39. Effect of CH₃COOK on Fe³⁺ reduction by endogenous substrates in the absence and presence of complex I inhibitors at pH 3.5.

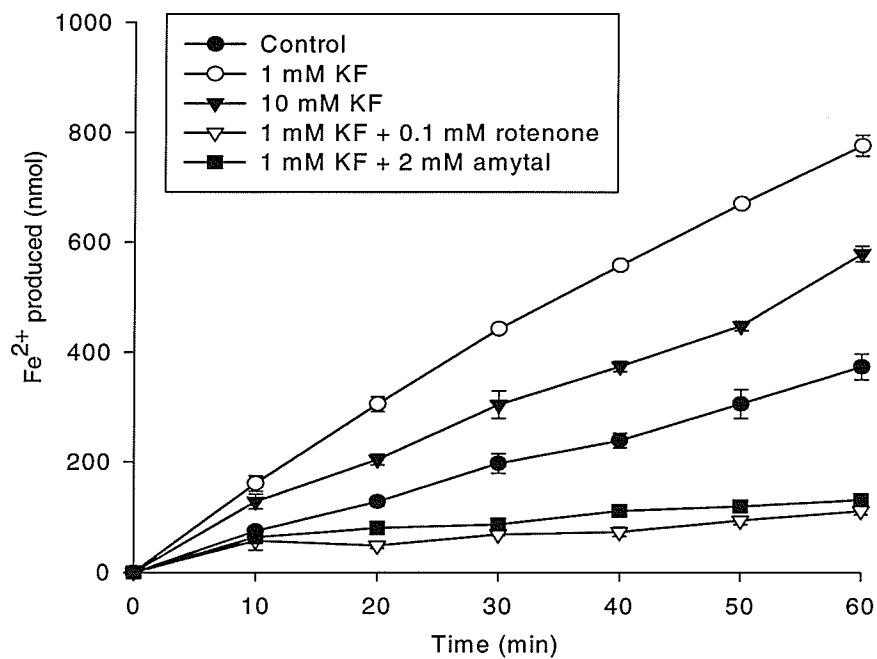


Fig. 2-40. Effect of KF on Fe³⁺ reduction by endogenous substrates in the absence and presence of complex I inhibitors at pH 3.5.

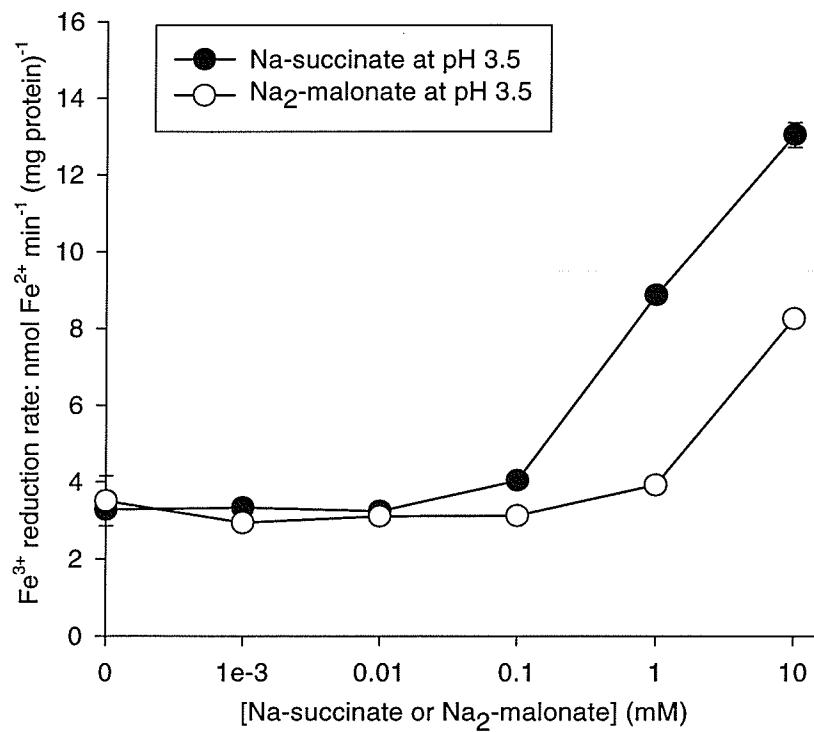


Fig. 2-41. Effect of Na₂-succinate and Na₂-malonate on Fe³⁺ reduction by endogenous substrates at pH 3.5.

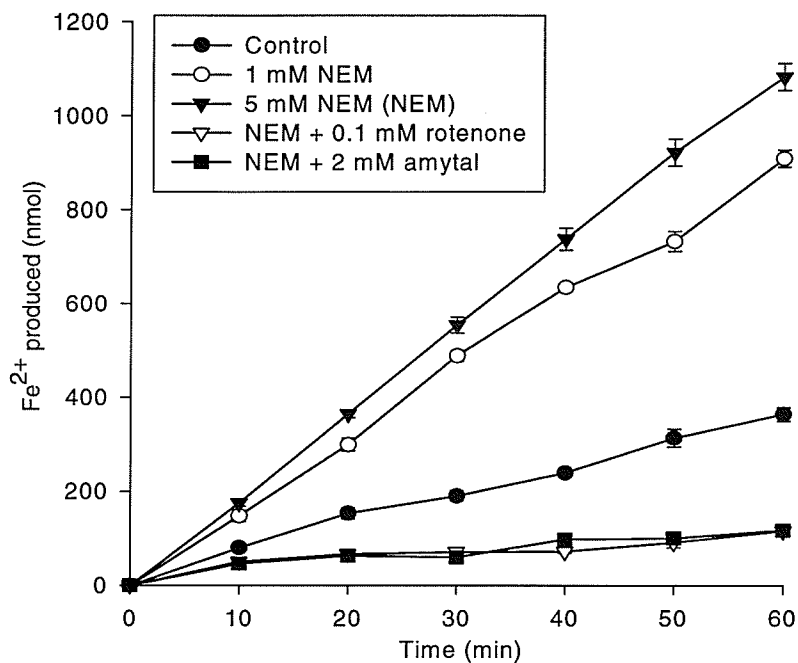


Fig. 2-42. Effect of NEM on Fe^{3+} reduction by endogenous substrates in the absence and presence of complex I inhibitors at pH 3.5.

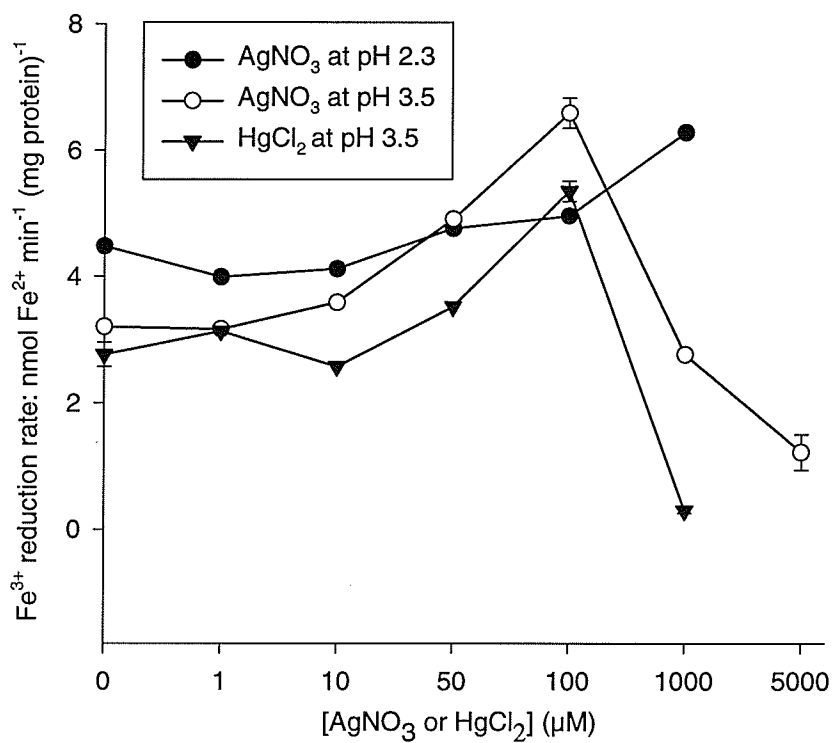
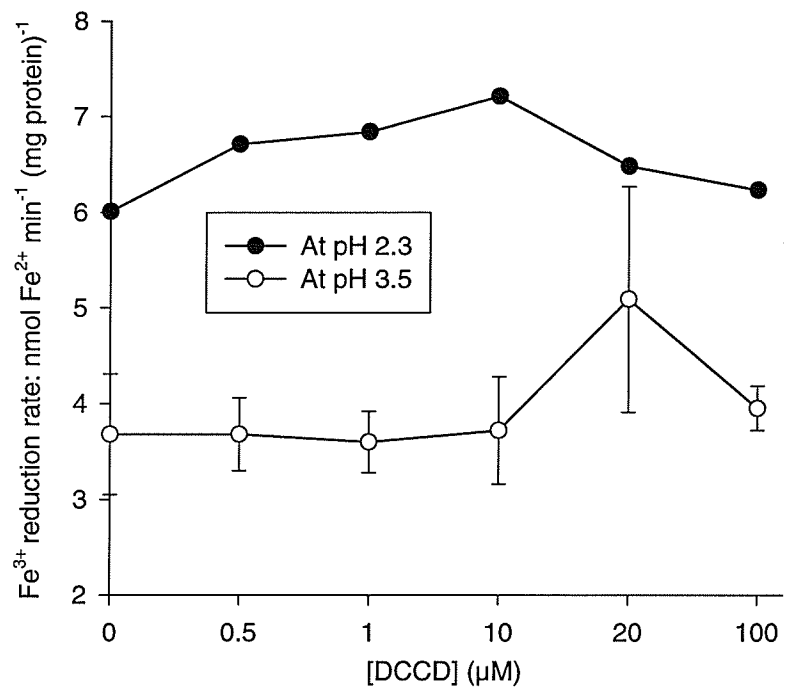
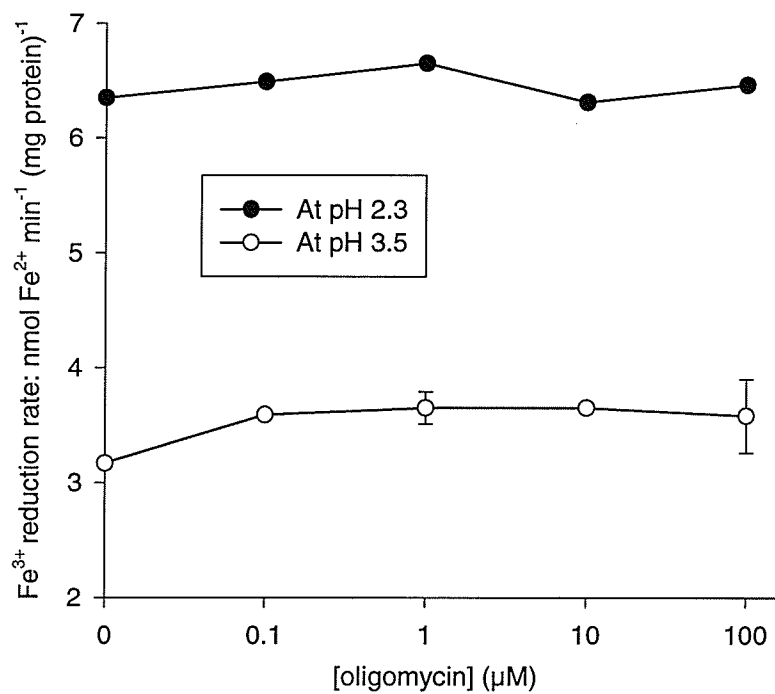


Fig. 2-43. Effect of HgCl_2 and AgNO_3 on Fe^{3+} reduction by endogenous substrates at pH 2.3 and pH 3.5.



(a)



(b)

Fig. 2-44. Effect of inhibitors of ATP synthase, DCCD (a) and oligomycin (b), on Fe^{3+} reduction by endogenous substrates at pH 2.3 and pH 3.5.

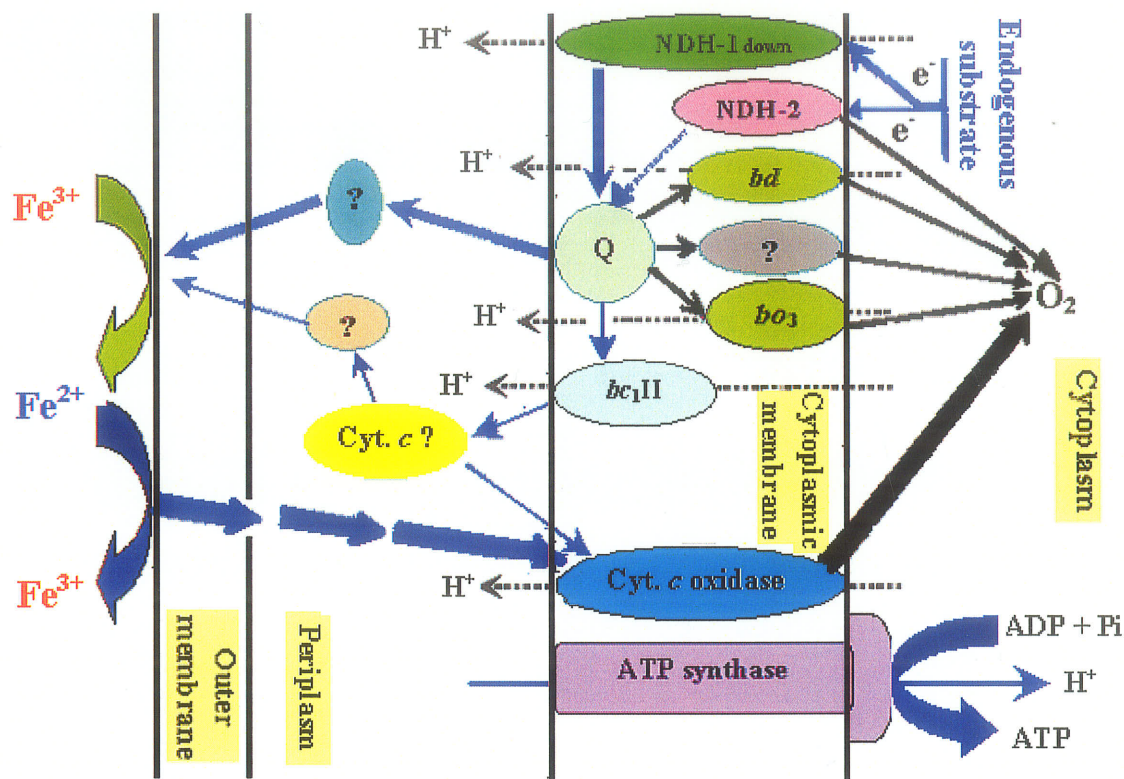


Fig. 2-45. Proposed model for electron transport pathways of oxidation of endogenous substrates in *A. ferrooxidans*. Q: ubiquinone/ubiquinol pool; NDH-1_{down}: the complex I (a NADH-ubiquinol oxidoreductase) involving proton pumping and operating in downhill reaction; NDH-2: a NADH-ubiquinol oxidoreductase involving no proton pumping; *bd* and *bo*₃: cytochrome *bd* and *bo*₃ quinol oxidases involving proton pumping; *bc*₁II: the complex III involved in downhill reaction; Cyt.: cytochrome. The thickness of straight arrows (not including the arrows pointing at H^+) represents the speed of electron flow in a qualitative manner.

Part III
Oxidation of Fructose

Abstract

Fructose was oxidized by *A. ferrooxidans* possibly after a concentration-dependent diffusion into the cells. Complex I inhibitors rotenone, amytal and piericidin A, and complex IV inhibitors KCN and NaN_3 , strongly inhibited fructose oxidation, but complex I inhibitor atabrine had no effect. The effect of complex III inhibitors antimycin A, myxothiazol and HQNO (also an inhibitor of quinol oxidase) have also been tested. HQNO and antimycin A showed no effect on fructose oxidation by O_2 but slightly stimulated the oxidation by Fe^{3+} . Myxothiazol showed no effect on the oxidation by both O_2 and Fe^{3+} . Uncouplers and iron chelators showed no effect. The respiratory quotient (CO_2 / O_2 ratio) of fructose oxidation was close to 1.0 in agreement with the complete oxidation of fructose to CO_2 and H_2O . The external pH of cells decreased during fructose oxidation indicating proton pumping. It was concluded that the oxidation of fructose required the same electron transport pathways as endogenous oxidation.

Introduction

A. ferrooxidans is not expected to grow by oxidizing organic compounds for energy and carbon source because it is a chemoautotrophic bacterium. However, since the respiratory quotient of 1.0 (CO_2 / O_2 ratio) for endogenous respiration indicates the carbohydrate nature $((\text{CH}_2\text{O})_n)$ of endogenous substrates, a question must be asked if any external organic compounds could be oxidized by the cells of *A. ferrooxidans*.

The oxidation of organic compounds by *A. ferrooxidans* has been investigated previously. In 1960s – 1970s, there were reports showing that *A. ferrooxidans* could grow on glucose after it used up ferrous iron in a medium containing ferrous iron and glucose (Shafia et al. 1972; Shafia and Wilkinson 1961; Tabita and Lundgren 1971a, 1971b). Later it was found that the oxidation of glucose was due to the contamination of an acidophilic heterotrophic bacterium which could oxidize glucose but not sulfur or ferrous iron (Harrison et al. 1980). Sugio et al. (1982) investigated the glucose transport system in a facultative Fe^{2+} -oxidizing bacterium *A. ferrooxidans* strain AP-44 which was able to obtain energy by oxidizing Fe^{2+} or elemental sulfur in addition to organic substances such as glucose. $[^{14}\text{C}]$ glucose was taken up by AP-44 cells and was incorporated into $^{14}\text{CO}_2$ produced during glucose oxidation. The electron transport pathway of glucose oxidation was not studied but effects of electron transport inhibitors and uncoupler were investigated on the uptake activity of $[^{14}\text{C}]$ glucose. Complex I inhibitors 50 μM amytal, 50 μM rotenone and 1 mM atabrine inhibited glucose uptake activity in Fe^{2+} -grown cells by 100%, 100% and 22%, respectively. Complex IV inhibitors 1 mM KCN and 1 mM NaN_3 showed 94% and 100% inhibition, respectively.

ATP synthase inhibitor 50 μ M DCCD and uncoupler 1 mM DNP showed 100% and 88% inhibition, respectively.

In this study, O₂ consumption by the cells of *A. ferrooxidans* with the addition of different sugars and sugar alcohols was investigated to see if any of them could increase the respiration by the cells. Furthermore, the effects of electron transport inhibitors and uncouplers on O₂ consumption and Fe³⁺ reduction (if possible) in the presence of the compound(s) that significantly stimulated endogenous oxidation would be investigated.

Results

3.1. Fructose may be oxidized by *A. ferrooxidans*

Twenty compounds including 7 sugar alcohols (D-forms) and 13 sugars (D-forms) have been tested to see if the cells could oxidize any of them faster than endogenous respiration by using 24 mg cells in Oxygraph (1.2 mL). Fig. 3-1 lists these compounds and their relative oxidation activities when compared to endogenous respiration rates (O_2 consumption rates). Only in the presence of fructose (80 mM) the rate was appreciably faster (3 – 4 times) than endogenous respiration rate. It is unlikely that the stimulated rate was due to the acceleration of endogenous respiration by fructose as uncouplers, weak acids, HQNO and other compounds do. It is quite possible that fructose is oxidized by the cells. When the concentration of fructose was increased with either 10 mg or 24 mg cells, the rate of fructose oxidation increased almost linearly up to 80 mM but slowed down at 160 mM (Fig. 3-2). Fig. 3-3 shows that the rate of O_2 consumption with 80 mM fructose was linear for 40 min until all the O_2 was consumed but the rate with 160 mM fructose slowed down further after 15 min. Sucrose at 0.3 M inhibited the activity in the presence of 80 mM fructose by 64% although the rate of endogenous respiration was stimulated by 21% (Fig. 3-3). The respiration of cells in the presence of the phosphorylated forms of fructose and glucose was also tested and negative results were observed (Fig. 3-4). The genes coding for the transporter of fructose were not found in the partial genome sequence of *A. ferrooxidans* (data not shown). Experiment trying to grow this organism for two weeks by replacing $FeSO_4$ with fructose in M-9-K medium was not successful (data not shown). Therefore, fructose is probably metabolized after a concentration-dependent diffusion into the cells

and a high osmotic pressure in the presence of 160 mM fructose or 0.3 M sucrose was inhibitory.

Since *A. ferrooxidans* is an autotroph it is not expected to oxidize organic compounds to provide energy for its growth. It is understandable that much of the studies have been carried out on the oxidation of inorganic compounds (Fe^{2+} and sulfur compounds). Glucose oxidation by *A. ferrooxidans* has been reported only in a special facultative strain AP-44 (Sugio et al. 1982). Thus detailed studies of fructose oxidation by *A. ferrooxidans* are necessary.

Fructose is an organic compound and may be indirectly oxidized via a downhill electron transport pathway. Since fructose and the endogenous substrates in this organism are both carbohydrate compounds ($(\text{CH}_2\text{O})_n$), experiments have been carried out to see if oxidation of fructose is following the same electron transport pathways as the oxidation of endogenous substrates (Fig. 2-45). Fructose could be oxidized by *A. ferrooxidans* either by using O_2 (as shown above) or by using Fe^{3+} (the following data) as a terminal electron acceptor. In the following experiments, oxidation of fructose by O_2 was studied by using 80 mM fructose and 24 mg cells in Oxygraph (1.2 mL) or 80 mM fructose and 64 mg cells in Warburg (3.2 mL). Oxidation of fructose by Fe^{3+} was studied by using 80 mM fructose, 2 mM KCN, 4 mM FeCl_3 and 20 mg cells in 1 mL reaction system. Unless otherwise stated, all the experiments were carried out in 0.1 M β -alanine- H_2SO_4 , pH 3.5 at 25 °C.

3.2. Effect of uncouplers and iron chelators

Uncoupler CCCP at 10 μM inhibited fructose oxidation by only 3% (data not shown). FeCl_3 at 4 mM had little effect on fructose oxidation (Fig. 3-4). Iron chelators, 8 mM EDTA, 10 mM 2,2'-dipyridyl and 1.2 mM o-phenanthroline had no effect on it but 4 mM tiron stimulated it by 59% (data not shown). The fact that CCCP, EDTA, 2,2'-dipyridyl and o-phenanthroline stimulated endogenous respiration (see Part II) but failed to stimulate fructose oxidation may suggest that the rate of fructose oxidation already reached the maximum and could no longer be increased by the stimulators used in endogenous respiration. The stimulation by tiron was due to the oxidation of tiron itself as showed in Part I but not due to the real stimulation of fructose oxidation.

3.3. Effect of complex I inhibitors

Table 3-1 and Fig. 3-5 show the effect of complex I inhibitors on fructose oxidation by O_2 and Fe^{3+} . Atabrine at 2 mM had no effect on fructose oxidation by O_2 . If the rate over the endogenous oxidation rate is the real oxidation rate of fructose, fructose oxidation by either O_2 or Fe^{3+} was inhibited nearly completely by 0.1 mM rotenone or 2 mM amytal, although endogenous oxidation was only inhibited by complex I inhibitors by 50% (see Part II). Piericidin A at 0.5 μM also showed nearly complete inhibition of oxidation by Fe^{3+} . The results indicate that electrons from fructose mainly enter the electron transport pathways at $\text{NDH-1}_{\text{down}}$ as shown in Fig. 2-45.

3.4. Effect of inhibitors of complex IV

Fig. 3-6 shows the effect of complex IV inhibitors, KCN and NaN_3 , on fructose oxidation by O_2 . If the oxidation rate of endogenous substrates is subtracted 2 mM KCN and 1 mM NaN_3 nearly completely inhibited fructose oxidation. NaN_3 at 0.1 mM failed to stimulate fructose oxidation as it did in endogenous respiration but showed 11% inhibition. This may be because that fructose oxidation already reached the fastest speed similar to uncoupler-stimulated endogenous respiration and took the pathway to cytochrome *c* oxidase to O_2 . Failure of an uncoupler, CCCP, to stimulate fructose oxidation agrees with this interpretation. In the presence of fructose and 2 mM KCN or 1 mM NaN_3 , the rate before 10 min was slower than the rate after 10 min. This may indicate the shifting of electrons from the cytochrome *c* oxidase pathway to the pathways to other terminal oxidases (see Fig. 2-45).

3.5. Effect of inhibitors of complex III and quinol oxidase

Table 3-2 and Fig. 3-7 show the effect of inhibitors of complex III and quinol oxidase. Antimycin A, HQNO showed no effect on fructose oxidation by O_2 but showed 27% and 17% stimulation on the oxidation by Fe^{3+} , respectively. Myxothiazol at 40 μM showed inhibition of around 10% either with O_2 or Fe^{3+} as the terminal electron acceptor. However, the inhibition was mainly due to low rate in the last 10 min in Fe^{3+} reduction (Fig. 3-6) and in the last 15 min in O_2 reduction (data not shown). So myxothiazol may not really inhibit fructose oxidation. No inhibition of fructose by these three compounds indicates that electrons from $\text{NDH-1}_{\text{down}}$ could directly flow from Q to Fe^{3+} . Stimulation indicates that some electrons flow from Q to $bc_1\text{II}$ to cyt. *c*? and then either to O_2 or to

Fe^{3+} as shown in Fig. 2-45 and the inhibition of the pathway forces more electrons to go from Q to Fe^{3+} directly which is more efficient and faster.

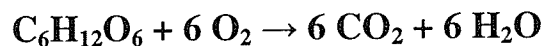
Fig. 3-8 shows the effect of CCCP and HQNO on fructose oxidation after cells were preincubated with 2 mM KCN for 25 min before the addition of fructose with or without 10 μM CCCP and / or 40 μM HQNO. In the presence of KCN, fructose was oxidized by the cells with an activity 73% higher than that without fructose. The activity with fructose in the presence of KCN was stimulated by CCCP by 104% although the activity with KCN alone (endogenous oxidation) was also stimulated by CCCP by 113%. The activity in the presence of KCN, fructose and CCCP, which was 66% higher than the activity in the presence of KCN and CCCP, was inhibited by HQNO by 48% to the level similar to the activity in the presence of KCN and fructose. As shown in Part II (Fig. 2-8 & 2-14), electrons mainly flow to the terminal oxidases (*bd*, *bo₃* and the unknown oxidase in Fig. 2-45) other than cytochrome *c* oxidase after 25 min in the presence of 2 mM KCN. The results shown in Fig. 3-8, therefore, indicate that fructose could be oxidized by the proton pumping quinol oxidases *bd* and / or *bo₃* as well as the unknown oxidase (?) as shown in Fig. 2-45 after cytochrome *c* oxidase (*aa₃ / ba₃*) was inhibited by KCN.

3.6. Respiratory quotient of fructose oxidation

Since both fructose and endogenous substrates belong to carbohydrate compounds and the respiratory quotient (CO_2 / O_2) of endogenous respiration was 1.0, it was essential to test if the respiratory quotient of fructose oxidation was also 1.0. Fig. 3-9 shows that the respiratory quotient of fructose oxidation was indeed close to 1.0 with

rates of CO₂ production and O₂ consumption of 5.39 ± 0.04 nmol CO₂ min⁻¹ (mg protein)⁻¹ (\pm SD, n=2) and 5.06 ± 0.09 nmol O₂ min⁻¹ (mg protein)⁻¹ (\pm SD, n=2), respectively.

Therefore, fructose is completely oxidized to CO₂ and H₂O as showed in reaction 8.



Reaction 8. Respiration of fructose by *A. ferrooxidans*.

3.7. Change of external pH of cells during fructose oxidation

Fig. 3-10 shows the changes in external pH of cells during fructose oxidation and endogenous substrates when cells were kept at room temperature before testing. During fructose oxidation, pH decreased from 3.3 to 3.22. This indicated that the speed of proton pumping out of cells was faster than that of proton leaking in and protons were generated in the outside of cells during fructose oxidation, which was opposite to the situation during endogenous respiration (Figs. 2-22 & 3-10). The value of pH increased from 3.2 to 3.33 during endogenous respiration in Fig. 3-10. In another experiment, pH changed from 3.24 to 3.21 within 30 min during fructose oxidation when cells were kept at 4°C (data not shown).

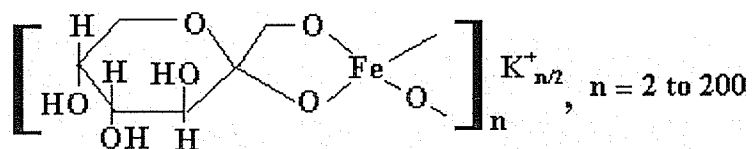
3.8. Fructose oxidation by spheroplasts and cell free extracts

Fructose, F-1,6-P and F-6-P were not oxidized by cell free extracts tested at pH 3.5, 6.5 and 7 (data not shown). Ability to oxidize fructose was almost totally gone after cells were treated to form spheroplasts. In the presence of 80 mM fructose the O₂

consumption rate ($0.93 \pm 0.03 \text{ nmol O}_2 \text{ min}^{-1} (\text{mg protein})^{-1}$) was only 10% higher than the rate of endogenous respiration ($0.84 \text{ nmol O}_2 \text{ min}^{-1} (\text{mg protein})^{-1}$) although the rate of endogenous respiration did not change compared to that of whole cells. Loss of fructose oxidizing activity by spheroplasts may be explained by the hypothesis that the pathway from Q to Fe^{3+} to cytochrome *c* oxidase to O_2 as shown in Fig. 2-45 was damaged during the preparation of spheroplasts.

Discussion and conclusions

Fructose among the 20 sugars and sugar alcohols tested, was the only compound that greatly stimulated the O₂ consumption rate by the cells of *A. ferrooxidans* (Fig. 3-1) indicating that it may have been oxidized by the cells. Experiments to grow this organism for two weeks in the medium containing fructose instead of FeSO₄ (data not shown) was not successful. The failure of growth on fructose may be due to the lack of the transporter system of fructose since the genes coding for the transporter proteins of fructose were not found in the partial genome sequence of *A. ferrooxidans* (data not shown). The rate of fructose oxidation increased with the increase of fructose concentration and reached a maximal level at 80 mM, and then the rate decreased at higher concentrations of fructose (Fig. 3-2) probably due to deleterious effect of high osmotic pressure. Fructose oxidation was inhibited 64% by 0.3 M sucrose (Fig. 3-3). Thus it is quite possible that fructose entered the cells by a concentration-dependent diffusion. It is not clear why fructose was oxidized much faster than other sugars such as glucose. One possible reason may be the ability fructose to form ferric fructose (potassium salt) complex (Windholz et al. 1983) with the structure:



The formation of the complex with the ferric iron on the cell surface of *A. ferrooxidans* may somehow facilitate the entrance of fructose into the cells, although this is only a speculation.

Since fructose has the carbohydrate nature as the endogenous substrates of *A. ferrooxidans* do, it is expected that fructose will be oxidized through the glycolytic pathway, the TCA cycle oxidation and the same electron transport pathways as observed

for endogenous oxidation. The genes coding for fructokinase have been found in the partial genome sequence of this organism (data not shown) indicating that fructose 6-phosphate is the entry point on the glycolytic pathway during fructose oxidation. The respiratory quotient of fructose oxidation was close to 1.0 (Fig. 3-9) agreeing with its carbohydrate nature and indicating that fructose was completely oxidized to CO_2 and H_2O (Reaction 8). The latter interpretation is supported by the fact that all enzymes on the glycolytic pathway and the TCA cycle exist in *A. ferrooxidans* as discussed in Part II.

Fructose, as well as endogenous substrates in this organism, could be oxidized by Fe^{3+} as well as O_2 . Complex I inhibitors rotenone, amytal and piericidin A strongly inhibited fructose oxidation (Fig. 3-5) indicating that electrons from fructose enter the electron transport pathways mainly from $\text{NDH-1}_{\text{down}}$. Atabrine showed no effect but piericidin A showed strong inhibition (Fig. 3-5) indicating that fructose oxidation is different from Fe^{2+} oxidation (see Part I). Complex IV inhibitors KCN and NaN_3 showed stronger inhibition on fructose oxidation (Fig. 3-6) than on endogenous respiration (see Part II) possibly suggesting that the rate of fructose oxidation was very close to the maximal rate which could be achieved only by using the cytochrome *c* oxidase pathway. This interpretation is also supported by the effect of CCCP (10 μM), HQNO (40 μM) and iron chelators which showed no effect on fructose oxidation but greatly stimulated endogenous respiration (see Part II).

Since the first step of sugar metabolism needs energy (ATP) (sugar phosphorylation), it was suspected that the lack of stimulation by uncouplers on fructose oxidation in *A. ferrooxidans* was due to the inhibition of ATP generation through the electron transport chain. However, it was reported that CCCP at 1 μM stimulated glucose oxidation by

30% but inhibited succinate oxidation almost completely in the cells of *E. coli* (Cavari and Avi-Dor 1967). The lack of inhibition of glucose oxidation by CCCP is due to that the generation of ATP through the glycolytic pathway (providing energy for glucose phosphorylation) was unaffected by CCCP (Cavari and Avi-Dor 1967). Succinate oxidation was strongly inhibited by CCCP because: (1) oxaloacetate (OAA), which acts as a feedback inhibitor of succinate oxidation, has to be converted to phosphoenolpyruvate (PEP); (2) the energy (ATP) for the conversion of OAA into PEP is produced via the electron transport chain (ETC); and (3) ATP generation via ETC is inhibited by CCCP (Cavari and Avi-Dor 1967). Therefore, it is more likely that the lack of inhibition of fructose by uncouplers in *A. ferrooxidans* is due to that the rate of fructose oxidation is close to the maximum which is limited by the low activities of the key enzymes on the glycolytic pathway, the TCA cycle and also the electron transport pathways in the downhill direction. This interpretation is supported by the report by Tian et al. (2003). Tian et al. (2003) transferred the phosphofructokinase gene (*pfkA*) from *E. coli* into the chemoautotrophic bacterium *A. thiooxidans* Tt-7 by conjugation. The enzyme expressed from the *pfkA* gene in the Tt-7 transconjugant showed 20% activity of that in *E. coli*. The addition of glucose to the Starkey-S⁰ inorganic medium doubled the cell yield of *A. thiooxidans* Tt-7 transconjugant compared to the case without glucose addition after this strain has been grown for 11 days. The authors explained that the synthesis of partial cell materials from glucose instead of CO₂ could save some energy for the increase of cell yield.

Complex III inhibitors 40 μM HQNO and 0.1 mM antimycin A stimulated fructose oxidation by Fe³⁺ (Fig. 3-7) only by 20 – 30%, which was much less than the

stimulation of endogenous oxidation by Fe^{3+} (136% stimulation by 40 μM HQNO as shown in Fig. 2-32), indicating that (1) most electrons flowed via the fast pathway from Q to Fe^{3+} but smaller portion of electrons flowed via the slow pathway from Q to $bc_1\text{II}$ and finally to Fe^{3+} (see Fig. 2-45) in the absence of complex III inhibitors; and (2) electrons on the pathway involving $bc_1\text{II}$ were shifted to the fast pathway from Q to Fe^{3+} after $bc_1\text{II}$ (complex III) was inhibited by HQNO or antimycin A.

Fructose was oxidized after the cells were preincubated with 2 mM KCN for 25 min and the activity was greatly increased by 10 μM CCCP, but the increase in activity totally disappeared in the presence of 40 μM HQNO (Fig. 3-8) indicating the CCCP stimulatory site at quinol oxidase. The results suggest that fructose was oxidized by the proton pumping quinol oxidases bd and / or bo_3 and the unknown oxidase (see Fig. 2-45) after cytochrome c oxidase (aa_3 / ba_3) was inhibited by KCN. The stimulation by CCCP on fructose oxidation through quinol oxidases further supports that the ATP required for fructose phosphorylation can be provided by substrate.

Therefore, all the results indicate that fructose oxidation used the same pathways as endogenous oxidation as shown in Fig. 2-45.

The failure of spheroplasts in oxidizing fructose may be due to (1) the damage of the electron carriers on the fast pathway from Q to Fe^{3+} , (2) the loss of the periplasmic content during the preparation of spheroplasts, and (3) the inhibition by high osmotic pressure (see Fig. 3-3). The decrease of the external pH of the cells during fructose oxidation indicates proton pumping.

Tables of Part III

Table 3-1. Effect of complex I inhibitors on fructose oxidation.

Concentration		Oxidation by O ₂		Oxidation by Fe ³⁺	
		Rate *	R.A	Rate *	R.A
Endogenous		0.80 ± 0.03	0.23	2.79 ± 0.19	0.27
Control		3.43 ± 0.26	1.00	10.28 ± 1.09	1.00
Atabrine	2 mM	3.36 ± 0.26	0.98		
Amytal	0.5 mM	2.08 ± 0.05	0.61		
	2 mM	0.80 ± 0.07	0.23	1.78 ± 0.34	0.17
Rotenone	10 µM	1.17 ± 0.03	0.34		
	0.1 mM	0.63 ± 0.01	0.18	1.43 ± 0.10	0.14
Piericidin A	0.5 µM			0.91 ± 0.00	0.09

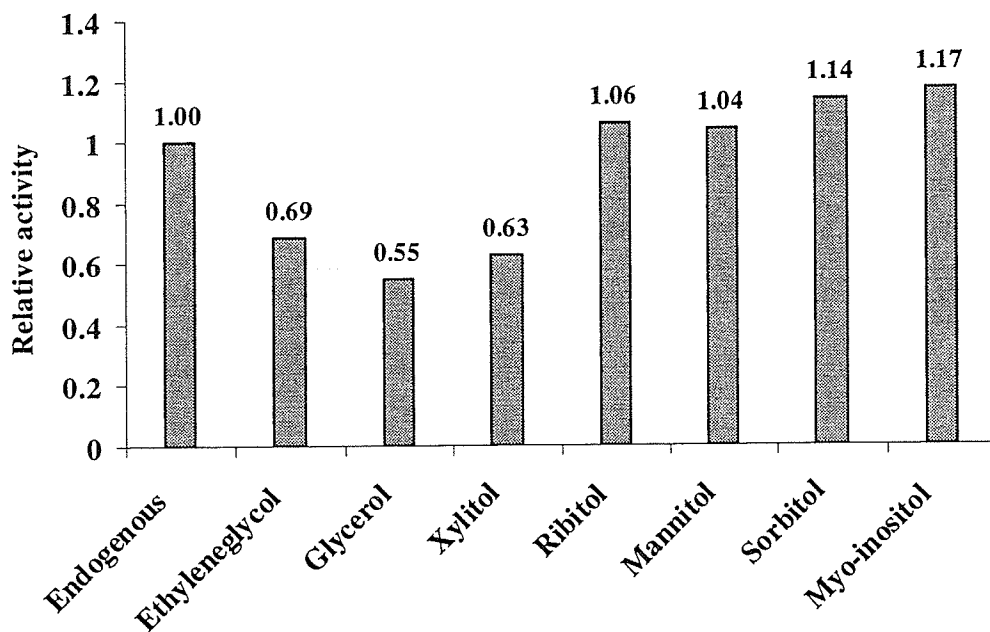
* Rate: nmol O₂ or Fe²⁺ min⁻¹ (mg protein)⁻¹ (± SD, n = 2); R.A: relative activity, a ratio of a rate over that of control.

Table 3-2. Effect of inhibitors of complex III and quinol oxidase on fructose oxidation.

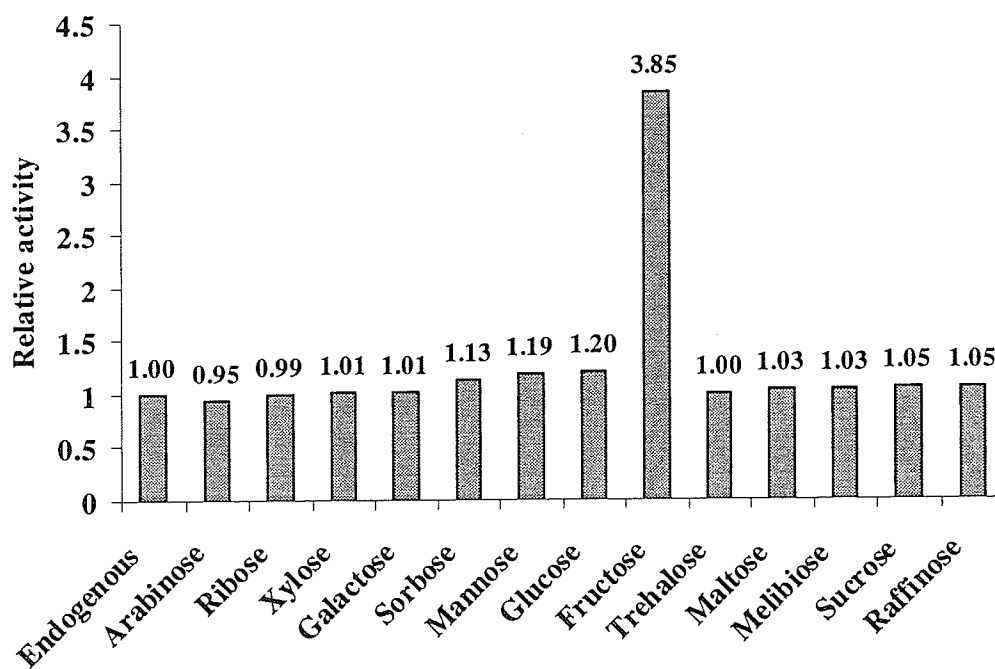
Concentration		Oxidation by O ₂		Oxidation by Fe ³⁺	
		Rate *	R.A	Rate *	R.A
Endogenous		0.94 ± 0.02	0.26	2.79 ± 0.19	0.27
Control		3.65 ± 0.05	1.00	10.28 ± 1.09	1.00
Antimycin A	10 µM	3.59 ± 0.07	0.98		
	0.1 mM	3.60 ± 0.04	0.99	13.08 ± 1.55	1.27
Myxothiazol	40 µM	3.28 ± 0.11	0.90	9.50 ± 1.04	0.92
HQNO	40 µM			12.00 ± 2.04	1.17
Control		4.40 ± 0.23	1.00		
HQNO	10 µM	4.58 ± 0.08	1.04		
	40 µM	4.44 ± 0.20	1.01		

* Rate: nmol O₂ or Fe²⁺ min⁻¹ (mg protein)⁻¹ (± SD, n = 2); R.A: relative activity, a ratio of a rate over that of control.

Figures of Part III



(a)



(b)

Fig. 3-1. Relative activities of respiration by 24 mg cells in Oxygraph (1.2 mL) in the presence of different alcohols (a) and sugars (b). Except for myo-inositol (50 mM) and raffinose (16 mM), all alcohols and sugars were present at 80 mM.

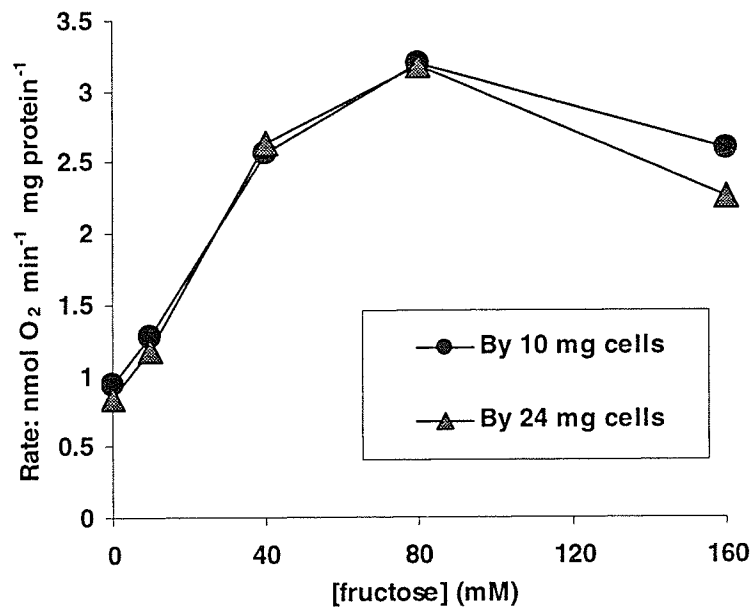


Fig. 3-2. Rates of oxidation of fructose at different concentrations by 10 mg and 24 mg cells in Oxygraph (1.2 mL).

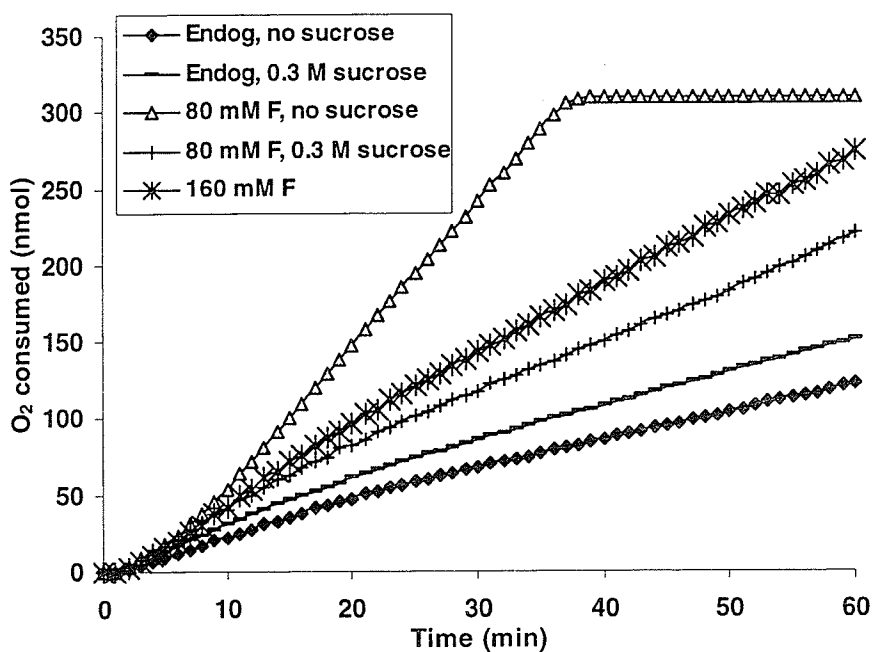


Fig. 3-3. Oxidation of fructose (F) at 80 mM and 160 mM and effect of sucrose on fructose oxidation and endogenous respiration by 24 mg cells in Oxygraph (1.2 mL).

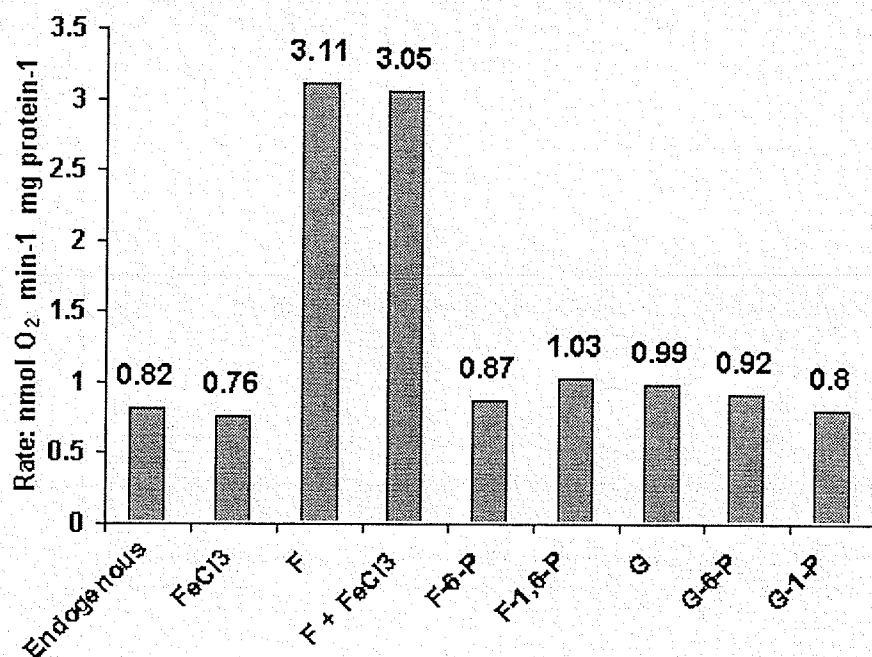
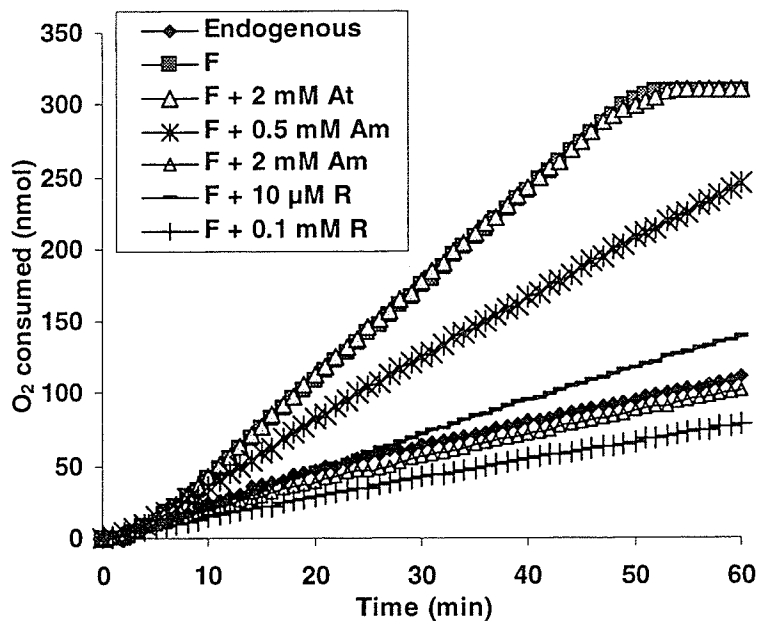
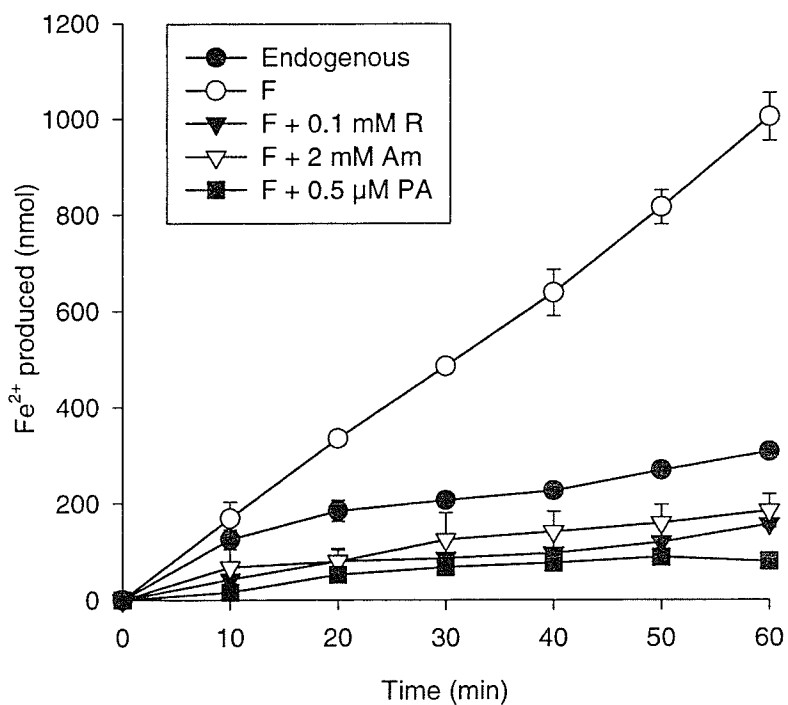


Fig. 3-4. Rates of respiration by 24 mg cells in Oxygraph (1.2 mL) in the presence of 4 mM FeCl₃, fructose (F), fructose-6-phosphate (F-6-P), fructose-1,6-diphosphate (F-1,6-P), glucose (G), glucose-6-phosphate (G-6-P) and glucose-1-phosphate (G-1-P). Except for F-6-P (14 mM), all sugars were present in 80 mM.



(a)



(b)

Fig. 3-5. Effect of complex I inhibitors on fructose oxidation by O₂ (a) and Fe³⁺ (b). At: atabrine; Am: amytal; R: rotenone; PA: piericidin A.

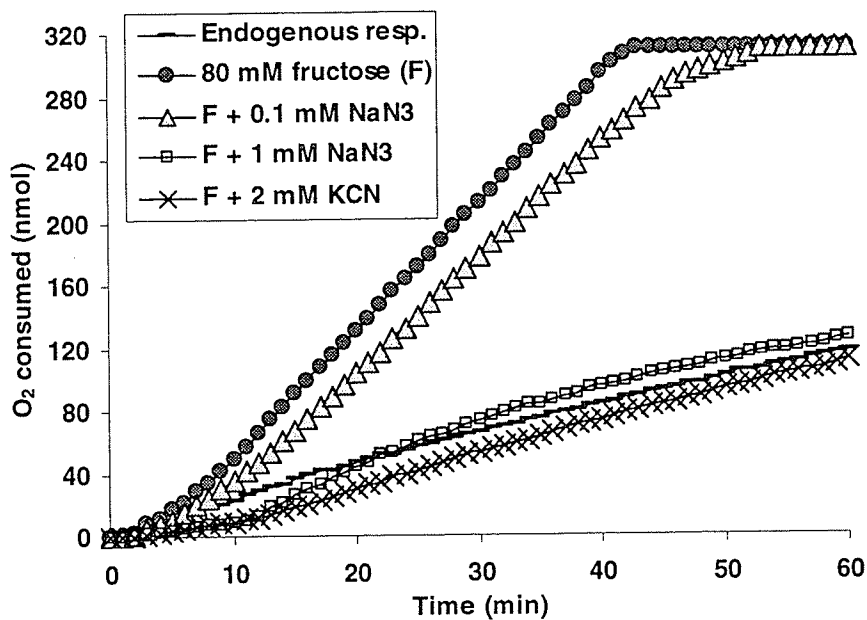


Fig. 3-6. Effect of KCN and NaN₃ on fructose oxidation.

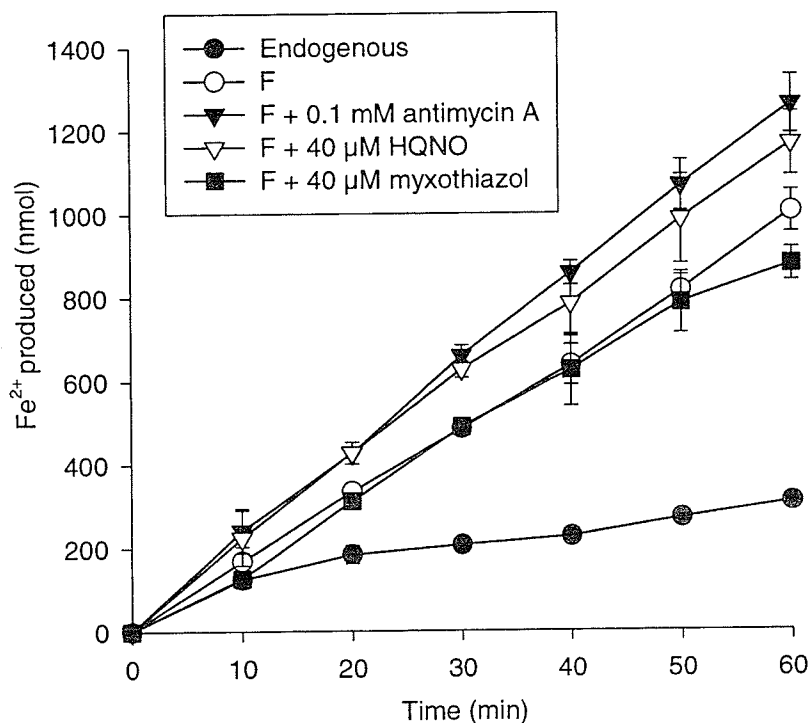


Fig. 3-7. Effect of antimycin A, myxothiazol and HQNO on fructose oxidation by Fe³⁺.

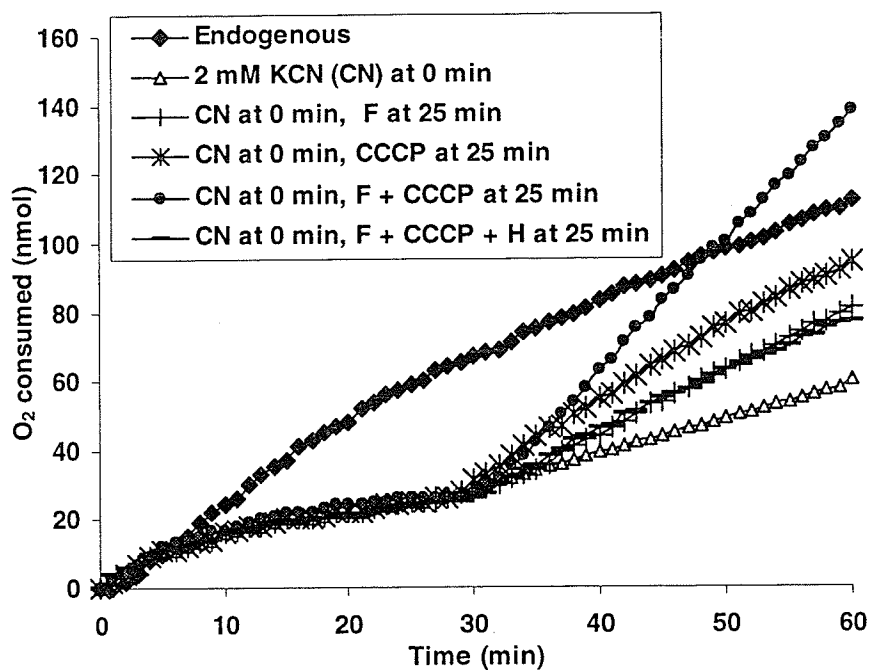


Fig. 3-8. Oxidation of fructose (F, 80 mM) with and without the combinations of CCCP (10 μ M) and HQNO (H, 40 μ M) after cells (24 mg / 1.2 mL) had been preincubated with 2 mM KCN for 25 min.

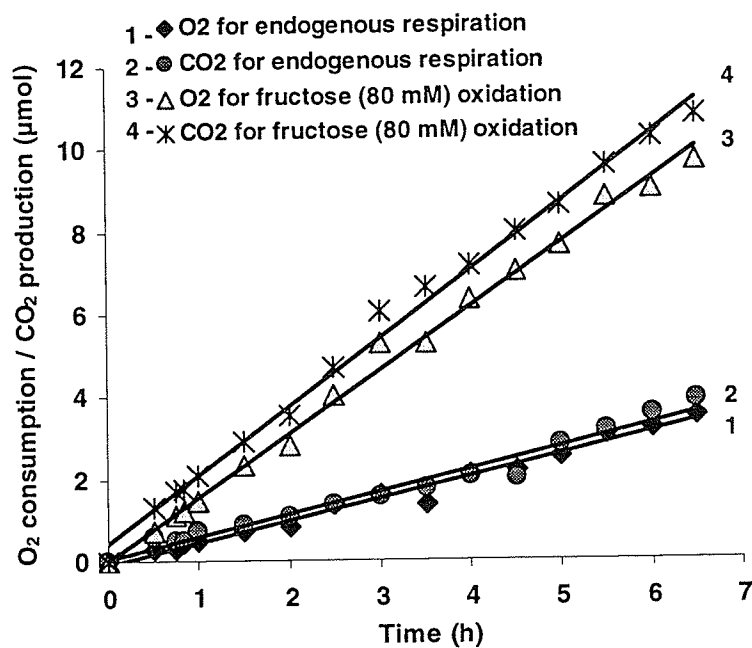


Fig. 3-9. O₂ consumption and CO₂ production during endogenous and fructose oxidation.

Tests were done at 30°C in Warburg respirometer with 64 mg cells in 3.2 mL reaction system.

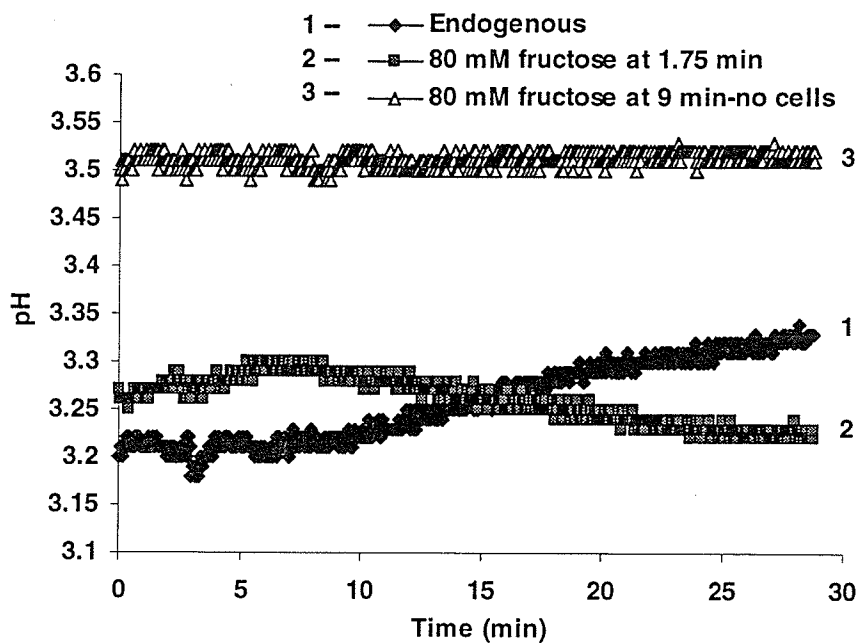


Fig. 3-10. Change of external pH of cells during endogenous and fructose oxidation tested in 2 mL system included 40 mg cells in water of pH 3.5. Cells were harvested and suspended in water of pH 3.5 and kept at room temperature before testing. The pH values were continuously recorded by a computer connected to the pH meter. The initial pH may shift within 0.1 unit due to the sensitivity change of the electrode of pH meter after more than long time of tests. In another experiment, when cells were kept at 4 °C, the pH decreased from 3.24 to 3.21 during fructose oxidation (data not shown).

Part IV

Oxidation of Yeast Extract (YE) and Casamino Acids (CA)

Abstract

Unknown compounds in yeast extract (YE) and casamino acids (CA) were oxidized by *A. ferrooxidans* using O₂ as the terminal electron acceptor. Complex I inhibitors rotenone, amytal and piericidin A partially inhibited the oxidations of YE and CA but atabrine had no effect. Complex III inhibitors myxothiazol and antimycin A showed partial inhibition but HQNO, an inhibitor of complex III and quinol oxidase, as well as complex IV inhibitors KCN and NaN₃ strongly inhibited the oxidations. FeCl₃ had no effect. Uncouplers slightly stimulated the oxidations at concentrations much lower than those used to stimulate Fe²⁺ oxidation. Although the nature of the oxidizable compounds is unknown, the results suggest that their oxidation possibly used the downhill electron transport pathways similar to the pathways of endogenous oxidation except that an HQNO-sensitive dehydrogenase may also be involved.

Introduction

Amino acid L-cysteine was oxidized by *A. ferrooxidans* by first reducing Fe^{3+} to Fe^{2+} on the cell surface and then Fe^{2+} being oxidized via the Fe^{2+} oxidation system as shown in Part I. A question that may be asked is if other amino acids could also be oxidized by this organism. Thus other 19 standard amino acids, casamino acids and vitamin-containing yeast extract were tested to see if any could be oxidized by the cells. Furthermore, if any of the potential substrates has been found to be oxidized by the cells, the effects of electron transport inhibitors, uncouplers and Fe^{3+} will be investigated trying to figure out the possible electron transport pathways.

Results

4.1. Oxidation of YE and CA by O₂ and Fe³⁺

L-cysteine was oxidized by *A. ferrooxidans* using the Fe²⁺ oxidation system as shown in Part I. The 19 standard amino acids at a concentration of 2 – 8 mM were tested by using 4.8 mg cells in Oxygraph (1.2 mL) but none showed an oxidation rate fast enough to carry out further detailed studies (data not shown). However, unknown compounds in yeast extract (YE) and casamino acids (CA), could be oxidized by this organism using O₂ as a terminal electron acceptor. The unknown compounds in 1% YE and 3% CA was quickly oxidized by the cells in Oxygraph (1.2 mL) consuming about 60 - 70 nmol and 30 – 40 nmol O₂, respectively and then the oxidation rates slowed down (Fig. 4-1). YE and CA could also be oxidized by the organism using Fe³⁺ as a terminal electron acceptor, and Fe³⁺ reduction by YE (1%) or CA (3%) in 4 mg cells in 1 mL reaction system finished in 10 min and produced the theoretical amount of Fe²⁺ corresponding to the amount of O₂ consumed in Oxygraph (200 - 250 nmol Fe²⁺ from 1% YE and 100 - 150 nmol Fe²⁺ from 3% CA) (data not shown). Detailed studies of Fe³⁺ reduction by YE and CA were not carried out due to (1) the nature of the oxidizable compounds in YE and CA is unknown; (2) the reaction was too fast (finished in 10 min) to be measured accurately; (3) the quantity of Fe²⁺ produced is small and higher concentrations of YE and CA would make the samples more turbid. Further studies of oxidation of YE and CA by O₂ have been carried out to figure out the possible electron transport pathway(s).

The rates in all experiments were calculated in the time periods of controls consuming 60 nmol O₂ for YE oxidation and 30 nmol O₂ for CA oxidation.

4.2. Effect of electron transport inhibitors

Table 4-1 and Figs. 4-1, 4-2, 4-3 show the effect of electron transport inhibitors on oxidation of YE and CA. Complex I inhibitors, 0.1 mM rotenone, 2 mM amytal and piericidin A, inhibited YE oxidation by 8 – 37% and CA oxidation by 23 – 48%, but 2 mM atabrine showed no effect. Inhibitors of complex III (bc_1 complex), 10 μ M antimycin A and 40 μ M myxothiazol, inhibited oxidation of YE and CA by 8 – 44%. HQNO, an inhibitor of complex III and quinol oxidase, showed a strong inhibition by up to 90% on oxidation of both YE and CA. Complex IV inhibitors, 2 mM KCN and 1 mM NaN_3 , strongly inhibited oxidation of YE and CA almost completely.

4.3. Effect of uncouplers and FeCl_3

Table 4-2 shows the effect of uncouplers on oxidation of YE and CA. CCCP at 0.5 μ M stimulated Fe^{2+} oxidation (see Part I) and at 10 μ M stimulated endogenous respiration (see Part II) but it inhibited oxidation of YE and CA at both concentrations. DNP at 20 μ M stimulated Fe^{2+} oxidation (see Part I) and at 30 μ M stimulated endogenous respiration (see Part II) but DNP at 20 μ M inhibited oxidation of YE and CA. The stimulation could be demonstrated when even lower concentrations of uncouplers were used. DNP at 0.5 μ M and 1 μ M showed stimulation on CA oxidation by 21% and 26%, respectively. Thus oxidations of YE and CA are more sensitive to inhibition by uncouplers than oxidation of Fe^{2+} or endogenous substrates.

FeCl_3 at 4 mM had no effect on oxidation of YE and CA (Fig. 4-4). The fast rate in the initial 1 min was due to the oxidation of Fe^{2+} contained in FeCl_3 stock solution.

4.4. Oxidation of YE and CA by spheroplasts and cell free extracts

Both YE and CA were not oxidized by cell free extracts (data not shown), but they were oxidized by spheroplasts (Fig. 4-5) with an activity of 50% of that of whole cells (Table 4-3).

Discussion and conclusions

The inhibition of YE and CA oxidations by rotenone, amytal and piericidin A but not by atabrine (Table 4-1 and Figs. 4-1) indicates the oxidation of the unknown compound(s) in YE or CA used an downhill electron transport pathway that starts at NDH-1_{down} (see Fig. 2-45), but did not use the Fe²⁺ oxidation system by directly reducing Fe³⁺ to Fe²⁺ on the cell surface (as in cysteine oxidation) as discussed in Part I. This is also supported by the observation that FeCl₃ showed no effect on the oxidation (Fig. 4-4).

That HQNO strongly inhibited the oxidation of YE and CA (Table 4-1 and Fig. 4-2) possibly suggests that (1) electrons from Q were transferred to quinol oxidases *bd* and *bo₃* and / or to *bc₁II* (see Fig. 2-45), and / or (2) electrons from YE or CA may be first transferred to an unknown dehydrogenase which is sensitive to the inhibition by HQNO. An example of such an enzyme in this organism is the thiosulfate-quinol reductase which was strongly inhibited by HQNO (Brasseur et al. 2004). Complex III inhibitors myxothiazol and antimycin A also showed partial inhibition on the oxidation of YE and CA (Table 4-1 and Fig. 4-2). This indicates that at least some electrons from Q were transferred to *bc₁II* but does not mean that all electrons went to *bc₁II*. Since the oxidation rates of YE and CA were 10 – 20 times faster than the endogenous oxidation rate, it is possible that the oxidation rates of YE and CA were very close to the maximal levels which could only be achieved by using both the fast pathway from Q to Fe³⁺ and the slow pathway from Q to *bc₁II*, similar to the situation in fructose oxidation.

Complex IV inhibitors KCN and NaN₃ strongly inhibited the oxidation of YE and CA (Table 4-1 and Fig. 4-3) indicating that the main portion of electrons was transferred through *aa₃* / *ba₃* to O₂ as shown in Fig. 2-45 and supporting the hypothesis that the

oxidation rates of YE and CA were close to the maximal and that the oxidation requires the fast Fe-containing pathway. This hypothesis is also supported by the high sensitivity of the oxidation to the inhibition by uncouplers (Table 4-2) and the decrease of oxidation rates by spheroplasts compared to the rates by the whole cells. An electron carrier system operating at maximal rates may be sensitive to a small change in proton concentration caused by uncouplers and also may be disrupted during the preparation of spheroplasts.

Since YE and CA contain L-cysteine (Cys) which can be oxidized by *A. ferrooxidans* using the Fe^{2+} oxidation system (see Part I), it was suspected that the oxidation of YE and CA was due to the oxidation of Cys. According to the amino acid composition of YE and CA reported by Farrell et al. (1993), YE and CA contain 1% and 0.07% Cys, respectively. Thus 1% YE and 3% CA contain 0.1 mM and 0.17 mM Cys, respectively. Although the rates and total oxygen consumption of the oxidation of 1% YE and 3% CA are close to the theoretical values based on the oxidation of Cys in 1% YE and 3% CA, the effects of Fe^{3+} and electron transport inhibitors on Cys oxidation and the oxidation of YE and CA are different (Table 4-4). Cys oxidation was greatly stimulated by Fe^{3+} , strongly inhibited by atabrine and not highly sensitive to the inhibition by rotenone, amytal and HQNO, while the oxidation of YE and CA was not affected by Fe^{3+} and atabrine but was more sensitive to the inhibition by rotenone, amytal and HQNO. These results indicate that the oxidation of YE and CA may not be due to the oxidation of Cys. The oxidation of YE and CA may be due to the oxidation of other unknown components instead of Cys. The concentrations of other amino acids are much higher than those of Cys in YE and Cys according to the calculation based on the data reported by Farrell et

al. (1993). For example, the concentrations of lysine (2.3 mM and 16.7 mM) are 20 and 100 times higher than the concentrations of Cys (0.1 mM and 0.17 mM) in 1% YE and 3% CA, respectively. So it is possible that other amino acids preferentially chelated the ferric iron on the cell surface of *A. ferrooxidans* before Cys had a chance to chelate it.

Therefore, the oxidation of YE and CA is similar to oxidation of endogenous substrates and fructose, in using the downhill electron transport pathways starting at NDH-1_{down} or NDH-2 as shown in Fig. 2-45. Furthermore an unknown HQNO-sensitive dehydrogenase may also be engaged in the reaction.

Tables of Part IV

Table 4-1. Effect of electron transport inhibitors on oxidation of YE and CA.

	Concentration	YE (1%) oxidation		CA (3%) oxidation	
		Rate *	R.A	Rate *	R.A
Effect of complex IV inhibitors					
Endogenous		0.65 ± 0.10	0.03	0.00 ± 0.00	0
Control		18.80 ± 0.81	1.00	15.26 ± 0.42	1.00
KCN	2 mM	1.20 ± 0.05	0.06	0.00 ± 0.00	0
NaN ₃	1 mM	2.58 ± 0.00	0.14	0.00 ± 0.00	0
Effect of complex I inhibitors					
Control		18.80 ± 0.81	1.00	15.26 ± 0.42	1.00
Atabrine (At)	2 mM	19.09 ± 0.23	1.02	14.89 ± 0.21	0.98
Rotenone (R)	0.1 mM	13.05 ± 0.78	0.69	10.18 ± 0.21	0.67
Amytal (Am)	2 mM	17.37 ± 0.70	0.92	11.12 ± 0.05	0.73
R + Am		11.93 ± 0.52	0.63	7.99 ± 0.05	0.52
Control		18.39 ± 0.47	1.00	11.43 ± 0.39	1.00
Piericidin A	0.5 μM	12.32 ± 0.76	0.67	8.80 ± 0.44	0.77
Effect of inhibitors of complex III and quinol oxidases					
Control		17.40 ± 0.81	1.00	15.34 ± 0.10	1.00
Antimycin A (An)	10 μM	13.85 ± 1.02	0.80	9.97 ± 0.31	0.65
Myxothiazol (My)	40 μM	15.94 ± 0.08	0.92	13.20 ± 0.36	0.86
An + My		12.84 ± 0.16	0.74	8.57 ± 0.31	0.56
HQNO (H)	4 μM	2.24 ± 0.81	0.13	2.94 ± 0.57	0.19
	40 μM	2.94 ± 0.63	0.17	1.15 ± 0.16	0.07

* Rate: nmol O₂ min⁻¹ (mg protein)⁻¹ (± SD, n = 2); R.A: relative activity, a ratio of a rate over that of control.

Table 4-2. Effect of uncouplers on oxidation of YE and CA.

Concentration		YE (1%) oxidation		CA (3%) oxidation	
		Rate *	R.A	Rate *	R.A
Control		18.39 ± 0.47	1.00	11.43 ± 0.39	1.00
CCCP	0.5 μM	16.38 ± 0.16	0.89	10.7 ± 0.26	0.94
	10 μM	10.08 ± 0.26	0.55	8.19 ± 0.13	0.72
DNP	20 μM	14.95 ± 0.76	0.81	10.78 ± 0.00	0.94
	0.1 mM	11.17 ± 0	0.61	8.70 ± 0.34	0.76
Control				13.98 ± 0.10	1.00
DNP	0.5 μM			16.93 ± 1.85	1.21
	1 μM			17.58 ± 0.91	1.26

* Rate: $\text{nmol O}_2 \text{ min}^{-1} (\text{mg protein})^{-1}$ (\pm SD, $n = 2$); R.A: relative activity, a ratio of a rate over that of control.

Table 4-3. Comparison of the rates of oxidation of YE and CA by spheroplasts and whole cells.

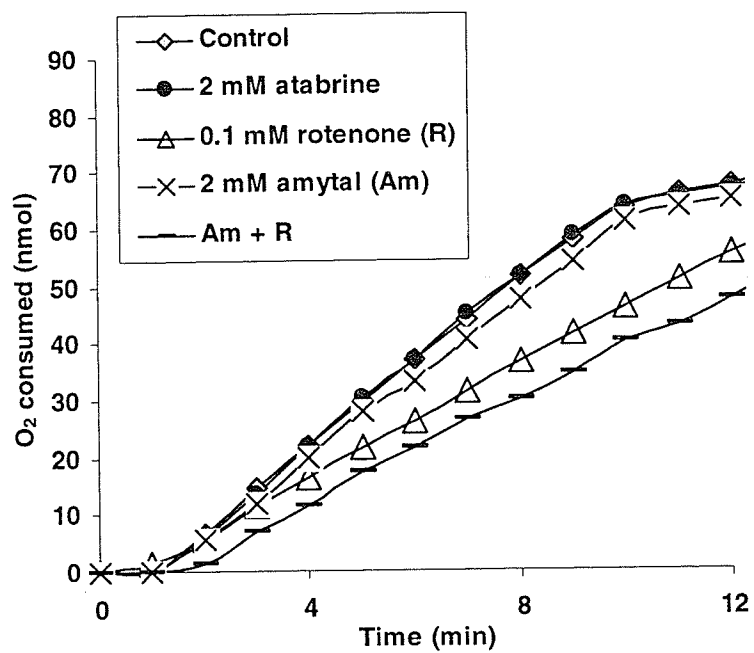
	Rate: $\text{nmol O}_2 \text{ min}^{-1} (\text{mg protein})^{-1}$ (\pm SD, $n = 2$)		Rs / Rc
	Cells (Rc)	Spheroplasts (Rs)	
Endogenous	0.89 ± 0.03	0.90 ± 0.04	1.00
YE (1%)	18.01 ± 1.03	9.22 ± 0.78	0.51
CA (3%)	14.86 ± 0.76	7.84 ± 0.00	0.53

Table 4-4. Summary of the oxidation of 2 mM Cys, 1% YE and 3% CA by *A. ferrooxidans*. *

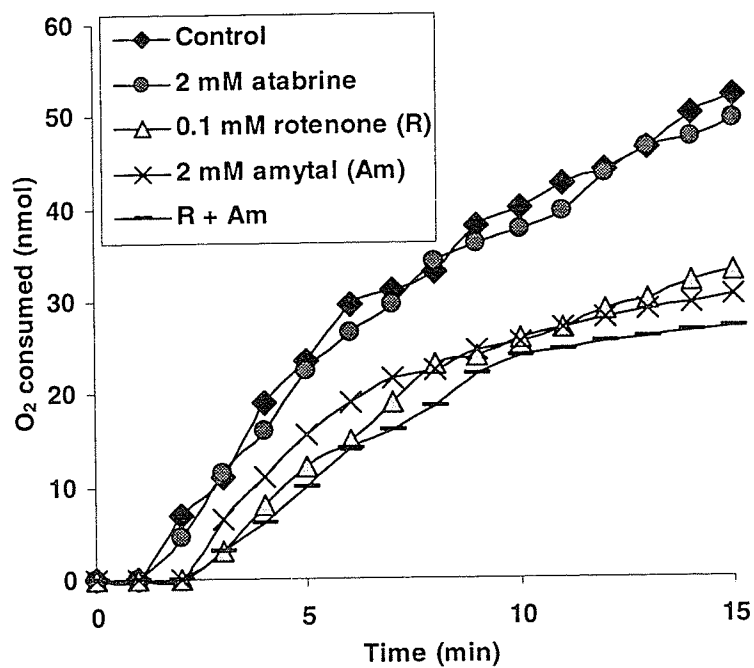
	2 mM Cys	1% YE	3% CA
Cys contained		0.1 mM	0.17 mM
Rate **	300	20	15
O ₂ (nmol) in 1.2 mL **	>310	60-70	30-40
Rate ***		15	26
O ₂ (nmol) in 1.2 mL***		30	51
Inhibition (%) by electron transport inhibitors			
R (0.1 mM rotenone)	5	31	33
Am (2 mM amytal)	11 (1mM Am)	8	27
R+Am	10	37	48
0.4 mM atabrine	63		
2 mM atabrine	85	0	2
0.5 μM piericidin A	2	33	23
An (10 μM antimycin A)	12	20	35
My (40 μM myxothiazol)	24	8	24
An+My		26	44
4 μM HQNO		87	81
40 μM HQNO	30	83	93
An + My + 40 μM HQNO	39		
Stimulation (%) by FeCl ₃			
1 mM FeCl ₃	370		
4 mM FeCl ₃	340	No effect	No effect
O ₂ consumption (nmol) within 1 min in 1.2 mL (4.8 mg cells were used)			
4 mM FeCl₃	62 (0.2 mM Cys)	0	0

*Rate (nmol O₂ min⁻¹ (mg of protein)⁻¹) and some data are taken from Part I; ** Experimental data; *** Theoretical data based on Cys oxidation.

Figures of Part IV

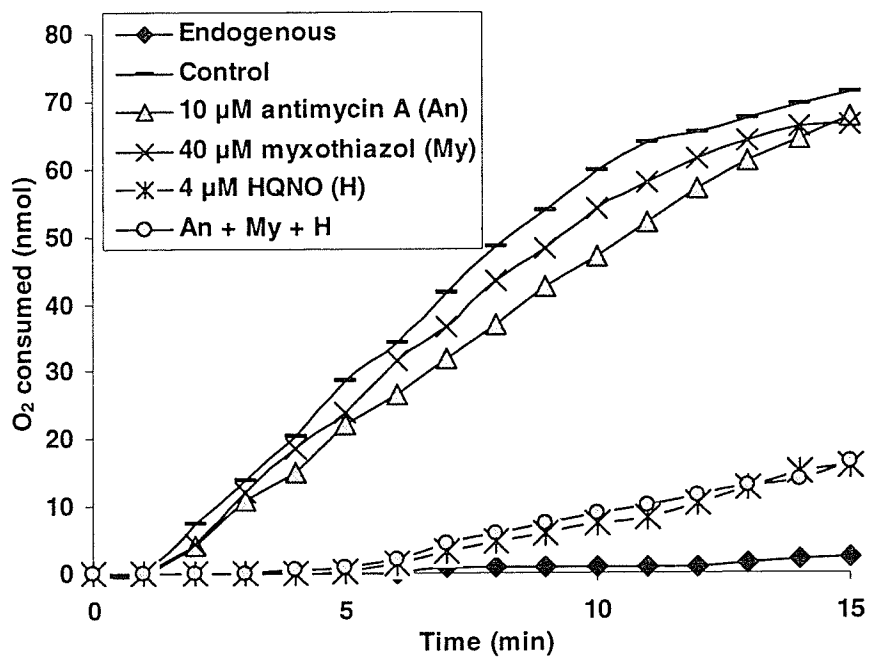


(a)

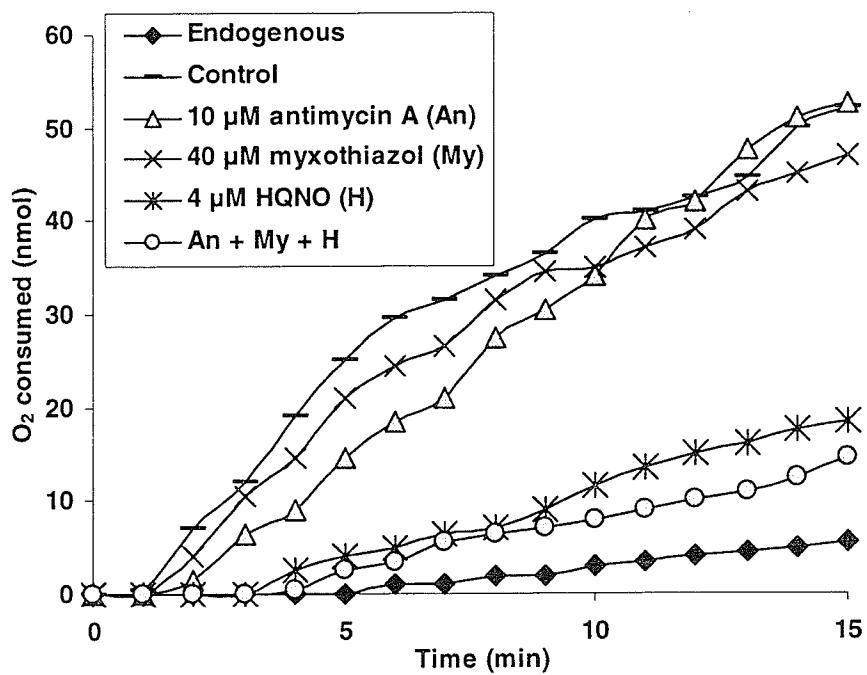


(b)

Fig. 4-1. Effect of complex I inhibitors on oxidation of YE (1%, a) and CA (3%, b).

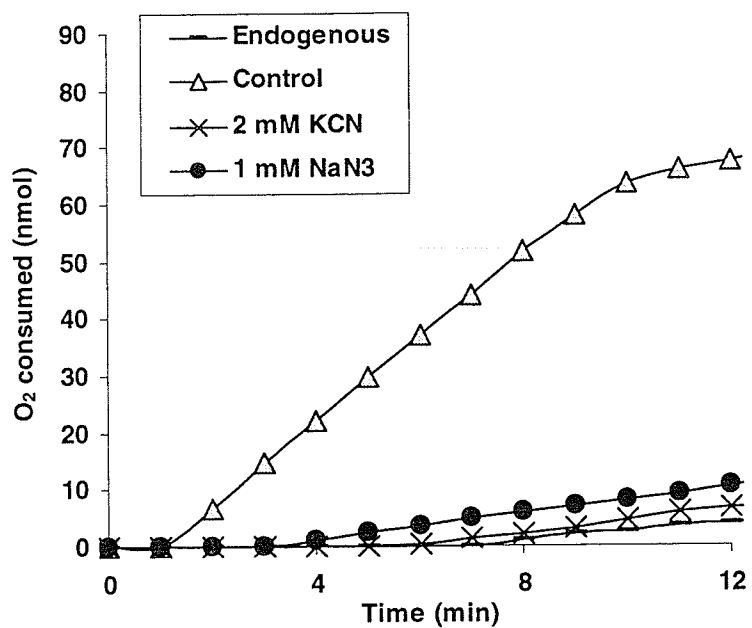


(a)

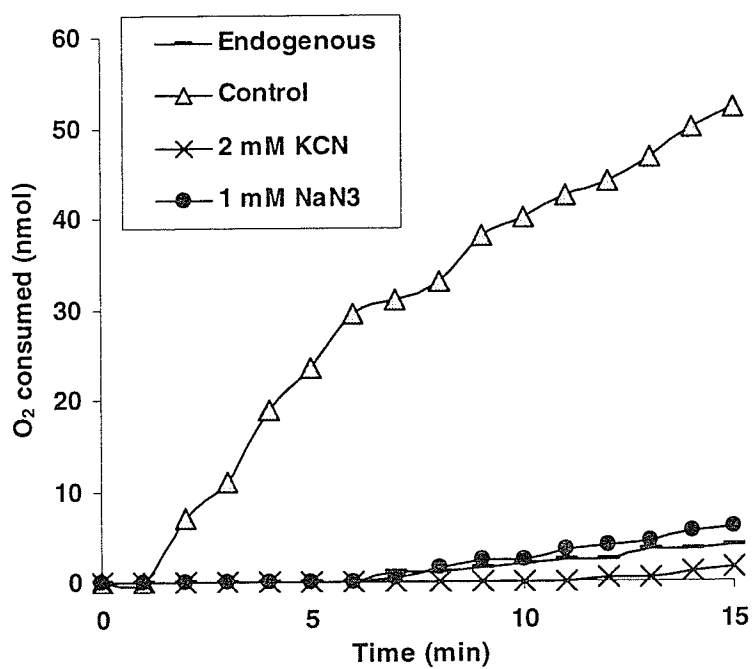


(b)

Fig. 4-2. Effect of complex III inhibitors on oxidation of YE (1%, a) and CA (3%, b).

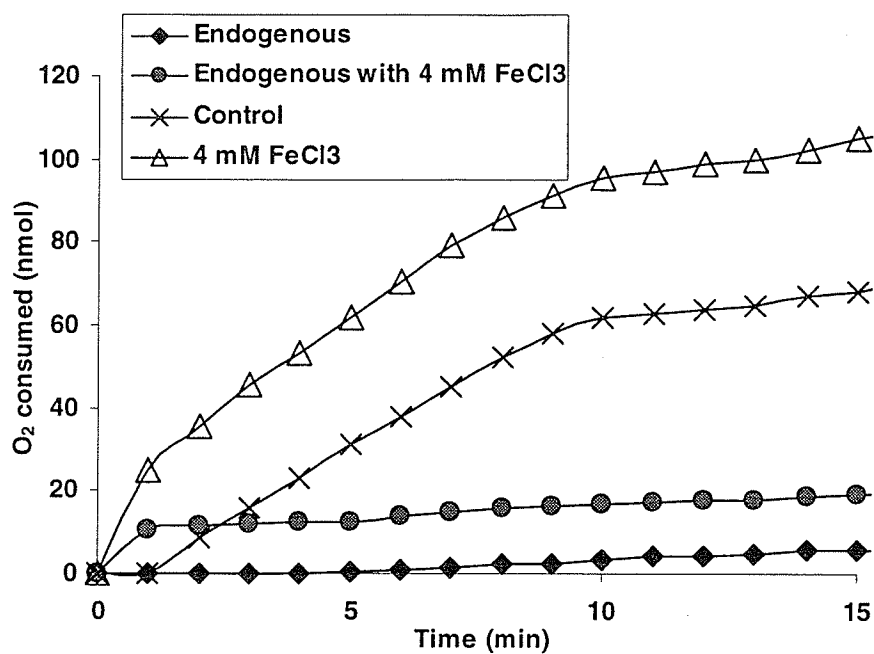


(a)

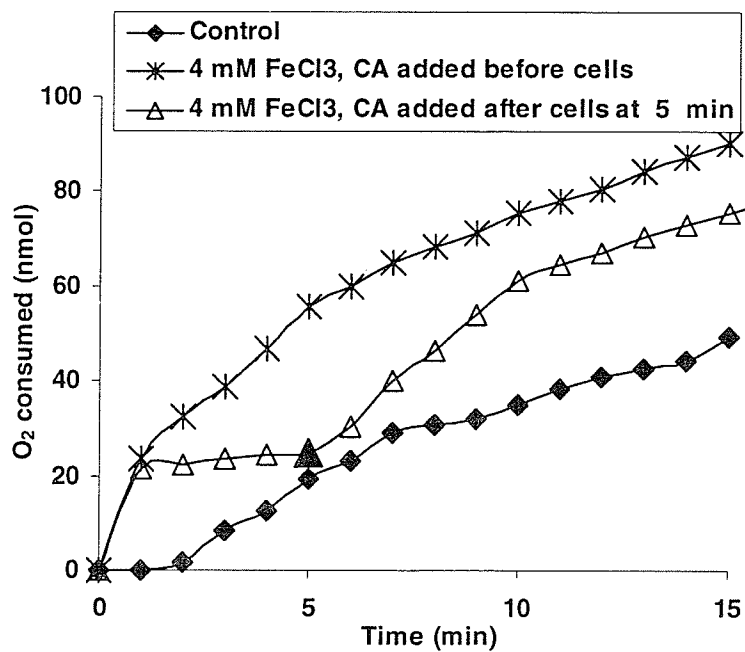


(b)

Fig. 4-3. Effect of complex IV inhibitors on oxidation of YE (1%, a) and CA (3%, b).



(a)



(b)

Fig. 4-4. Effect of FeCl₃ on oxidation of YE (1%, a) and CA (3%, b).

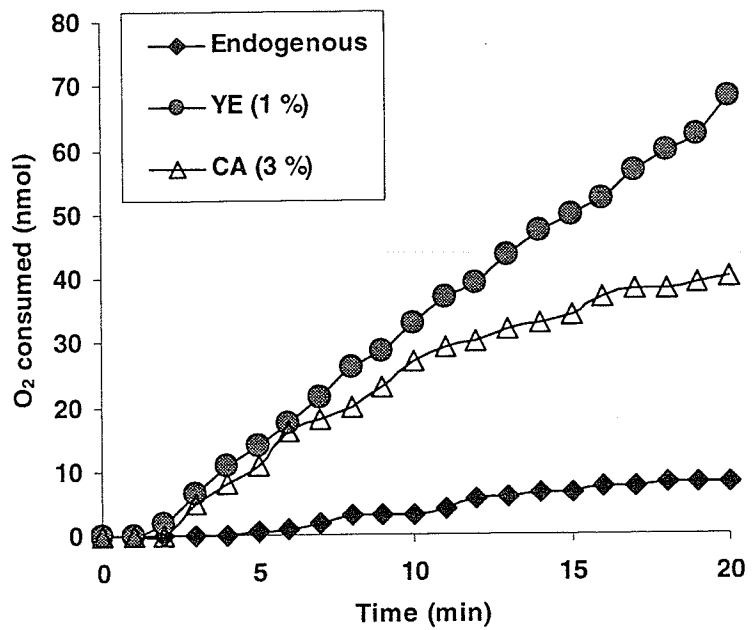


Fig. 4-5. Oxidation of YE and CA by spheroplasts. Spheroplasts (4.8 mg) was added to start the reaction.

Part V

Oxidation of Formic Acid

Abstract

Different electron transport inhibitors and uncouplers have been tested for formic acid oxidation by O_2 and Fe^{3+} in *A. ferrooxidans*. Complex I inhibitors rotenone and piericidin A only partially inhibited formic acid oxidation but atabrine and amytal had no effect. Complex III inhibitors antimycin A and myxothiazol also partially inhibited it but HQNO, an inhibitor of both complex III and quinol oxidases, inhibited it by about 90% even at low concentrations. Complex IV inhibitors KCN and NaN_3 showed much less inhibition on formic acid oxidation than on Fe^{2+} oxidation at low concentrations, but inhibited formic acid oxidation nearly completely at 1 mM. The inhibitors of plant alternative oxidase, SHAM and propyl gallate which are iron chelators, inhibited formic acid oxidation by 30 – 70%, but other iron chelators had no effect. Uncouplers CCCP and DNP only inhibited O_2 reduction but 0.5 μ M DNP 20 nM CCCP stimulated Fe^{3+} reduction for the first 10 min. Possible electron transport pathways for oxidation of formic acid were proposed and the effects of uncouplers were explained.

Introduction

It has been reported that *A. ferrooxidans* could grow on formic acid aerobically by using O₂ as a terminal electron acceptor (Ponk et al. 1991b) and anaerobically by using Fe³⁺ as a terminal electron acceptor (Ponk et al. 1991a). However, the electron transport pathways for oxidation of formic acid are still unknown in this organism.

Formate oxidation is catalyzed by a formate dehydrogenase (FDH) producing CO₂ and 2H. FDHs have been found in bacteria, fungi, mammals as well as in plants and are involved in cell respiration under various environmental conditions (de Bok et al. 2003; Ferry 1990; Oro and Rappoport 1959; Overkamp et al. 2002; Hourton-Cabassa et al. 1998; Sawers 1994).

Under aerobic conditions in aerobic organisms, formate is mainly oxidized by the NAD⁺-dependent oxygen-insensitive FDHs while under anaerobic conditions, formate is oxidized by NAD⁺-independent oxygen-sensitive FDHs (de Bok et al. 2003; Ferry 1990; Oh and Bowien 1998). The NAD⁺-dependent FDHs do not contain metals and cofactors. The NAD⁺-independent FDHs contain molybdenum or tungsten cofactors and iron sulfur centers.

Among prokaryotes, *E. coli* which is a proteobacterium as *A. ferrooxidans*, is the organism whose FDHs have been studied most extensively. There are three types of FDHs in *E. coli* including FDH-N, FDH-O and FDH-H (Benoit et al. 1998; Boyington et al. 1997; Jormakka et al. 2002; Jormakka et al. 2003; Søballe and Poole 1999). Both FDH-N and FDH-O contain molybdenum, heme and non-heme iron, *bis*-molybdenum guanine dinucleotide (*bis*-MGD) cofactors and intrinsic selenocysteine (SeCys). They contain three subunits (α , β , γ) and the corresponding subunits from these two enzymes

have 45 – 75% identity. Their γ -subunits are the transmembrane segments and contain heme b groups which can bind the inhibitor HQNO. The α - and β -subunits are located in the periplasm in FDH-N but in the cytoplasm in FDH-O. FDH-N is expressed in anaerobic conditions when nitrate is available and is also a part of a respiratory chain by reducing menaquinone (MQ) to menaquinol (MQH₂) which then reduces nitrate to nitrite. FDH-O is mainly expressed under aerobic conditions and is slightly induced by nitrate under anaerobic conditions. It is also a part of a respiratory chain by reducing ubiquinone (UQ) to ubiquinol (UQH₂) which then reduces nitrate to nitrite. FDH-H is expressed during fermentative growth and is a part of the hydrogen lyase complex which decomposes formate to CO₂ and H₂. It is a membrane-bound but cytoplasmically-oriented enzyme with a four-domain $\alpha\beta$ -structure containing SeCys, a Fe₄S₄ cluster, molybdenum, two *bis*-MGD cofactors.

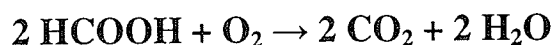
The FDH(s) in *A. ferrooxidans* has not been characterized but formate oxidation by the cell extracts of formate-grown cells was found to be NAD(P)⁺ independent (Pronk et al. 1991*b*).

In this study, different electron transport inhibitors and uncouplers have been studied on oxidation of formic acid by O₂ and Fe³⁺ trying to build the possible electron transport pathways for formate oxidation in *A. ferrooxidans*.

Results

5.1. Oxidation of formic acid at different concentrations

Fig. 5-1 shows the oxidation of formic acid at different concentrations. The oxidation rate of formic acid reached the maximum of approximately $20 \text{ nmol O}_2 \text{ min}^{-1} (\text{mg protein})^{-1}$ at 0.1 mM formic acid when O_2 was used as the terminal electron acceptor, and of $33 \text{ nmol Fe}^{2+} \text{ min}^{-1} (\text{mg protein})^{-1}$ at 5 mM formic acid when Fe^{3+} was used as the terminal electron acceptor and cytochrome *c* oxidase was inhibited by 2 mM KCN. Higher concentrations of formic acid became inhibitory. The maximal rate of Fe^{3+} reduction in terms of electrons transferred was less than 50% of that of O_2 reduction. The amount of Fe^{2+} produced during Fe^{3+} reduction never reached the stoichiometric values based on the calculation of the complete oxidation of formic acids to CO_2 (Fig. 5-1). However, the oxidation of 0.1 mM formic acid (120 nmol) in Oxygraph (1.2 mL) consumed 60 nmol O_2 (Fig. 5-3a). This agrees with the stoichiometry of formic acid oxidation following reaction 9.



Reaction 9. Oxidation of formic acid by O_2 in *A. ferrooxidans*.

Substrate inhibition at high concentrations of formic acid was expected because of known toxic effects of formic acid to this acidophilic bacterium (Ingledew 1982; Pronk et al. 1991*b*), but the shift in the optimal formate concentration from 0.1 mM to 5 mM when O_2 was replaced with Fe^{3+} as electron acceptor (Fig. 5-1) was unexpected. Formate-grown cells (Pronk et al. 1991*a*) in the presence of 0.1 mM formate reduced 0.2 mM Fe^{3+} anaerobically while aerobically in 10 μM azide reduced less than 0.1 mM

Fe^{3+} and more slowly. Since no anaerobic experiments have been carried out in this study, the reasons for the unexpected results in Fig. 5-1 are unknown.

5.2. Effect of uncouplers

CCCP and DNP inhibited only the formic acid oxidation by O_2 , even at the concentrations lower than those stimulating Fe^{2+} oxidation (Table 5-1). CCCP and DNP also inhibited formic acid oxidation by Fe^{3+} , but the inhibition was not as strong and 20 nM CCCP and 0.5 μM DNP stimulated the oxidation in the initial 10 min by 13% and 93%, respectively (Fig. 5-2).

5.3. Effect of complex I inhibitors

Table 5-2 and Fig. 5-3 show the effect of complex I inhibitors on formic acid oxidation by O_2 and Fe^{3+} . Atabrine had no effect on O_2 reduction and amytal had no effect on both O_2 and Fe^{3+} reduction. Formic acid oxidation was inhibited by rotenone and piericidin A but the oxidation was less sensitive to the inhibition than the oxidation of endogenous substrates and fructose (see Part II and III). Rotenone at 0.1 mM and 0.5 mM inhibited formic acid oxidation by O_2 by 34% and 48%, respectively and inhibited the oxidation by Fe^{3+} by 27% and 41%, respectively. Piericidin A at 0.5 μM and 2.5 μM inhibited the O_2 reduction by 11% and 26%, respectively and inhibited the Fe^{3+} reduction by 10% and 27%, respectively. This inhibition pattern is different from that of Fe^{2+} oxidation, oxidation of endogenous substrates, fructose, YE or CA (Table 5-3). Formic acid oxidation is different from the oxidation of Fe^{2+} and the compounds interacting with iron (as shown in Part I) also in the combined effect of atabrine and

CCCP. Combination of 2 mM atabrine and 10 μ M CCCP had a similar inhibitory effect as 10 μ M CCCP alone (Fig. 5-4). It should be mentioned that formate dehydrogenase in this organism is NAD(P)⁺-independent (Pronk et al. 1991b).

5.4. Effect of inhibitors of complex III and quinol oxidase

Table 5-4 and Fig. 5-5 show the effect of the inhibitors of complex III and quinol oxidase on formic acid oxidation by O₂ and Fe³⁺. Antimycin A at 0.1 mM and 80 μ M myxothiazol, inhibited O₂ reduction and Fe³⁺ reduction by 15 – 18%, respectively (Table 5-4). HQNO, an inhibitor of complex III and quinol oxidase, showed strong inhibition on O₂ and Fe³⁺ reduction even at low concentrations. HQNO at 4 μ M inhibited O₂ and Fe³⁺ reduction by 86% and 78%, respectively. HQNO is an inhibitor of sulfide or thiosulfate quinone reductase of *A. ferrooxidans* (Brasseur et al. 2004) and heme *b*-containing formate dehydrogenase of *E. coli* (Benoit et al. 1998; Jormakka et al. 2002; Jormakka et al. 2003). The response of formic acid oxidation to inhibitors of complex III and quinol oxidase is similar to oxidation of Fe²⁺, YE and CA (inhibited by the inhibitors, although Fe²⁺ oxidation was less sensitive to inhibition) but different from oxidation of endogenous substrates and fructose (not inhibited by the inhibitors).

5.5. Effect of complex IV inhibitors

A detailed study of complex IV inhibitors KCN and NaN₃ inhibition of 0.1 mM HCOOH oxidation by 2.4 mg cells at changing inhibitor concentrations is shown in Fig. 5-6. It is obvious that KCN inhibition was progressive with time at 0.1 and 0.2 mM while NaN₃ inhibited the oxidation instantly and then some activity recovered. Similar

inhibition patterns by KCN and NaN_3 were obtained for Fe^{2+} oxidation also when the reaction was started with addition of cells (see Part I, Figs. 1-7 & 1-8). KCN at 50 μM and 0.1 mM showed progressive inhibition while NaN_3 inhibition was instant and then some activity recovered. As mentioned in Part I, the pattern of KCN inhibition is possibly due to the time-dependent penetration of cyanide anion into the cells and the pattern of NaN_3 inhibition may be due to the instant inhibition of ATP synthase followed by the weak acid effect of NaN_3 . Fe^{2+} oxidation, however, was much more sensitive to KCN and NaN_3 inhibition than formate oxidation. For example, 50 μM KCN inhibited Fe^{2+} oxidation by 97%, but formate oxidation only by 28% and 5 μM NaN_3 inhibited Fe^{2+} oxidation by 92%, but formate oxidation only by 11%. This difference is understandable since the rate of Fe^{2+} oxidation is around 50 times faster than formate oxidation. If the same cytochrome oxidase is used for both oxidations formate oxidation theoretically was only 2% of the cytochrome oxidase activity used for Fe^{2+} oxidation.

When the cell concentration was increased by 10-fold from 2.4 mg to 24 mg cells and the formate concentration was increased by 5-fold to 0.5 mM the rate of oxidation was around 10-fold (Fig. 5-7). KCN at 2 mM inhibited the oxidation by 97%, but the remaining activity was still higher than endogenous respiration, perhaps due to electrons flowing to KCN insensitive oxidases.

5.6. Effect of iron chelators

In the presence of 4 mM FeCl_3 the rate of formate oxidation slowed down initially and then became faster (Figs. 5-8 & 5-9), but the addition of 4 mM FeCl_3 stopped the

residual activity in the presence of 2 mM KCN (Fig. 5-7). The inhibitors of plant alternative oxidases, SHAM and PG which are iron chelators (Siedow and Bickett 1981), also inhibited formate oxidation. SHAM at 2 mM inhibited it by 70% when either 2.4 mg cells (Fig. 5-8) or 24 mg cells (Fig. 5-7) were used. PG at 2 mM inhibited formate oxidation by 30% although 2 mM PG alone was oxidized by cells (see Part I) with an O_2 consumption rate of 85% of that of control formate oxidation (Fig. 5-10). Other iron chelators, 4 mM tiron (Fig. 5-8), 8 mM EDTA and 0.44 mM o-phenanthroline (data not shown), had no effect. The effects of Fe^{3+} , SHAM and PG will be interpreted later.

5.7. Oxidation of formic acid by spheroplasts and cell free extracts

Formic acid was not oxidized by cell free extracts at pH 3.5 and 6.5 (data not shown), but it was oxidized by spheroplasts with an activity ($9.06 \pm 0.36 \text{ nmol } O_2 \text{ min}^{-1} (\text{mg protein})^{-1}$) or 34% of the activity by whole cells ($26.57 \pm 3.11 \text{ nmol } O_2 \text{ min}^{-1} (\text{mg protein})^{-1}$).

Discussion and conclusions

Formic acid was oxidized by *A. ferrooxidans* (Fig. 5-1) with a maximal rate at 0.1 mM when O₂ was used as the terminal electron acceptor and a maximal rate at 5 mM when Fe³⁺ was used as the terminal electron acceptor. Higher concentrations of formic acid became inhibitory. The substrate inhibition at high concentrations of formate was also reported by Pronk et al. (1991b) who also showed that the maximal O₂ reduction rate was achieved by 0.1 mM formate. The reason for the substrate inhibition of formate oxidation was due to the toxicity of organic acids (Pronk et al. 1991b). The formate concentration required for maximal Fe³⁺ reduction rate was 50-times of the concentration for the maximal O₂ reduction rate. This was unexpected since substrate inhibition was applied to both O₂ and Fe³⁺ reduction. Furthermore, the amount of Fe²⁺ produced from Fe³⁺ reduction was much less than the theoretical stoichiometric values (Fig 5-1b) based on the calculation of the complete oxidation of formic acid to CO₂. This agrees with the report by Pronk et al. (1991a) that in the presence of 10 μM NaN₃ the aerobic reduction of Fe³⁺ did not produce the stoichiometric amounts of Fe²⁺. However, the authors demonstrated that in the absence and presence of 10 μM NaN₃ Fe³⁺ reduction by formate showed stoichiometric amounts of Fe²⁺ under anaerobic conditions. Therefore, the presence of O₂ may interfere with the Fe³⁺ reduction by formate.

Complex I inhibitor atabrine had no effect on formate oxidation (Table 5-2) and the combination of 2 mM atabrine and 0.5 μM CCCP did not produce higher inhibition than CCCP alone (Fig 5-4). This indicates that formate oxidation is different from the oxidation of Fe²⁺ and the compounds interacting with iron (see Part I). Complex I inhibitors 0.1 mM rotenone and 0.5 μM piericidin A showed less inhibition on formate

oxidation than on endogenous and fructose oxidation while amytal had no effect on formate oxidation but significantly inhibited endogenous and fructose oxidation (Table 5-3), suggesting that complex I may not be involved in formate oxidation. This is in agreement with the finding that formate oxidation by cell extracts of this organism was NAD(P)⁺-independent (Pronk et al. 1991b). Since it is well known that some electron transport inhibitors are not specific and can inhibit more than one enzyme, one possibility for the partial inhibition of formate oxidation by rotenone and piericidin A was the inhibition of formate dehydrogenase (FDH). However, the FDH(s) in *A.ferrooxidans* has not been isolated and its genes have not been identified and cloned although the ability of this organism in growing on formate (Pronk et al. 1991a, 1991b) and oxidizing formate by iron-grown cells indicates the existence of FDH(s) in this organism. Preliminary bioinformatics searches of the partial genome sequence of *A.ferrooxidans* only identify the genes coding for the subunits of formate hydrogenlyase and formate dependant nitrate reductase (data not shown). The identification of formate hydrogenlyase agrees with the possession of hydrogenase and the ability of growth on H₂ by this organism (Drobner et al.1990). The amino acid sequences of the subunits of formate hydrogenlyase have high similarities to the amino acid sequences of the subunits of NDH-1s in this organism (data not shown) indicating that the hydrogenlyase may have the binding sites for rotenone and Piericidin A. Since formate hydrogenlyase directly oxidizes formate to CO₂ and H₂ and is not supposed to be a part of an electron transport chain, it is unknown if *A. ferrooxidans* uses the same enzyme in the course of O₂ and Fe³⁺ reduction by formate.

The identification of the gene coding for the formate-dependent nitrate reductase in this organism (data not shown) indicates the existence of the FDH-O like enzyme which could directly transfer electrons to ubiquinone pool, similar to the case in *E. coli* (see "Introduction"). Although not proved, it is possible that the FDH-O in *A. ferrooxidans* shares similarities with NDH-1s and so has rotenone and piericidin A binding sites. The difficulty in identifying the FDH-O and other types of FDHs may be due to the poor similarities of these enzymes in this organism with the known FDHs in other organism or due to the incompleteness of the genome information in this organism.

The growth on formate is still considered to be autotrophic growth in *A. ferrooxidans*. If formate was oxidized by donating electrons to FDH to ubiquinone / ubiquinol pool (Q) and finally to O_2 or Fe^{3+} , the reducing power (NADH) for CO_2 fixation must be produced via an uphill reaction from Q to NDH-1_{up} to NAD^+ since the FDH involved in O_2 or Fe^{3+} reduction was indicated to be $NAD(P)^+$ - independent in this organism (Pronk et al. 1991b). This seems to be contradictory with the results that atabrine and amytal inhibited the uphill reaction during Fe^{2+} oxidation (see Part I and Elbehti et al. 2000) but had no effect on formate oxidation (Table 5-2 and Fig. 5-4). The lack of inhibition of formate oxidation by atabrine and amytal may be due to that even smaller proportion of electrons flowed along the uphill reaction (NAD^+ reduction) compared to the case in Fe^{2+} oxidation. The rate of formate oxidation, similar to the rate of GSH and PG oxidation (See Part I), was 50 times slower than the rate of Fe^{2+} oxidation. As discussed in Part I, when the reaction rate is slow, the proportion of electrons going to the uphill reaction would be smaller and so less inhibition by complex I inhibitors would be expected. In fact, formate oxidation (Table 5-2), similar to the

oxidation of GSH and PG (Table 1-26), was not inhibited by amytal. The inhibition of atabrine on the oxidation of GSH and PG was due to other effect of atabrine on Fe^{2+} oxidation other than inhibiting NDH-1. The high sensitivity of formate oxidation to the inhibition by uncouplers DNP and CCCP (Table 5-1 and Fig. 5-2) may also indicate the involvement of the uphill reaction which requires Δp or the fact that formic acid already uncoupled the cells (pKa value of HCOOH is 3.8).

Complex III inhibitors antimycin A and myxothiazol partially inhibited formate oxidation by 15% (Table 5-4) indicating the involvement of complex III ($bc_1\text{II}$) during the oxidation. HQNO, an inhibitor of complex III and quinol oxidase, inhibited formate oxidation by 90% at a low concentration of 4 μM using O_2 or Fe^{3+} as the terminal electron acceptor (Table 5-4 and Fig. 5-5). The strong inhibition of formate oxidation by HQNO, different from the great stimulation of endogenous oxidation by HQNO, is most likely due to the inhibition of FDH especially considering that Fe^{3+} reduction by formate was almost completely inhibited by 10 μM HQNO (Table 5-4 and Fig. 5-5b). In *E. coli*, the anaerobically functioned FDH-N contains heme *b* and has been shown to have HQNO binding site and the aerobically functioned FDH-O also contains heme *b* and is supposed to be inhibited by HQNO (see "Introduction"). It is quite possible that the putative FDH-O in *A. ferrooxidans* also contains heme *b* and could be inhibited by HQNO. The effect of HQNO on formate oxidation may also suggest the involvement of $bc_1\text{II}$ and quinol oxidases *bd* and *l* or bo_3 since the strong inhibition of formate oxidation by HQNO in both O_2 and Fe^{3+} reduction occurred initially and then some activity recovered (Fig. 5-5). The later-time activity recovery is perhaps caused by the shift of

electrons to the pathway from Q to Fe^{3+} after $bc_1\text{II}$ and quinol oxidases bd and bo_3 have been inhibited by HQNO (see Fig. 2-45).

When 2.4 mg cells were used, complex IV inhibitors KCN and NaN_3 at low concentration showed less inhibition on formate oxidation (Fig. 5-6) than on Fe^{2+} oxidation (Figs. 1-7 & 1-8). This may be because of the remaining activity of cytochrome c oxidase (aa_3 / ba_3) after inhibition by low concentrations of KCN or NaN_3 still performing a substantial oxidation of formate. However, KCN and NaN_3 at 1 mM almost completely inhibited formate oxidation when 2.4 mg cells were used (Fig. 5-6). This may be interpreted by the inhibition of both cytochrome c oxidase and FDH by KCN and NaN_3 since it was reported that the FDH of *Pseudomonas oxalaticus* was inhibited by KCN and NaN_3 (Quayle 1966) although there is no available direct evidence showing KCN and NaN_3 inhibition of the FDH(s) in *A. ferrooxidans*. When 24 mg cells were used, 2 mM KCN inhibited the oxidation of 0.5 mM formic acid by 97% with the remained activity higher than the endogenous oxidation activity (Fig. 5-7) suggesting the shift of electrons to the oxidases other than cytochrome c oxidase (see Fig. 2-45).

FeCl_3 at 4 mM strongly inhibited the activity in the presence of 2 mM KCN and 0.5 mM formic acid (Fig. 5-7) indicating that electrons were preferentially transferred to Fe^{3+} making the oxidation more sensitive to KCN inhibition. In the presence of 4 mM Fe^{3+} , the O_2 consumption rate during formate oxidation was slow initially and then increased (Figs. 5-8 & 5-9) although stoichiometry for 0.5 O_2 per formate was maintained (Fig. 5-9). Formate at 5 mM showed a substrate inhibition with a reduced rate of O_2 consumption and a more pronounced inhibition by 4 mM Fe^{3+} (Fig. 5-9b). The

time course of O_2 consumption suggests again that formic acid is perhaps oxidized by Fe^{3+} preferentially and Fe^{2+} formed is oxidized by O_2 under these conditions. These conditions are similar to the conditions used in Fe^{3+} reduction experiments in Fig. 5-1 where Fe^{3+} reduction rate by formate was optimal. One plausible explanation for the “slow-fast” oxidation pattern of formate oxidation in the presence of Fe^{3+} (Fig. 5-9) and the slow reduction of Fe^{3+} by formate (Fig. 5-1) may be due to the change of the midpoint redox potential from +0.77 V (Fe^{3+} / Fe^{2+} couple) to +0.67 V ($HCOOFe^{2+} / Fe^{2+}$) caused by the chelation of formate to Fe^{3+} . However, the small decrease (0.10 V) of the midpoint redox potential may have not led to the dramatic effect of formate oxidation by Fe^{3+} . The dramatic effect is perhaps accounted for by the interference of O_2 with the stepwise oxidation of $HCOOH$ to CO_2 with Fe^{3+} when Fe^{2+} oxidation is inhibited as in Fig. 5-1 since aerobically the reduction of Fe^{3+} by formate is slow and non-stoichiometric compared to the anaerobic reduction of Fe^{3+} (Pronk et al 1991a).

Inhibition of formate oxidation by the inhibitors of plant AOX (alternative oxidase), SHAM and PG, (Figs. 5-7 & 5-10) raises again the possibility of AOX involvement or the inhibition of bc_1II and quinol oxidases bd and bo_3 by SHAM and PG as discussed in endogenous respiration (Part II). It is also possible that SHAM and PG could inhibit the putative FDH-O in *A. ferrooxidans* by binding to the non-heme iron of FDH-O as it was reported that the FDH-N and FDH-O contain non-heme iron in *E. coli* (see “Introduction”).

The lower activity of formate oxidation by spheroplasts compared to the activity by whole cells may be due to the damage or disorganization of electron transport enzymes

or the loss of periplasmic content during the preparation of spheroplasts as discussed in the previous parts.

According to the above discussion and the results, a possible model for the electron transport pathways of formate oxidation in *A. ferrooxidans* is shown in Fig. 5-11. It was proposed that during formate oxidation, electrons are transferred to Q and then mainly go through the same pathways as used for endogenous oxidation and a portion of electrons released would go to the uphill pathway from Q to NDH-1_{up} to reduce NAD⁺.

Tables of Part V

Table 5-1. Effect of uncouplers on oxidation of formic acid by O₂.

	Concentration	Rate *	R.A
Control		23.75 ± 0.73	1.00
DNP	0.1 μM	22.71 ± 0.47	0.96
	0.2 μM	22.76 ± 0.00	0.96
	0.5 μM	21.67 ± 0.05	0.91
	1 μM	21.15 ± 0.16	0.89
	5 μM	18.39 ± 0.26	0.77
	10 μM	16.35 ± 0.26	0.69
	20 μM	13.39 ± 0.42	0.56
	Control		23.44 ± 0.52
CCCP	1 nM	23.44 ± 1.15	1.00
	2 nM	22.55 ± 0.21	0.96
	5 nM	22.40 ± 0.31	0.96
	10 nM	22.19 ± 0.21	0.95
	20 nM	22.14 ± 0.16	0.94
	50 nM	21.67 ± 0.21	0.92
	0.1 μM	21.46 ± 0.21	0.92
	0.2 μM	20.47 ± 0.05	0.87
	0.5 μM	18.44 ± 0.05	0.79
	1 μM	16.56 ± 0.21	0.71
	5 μM	7.71 ± 0.36	0.33

* Rate: nmol O₂ min⁻¹ (mg protein)⁻¹; R.A: relative activity, a ratio of a rate over that of control.

Table 5-2. Effect of complex I inhibitors on formic acid oxidation.

		Oxidation by O ₂		Oxidation by Fe ³⁺	
	Concentration	Rate *	R.A	Rate **	R.A
Control		23.28 ± 0.45	1.00	33.72 ± 0.25	1.00
Rotenone	10 μM	20.47 ± 0.36	0.88		
	50 μM	17.5 ± 0.57	0.75		
	0.1 mM	15.42 ± 0.63	0.66	24.63 ± 3.44	0.73
	0.5 mM	12.03 ± 0.10	0.52	20.01 ± 1.63	0.59
Control		24.32 ± 0.47	1.00	33.75 ± 3.51	1.00
Amytal	0.1 mM	24.69 ± 0.05	1.02		
	0.5 mM	24.27 ± 0.52	1.00		
	1mM	24.58 ± 0.89	1.01		
	2 mM	23.23 ± 0.31	0.96	33.38 ± 3.80	0.99
Control		21.15 ± 0.21	1.00		
Atabrine	0.1 mM	20.99 ± 0.31	0.99		
	1mM	20.42 ± 0.31	0.97		
	2 mM	20.83 ± 0.78	0.98		
Control	0 μM	26.67 ± 0.31	1.00	33.75 ± 3.51	1.00
Piericidin A	0.5 μM	23.70 ± 0.00	0.89	30.32 ± 2.52	0.90
	2.5 μM	19.69 ± 0.63	0.74		

* Rate: nmol O₂ min⁻¹ (mg protein)⁻¹; ** Rate: nmol Fe²⁺ min⁻¹ (mg protein)⁻¹; R.A: relative activity, a ratio of a rate over that of control.

Table 5-3. Comparison of inhibition (%) of complex I inhibitors on oxidation of different substrates by *A. ferrooxidans* at pH 3.5.

Complex I Inhibitor	Terminal <i>e</i> -acceptor	Oxidized substrate *					
		Fe ²⁺	Endog	Fructose	YE	CA	formic
2 mM atabrine	O ₂	17	0	0	0	0	0
	Fe ³⁺		0	ND	ND	ND	ND
2 mM amytal**	O ₂	15	42	77	8	27	0
	Fe ³⁺		45	83	ND	ND	0
0.1 mM rotenone	O ₂	18	48	82	31	33	34
	Fe ³⁺		46	86	ND	ND	27
0.5 μM piericidin A	O ₂	0	46	ND	33	23	11
	Fe ³⁺		92	91	ND	ND	10

*: Numbers in table represent the values of percentage (%) of inhibition; Endog: endogenous substrates; YE: yeast extract; CA: casamino acids; formic: formic acid; ND: not determined. ** Concentration was 1 mM in Fe²⁺ oxidation. The values other than in formic acid oxidation were taken from Part I, II, III, and IV.

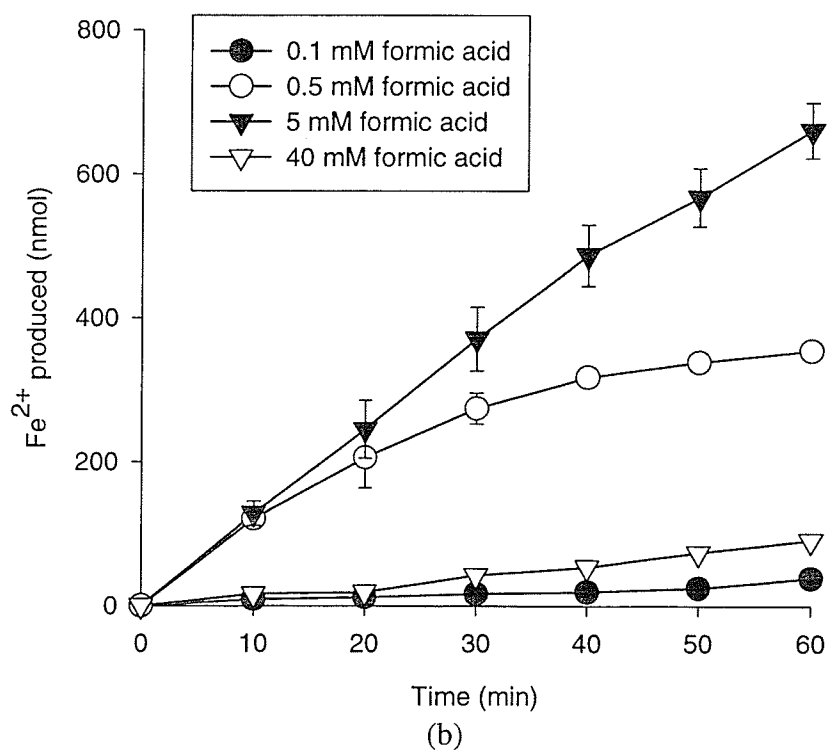
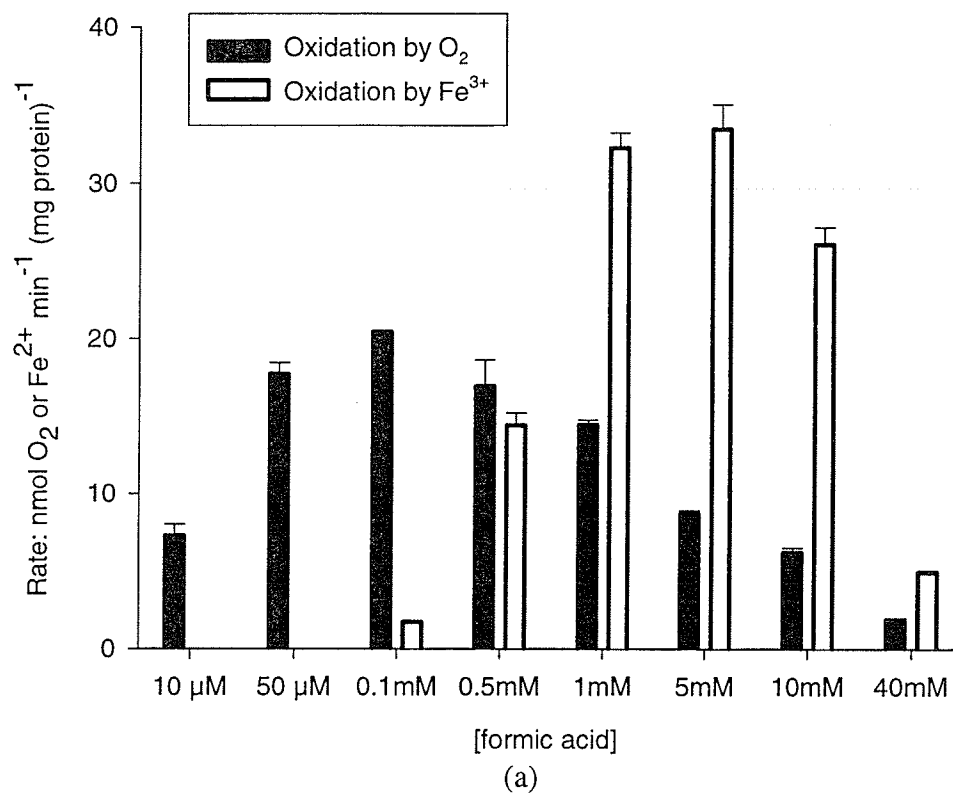
Table 5-4. Effect of inhibitors of complex III and quinol oxidases on formic acid oxidation.

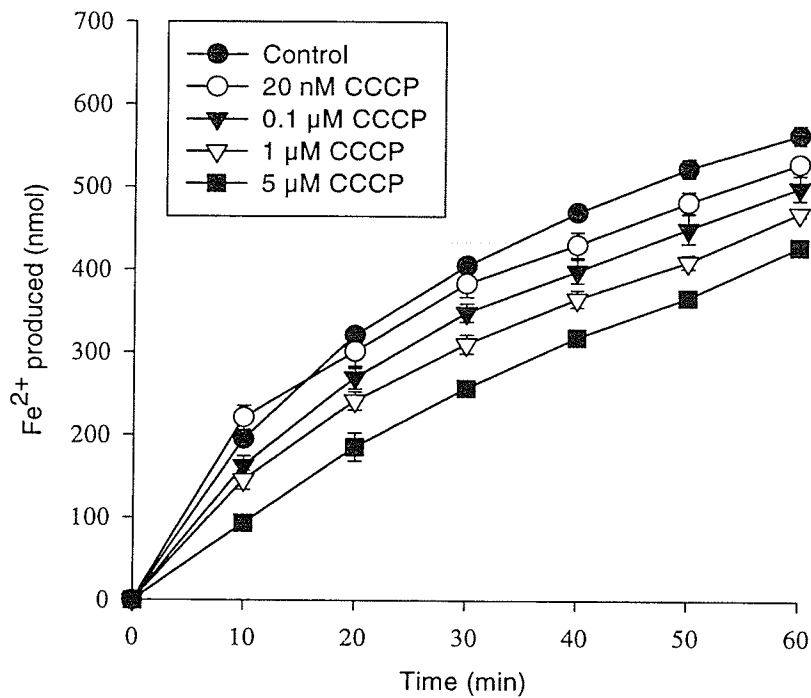
		Oxidation by O ₂		Oxidation by Fe ³⁺	
	Concentration	Rate *	R.A	Rate **	R.A
Control		23.28 ± 0.45	1.00	33.75 ± 3.51	1.00
Antimycin A	1 μM	22.66 ± 0.05	0.97		
	10 μM	20.21 ± 0.05	0.87		
	50 μM	20.05 ± 0.42	0.86		
	0.1 mM	19.48 ± 0.16	0.84	27.78 ± 1.52	0.82
Control	Myxothizol	24.38 ± 0.47	1.00	33.75 ± 3.51	1.00
	4 μM	23.59 ± 0.21	0.97		
	10 μM	22.92 ± 0.52	0.94		
	40 μM	22.08 ± 0.05	0.91		
	80 μM	20.57 ± 0.36	0.84	28.64 ± 2.13	0.85
Control		19.38 ± 0.63	1.00	35.31 ± 3.78	1.00
HQNO	0.1 μM	16.25 ± 0.05	0.84		
	0.4 μM	9.90 ± 0.42	0.51	9.53 ± 2.28	0.27
	1 μM	4.90 ± 0.05	0.25	5.78 ± 1.41	0.16
	4 μM	2.66 ± 0.42	0.14	4.03 ± 0.63	0.11
	10 μM			1.63 ± 2.31	0.05

* Rate: nmol O₂ min⁻¹ (mg protein)⁻¹; ** Rate: nmol Fe²⁺ min⁻¹ (mg protein)⁻¹; R.A: relative activity, a rate relative to that of the control rate.

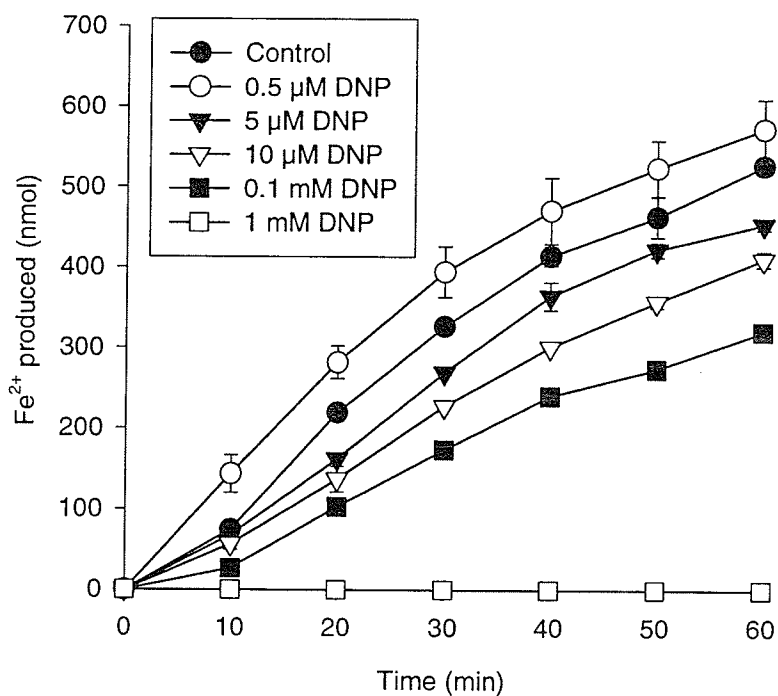
Figures of Part V

Fig. 5-1. Oxidation of formic acid at different concentrations by O_2 and Fe^{3+} . (a) Rate comparisons; (b) time course of Fe^{3+} (4 mM) reduction by formic acid at several concentrations. Error bars represent standard deviation ($n = 3$) (a) or standard errors ($n = 3$) (b). In O_2 reduction, 2.4 mg cells were added to start the reaction in a 1.2 mL system. In Fe^{3+} reduction, 4 mg cells were added to start the reaction in a 1 mL system.



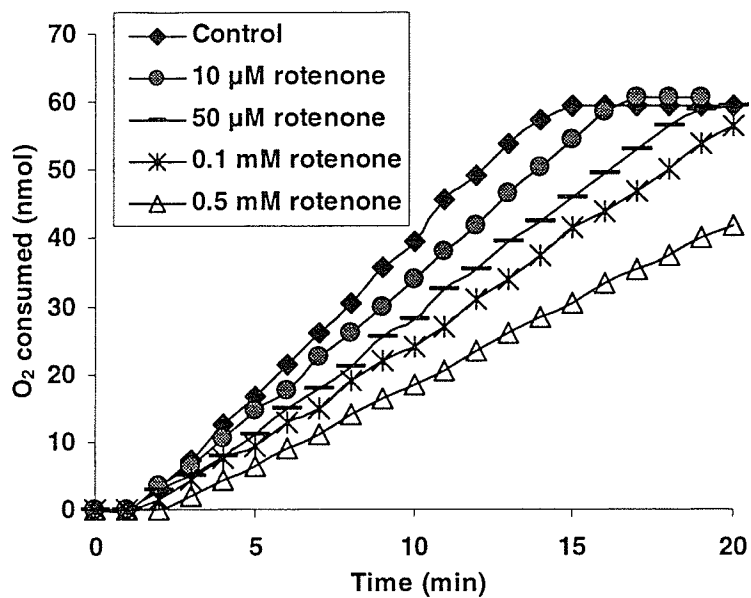


(a)

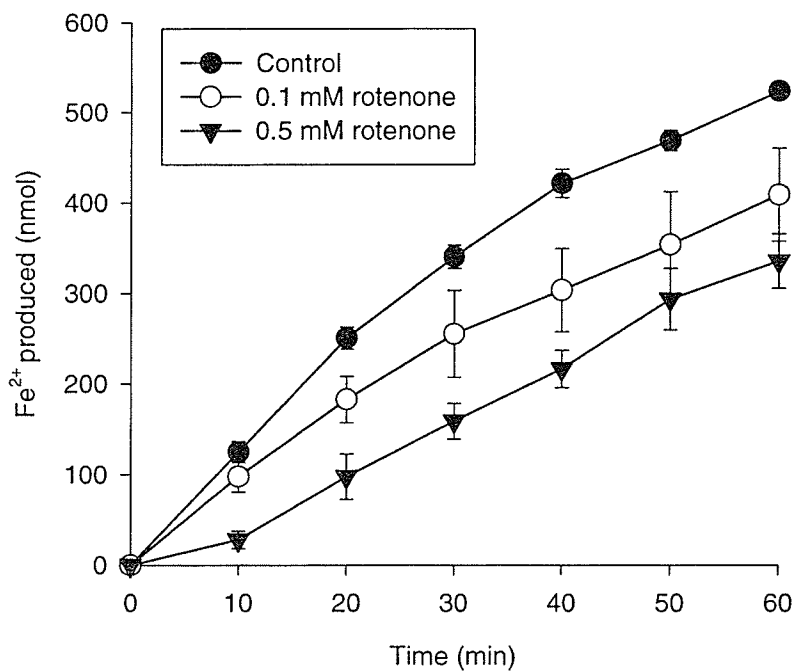


(b)

Fig. 5-2. Effect of uncouplers CCCP (a) and DNP (b) on formate oxidation by Fe^{3+} (4 mM). Cells (4 mg) and 1 mM formic acid were used in 1 mL system.



(a)



(b)

Fig. 5-3. Effect of rotenone on formic acid oxidation by O₂ (a) and Fe³⁺ (b). In O₂ reduction, 2.4 mg cells and 0.1 mM formic acid were used in 1.2 mL system. In Fe³⁺ (4 mM) reduction, 4 mg cells and 1 mM formic acid were used in 1 mL system.

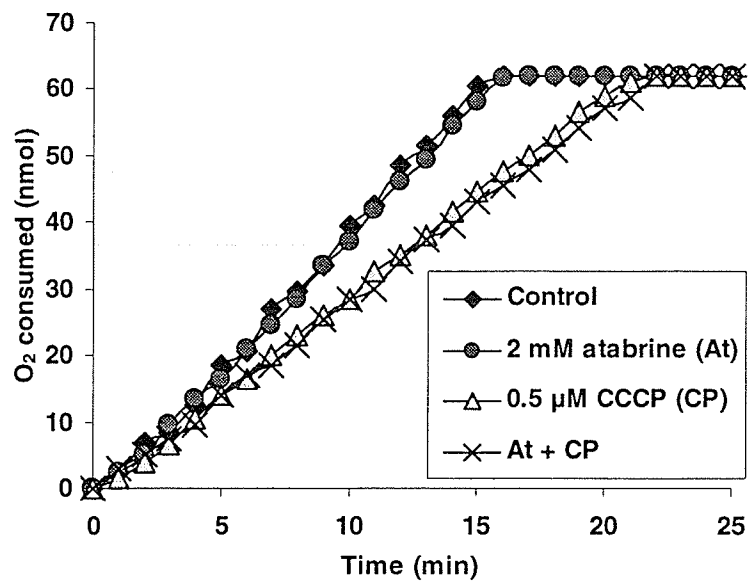
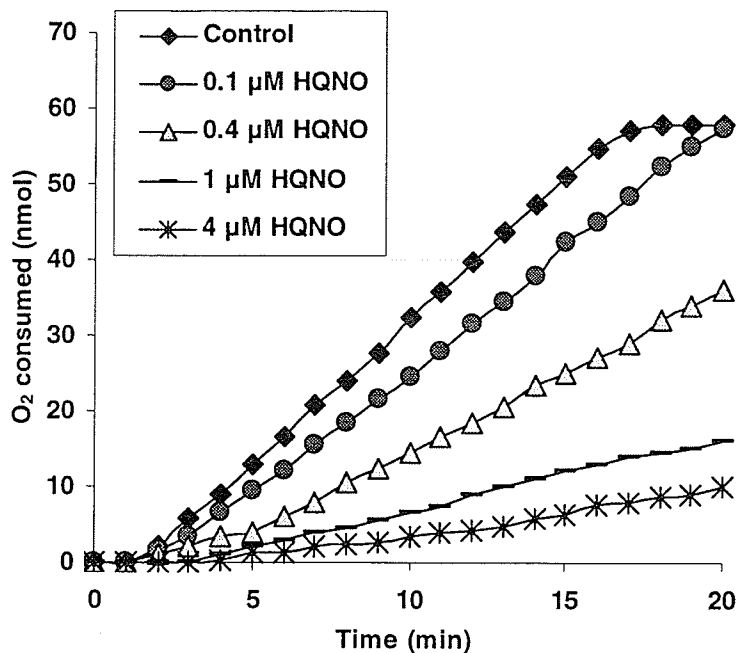
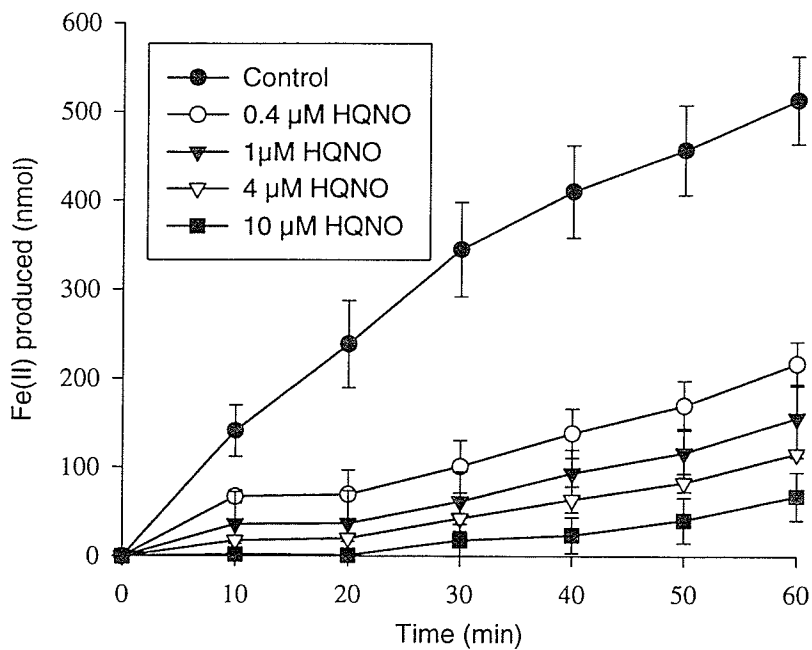


Fig. 5-4. Effect of combination of CCCP and atabrine on formate oxidation by O_2 . Cells (2.4 mg) were added to start the reaction following the addition of formic acid (0.1 mM) in 1.2 mL system.

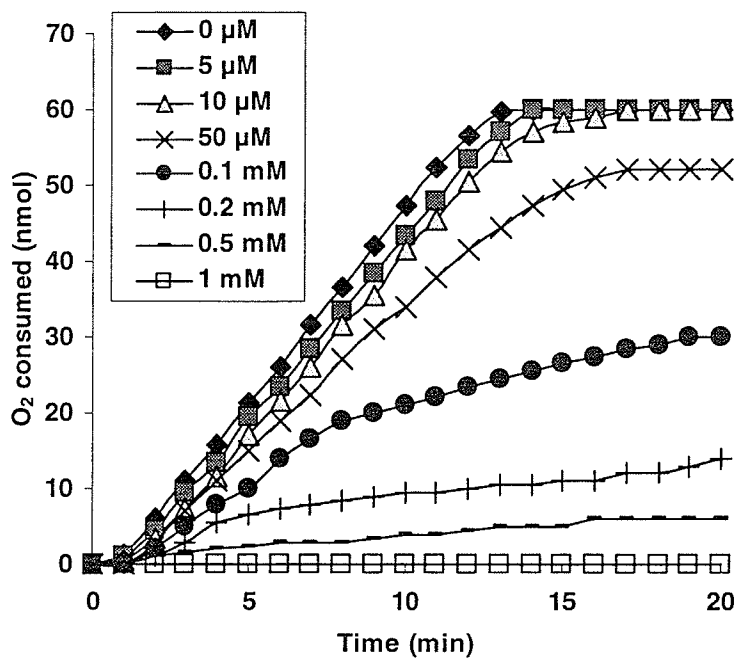


(a)

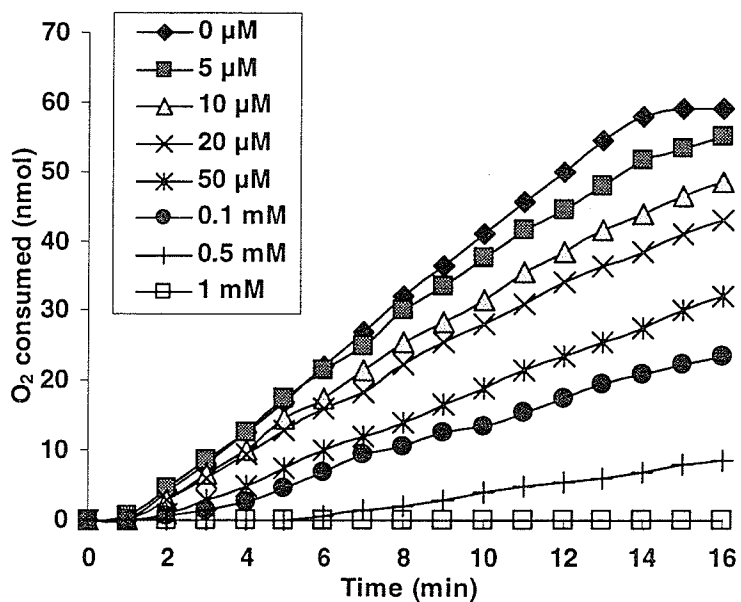


(b)

Fig. 5-5. Effect of HQNO on formate oxidation by O₂ (a) and Fe³⁺ (b). Conditions were same as Fig. 5-3.



(a)



(b)

Fig. 5-6. Effect of KCN (a) and NaN_3 (b) on formate oxidation by O_2 . Cells (2.4 mg) were added to start the reaction after formic acid (0.1 mM) in 1.2 mL system.

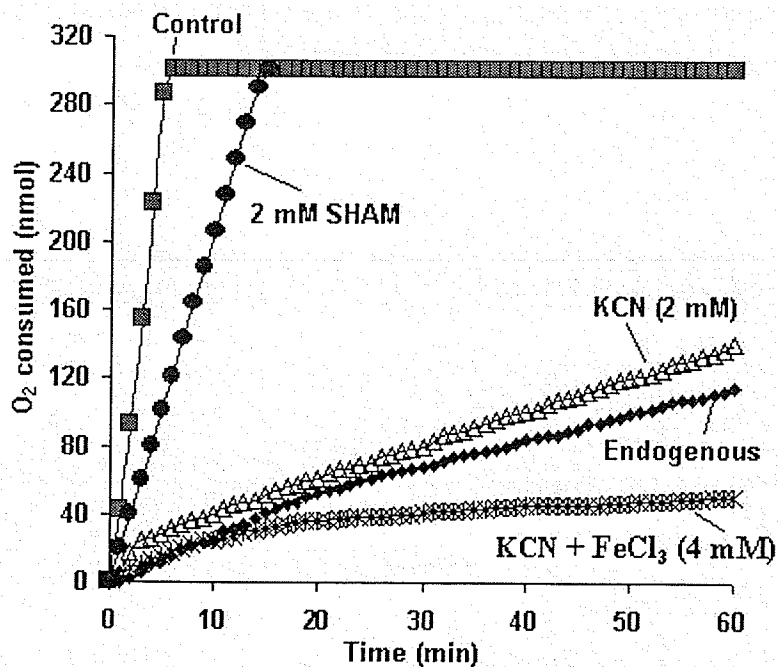


Fig. 5-7. Effect of KCN, SHAM and FeCl₃ on formate (0.5 mM) oxidation by 24 mg cells. Cells were added to start the reaction in 1.2 mL system.

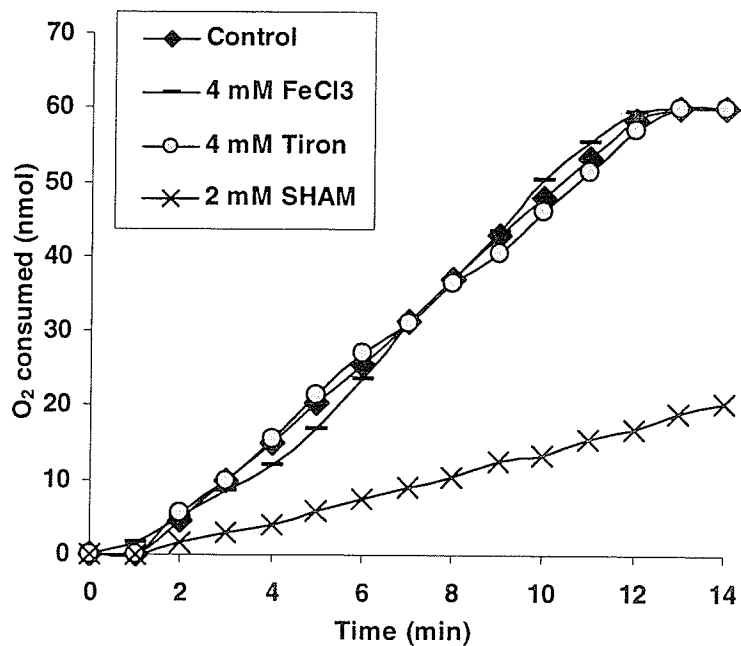
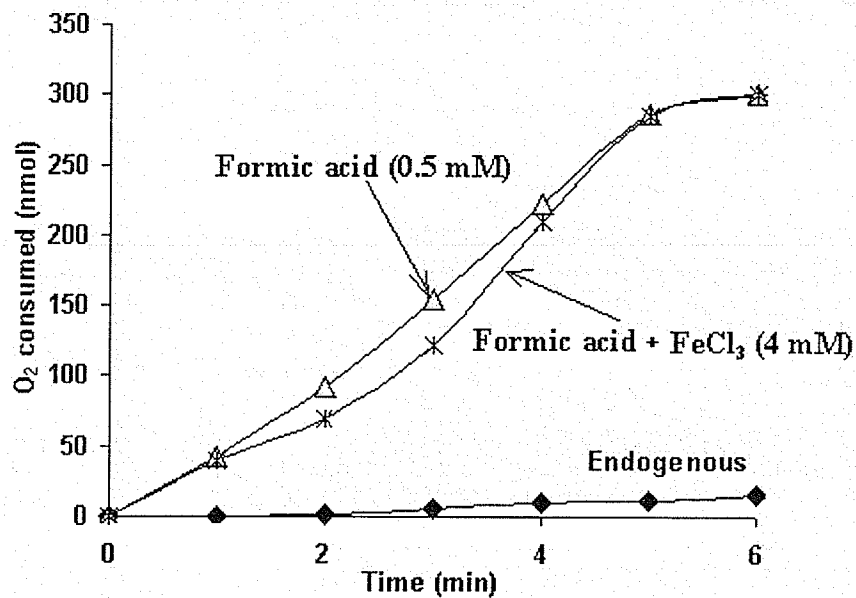
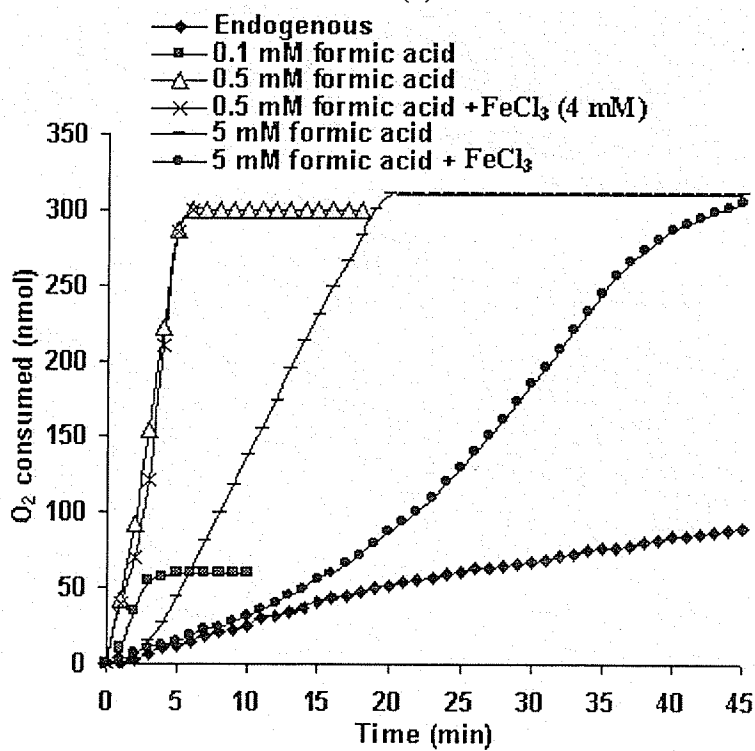


Fig. 5-8. Effects of FeCl₃, tiron and SHAM on formic acid oxidation. Cells (2.4 mg) were added to start the reaction after formic acid (0.1 mM) in 1.2 mL system.



(a)



(b)

Fig. 5-9. Formate oxidation in the absence and presence of FeCl_3 . Cells (24 mg) were added to start the reaction in 1.2 mL system. (a) Shows the short time scale of the oxidation of 0.5 mM of formic acid while (b) shows the long time scale of the oxidation of 0.1 mM, 0.5 mM and 5 mM formic acid.

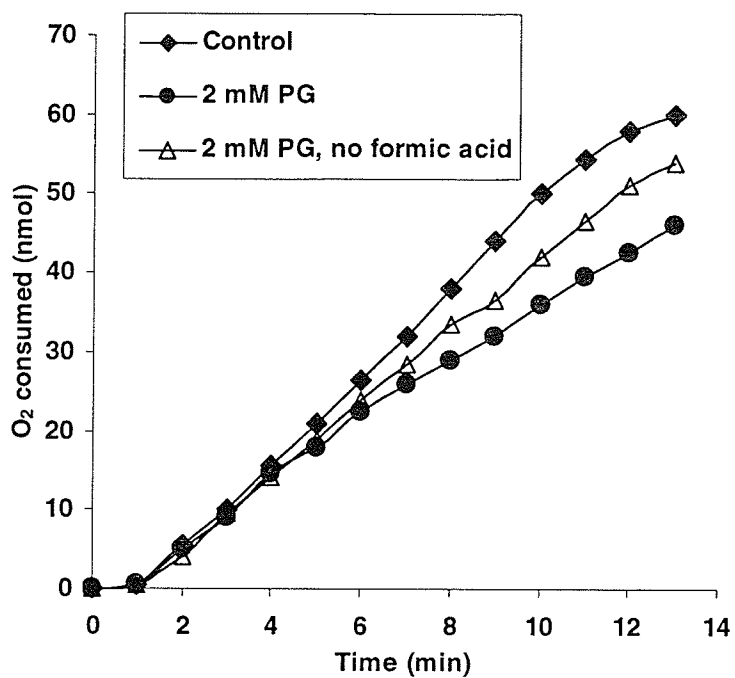


Fig. 5-10. Effects of PG on formate oxidation. Cells (2.4 mg) were added to start the reaction following the addition of formic acid (0.1 mM) in 1.2 mL system.

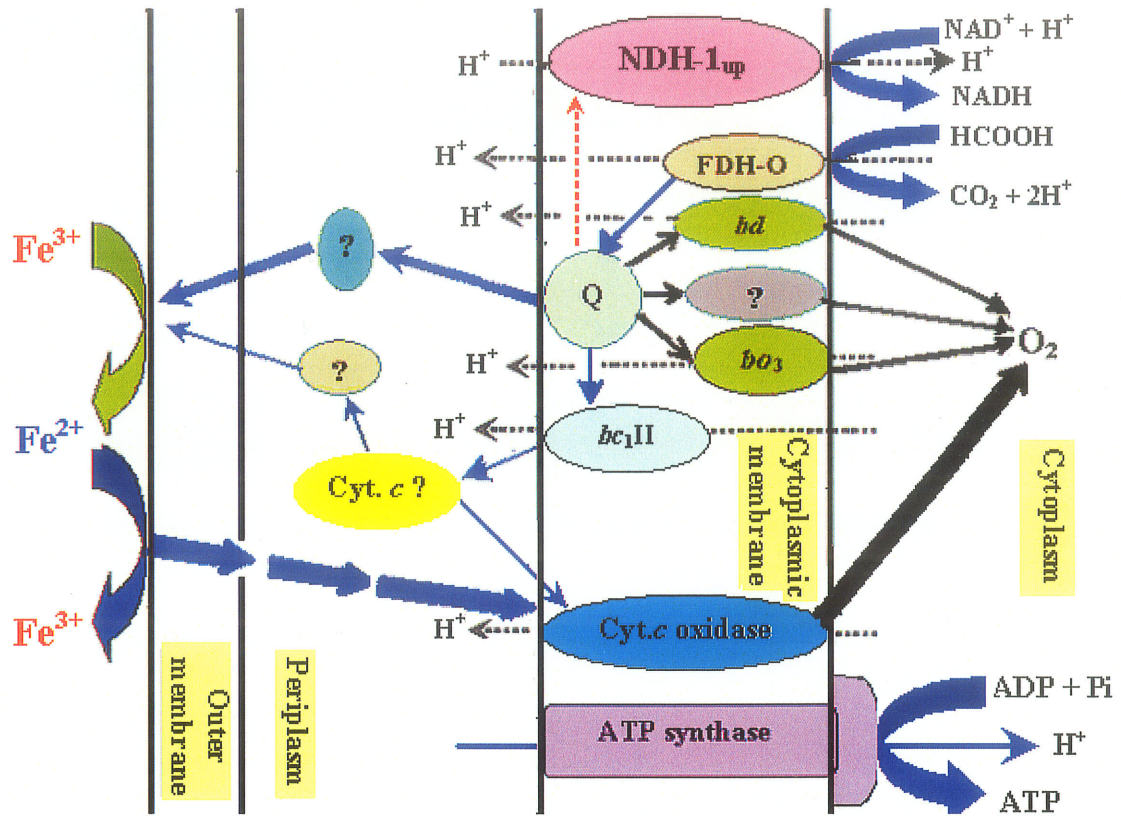


Fig. 5-11. Proposed model for electron transport pathways of formate oxidation in *A. ferrooxidans*. Q: ubiquinone/ubiquinol pool; NDH-1_{up} : the NDH-1 involved in the uphill reaction (NAD^+ reduction); FDH-O : formate dehydrogenase that operates under aerobic condition; bd and bo_3 : cytochrome bd and bo_3 quinol oxidases involving proton pumping; $bc_1\text{II}$: the complex III involved in downhill reaction; Cyt.: cytochrome. The thickness of straight arrows (not including the arrows pointing at H^+) represents the speed of electron flow in a qualitative manner.

Chapter IV
General Summary

The effects of uncouplers and electron transport inhibitors on the oxidation of Fe^{2+} , some Fe^{3+} -reacting organic compounds, endogenous substrates, fructose, yeast extract (YE), casamino acids (CA) and formic acid in *A. ferrooxidans* have been investigated.

Fe^{2+} is oxidized by using the cytochrome *c* oxidase as the terminal oxidase and during this reaction some electrons are transferred along an uphill pathway to reduce NAD^+ (Fig. 1-26). The uphill reaction (NAD^+ reduction) during Fe^{2+} oxidation was indirectly proved by using the concept of respiratory control. The energy in the form of ΔE ($E_{\text{H}_2\text{O}/1/2 \text{O}_2} - E_{\text{Fe}^{3+}/\text{Fe}^{2+}}$) will be converted to proton motive force (Δp) and an equilibrium tends to occur between ΔE and Δp during Fe^{2+} oxidation. Any process that decreases Δp will increase the disequilibrium between ΔE and Δp leading to the acceleration of Fe^{2+} oxidation. Conversely, a process that increases Δp will decrease the disequilibrium between ΔE and Δp leading to the inhibition of Fe^{2+} oxidation.

Uncouplers CCCP and DNP, which dissipate Δp , stimulated Fe^{2+} oxidation maximally by 30% (Table 1-1 and Fig. 1-1) indicating a normal respiratory control during Fe^{2+} oxidation.

During Fe^{2+} oxidation, Δp is mainly consumed in two processes: ATP generation through ATP synthase and NAD^+ reduction via the hypothetical uphill electron transport pathway (from cytochrome *c* to NDH-1_{up}) (Fig. 1-26). If the hypothetical uphill electron transport pathway is involved in Fe^{2+} oxidation, the inhibition of this pathway by the inhibitors of NDH-1_{up} or $bc_1\text{I}$ would increase Δp leading to the inhibition of Fe^{2+} oxidation. Under this condition, the increased Δp caused by the inhibitors of NDH-1_{up} or $bc_1\text{I}$ will be destroyed by an uncoupler leading to the stimulation of Fe^{2+} oxidation. Tables 1-5 and 1-6 and Fig. 1-13 show that Fe^{2+} oxidation was inhibited by complex I

(NDH-1_{up}) inhibitors (rotenone, amytal and atabrine) and complex III (*bc₁I*) inhibitors (HQNO, antimycin A and myxothiazol) and the reduced activities caused by the addition of these inhibitors were stimulated by 10 μ M or 100 μ M DNP with the exception of atabrine-reduced activity. The results, as expected, indicate the existence of the uphill reaction (NAD⁺ reduction) during Fe²⁺ oxidation (Fig. 1-26).

The Fe³⁺-reacting organic compounds ascorbic acid (Vc), propyl gallate (PG), SHAM, L-cysteine (Cys), glutathione (GSH) and tiron are oxidized by first reducing Fe³⁺ on the cell surface of *A. ferrooxidans* to Fe²⁺ and Fe²⁺ is oxidized via the Fe²⁺-oxidizing system (Fig. 1-26). The evidences include: (1) these organic compounds chemically reduce Fe³⁺ to Fe²⁺ (Table 1-23); (2) the oxidation of these organic compounds by O₂ is greatly stimulated by FeCl₃ (Table 1-26); (3) the oxidation of these compounds and the oxidation of Fe²⁺ are affected similarly by uncouplers (Table 7 and Fig. 1-18) and the inhibitors of complex I (Table 1-26), complex III (Table 1-26) and complex IV (Table 7).

Among the NDH-1 inhibitors, atabrine showed an unique inhibitory effect on the oxidation of Fe²⁺ and the above-mentioned Fe³⁺-reacting organic compounds. If atabrine is an specific inhibitor of NDH-1_{up} (Fig. 1-26), two phenomena should be observed: (1) the reduced oxidation activities caused by atabrine should be stimulated by an uncoupler as those by rotenone and amytal (Figs. 1-13 & 1-18); and (2) atabrine should show less inhibition on the oxidation of the Fe³⁺-reacting organic compounds than on Fe²⁺ oxidation as rotenone and amytal did (Table 1-26). However, atabrine showed stronger inhibition on the oxidation of the Fe³⁺-reacting organic compounds than on Fe²⁺ oxidation (except on PG oxidation) (Table 1-26), and the reduced oxidation activities

caused by atabrine were further inhibited by uncouplers (Table 8). The results indicate that atabrine is not an specific inhibitor of NDH-1_{up} (Fig. 1-26) and it must also inhibit Fe²⁺ oxidation at other site(s) other than NDH-1_{up}. Since the oxidation of other substrates (endogenous substrates, fructose, YE, CA, formic acid, etc.) was not significantly stimulated by Fe³⁺ (Table 9), and was not inhibited by atabrine (Table 9), atabrine can be used to quickly determine if the oxidation of a compound by *A. ferrooxidans* is mainly using the Fe²⁺-oxidizing system. It is possible that one of the functional sites of atabrine inhibition is at complex I. The uphill reaction from cytochrome *c* to NDH-1 (Fig. 1-26) was inhibited by 65% by 0.7 mM atabrine when the oxidation of external reduced cytochrome *c* instead of Fe²⁺ was studied (Elbehti et al. 2000). Since NDH-1 contains flavin, it is possible that at least part of the inhibition of the uphill reaction was due to the inhibition of NDH-1_{up}.

Two types of complex I (NDH-1) may exist in *A. ferrooxidans* because (1) the opposite effects of atabrine and piericidin A have been observed on Fe²⁺ oxidation and the oxidation of endogenous substrates and fructose (Tables 1-26 and 9); and (2) the genes coding for the subunits of two types of NDH-1 have been identified in the partial genome sequence of this organism (see the example in Fig. 1-25). NDH-1_{up} is involved in NAD⁺ reduction (Fig. 1-26) and NDH-1_{down} in NADH oxidation (Fig. 2-45).

Endogenous substrates can be oxidized by O₂ or Fe³⁺ (see Part II of Chapter III). The electron transport pathways of endogenous oxidation start from NDH-1_{down} and NDH-2 and end at cytochrome *c* oxidases (*aa*₃ and *ba*₃) and / or quinol oxidases (*bd*, *bo*₃ and the unknown oxidase) under aerobic conditions and at a Fe³⁺ reductase on the cell surface (not shown in figure) under anaerobic conditions or in the presence of CN⁻ or N₃⁻ (Fig.

2-45). Since the respiratory quotient (CO_2 / O_2) of endogenous respiration is close to 1.0 (Table 2-3 and Fig. 2-24), it suggests that the endogenous substrates in *A. ferrooxidans* belong to carbohydrate of which complete oxidation to CO_2 requires an operational TCA cycle. The carbohydrate nature of endogenous substrates agrees with the early studies in that most prokaryotes accumulate and oxidize glycogen for survival and energy of maintenance (Dawes 1976). As discussed in Part II of Chapter III, a complete TCA cycle may exist in this organism and the low activities of some key enzymes are fast enough for endogenous metabolism. Although the stimulation of endogenous respiration by the complex II inhibitor TTFA (Table 2-7 and Fig. 2-16) does not fit the expectation that complex II (succinate dehydrogenase) should be involved in endogenous metabolism, the major parts of the model (Fig. 2-45) for endogenous oxidation are supported by this study. Endogenous oxidation was inhibited by complex I inhibitors only by 50% (Table 9) indicating the involvement of both complex I ($\text{NDH-1}_{\text{down}}$) and NDH-2 (Fig. 2-45). Although specific inhibitors of NDH-2 are not available to confirm its involvement, the electron donor produced from the TCA cycle should mainly be NADH since complex II inhibitor TTFA did not inhibit endogenous respiration (Table 2-7 and Fig. 2-16). The NDH-1 inhibitor rotenone at 0.1 mM inhibited endogenous respiration in the presence of the uncoupler 30 μM DNP more strongly (90%) (Fig. 2-1a) than in the absence of an uncoupler (50%) (Table 9), supporting that $\text{NDH-1}_{\text{down}}$ pumps protons but NDH-2 does not (Fig. 2-45). In the absence or presence of 10 μM CCCP, endogenous respiration was strongly inhibited by 2 mM KCN initially but the activity recovered later (Fig. 2-14) indicating that electrons mainly flow to cytochrome *c* oxidase in the absence of KCN but shifted to quinol oxidases (*bd*, *bo*₃

and ?) after 2 mM KCN was added (Fig. 2-45). CCCP (added at zero time) greatly stimulated endogenous respiration in the absence of KCN (Fig. 2-14b) indicating that cytochrome *c* oxidase pumps protons (Fig. 2-45). The rate of endogenous respiration in the presence of CCCP and KCN (both added at zero time) was much higher than that in the presence of KCN (added at zero time) during 20 to 60 min (Fig. 2-14b) indicating that quinol oxidases *bd* and / or *bo*₃ are involved in proton-pumping (Fig. 2-45). Since HQNO inhibits *bc*₁II, *bd* and *bo*₃ (Fig. 2-45), the great stimulation of endogenous respiration by HQNO (Fig. 2-14a) supports that electrons bypassed *bc*₁II, *bd* and *bo*₃ and went to cytochrome *c* oxidase. Since Fe²⁺ oxidation via the pathway from Fe²⁺ to cytochrome *c* oxidase is 1000 times faster than endogenous oxidation via the pathway going through Q to *bc*₁II (Fig. 2-45), the pathway directly from Q to an unknown electron carrier, Fe³⁺, and to cytochrome *c* oxidase can be much more efficient than the pathway going through Q to *bc*₁II. HQNO at 40 μM greatly stimulated endogenous respiration and the increased activity was strongly inhibited by KCN are remained inhibited over 60 min period (Fig. 2-14a) supporting the possibility of the pathway from Q to the unknown electron carrier (?) to Fe³⁺ (Fig. 2-45). The cells must “open” this new pathway when the ratio of the reduced ubiquinone over the oxidized ubiquinone is high (in the presence of HQNO). The activity or the quantity of the *bc*₁II was too low in the Fe²⁺-grown cells (in this study) to perform a reaction faster than the normal endogenous respiration as Brasseur et al. (2004) reported that *bc*₁II was detectable only in the sulfur-grown cells and *bc*₁I only in the Fe²⁺-grown cells. The activity in the presence of CCCP and KCN was strongly inhibited by HQNO (Fig. 2-14b) confirming that *bd* and *bo*₃ were inhibited by HQNO, and the remaining activity was further strongly inhibited by

0.1 mM rotenone (Fig. 2-14b) indicating the involvement of an unknown quinol oxidase which is not sensitive to KCN and HQNO (Fig. 2-45). The activity in the presence of KCN and HQNO (Fig. 2-14a) was not stimulated by the addition of CCCP (Fig. 2-14b, KCN + HQNO + CCCP) indicating that the unknown quinol oxidase is not involved in proton-pumping (Fig. 2-45).

Among the 20 sugars and sugar alcohols tested, fructose was the only one that greatly increased the respiration rate compared to the endogenous rate (Fig. 3-1) suggesting the metabolism of fructose by *A. ferrooxidans*. Since the genes coding for the fructose transporter proteins have not been found in the partial genome sequence of this organism, it may suggest that fructose enters the cells by a concentration-dependent diffusion and this is supported by: (1) the rate of fructose oxidation increased almost linearly with the increase of fructose concentration up to 80 mM and higher concentrations showed inhibition (Fig. 3-2); (2) fructose oxidation was strongly inhibited by 0.3 M sucrose (Fig. 3-3). The respiratory quotient (CO_2 / O_2) of fructose respiration, similar to that of endogenous respiration, was close to 1.0 (Fig. 3-9) agreeing with its carbohydrate nature. As discussed in Part III of Chapter III, CO_2 may be produced from the TCA cycle. The electron transport inhibitors and uncouplers showed similar effects on fructose oxidation as on endogenous respiration (Table 9) supporting that fructose oxidation is using the same electron transport pathway that are used for endogenous oxidation (Fig. 2-45). Complex I inhibitors showed higher inhibition on fructose oxidation than on endogenous respiration (Table 9) suggesting that more electrons flowed to $\text{NDH-1}_{\text{down}}$ (Fig. 2-45). Compared to the great stimulation on endogenous respiration, HQNO and the uncoupler CCCP showed no effect on

fructose oxidation (Table 9) possibly because fructose oxidation was close to the maximal rate and was using the maximal capacity (all enzymes are operating at their maximal rates) of the electron transport pathways (Fig. 2-45) as discussed in Part III of Chapter III. In fact, the rate of fructose oxidation was close to the rate of endogenous respiration in the presence of 40 μM HQNO or 10 μM CCCP (see Part II and Part III of Chapter III). Complex IV inhibitors showed almost complete inhibition on fructose oxidation (Table 9) supporting that fructose oxidation must use the fast pathway from Q to an unknown electron carrier, Fe^{3+} , to cytochrome *c* oxidase (Fig. 2-45).

The oxidation of YE, CA and formic acid was not affected by atabrine and Fe^{3+} (Table 9) indicating that the oxidation was different from that of the Fe^{3+} -interacting organic compounds (Table 1-26). The oxidation of YE, CA and formic acid was significantly inhibited by complex I inhibitors rotenone and piericidin A (Table 9) suggesting that the electron transport pathways for endogenous metabolism (Fig. 2-45) may be used for the oxidation of YE, CA and formic acid. However, HQNO at a low concentration (4 μM) almost completely inhibited the oxidation of YE, CA and formic acid (Table 9) indicating that a HQNO-sensitive dehydrogenase(s) instead of $\text{NDH-1}_{\text{down}}$ may be the first electron transport enzyme(s) for the oxidation of YE, CA and formic acid and some electrons may be transferred to NDH-1_{up} (Fig. 5-11). The strong inhibition of the oxidation of YE, CA and formic acid by complex IV inhibitors (Table 9) suggests the oxidation must use the fast pathway from Q to an unknown electron carrier, Fe^{3+} , to cytochrome *c* oxidase (Fig. 2-45). Compared to endogenous respiration, the oxidation of YE, CA and formic acid was more sensitive to the inhibition by uncouplers (Table 9). The reasons may be due to: (1) the energy requirement of substrate uptake

(YE, CA) or (2) the weak acid property and unknown detrimental effects (of formic acid) as discussed in Chapter III.

Based on this study and the currently available information in the literature, a general model of the electron transport pathways in *A. ferrooxidans* is shown in Fig. 8.

Tables of Chapter IV

Table 7. Comparison of the effects of uncouplers (CCCP and DNP) and complex IV inhibitors (KCN and NaN_3) on the oxidation of Fe^{2+} , Vc, PG, Cys, GSH and tiron.*

	Fe^{2+}	Vc	PG	Cys	GSH	Tiron
0.5 μM CCCP	25 (S)	13 (S)	12 (I)	0	14 (S)	13 (I)
10 μM CCCP	10 (I)	19 (I)	26 (I)	19 (I)	4 (S)	57 (I)
20 μM DNP	28 (S)	12 (S)	12 (I)			17 (I)
30 μM DNP	20 (S)	11 (S)		7 (S)	8 (S)	
1 mM KCN	100 (I)	100 (I)	95 (I)			
2 mM KCN	100 (I)		96 (I)	100 (I)	99 (I)	99 (I)
0.1 mM NaN_3	100 (I)	100 (I)	84 (I)			
1 mM NaN_3	100 (I)		96 (I)	100 (I)	99 (I)	99 (I)

* The numbers in the table represent percentage (%). S: stimulation; I: inhibition. Tiron oxidation was measure in the presence of 4 mM FeCl_3 and detailed studies of SHAM oxidation were not carried out (see Part I of Chapter III).

Table 8. Effect of an uncoupler (CCCP or DNP) on the atabrine-reduced activities during the oxidation of Fe^{2+} and the organic compounds that interact with Fe^{3+} . *

	Fe^{2+}	Vc	PG	Cys	GSH	Tiron
Concentrations used						
Atabrine (At)	2 mM	0.1 mM	2 mM	0.4 mM	2 mM	2 mM
DNP	0.1 mM					
CCCP		10 μM	10 μM	10 μM	100 μM	10 μM
Inhibition (%)						
At	17	46	9	63	25	58
Uncoupler	16	27	11	19	14	57
At + uncoupler	56	62	23	72	65	74

* Tiron oxidation was measure in the presence of 4 mM FeCl_3 and detailed studies of SHAM oxidation were not carried out (see Part I of Chapter III).

Table 9. Comparison of the effects of the inhibitors of complex I, complex III and complex IV, uncouplers and Fe^{3+} on the oxidation of different substrates.*

	Substrate	Fe^{2+}	Endog.	Fructose	YE	CA	Formate
Complex I inhibitors	2 mM At	17 (I)	0	0	0	0	0
	2 mM Am	15 (I)	42 (I)	77 (I)	8 (I)	27 (I)	0
	0.1 mM R	18 (I)	48 (I)	82 (I)	31 (I)	33 (I)	34 (I)
	0.5 μM PA	0	46 (I)		33 (I)	23 (I)	11 (I)
Complex III inhibitors	4 μM H		100 (S)		90 (I)	80 (I)	90 (I)
	40 μM H	14 (I)	150-360 (S)	1 (S)	80 (I)	90 (I)	
	10 μM An	16 (I)		2 (I)	20 (I)	35 (I)	13 (I)
	0.1 mM An		3 (I)	1 (I)			16 (I)
	10 μM My	7 (I)	5 (S)				6 (I)
	40 μM My				0-10 (I)	8 (I)	14 (I)
Complex IV inhibitors	2 mM KCN	100 (I)	40-60 (I) → 80-90 (I) → 0-30(I)	80 (I)	90 (I)	100 (I)	100 (I)
	1 mM NaN_3	100 (I)	70 (I) → 40 (S)	80 (I)	90 (I)	100 (I)	100 (I)
Uncouplers	0.5 μM CCCP	25 (S)			11 (I)	6 (I)	21 (I)
	10 μM CCCP	10 (I)	170-250 (S)	3 (I)	45 (I)	38 (I)	
	20 μM DNP	28 (S)			19 (I)	6 (I)	44 (I)
	30 μM DNP	20 (S)	170 (S)				
Fe^{3+}	4 mM FeCl_3		10-20 (S) → 0-10 (I)	2 (I)	0-10 (S)	0-20 (S)	4 (S)

* The numbers in the table represent percentage (%). S: stimulation; I: inhibition. Endog.: endogenous substrates; At: atabrine; Am: amytal; R: rotenone; PA: piericidin A; H: HQNO; An: antimycin A; My: mythoxiazol. Data with O_2 reduction at pH 3.5 are compared. Rate comparison during endogenous oxidation: 2 mM KCN (0 – 15 min, 15 – 25 min, 25 – 60 min), 1 mM NaN_3 (0 – 8 min, 8 – 60 min), 4 mM FeCl_3 (0 – 30 min, 30 – 60 min).

Figures of Chapter IV

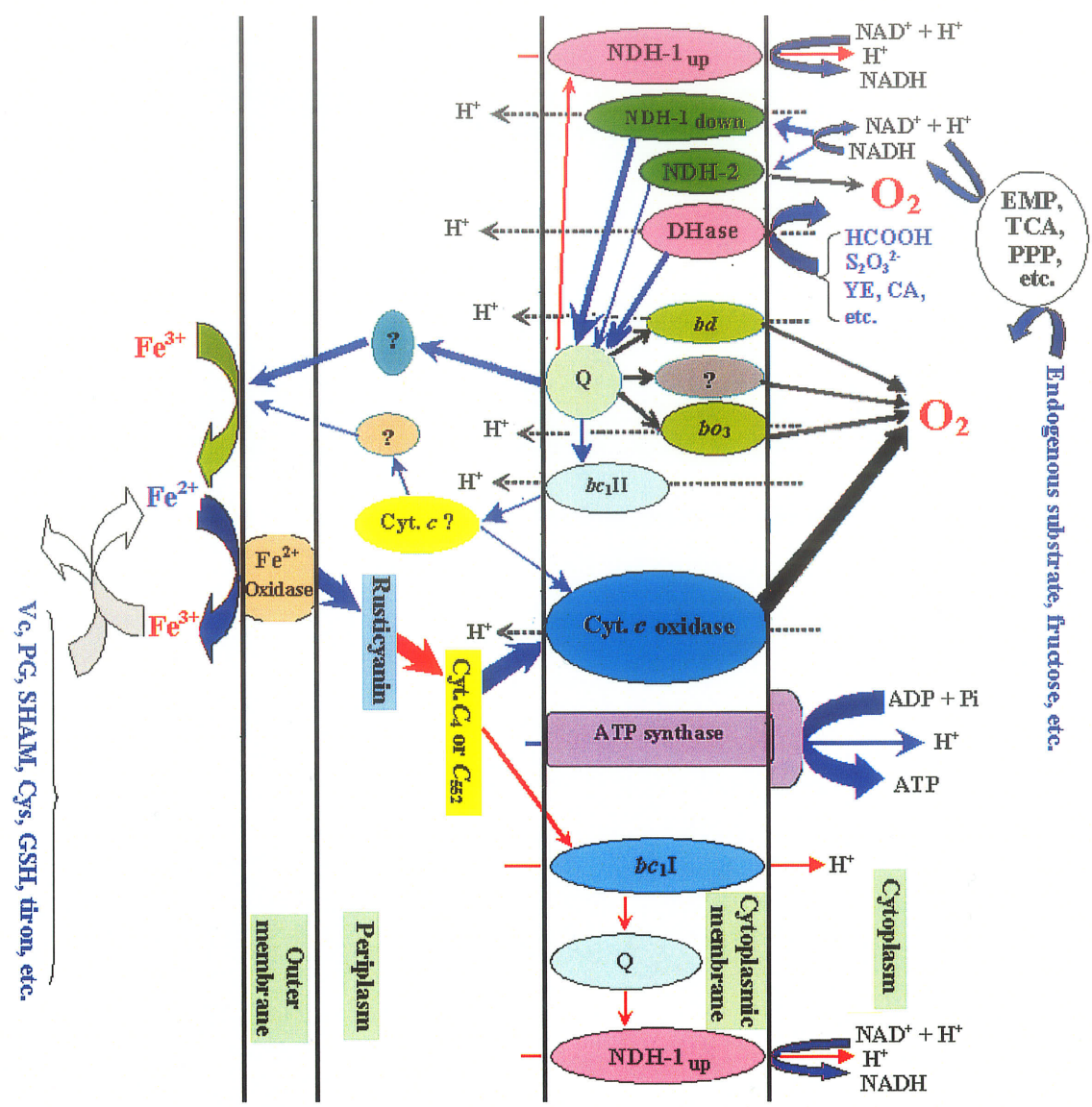


Fig. 8. The electron transport pathways in *A. ferrooxidans*. The oxidation of HCCOH, $S_2O_3^{2-}$, YE (yeast extract) and CA (casamino acids) involves an uphill reaction from Q to NDH-1_{up}. The oxidation of NADH does not involve an uphill reaction from Q to NDH-1_{up}. Fe^{2+} oxidation involves the uphill reaction from rusticyanin to cytochrome c_4 or cytochrome c_{552} and the uphill reaction from Cyt. c_4 or c_{552} to bc_1I , Q and NDH-1_{up}. bc_1I and NDH-1_{up} are involved in the uphill (endergonic) pathway. bc_1II and NDH-1_{down} are involved in the downhill (exergonic) pathway. Cyt. c oxidase represents aa_3 and / or ba_3 oxidase. Q: ubiquinone / ubiquinol pool; EMP: the Embden-Meyehof pathway; TCA: the tricarboxylic Acid cycle; PPP: the Pentose Phosphate Pathway; Vc: ascorbic acid; PG: propyl gallate; Cys: L-cysteine; GSH: glutathione.

Chapter V
Discoveries and Future Studies

Major discoveries made in this study are:

- (1) Stimulation of Fe^{2+} oxidation in *A. ferrooxidans* by uncouplers has been demonstrated. Uncoupler stimulation on Fe^{2+} oxidation indicates respiratory control during Fe^{2+} oxidation and may also suggest proton pumping by cytochrome *c* oxidase.
- (2) The uphill reaction (NAD^+ reduction) during Fe^{2+} oxidation was clearly demonstrated by the effects of the inhibitors of complex I (rotenone, amytal and atabrine) and complex III (antimycin A, myxothiazol and HQNO) in the absence and presence of an uncoupler. In the absence of uncoupler, Fe^{2+} oxidation was reduced by these inhibitors and these reduced activities were stimulated by the addition of an uncoupler with the exception of atabrine inhibition. This indicates that some electrons were flowing along the uphill electron transport pathway to NDH-1_{up} during Fe^{2+} oxidation (Fig. 1-26) and the uphill electron transport pathway is the other “valve” in addition to ATP synthase in controlling the respiration.
- (3) Fe^{2+} oxidation was inhibited by atabrine and the reduced activity could be further inhibited by the addition of an uncoupler. These two reactions are the special features for Fe^{2+} oxidation in *A. ferrooxidans*. Some Fe^{3+} -interacting organic compounds such as ascorbic acid (Vc), propyl gallate (PG), salicylhydroxamic acid (SHAM), L-cysteine (Cys), glutathione (GSH) and tiron could be oxidized by this organism using the Fe^{2+} -oxidizing system but with a lower rate. The oxidation of these organic compounds was also inhibited by atabrine and the reduced activities were further inhibited by the addition of an uncoupler.

- (4) The inhibition of Fe^{2+} oxidation and formate oxidation by KCN was time-dependent in agreement with what was expected. In the presence of NaN_3 , Fe^{2+} oxidation and formate oxidation stopped instantly but some activities recovered after a while. The instant inhibition was possibly due to the inhibition of ATP synthase by NaN_3 and the later activity recovery was due to the uncoupling effect of the weak acid property of HN_3 . Therefore proton flowing into the cells via ATP synthase is possibly obligatorily coupled to the oxidation of Fe^{2+} and formic acid.
- (5) The oxidation of endogenous substrates in *A. ferrooxidans* by O_2 or Fe^{3+} (endogenous oxidation) was successfully demonstrated by using a large amount of cells. Endogenous oxidation was greatly stimulated by uncouplers, ionophores and weak acids indicating a normal respiratory control during endogenous oxidation. The extent of stimulation on an oxidation (endogenous oxidation) by these Δp dissipaters was shown for the first time in this organism to be similar to the extent of stimulation on the respiration by uncouplers in mitochondria and heterotrophic bacteria.
- (6) Endogenous oxidation was strongly inhibited by complex I inhibitors rotenone, amytal and piericidin A indicating a downhill electron transport pathway starting from NDH-1 for this oxidation. This is the first report showing an electron transport pathway starting from NDH-1 for an oxidation in this organism.
- (7) Complex I inhibitors atabrine and piericidin A showed opposite effects on Fe^{2+} oxidation and endogenous oxidation. Atabrine did not inhibit endogenous oxidation but inhibited Fe^{2+} oxidation, while piericidin A inhibited endogenous oxidation but did not inhibit Fe^{2+} oxidation, suggesting the possibility of two types of complex I

(NDH-1) in this organism: one (NDH-1_{down}) involved in the downhill reaction (endogenous oxidation) and the other (NDH-1_{up}) involved in the uphill reaction (Fe²⁺ oxidation). This is also supported by the identification of the genes coding for two types of NDH-1 in the partial genome sequence of *A. ferrooxidans*.

- (8) Complex IV inhibitors, KCN and NaN₃, only partially inhibited endogenous respiration indicating the involvement of other terminal oxidases in addition to cytochrome *c* oxidase. The reduced activity of endogenous respiration by KCN or NaN₃ was further inhibited by the addition of HQNO, an inhibitor of complex III and heme *b*-containing quinol oxidases, and the remained activity was strongly inhibited by rotenone, indicating the involvement of quinol oxidases (*bd* and *bo*₃) and an unknown terminal oxidase that is not sensitive to KCN, NaN₃ and HQNO.
- (9) HQNO, an inhibitor of complex III and heme *b*-containing quinol oxidases, greatly stimulated endogenous oxidation. KCN or NaN₃ more strongly inhibited the stimulated activity of endogenous respiration by HQNO than that by uncouplers. It was proposed that HQNO stimulation was due to the shifting of electrons to a fast electron transport pathway involving iron and the cytochrome *c* oxidase pathway.
- (10) Among the 20 sugars and sugars alcohols tested, fructose is unique in that it was oxidized with a significant rate by this organism using the electron transport pathways used for endogenous oxidation.
- (11) Unknown compounds in yeast extract (YE) and casamino acids (CA) were oxidized by this organism by using the same electron transport pathways as endogenous oxidation except that the oxidation may involve an HQNO-sensitive dehydrogenase other than NDH-1_{down}.

- (12) Formate oxidation was strongly inhibited by HQNO at low concentrations indicating that the FDH in this organism contains a quinone-reacting *b* type cytochrome.
- (13) The studies of the effects of electron transport inhibitors on formate oxidation indicate that formate oxidation may use the electron transport pathways used for endogenous oxidation after electrons have been transferred to Q (see Figs. 5-11 and 8).
- (14) The inhibitors of plant alternative oxidase (AOX), SHAM and PG, significantly inhibited formate oxidation. This indicates that the unknown terminal oxidase in Fig. 9 may be AOX or alternatively other enzyme(s) which may be inhibited by SHAM and PG.

The discoveries in this work initiated many topics that need to be further investigated.

The following lists some directions in future studies.

- (a) The existence of two types of NDH-1 in this organism needs to be confirmed by cloning and expressing the genes of these two enzymes. Furthermore, the effects of different inhibitors such as atabrine and piericidin A on each type of NDH-1 should be investigated.
- (b) Atabrine is supposed to inhibit NDH-1_{up} but this study showed that it also inhibits Fe²⁺ oxidation at somewhere other than NDH-1_{up}. The study of the atabrine inhibition sites will greatly help the understanding of the mechanism of Fe²⁺ oxidation.

- (c) Inhibition of the oxidation of the Fe^{3+} -interacting organic compounds (essentially Fe^{2+} oxidation) by complex I and complex III electron transport inhibitors except atabrine was less than the inhibition of Fe^{2+} oxidation by these inhibitors. Since the latter oxidation was much faster than the former oxidation, this study proposed that the faster Fe^{2+} oxidation is, the higher the proportion of electrons will flow to the uphill pathway to NDH-1_{up} and so the higher the inhibition of Fe^{2+} oxidation by electron transport inhibitors will be. This hypothesis needs to be further confirmed with more experiments.
- (d) The model for the electron transport pathways of endogenous oxidation proposed in this study is still a preliminary model. More studies are needed to make this model complete since it may be the “central model” for the oxidation of many compounds such as formate and fructose. Some electron carriers are still not clear in this model (Fig. 2-45). The unknown terminal oxidase needs to be investigated and even the types of heme *b* containing quinol oxidases need to be further confirmed.
- (e) SHAM, an AOX inhibitor, greatly stimulated endogenous respiration but inhibited the HQNO-stimulated activity of endogenous respiration, the activity of endogenous respiration in the presence of 10 μM CCCP and 2 mM KCN, and the activity of formate oxidation. This indicates the possibility of the existence of AOX in *A. ferrooxidans* although the genes coding for AOX have not been identified in the partial genome sequence of this organism. It is physiologically and evolutionarily important to further investigate the existence of AOX in this organism.
- (f) Some iron chelators such as *o*-phen. and EDTA stimulated endogenous respiration. In this study it was interpreted as due to the redox potential changing of the iron on

the cell surface but the exact reason for the stimulation should be further investigated.

- (g) Formate oxidation was strongly inhibited by HQNO and partially inhibited by complex I inhibitors rotenone and piericidin A. In this study it was explained that the FDH in this organism contains heme *b* and it is NAD(P)⁺-independent but has binding site(s) for rotenone and piericidin A. Purification of the FDH(s) is required to confirm these findings.
- (h) In the presence of FeCl₃ formate oxidation by O₂ was initially slow but became faster with time. The O₂ reduction by formate was much faster than Fe³⁺ reduction by formate in the presence of KCN aerobically, and the former reaction was stoichiometric but the latter was not. The unusual effects of Fe³⁺ on formate oxidation need to be further studied.
- (i) In this study it was proposed that an uphill reaction from Q to NDH-1_{up} (Fig. 5-11) is required to generate NADH during formate oxidation. More experiments are required to confirm this hypothesis.
- (j) Fructose was shown to be oxidized by *A. ferrooxidans* but the mechanism of the entry of fructose into the cells is unknown. Further investigation of this mechanism will help the understanding of the autotrophic feature of this organism and make it possible to grow this organism heterotrophically which may be industrially and evolutionarily significant.

References

- Adapoe, C., and Silver, M. 1975. The soluble adenosine triphosphatase of *Thiobacillus ferrooxidans*. *Can. J. Microbiol.* **21**: 1 – 7.
- Albury, M. S., Affourtit, C., Crichton, P. G., and Moore, A. L. 2002. Structure of the plant alternative oxidase: site-directed mutagenesis provides new information on the active site and membrane topology. *J. Biol. Chem.* **277**: 1190 – 1194.
- Aleem, M. I. H. 1977. Coupling of energy with electron transfer reactions in chemoautotrophic bacteria. In: *Microbial Energetics* (Haddock, B. A., and Hamilton, W. A., Eds.), pp. 351 – 381. Cambridge University Press, London, UK.
- Alexeeva, S., Hellingwerf, K. J., and Teixeira de Mattos, M. J. 2002. Quantitative assessment of oxygen availability: perceived aerobiosis and its effect on flux distribution in the respiratory chain of *Escherichia coli*. *J. Bacteriol.* **184**: 1402 – 1406.
- Alexeeva, S., Hellingwerf, K. J., and Teixeira de Mattos, M. J. 2003. Requirement of ArcA for redox regulation in *Escherichia coli* under microaerobic but not anaerobic or aerobic conditions. *J. Bacteriol.* **185**: 204 – 209.
- Altschul, S. F., Madden, T. L., Schaffer, A. A., Zhang, J., Zhang, Z., Miller, W., and Lipman, D. J. 1997. Gapped BLAST and PSI-BLAST: a new generation of protein database search programs. *Nucl. Acids Res.* **25**: 3389 – 3402.
- Apel, W. A., Dugan, P. R., and Tuttle, J. H. 1980. Adenosine 5'-triphosphate formation in *Thiobacillus ferrooxidans* vesicles by H⁺ ion gradients comparable to those of environmental conditions. *J. Bacteriol.* **142**: 295 – 301.
- Armitage, J. P., Ingham, C., and M C Evans, M. C. 1985. Role of proton motive force in phototactic and aerotactic responses of *Rhodospseudomonas sphaeroides*. *J. Bacteriol.* **161**: 967 – 972.
- Arnold, R. G., DiChristina, T. J., and Hoffmann, M. R. 1986. Inhibitor studies of dissimilative Fe(III) reduction by *Pseudomonas* sp. Strain 200 (“*Pseudomonas ferrireductans*”). *Appl. Environ. Microbiol.* **52**: 281 – 289.
- Atkin, O. K., Villar, R., and Lambers, H. 1995. Partitioning of electrons between the cytochrome and the alternative pathways in intact roots. *Plant Physiol.* **108**: 1179 – 1183.
- Azarkina, N., Siletsky, S., Borisov, V., von Wachenfeldt, C., Hederstedt, L., and Konstantinov, A. A. 1999. A cytochrome *bb'*-type quinol oxidase in *Bacillus subtilis* strain 168. *J. Biol. Chem.* **274**: 32810 – 32817.
- Beck, J. V., and Shafia, F. M. 1964. Effect of phosphate ion and 2,4-dinitrophenol on the activity of intact cells of *Thiobacillus ferrooxidans*. *J. Bacteriol.* **88**: 850 – 857.

- Benoit, S., Abaibou, H., and Mandrand-Bertholot, M. A. 1998. Topological analysis of the aerobic membrane-bound formate dehydrogenase of *Escherichia coli*. *J. Bacteriol.* **180**: 6625 – 6634.
- Bertsova, Y. V., Bogachev, A. V., and Skulachev, V. P. 2001. Noncoupled NADH:ubiquinone oxidoreductase of *Azotobacter vinelandii* is required for diazotrophic growth at high oxygen concentrations. *J. Bacteriol.* **183**: 6869 – 6874.
- Blake, R. C., and Shute, E. A. 1994. Respiratory enzymes of *Thiobacillus ferrooxidans*. Kinetic properties of an acid-stable iron: rusticyanin oxidoreductase. *Biochemistry.* **33**: 9220 – 9228.
- Blaylock, B. A., and Nason, A. 1963. Electron transport systems of the chemoautotroph *Ferrobacillus ferrooxidans*. I. Cytochrome *c*-containing iron oxidase. *J. Biol. Chem.* **238**: 3453 – 3462.
- Bodo, C., and Lundgren, D. G. 1974. Iron oxidation by cell envelopes of *Thiobacillus ferrooxidans*. *Can. J. Microbiol.* **20**: 1647 – 1652.
- Booth, I. R., Douglas, R.M., Ferguson, G. P., Lamb, A. J., Munro, A. W., and Ritchie, G. Y. 1993. K⁺ efflux systems. *In* Alkali cation transport systems in prokaryotes, *Edited by* E. P. Bakker. CRC Press, Boca Raton Florida. pp. 291 – 308.
- Bosecker, K. 1997. Bioleaching: metal solubilization by microorganisms. *FEMS Microbiol. Rev.* **20**: 591 – 604.
- Bott, C. B., and Love, N. G. 2004. Implicating the glutathione-gated potassium efflux system as a cause of electrophile-induced activated sludge deflocculation. *Appl. Environ. Microbiol.* **70**: 5569 – 5578.
- Boyington, J. C., Gladyshev, V.N., Byrne, B., Khangulov, S. V., Stadtman, T.C., and Sun, P. D. 1997. Crystal structure of formate dehydrogenase H: catalysis involving Mo, molybdopterin, selenocysteine, and an Fe₄S₄ cluster. *Science.* **275**: 1305 – 1308.
- Brasseur, G., Bruscella, P., Bonnefoy, V., and Lemesle-Meunier, D. 2002. The *bc*₁ complex of the iron-grown acidophilic chemolithotrophic bacterium *Acidithiobacillus ferrooxidans* functions in the reverse but not in the forward direction. Is there a second *bc*₁ complex? *Biochim. Biophys. Acta.* **1555**:37 – 43.
- Brasseur, G., Levican, G., Bonnefoy, V., Holmes, D., Jedlick, E., and Lemesle-Meunier, D. 2004. Apparent redundancy of electron transfer pathways via *bc*₁ complexes and terminal oxidases in the extremophilic chemolithoautotrophic *Acidithiobacillus ferrooxidans*. *Biochem. Biophys. Acta.* **1656**: 114 – 126.

- Brdar, B., Kos, E., and Drakulić, M. 1965. Metabolism of nucleic acids and protein in starving bacteria. *Nature*, London. **208**: 304-3 – 304.
- Casimiro, D. R., Toy-Palmer, A., Blake II, R. C., and Dyson, H. J. 1995. Gene synthesis, high-level expression, and mutagenesis of *Thiobacillus ferrooxidans* rusticyanin: His 85 is a ligand to the blue copper center. *Biochemistry*. **34**: 6640 – 6648.
- Cavari, B. Z., and Avi-Dor, Y. 1967. Effect of carbonyl cyanide m-chlorophenylhydrazone on respiration and respiration-dependent phosphorylation in *Escherichia coli*. *Biochem. J.* **103**: 601 – 608.
- Chen, Y., and Suzuki, I. 2004. Effect of uncouplers on endogenous respiration and ferrous iron oxidation in a chemolithoautotrophic bacterium *Acidithiobacillus ferrooxidans*. *FEMS Microbiol. Lett.* **237**: 139 – 145.
- Chen, Q., Vazquez, E. J., Moghaddas, S., Hoppel, C. L., and Lesnefsky, E. J. 2003. Production of reactive oxygen species by mitochondria: central role of complex III. *J. Biol. Chem.* **278**:36027 – 36031
- Cobley, J. G. 1976a. Energy-conserving reactions in phosphorylating electron-transport particles from *Nitrobacter winogradskyi*. Activation of nitrite oxidation by the electrical component of the proton motive force. *Biochem.J.* **156**: 481 – 491.
- Cobley, J. G. 1976b. Reaction of cytochromes by nitrite in electron-transport particles from *Nitrobacter winogradskyi*. Proposal of a mechanism for H⁺ translocation. *Biochem.J.* **156**: 493 – 498.
- Colmer, A. R., and Hinkle, M. E. 1947. The role of microorganisms in acid mine drainage: a primary report. *Science*. **106**: 253 – 256.
- Cournac, L., Guedeney, G., Peltier G., and Vignais, P. M. 2004. Sustained photoevolution of molecular hydrogen in a mutant of *Synechocystis* sp. strain PCC6803 deficient in the Type I NADPH-dehydrogenase complex. *J. Bacteriol.* **186**: 1737 – 1746.
- Cox, J. C., and Boxer, D. H. 1986. The role of rusticyanin, a blue copper protein, in the electron transport chain of *Thiobacillus ferrooxidans* grown on iron or thiosulfate. *Biotechnol. Appl. Biochem.* **8**: 269 – 275.
- Cox, J. C., Nicholls, D. G., and Ingledew, W. J. 1979. Transmembrane electrical potential and transmembrane pH gradient in the acidophile *Thiobacillus ferrooxidans*. *Biochem. J.* **178**: 195 – 200.
- Crane, R. K., and Lipmann, F. 1953. The effect of arsenate on aerobic phosphorylation. *J. Biol. Chem.* **201**: 235 – 243.

- Dagley, S., and Sykes, J. 1957. Effect of starvation upon the constitution of bacteria. *Nature*, London. **179**: 1249 – 1250.
- Daldal, F., Mandaci, S., Winsterstein, C., Myllykallio, H., Duyck, K., and Zannoni, D. 2001. Mobile cytochrome c_2 and membrane-anchored cytochrome c_y are both efficient electron donors to cbb_3 - and aa_3 - type cytochrome c oxidases during respiratory growth of *Rhodobacter sphaeroides*. *J. Bacteriol.* **183**: 2013 – 2024.
- Das, H. K., Goldstein, A., and Kanner, L. C. 1966. Inhibition by chloramphenicol of the growth of nascent protein chains in *Escherichia coli*. *Mol. Pharmacol.* **2**: 158 – 170.
- Dawes, E. A. 1963. Endogenous metabolism with special reference to bacteria. Concluding remarks. *Ann. N. Y. Acad. Sci.* **102**: 789 – 793.
- Dawes, E. A. 1976. Endogenous metabolism and the survival of starved prokaryotes. *Symp. Soc. Gen. Microbiol.* **26**: 19 – 53.
- Dawes, E. A., and Ribbons, D. W. 1962. The endogenous metabolism of microorganisms. *Annu. Rev. Microbiol.* **16**: 241 – 264.
- Dawes, E. A., and Ribbons, D. W. 1963. Endogenous metabolism and survival of *Escherichia coli* in aqueous suspensions. *J. Appl. Bacteriol.* **26**: vi.
- Dawes, E. A., and Ribbons, D. W. 1964. Some aspects of the endogenous metabolism of bacteria. *Bacteriol. Rev.* **28**: 126 – 149.
- Dawes, E. A., and Ribbons, D. W. 1965. Studies on the endogenous metabolism of *Escherichia coli*. *Biochem. J.* **95**: 332 – 343.
- Day, D. A. 1992. Can inhibitors be used to estimate the contribution of the alternative oxidase to respiration in plants? In Lambers, H., van der Plas, L. H. W., eds, *Molecular, Biochemical and Physiological Aspects of Plant Respiration*. SPB Academic Publishing, The Hague, pp 37 – 42.
- de Bok, F. A., Hagedoorn, P. L., Silva, P. J., Hagen, W. R., Schiltz, E., Fritsche, K., and Stams, A. J. 2003. Two W-containing formate dehydrogenases (CO₂-reductases) involved in syntrophic propionate oxidation by *Syntrophobacter fumaroxidans*. *Eur. J. Biochem.* **270**: 2476 – 2485.
- Degli Esposti, M. 1998. Inhibitors of NADH-ubiquinone reductase: an overview. *Biochim. Biophys. Acta.* **1364**: 222 – 235.
- Degli Esposti, M., Crimi, M., and Ghelli, A. 1994. Natural variation in the potency and binding sites of mitochondrial quinone-like inhibitors. *Biochem. Soc. Trans.* **22**: 209 – 213

- Diehl, H., and Smith, G. F. 1952. Quantitative analysis: elementary principles and practice. John Wiley & Sons. Inc., New York Chapman & Hall, Ltd., London, pp 249 – 252.
- Donaire, A., Jiménez, B., Fernández, C. O., Pierattelli, R., Niizeki, T., Moratal, J., Hall, J. F., Kohzuma, T., Hasnain, S. S., and Vila, A. J. 2002. Metal-ligand interplay in blue copper proteins studied by ¹H NMR spectroscopy: Cu(II)-pseudoazurin and Cu(II)-rusticyanin. *JACS*. **124**: 13698 – 13708.
- Dominy, C. N., Deane, S. M., and Rawlings, D. E. 1997. A geographically widespread plasmid from *Thiobacillus ferrooxidans* has genes for ferrexoxin-, FNR-, prismsane-, and NADH-oxidoreductase-like proteins which are also located on the chromosome. *Microbiology*, **143**: 3123 – 3136.
- Dopson, M., Lindström, E. B., and Hallberg, K. B. 2002. ATP generation during reduced inorganic sulfur compound oxidation by *Acidithiobacillus caldus* is exclusively due to electron transport phosphorylation. *Extremophiles*. **6**:123 – 129.
- Douce, R., and Neuberger, M. 1989. The uniqueness of plant mitochondria. *Annu Rev Plant Physiol. Plant Mol. Biol.* **40**: 371 – 414.
- Drobner, E., Huber, H., and Stetter, K. O. 1990. *Thiobacillus ferrooxidans*, a facultative hydrogen oxidizer. *Appl. Environ. Microbiol.* **56**: 2922 – 2923.
- Edwart, D. K., and Hugues, N. H. 1991. The extraction of metals from ores using bacteria. *Adv. Inorg. Chem.* **36**: 103 – 135.
- Elbehti, A., Brasseur, G., and Lemesle-Meunier, D. 2000. First evidence for existence of an uphill electron transfer through the *bc₁* and NADH-Q oxidoreductase complexes of the acidophilic obligate chemolithotrophic ferrous ion-oxidizing bacterium *Thiobacillus ferrooxidans*. *J. Bacteriol.* **182**:3602 – 6.
- Farrell, R. E., Germida, J. J., Huang, P. M. 1993. Effects of chemical speciation in growth media on the toxicity of mercury (II). *Appl. Environ. Microbiol.* **59**: 1507 – 1514.
- Ferguson-Millers, S., and Babcock, G. T. 1996. Heme/copper terminal oxidases. *Chem. Rev.* **96**: 2889 – 2907.
- Ferry, J. G. 1990. Formate dehydrogenase. *FEMS Microbiol. Rev.* **87**: 377 – 382.
- Fischer, J., Quentmeier, A., Kostka, S., Kraft, R., Friedrich, C. G. 1996. Purification and characterization of the hydrogenase from *Thiobacillus ferrooxidans*. *Arch. Microbiol.* **165**: 289 – 296.

- Friedrich, T., van Heek, P., Leif, H., Ohnishi, T., Forche, E., Kunze, B., Jansen, R., Trowitzsch-Kienast, W., Höfle, G., Reichenbach, H. X., and Weiss, H. 1994. Two binding sites of inhibitors in NADH: ubiquinone oxidoreductase (complex I). Relationship of one site with the ubiquinone-binding site of bacterial glucose:ubiquinone oxidoreductase. *Eur. J. Biochem.* **219**: 691 – 698.
- Friedrich, C. G., Rother, D., Bardischewsky, F., Quentmeier, A., and Fischer, J. 2001. Oxidation of reduced inorganic sulfur compounds by bacteria: emergence of a common mechanism? *Appl. Environ. Microbiol.* **67**: 2873 – 2882.
- Fukumori, Y., Yano, T., Sato, A., and Yamanaka, T. 1988. Fe(II)-oxidizing enzyme purified from *Thiobacillus ferrooxidans*. *FEMS Microbiol. Lett.* **50**: 169 – 172.
- Garcia-Horsman, J. A., Barquera, B., Rumbley, J., Ma, J., and Gennis, R. B. 1994. The superfamily of heme-copper respiratory oxidases. *J. Bacteriol.* **176**: 5587 – 5600.
- Giudici-Orticoni, M. T., Guerlesquin, F., Bruschi, M., and Nitschke, W. 1999. Interaction-induced redox switch in the electron transfer complex rusticyanin-cytochrome *c*₄. *J. Biol. Chem.* **274**: 30365 – 30369.
- González-Meler, M. A., Ribas-Carbo, M., Giles, L., and Siedow, J. N. 1999. The effect of growth and measurement temperature on the activity of the alternative respiratory pathway. *Plant Physiol.* **120**: 765 – 772.
- Grossmann, J. G., Hall, J. F., Kanbi, L. D., and Hasnain, S. S. 2002. The N-terminal extension of rusticyanin is not responsible for its acid stability. *Biochemistry.* **41**: 3613 – 3619.
- Harahuc, L., Lizama, H. M., and Suzuki, I. 2000. Selective inhibition of the oxidation of ferrous iron or sulfur in *Thiobacillus ferrooxidans*. *Appl. Environ. Microbiol.* **66**: 1031 – 1037.
- Harahuc, L., and Suzuki, I. 2001. Sulfite oxidation by iron-grown cells of *Thiobacillus ferrooxidans* at pH 3 possibly involves free radicals, iron, and cytochrome oxidase. *Can. J. Microbiol.* **47**: 424 – 430.
- Harold, F. M. 1972. Conservation and transformation of energy by bacterial membranes. *Bacteriol. Rev.* **36**: 172 – 230.
- Harrison, A. P., Jarvis, B. W., and Johnson, J. L. 1980. Heterotrophic bacteria from cultures of autotrophic *Thiobacillus ferrooxidans*: relationship as studied by means of deoxyribonucleic acid homology. *J. Bacteriol.* **143**: 448 – 454.
- Harvey, A. E., Smart, J. A., and Amis, E. S. 1955. Simultaneous spectrophotometric determination of iron(II) and total iron with 1,10-phenanthroline. *Anal. Chem.* **27**: 26 – 29.

- Heinhorst, S., Baker, S. H., Johnson, D. R., Davies, P. S., Cannon, G. C., and Shively, J. M. 2002. Two copies of form I RuBisCO genes in *Acidithiobacillus ferrooxidans* ATCC 23270. *Curr. Microbiol.* **45**: 115 – 117.
- Hesse, S. J. A., Ruijter, G. J. G., Dijkema, C., and Visser, J. 2002. Intracellular pH homeostasis in the filamentous fungus *Aspergillus niger*. *Eur. J. Biochem.* **269**: 3485 – 3494.
- Hoefnagel, M. H., Millar, A. H., Wiskich, J. T., and Day, D. A. 1995. Cytochrome and alternative respiratory pathways compete for electrons in the presence of pyruvate in soybean mitochondria. *Arch Biochem Biophys.* **318**: 394 – 400.
- Holt, P. J., Morgan, D. J., and Sazanov, L. A. 2003. The Location of NuoL and NuoM Subunits in the Membrane Domain of the *Escherichia coli* Complex I: Implications for the mechanism of proton pumping. *J. Biol. Chem.* **278**: 43114 – 43120.
- Hourton-Cabassa, C., Ambard-Bretteville, F., Moreau, F., Davy de Virville, J., Rémy, R., and Colas des Francs-Small, C. 1998. Stress induction of mitochondrial formate dehydrogenase in potato leaves. *Plant Physiol.* **116**: 627 – 635.
- Imkamp, F., and Müller, V. 2002. Chemiosmotic energy conservation with Na⁺ as the coupling ion during hydrogen-dependent caffeate reduction by *Acetobacterium woodii*. *J. Bacteriol.* **184**: 1947 – 1951.
- Ingledeu, W. J. 1982. *Thiobacillus ferrooxidans*, The bioenergetics of an acidophilic chemolithotroph. *Biochim. Biophys. Acta* **683**: 89-117.
- Ingledeu, W. J., Cox, J. C., and Halling, P. J. 1977. A proposed mechanism for energy conservation during Fe²⁺ oxidation by *Thiobacillus ferro-oxidans*: chemiosmotic coupling to net H⁺ influx. *FEMS Microbiol. Lett.* **2**: 193 – 197.
- Ingledeu, W. J., and Houston, A. 1986. The organization of the respiratory chain of *Thiobacillus ferrooxidans*. *Biotechnol. Appl. Biochem.* **8**: 242 – 248.
- Ishikawa, R., Ishido, Y., Tachikawa, A., Kawasaki, H., Matsuzawa, H., and Wakagi, T. 2002. *Aeropyrum pernix* K1, a strictly aerobic and hyperthermophilic archaeon, has two terminal oxidases, cytochrome *ba*₃ and cytochrome *aa*₃. *Arch. Microbiol.* **179**: 42 – 49.
- Jensen, A. B., and Webb, C. 1995. Ferrous sulphate oxidation using *Thiobacillus ferrooxidans*: a review. *Process Biochem.* **30**: 225 – 236.
- Jiménez, B., Piccioli, M., Moratal, J., and Donaire, A. 2003. Backbone dynamics of rusticyanin: the high hydrophobicity and rigidity of this blue copper protein is responsible for its thermodynamic properties. *Biochemistry.* **42**: 10396 – 10405.

- Jormakka, M., Byrne, B., and Iwata, S. 2003. Protonmotive force generation by a redox loop mechanism. *FEBS Lett.* **545**: 25 – 30.
- Jormakka, M., Törnroth, S., Byrne, B., and Iwata, S. 2002. Molecular basis of proton motive force generation: structure of formate dehydrogenase-N. *Science.* **295**: 1863 – 1968.
- Jørgensen, B. B. 1982. Mineralization of organic matter in the sea bed – the role of sulphate reduction. *Nature.* **296**: 643 – 645.
- Kamikura, K., Fujii, S., and Sugio, T. 2001. Purification and some properties of ubiquinol oxidase from obligately chemolithotrophic iron-oxidizing bacterium, *Thiobacillus ferrooxidans* NASF-1. *Biosci. Biotechnol. Biochem.* **65**: 63 – 71.
- Kanbi, L. D., Antonyuk, S., Hough, M. A., Hall, J. F., Dodd, F. E., and Hasnain, S. S. 2002. Crystal structure of the Met148Leu and Ser86Asp mutants of rusticyanin from *Thiobacillus ferrooxidans*: insight into the structural relationship with the cupredoxins and the multi copper proteins. *J. Mol. Biol.* **320**: 263 – 275.
- Kelly, D. P., and Wood, A. P. 2000. Reclassification of some species of *Thiobacillus* to the newly designated genera *Acidithiobacillus* gen. nov., *Halothiobacillus* gen. nov. and *Thermithiobacillus* gen. nov. *Int. J. Syst. Evol. Microbiol.* **50**: 511 – 516.
- Kim, H., Xia, D., Yu, C. A., Xia, J. Z., Kachurin, A. M., Zhang, L., Yu, L., Deisenhofer, J. 1998. Inhibitor binding changes domain mobility in the iron-sulfur protein of the mitochondrial bc₁ complex from bovine heart. *PNAS.* **95**: 8026 – 8033.
- Kiesow, L. A. 1967. Energy-linked reaction in chemoautotrophic organisms. In: *Current Topics in Bioenergetics* (Sanadi, D. R., Ed.), Vol.2. pp. 195 – 233. Academic Press, New York.
- Kramer, D. M., Roberts, A. G., Muller, F., Cape, J., and Bowman, M. K. 2004. Q-cycle bypass reactions at the Q_o site of the cytochrome bc₁ (and related) complexes. *Methods Enzymol.* **382**: 21 – 45.
- Kusano, T., Takeshima, T., Inoue, C., and Sugawara, K. 1991. Evidence for two sets of structural genes coding for ribulose biphosphate carboxylase in *Thiobacillus ferrooxidans*. *J. Bacteriol.* **173**: 7313 – 7323.
- Kusano, T., Takeshima, T., Sugawara, K., Inoue, C., Shirotori, T., Yano, T., Fukumori, Y., and Yamanaka, T. 1992. Molecular cloning of the gene encoding *Thiobacillus ferrooxidans* Fe(II) oxidase. High homology of the gene product with HiPP. *J. Biol. Chem.* **267**: 11242 – 11247.

- Lambers, H., Day, D. A., and Azcón-Bieto, J. 1983. Cyanide-resistant respiration in roots and leaves: measurements with intact tissues and isolated mitochondria. *Physiol. Plant.* **58**: 148 – 154.
- Leathen, W. W., and Kinskel, N.A., Bralley, S. A. Sr. 1956. *Ferrobacillus ferrooxidans*: a chemosynthetic autotrophic Bacterium. *J Bacteriol.* **72**: 700 – 704.
- Leduc, L. G., and Ferroni, G. D. 1994. The chemolithotrophic bacterium *Thiobacillus ferrooxidans*. *FEMS Microbiol. Rev.* **14**: 103 – 120.
- Lovley, D. R. 2003. Environmental microbe-metal interactions. ASM Press, Washington, D. C.
- Lowry, O. H., Rosebrough, N. J., Farr, A. L., and Randall, R. J. 1951. Protein measurement with the folin phenol reagent. *J. Biol. Chem.* **193**: 265 – 275.
- Maeda, S., Badger, M. R., and Price, G. D. 2002. Novel gene products associated with NdhD3/D4-containing NDH-1 complexes are involved in photosynthetic CO₂ hydration in the cyanobacterium, *Synechococcus* sp. PCC7942. *Mol. Microbiol.* **43**: 425 – 435.
- Masau, R. J., Oh, J. K., Suzuki, I. 2001. Mechanism of oxidation of inorganic sulfur compounds by thiosulfate-grown *Thiobacillus thiooxidans*. *Can. J. Microbiol.* **47**: 348 – 358.
- McDold, D. G., and Clark, R. H. 1970. The oxidation of aqueous ferrous sulfate by *Thiobacillus ferrooxidans*. *Can. J. Chem. Engng.* **48**: 669 – 675.
- Mignone, C.F., and Donati, E.R. 2004. ATP requirements for growth and maintenance of iron-oxidizing bacteria. *Biochem. Eng. J.* **18**: 211 – 216.
- Millar, A. H., Hoefnagel, M., Day, D. A., and Wiskich, J. T. 1996. Specificity of the organic acid activation of alternative oxidase in plant mitochondria. *Plant Physiol.* **111**: 613 – 618.
- Millenaar, F. F., and Lambers, H. 2003. The alternative oxidase: *in vivo* regulation and function. *Plant Biol.* **5**: 2 – 15.
- Miller, M. J., and Gennis, R. B. 1985. The cytochrome *d* complex is a coupling site in the aerobic respiratory chain of *Escherichia coli*. *J. Biol. Chem.* **260**: 14003 – 14008.
- Miyoshi, Y. 1998. Structure-activity relationships of some complex I inhibitors. *Biochim. Biophys. Acta.* **1364**: 236 – 244.
- Muller, F., Crofts, A. R., and Kramer, D. M. 2002. Multiple Q-cycle bypass reactions at the Qo site of the cytochrome *bc*₁ complex. *Biochemistry.* **41**: 7866 – 7874.

- Murphy, A. D., and Lang-Unnasch, N. 1999. Alternative oxidase inhibitors potentiate the activity of atovaquone against *Plasmodium falciparum*. *Antimicrob. Agents Chemother.* **43**: 651 – 654.
- Musser, S. M., and Chan, S. I. 1998. Evolution of the cytochrome *c* oxidase proton pump. *J. Mol. Evol.* **46**: 508 – 520.
- Namslauer, A., Pawate, A. S., Gennis, R. B., and Brzezinski, P. 2003. Redox-coupled proton translocation in biological systems: proton shuttling in cytochrome *c* oxidase. *PNAS.* **100**: 15543 – 15547.
- Nicholls, D. G., and Ferguson, S. J. 1992. *Bioenergetics*, 2nd Ed. Academic Press, London, UK.
- Nicholls, D. G., and Ferguson, S. J. 2002. *Bioenergetics*, 3rd Ed. Academic Press, London, UK.
- Nunoura, T., Sako, Y., Wakagi, T., and Uchida, A. 2003. Regulation of the aerobic respiratory chain in the facultatively aerobic and hyperthermophilic archaea on *Pyrobaculum oguniense*. *Microbiology.* **149**: 673 – 688.
- Oh, J. II., and Bowien, B. 1998. Structural analysis of the *fds* operon encoding the NAD⁺-linked formate dehydrogenase of *Ralstonia eutropha*. *J. Biol. Chem.* **273**: 26349 – 26360.
- Ohkawa, H., Pakrasi, H. B., and Ogawa, T. 2000. Two types of functionally distinct NAD(P)H dehydrogenases in *Synechocystis* sp. strain PCC6803. *J. Biol. Chem.* **275**: 31630 – 31634.
- Ohmura, N., Sasaki, K., Matsumoto, N., and Saiki, H. 2002. Anaerobic respiration using Fe³⁺, S⁰, and H₂ in the chemolithoautotrophic bacterium *Acidithiobacillus ferrooxidans*. *J. Bacteriol.* **184**: 2081 – 2087.
- Okun, J. G., Lümmlen, P., and Brandt, U. 1999. Three classes of inhibitors share a common binding domain in mitochondrial complex I (NADH:ubiquinone oxidoreductase). *J. Biol. Chem.* **274**: 2625 – 2630.
- Oro, J., and Rappoport, D. A. 1959. Formate metabolism by animal tissues. II. The mechanism of formate oxidation. *J. Biol. Chem.* **234**: 1661 – 1665.
- Overkamp, K. M., Kotter, P., van der Hoek, R., Schoondermark-Stolk, S., Luttik, M. A., van Dijken, J. P., and Pronk, J. T. 2002. Functional analysis of structural genes for NAD⁺-dependent formate dehydrogenase in *Saccharomyces cerevisiae*. *Yeast.* **19**: 509 – 520.

- Otten, M. F., Stork, D. M., Reijnders, W. N. M., Westerhoff, H. V., and van Spanning, R. J. M. 2001. Regulation of expression of terminal oxidases in *Paracoccus denitrificans*. *Eur. J. Biochem.* **268**: 2468 – 2497.
- Poole, R., and Hill, S. 1997. Respiratory protection of nitrogenase activity in *Azotobacter vinelandii* – roles of the terminal oxidases. *Biosci. Rep.* **17**: 303 – 317.
- Postage, J. R., and Hunter, J. R. 1962. The survival of starved bacteria. *J. Gen. Microbiol.* **29**: 233 – 263.
- Prochaska, L. J., Bisson, R., Capaldi, R. A., Steffens, G. C. M., and Buse, G. 1981. Inhibition of cytochrome c oxidase function by dicyclohexylcarbodiimide. *Biochim. Biophys. Acta.* **637**: 360 – 373.
- Pronk, J. T., Liem, K., Bos, P., and Kuenen, J. G. 1991a. Energy transduction by anaerobic ferric iron respiration in *Thiobacillus ferrooxidans*. *Appl. Environ. Microbiol.* **57**: 2063 – 2068.
- Pronk, J. T., Meijer, W. M., Haseu, W., van Dijken, J. P., Bos, P., and Kuenen, J. G. 1991b. Growth of *Thiobacillus ferrooxidans* on formic acid. *Appl. Environ. Microbiol.* **57**: 2057 – 2062.
- Purschke, W., Schmidt, C. L., Petersen, A., and Schäfer. 1997. The terminal quinol oxidase of the hyperthermophilic archaeon *Acidianus ambivalens* exhibits a novel subunit structure and gene organization. *J. Bacteriol.* **179**: 1344 – 1353.
- Puustinen, A., Finel, M., Vikkin, M., and Wikström, M. 1989. Cytochrome *o* (*bo*) is a proton pump in *Paracoccus denitrificans* and *Escherichia coli*. *FEBS Lett.* **249**: 163 – 167.
- Quayle, J. R. 1966. Formate dehydrogenase. *Methods Enzymol.* **9**: 360 – 364.
- Rawlings, D. E. 2002. Heavy metal mining using microbes. *Annu. Rev. Microbiol.* **56**: 65 – 91.
- Ribas-Carbo, M., Aroca, R., Gonzalez-Meler, M. A., Irigoyen, J. J., and Sanchez-Diaz, M. 2000. The electron partitioning between the cytochrome and alternative respiratory pathways during chilling recovery in two cultivars of maize differing in chilling sensitivity. *Plant Physiol.* **122**: 199 – 204.
- Rich, P. R., Wiegand, N. K., Blum, H., Moore, A. L., and Bonner, W. D. 1978. Studies on the mechanism of inhibition of redox enzymes by substituted hydroxamic acids. *Biochim. Biophys. Acta.* **525**: 325 – 337.
- Richardson, D. J. 2000. Bacterial respiration: a flexible process for a changing environment. *Microbiology.* **146**: 551 – 571.

- Rohwerder, T., Gehrke, T., Kinzler, K., and Sand, W. 2003. Bioleaching review part A: progress in bioleaching: fundamentals and mechanisms of bacterial metal sulfide oxidation. *Appl. Microbiol. Biotechnol.* **63**: 239 – 248.
- Ronk, M., Shively, J. E., Shute, E. A., and Blake, R. C. II. 1991. Amino acid sequence of the blue copper protein rusticyanin from *Thiobacillus ferrooxidans*. *Biochemistry.* **30**: 9435 – 9442.
- Sand, W. 1989. Ferric iron reduction by *Thiobacillus ferrooxidans* at extremely low pH-values. *Biogeochem.* **7**: 195 – 201.
- Sasaki, K., Ida, C., Ando, A., Matsumoto, N., Saiki, H., and Ohmura, N. 2003. Respiratory isozyme, two types of rusticyanin of *Acidithiobacillus ferrooxidans*. *Biosci. Biotechnol. Biochem.* **67**: 1039 – 1047.
- Sato, A., Fukumori, Y., Yano, T., Kai, M., and Yamanaka, T. 1989. *Thiobacillus ferrooxidans* c-552: purification and some of its molecular features. *Biochim. Biophys. Acta.* **976**: 129 – 134.
- Sawers, G. 1994. The hydrogenases and formate dehydrogenases of *Escherichia coli*. *Antonie Van Leeuwenhoek.* **66**: 57 – 88.
- Schafer, G., Purschke, W., and Schmidt, C. C. 1996. On the origin of respiration: electron transport proteins from archaea to man. *FEMS Microbiol. Rev.* **18**: 173 – 188.
- Shafia, F., Brinson, K. R., Heinzman, M. W., and Brady, J. M. 1972. Transition of the chemolithotroph *Ferrobacillus ferrooxidans* to obligate organotrophy and metabolic capabilities of glucose-grown cells. *J. Bacteriol.* **111**: 56 – 65.
- Shafia, F., and Wilkinson, Jr. 1961. Growth of *Ferrobacillus ferrooxidans* on organic matter. *J. Bacteriol.* **97**: 256 – 647.
- Shively, J., van Keulen, G., and Meijer, W. G. 1998. Something from almost nothing: carbon dioxide fixation in chemoautotrophs. *Annu. Rev. Microbiol.* **52**: 191 – 230.
- Siedow, J. N., and Bickett, D. M. 1981. Structural features required for inhibition of cyanide-insensitive electron transfer by propyl gallate. *Arch. Biochem. Biophys.* **207**: 32 – 39.
- Sierra, G., and Gibbons, N. E. 1962. Role and oxidation pathway of poly- β -hydroxybutyric acid in *Micrococcus halodenitrificans*. *Can. J. Microbiol.* **8**: 255 – 269.

- Silver, M., and Lundgren, D. G. 1968. The thiosulfate-oxidizing enzyme of *Ferrobacillus ferrooxidans* (*Thiobacillus ferrooxidans*). *Can. J. Biochem.* **46**:1215 – 1220.
- Skoog, D. A., West, D. M., and Holler, F. J. 2000. Analytical chemistry: an introduction, 7th ed., Fort Worth: Saunders College Pub., pp. 547 – 592.
- Smith, J. R., Luthy, G. R., and Middleton, T. L. 1988. Microbial ferrous iron oxidation in acidic solution. *J. Wat. Pollut. Control. Fed.* **60**: 518 – 530.
- Søballe, B., and Poole, R. 1999. Microbial ubiquinones: multiple roles in respiration, gene regulation and oxidative stress management. *Microbiology.* **145**: 1817 – 1830.
- Stenmark, P., Grünler, J., Mattsson, J., Sindelar, P. J., Nordlund, P., and Berthold, D. A. 2001. A new member of the family of di-iron carboxylate proteins. Coq7(cik-1), a membrane-bound hydroxylase involved in ubiquinone biosynthesis. *J. Biol. Chem.* **276**: 33297 – 33300.
- Stenmark, P., and Nordlund, P. 2003. A procaryotic alternative oxidase present in the bacterium *Novosphingobium aromaticivorans*. *FEBS Lett.* **552**: 189 – 192.
- Strange, R. E. 1968. Bacterial glycogen and survival. *Nature, London.* **220**: 606 – 607.
- Sugio, T., Kudo, S., Tano, T., and Imai, K. 1982. Glucose transport system in a facultative iron-oxidizing bacterium, *Thiobacillus ferrooxidans*. *J. Bacteriol.* **150**: 1109 – 1114.
- Sugio, T., Tano, T., and Imai, K. 1981. Isolation and some properties of two kinds of cytochrome *c* oxidase from iron-grown *Thiobacillus ferrooxidans*. *Agr. Biol. Chem.* **45**: 1791 – 1799.
- Suzuki, I. 1958. Fixation of carbon dioxide by chemoautotrophic bacteria. Ph.D. thesis. Iowa State University, Iowa, U.S.A.
- Suzuki, I. 2001. Microbial leaching of metals from sulfide minerals. *Biotechnol. Adv.* **19**: 119 – 132.
- Suzuki, I., Lee, D., Mackay, B., Harahuc, L., and Oh, J. K. 1999. Effect of various ions, pH, and osmotic pressure on oxidation of elemental sulfur by *Thiobacillus thiooxidans*. *Appl. Environ. Microbiol.* **65**: 5163 – 5168.
- Tabita, R., and Lundgren, D.G. 1971a. Utilization of glucose and the effect of organic compounds on the chemolithotroph *Thiobacillus ferrooxidans*. *J. Bacteriol.* **108**: 328 – 333.

- Tabita, R., and Lundgren, D.G. 1971*b*. Heterotrophic metabolism of the chemolithotroph *Thiobacillus ferrooxidans*. J. Bacteriol. **108**: 334 – 342.
- Temple, K. L., and Colmer, A. R. 1951. The autotrophic oxidation of iron by a new bacterium, *Thiobacillus ferrooxidans*. J Bacteriol. **62**: 605 – 611.
- Terada, H. 1981. The interaction of highly active uncouplers with mitochondria. Biochim. Biophys. Acta. **639**: 225 – 242.
- Thorn, M. B. 1953*a*. Inhibition by malonate of succinic dehydrogenase in heart-muscle preparations. Biochem J. **54**: 540 – 547.
- Thorn, M. B. 1953*b*. Malonate inhibition of succinic dehydrogenase. Biochem J. **53**: i.
- Tian, K., Lin, J., Liu, X., Liu, Y., Zhang, C., and Yan, W. 2003. Conversion of an obligate autotrophic bacteria to heterotrophic growth: expression of a heterogeneous phosphofructokinase gene in the chemolithotroph *Acidithiobacillus thiooxidans*. Biotech. Lett. **25**: 749 – 754.
- Tikhonova, G. V., Lisenkova, L. L., Doman, N. G., and Skulachev, V. P. 1967. Electron transport pathways in *Thiobacillus ferrooxidans*. Translated from Biokhimiya **32**: 725 – 734.
- Timmerman, M. M., and Woods, J. P. 1999. Ferric reduction is a potential iron acquisition mechanism for *Histoplasma capsulatum*. Infection and Immunity **67**: 6403 – 6408.
- Trumpower, B. L. 1990. The protonmotive Q cycle. Energy transduction by coupling of proton translocation to electron transfer by the cytochrome bc1 complex. J. Biol. Chem. **265**: 11409 – 11412.
- Tsubaki, M., Hori, H., Mogi, T. 2000. Probing molecular structure of dioxygen reduction site of bacterial quinol oxidases through ligand binding to the redox metal centers. J. Inorg. Biochem. **82**: 19 – 25.
- Tsuchiya, T., and B. P. Rosen. 1980. Respiratory control in *Escherichia coli*. FEBS Lett. **120**: 128 – 130.
- Ulvik, R., and Romslo, I. 1975. Effect of thenoyltrifluoroacetone on oxygen consumption and energy conservation in isolated rat liver mitochondria. FEBS Lett. **59**: 180 – 183.
- Umbreit, W. W., Burris, R. H., and Stauffer, J. F. 1949. Manometric techniques and tissue metabolism. Burgess Publ. Co., Minneapolis, Minnesota.

- Vanlerberghe, G. C., Robson, C. A., and Yip, J. Y.H. 2002. Induction of mitochondrial alternative oxidase in response to a cell signal pathway down-regulating the cytochrome pathway prevents programmed cell death. *Plant Physiol.* **129**: 1829 – 842.
- Vazquez, D. 1963. Antibiotics which affect protein synthesis: the uptake of ¹⁴C-chleramphenicol by bacteria. *Biochem. Biophys. Res. Commun.* **12**: 409 – 413.
- Watmough, N. J., Cheesman, M. R., Butler, C. S., Little, R. H., Greenwood, C., and Thomson, A. J. 1998. The dinuclear center of cytochrome *bo*₃ from *Escherichia coli*. *J. Bioenerg. Biomembr.* **30**: 55 – 62.
- Whittacker, M., Bergmann, D., Arciero, D., and Hooper, A. B. 2000. Electron transfer during the oxidation of ammonia by the chemolithotrophic bacterium *Nitrosomonas europaea*. *Biochim. Biophys. Acta.* **1459**: 346 – 355.
- Windholz, M., Budavari, S., Blumetti, R. F., Otterbein, E. S. 1983. The Merck Index, 10th edition. An encyclopedia of chemicals, drugs, and biologicals. Merck & Co., Inc., Pahway, N. J., USA. pp578.
- Winstedt, L., and von Wachenfeldt, C. 2000. Terminal oxidases of *Bacillus subtilis* strain 168: one quinol oxidase, cytochrome *aa*₃ or cytochrome *bd*, is required for aerobic growth. *J. Bacteriol.* **182**: 6557 – 6564.
- Yamanaka, T., Yano, T., Kai, M., Tamegai, H., Sato, A., and Fukumori, Y. 1991. *In* Mukohata, Y., eds, New Era of Bioenergetics. Academic Press, Tokyo, pp 223 – 246.
- Yano, T., Fukumor, Y., and Yamanaka, T. 1991. The amino acid sequence for rusticyanin isolated from *Thiobacillus ferrooxidans*. *FEBS Lett.* **288**: 159 – 162.
- Yarzabal, A., Appia-Ayme, C., Ratouchniak, J., and Bonnefoy, V. 2004. Regulation of the expression of the *Acidithiobacillus ferrooxidans rus* operon encoding two cytochromes *c*, a cytochrome oxidase and rusticyanin. *Microbiology.* **150**: 2113 – 2123.
- Yarzabal, A., Brasseur, G., and Bonnefoy, V. 2002a. Cytochromes *c* of *Acidithiobacillus ferrooxidans*. *FEMS Microbiol. Lett.* **209**: 189 – 195.
- Yarzabal, A., Brasseur, G., Ratouchniak, J., Lund, K., Lemesle-Meunier, D., DeMoss, J. A., and Bonnefoy, V. 2002b. The high-molecular-weight cytochrome *c* *Cyc2* of *Acidithiobacillus ferrooxidans* is an outer membrane protein. *J. Bacteriol.* **184**: 313 – 317.
- Zychlinsky, E., and Matin, A. 1983. Effect of starvation on cytoplasmic pH, proton motive force, and viability of an acidophilic bacterium, *Thiobacillus acidophilus*. *J. Bacteriol.* **153**: 371 – 374.